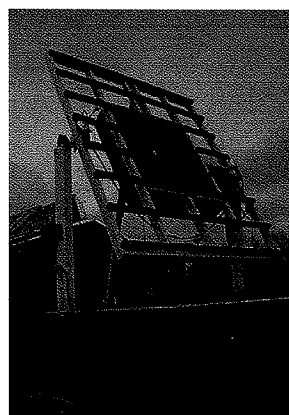
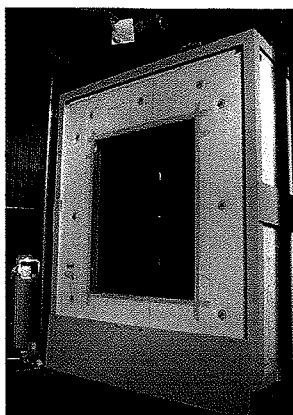


CHARACTERISATION OF ADVANCED WINDOWS

Determination of thermal properties
by measurements

KARSTEN DUER



RAPPORT

BYG•DTU R-007

2001

**ISSN 1396-4011
ISBN 87-7877-062-9**

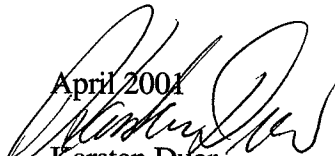
Preface

This report describes the main results of my ph.d. study carried out at the Department of Buildings and Energy, the Technical University of Denmark. The study was carried out under the supervision of professor Svend Svendsen.

The study was mainly funded by the Danish Ministry of Energy's EFP-programme and was for a large part carried out as an element in my participation in two international research projects:

1. The International Energy Agency, Solar Heating and Cooling Programme Task 18 "Advanced Glazings and Associated Materials for Solar and Building Applications" (IEA SHCP Task18).
2. The European project: Angular-dependent Light and Total Solar Energy Transmittance for Complex Glazings, ALTSET

I thank professor Svend Svendsen for his interest in the subject, my colleagues in the two projects mentioned above and the Danish Ministry of Energy for the funding that made the study possible.

April 2001

Karsten Duer.

CONTENTS

Preface

Summary

Resume (summary in Danish)

1	Introduction	1-1
1.1	Aim of the project	1-1
1.2	Methods	1-1
2	Background	2-1
3	Fundamental properties	3-1
3.1	General	3-1
3.2	Thermal transmittance, U-value	3-2
3.3	Solar direct transmittance, τ_e	3-4
3.4	Total solar energy transmittance, g-value	3-5
4	Calculation methods	4-1
4.1	General	4-1
4.2	Solar transmittance in a multilayer glazing	4-1
4.3	Total solar energy transmittance	4-3
4.3.1	Separate calculation of g	4-3
4.3.2	Determination of U and g by heat balance calculation	4-6
5	Measurement of thermal transmittance, U-value	5-1
5.1	General	5-1
5.2	Measurement of thermal transmittance and thermal resistance	5-2
5.3	Guarded hot box	5-2
5.4	Calibration of the guarded hot box	5-6
5.5	Measured calibration	5-7
5.6	Combined calibration	5-10
5.7	Determination of the U-value	5-12
5.7.1	Boundary conditions	5-12
5.7.2	The U-value measurement	5-13
5.7.3	Discussion of the two calibration principles	5-14
5.8	Roof windows	5-15
5.8.1	Detailed calibration procedure	5-16
5.8.2	Simple calibration procedure	5-17
5.8.3	Combined calibration procedure	5-17

5.8.4	Roof window measurements	5-18
5.8.5	Recommendations for U-value measurements on roof windows	5-21
5.9	Uncertainty of hot box measurements	5-22
5.10	U-value, ISO round robin test, measured calibration	5-23
5.10.1	Introduction	5-23
5.10.2	Description of the window	5-23
5.10.3	Calibration panels	5-25
5.10.4	Calibration measurements	5-25
5.10.5	U-value measurement	5-27
5.10.6	Inter-laboratory comparison	5-28
5.11	Nordic round robin test, combined calibration	5-29
5.11.1	Description of the windows	5-29
5.11.2	Calibration panels	5-29
5.11.3	Calibration measurements	5-30
5.11.4	U-value measurements	5-31
5.11.5	Inter-laboratory comparison, Nordic countries	5-32
5.12	Comparison of calculated and measured values	5-33
5.13	Conclusions	5-34
6	Calorimetric measurement of total solar energy transmittance, g-value	6-1
6.1	General	6-1
6.2	Reference conditions	6-3
6.3	Measuring devices	6-5
6.3.1	Collection of the transmitted energy	6-5
6.3.2	Solar simulator	6-5
6.3.3	Surface heat transfer	6-6
6.4	The METSET	6-6
6.4.1	Solar simulator	6-8
6.4.2	Metering box	6-10
6.4.3	Absorber	6-11
6.4.4	Guard box	6-12
6.4.5	Measurement of the collected energy	6-12
6.4.6	Auxiliary equipment	6-13
6.4.7	Technical characteristics summary	6-14
6.5	Measuring procedure, METSET	6-14
6.6	Determination of the g-value for experimental conditions (g_{exp})	6-16
6.6.1	Correction for heat flow across the test sample	6-16
6.6.2	Correction for heat flow across the metering box walls	6-17
6.6.3	Correction for heat flow through the sample edge	6-17
6.7	Determination of the g-value for reference conditions (g_{ref})	6-22
6.7.1	General	6-22
6.7.2	Correction to reference boundary conditions	6-24
6.7.3	Effect of the surface heat transfer coefficients	6-26
6.8	Calibration measurements	6-31
6.8.1	Float glass DGU	6-33
6.8.2	Low emissivity DGU	6-35
6.8.3	Solar control DGU	6-37

6.8.4	Simple correction data	6-41
6.8.5	Uncertainty of the g-value measurements	6-43
6.8.6	Conclusions and discussion	6-45
7	Measurement of direct solar transmittance, τ_e	7-1
7.1	General	7-1
7.2	Measuring principles	7-1
7.3	Solar tracker	7-2
7.4	Broadband measurements, SolTrans	7-5
7.4.1	Measuring the solar transmittance	7-7
7.4.2	Accuracy of the measurements	7-9
7.4.3	Test example	7-9
7.5	Measurement of τ^{dh} for three samples	7-12
7.5.1	Description of the samples	7-12
7.5.2	Measurements	7-13
7.5.3	Results	7-13
7.5.4	Interlaboratory comparison	7-14
7.6	Conclusion	7-17
8	Monolithic silica aerogel in glazings	8-1
8.1	Abstract	8-1
8.2	Introduction	8-1
8.3	Measurements	8-2
8.3.1	Measured solar and visible properties	8-2
8.3.2	Measured thermal properties	8-3
8.4	Aerogel double glazed unit	8-4
8.4.1	Production of an aerogel glazing	8-4
8.4.2	Measurement of key performance parameters	8-5
8.5	Conclusion	8-5
9	Conclusion	9-1
9.1	Outlook	9-3

Symbols

References

Appendices

- A U-value measurements on a roof window
- B U-value measurements on a roof window, second study
- C Uncertainty in guarded hot box measurement
- D Comparison of calculated and measured values.
Article submitted and under review to 'Solar Energy':
Energy labelling of glazings and windows in Denmark
- E Correction for heat flow through edge of sample
- F Monolithic silica aerogel in superinsulating glazings.
Article accepted and printed in 'Solar Energy' 1998:
Monolithic silica aerogel in superinsulating glazings

Summary

This report describes work carried out with the aim of facilitating a full energy performance characterisation of advanced windows and glazings by means of measurements. The energy performance of windows and glazings are characterised by two parameters: The thermal transmittance (U-value) and the total solar energy transmittance (g-value) and methods to determine these two parameters by measurements have been investigated. This process has included the improvement of existing equipment and existing measuring methods as well as the development of new measuring equipment and new methods of measuring and data treatment.

Measurements of the thermal transmittance of windows and glazings in a guarded hot box have been investigated. The calibration and measuring procedures for determining the U-values of facade windows were analysed and a suggestion for a new calibration and measuring procedure for determining the U-values of roof windows in a guarded hot box was elaborated. The accuracy of the guarded hot box measurements was examined by comparisons to measurements in a hot-plate device and excellent agreement between the results was obtained. Analysis showed that the expected uncertainty in the U-value measurement is about 5% for a specimen with a U-value of $1.75 \text{ W/m}^2\text{K}$. The U-values of three different windows were measured in two separate round robin tests applying two different calibration procedures. The window U-values were ranging from 1.1 to $2.5 \text{ W/m}^2\text{K}$ and all measured results were within the expected uncertainties of the measurements. On the basis of the investigations on hot box measurements a high degree of confidence in the measurement accuracy and the measuring procedure of the guarded hot box at the Department of Buildings and Energy has been obtained.

Indoor g-value measurements in a calorimetric test facility (the METSET) mounted in a solar simulator have been investigated and a number of problems regarding these measurements have been identified and (to a certain extent) solved. Procedures for performing the measurements in the METSET have been developed. As the measurements are carried out under conditions different from the defined reference conditions a number of corrections of the measured results must be applied. Procedures for these corrections have been developed and demonstrated. Especially the corrections for differences between the solar simulator spectrum and the reference spectrum draw attention and for some special types of specimens these corrections are still object for further development. For less special types the procedures outlined in this report are considered sufficiently accurate. The g-value as function of incidence angle for three different glazings have been measured in the METSET. The glazings had very different optical properties ranging from almost no spectral selectivity to significant spectral selectivity. However all glazings were clear and their g-values could be calculated using detailed calculation models. This enabled a comparison between measured and calculated g-values assuming that the uncertainty in the calculated values is $\pm 5\%$. An error analysis of the g-value measurements showed that the expected uncertainty for the measured g-value is about 4-10% for the investigated samples. The measured g-values were ranging from 0.29 to 0.75 and the difference between measured and calculated values

were all within the expected uncertainties (max difference 7%). This gives good reason to increase the confidence in the method used to obtain the measured/corrected g-values and shows that the calorimetric measurements - when properly corrected - give meaningful results.

Broadband transmittance values corresponding to solar simulator spectrum and to "real" solar spectrum are in some cases useful data for the correction of g-values measured indoor in the METSET. This is especially true if the sample cannot be characterised by an optical calculation model (e.g. many optically inhomogeneous materials). Therefore an outdoor test facility has been constructed in order to facilitate the measurement of direct solar transmittance of optically inhomogeneous samples under natural solar radiation and under any chosen angle of incidence. The test facility is based on a scanning pyranometer mounted in a tracking device.

Utilising the equipment and the procedures for measurements and data treatment described in this report will in most cases allow a full thermal characterisation of advanced windows and glazings to be carried out by measurements and with good accuracy. As an example of this the thermal and optical properties of a prototypical aerogel glazing have been determined by means of measurements.

Resume

Nærværende rapport beskriver undersøgelser gennemført med henblik på at muliggøre en karakterisering af avancerede vinduer og ruders energimæssige egenskaber ved hjælp af målinger. Vinduers og ruders energimæssige egenskaber er karakteriseret ved to værdier: Varmetransmissionskoefficienten (U-værdien) og den total solenergitransmittans (g-værdien) og der er udført undersøgelser og udvikling af metoder til at bestemme disse to værdier ved hjælp af målinger. Arbejdet har omfattet såvel forbedring af eksisterende måleudstyr og eksisterende målemetoder som udvikling af nyt måleudstyr og nye metoder til at foretage målinger og behandling af data.

Metoder til målinger af vinduers og ruders U-værdi i en guarded hot box er blevet grundigt undersøgt. Der er blevet gennemført analyser af kalibrerings- og måleprocedurer for måling af facadevinduers U-værdi og der er blevet udviklet et nyt forslag til at bestemme tagvinduers U-værdi ved hjælp af guarded hot box målinger. Nøjagtigheden af målinger udført i Institut for Bygninger og Energi's (IBE's) guarded hot box blev undersøgt ved sammenligning med resultater fra målinger i et hot plate apparat og der blev konstateret fremragende overensstemmelse mellem måleresultaterne. Usikkerhedsberegninger viste, at den forventede usikkerhed på U-værdimålingerne er ca 5% for et prøveemne med en U-værdi på $1,75 \text{ W/m}^2\text{K}$. I to ringkalibreringstests blev ialt tre vinduers U-værdi målt på basis af to forskellige kalibreringsrutiner. Vinduernes U-værdier lå mellem $1,1 \text{ W/m}^2\text{K}$ og $2,5 \text{ W/m}^2\text{K}$ og alle rapporterede resultater lå indenfor de forventede usikkerheder på målingerne. Med baggrund i de gennemførte undersøgelser af hot box målinger er der opnået en høj grad af tillid til såvel målenøjagtigheden som måleprocedurerne ved målinger i IBE's guarded hot box.

Måling af g-værdier i en indendørs kalorimetrisk prøvestand (METSET-en) placeret i en solsimulator er blevet grundigt undersøgt og en række problemer er blevet identificeret og (til en vis grad) løst, ligesom der er blevet udviklet procedurer for g-værdimålinger foretaget i METSET-en. Da de indendørs målinger udføres under forhold der er forskellige fra de definerede referenceforhold, skal der udføres en række korrektioner af de direkte målte data og metoder til at foretage disse korrektioner er blevet udviklet og demonstreret. Især korrektioner for spektrale forskelle mellem solsimulatorens og den "rigtige" sols spektra er vigtige og for visse meget specielle prøveemner er de udviklede korrektionsmetoder ikke tilstrækkelige. Yderligere udvikling af korrektionsmodeller er påkrævet. For de fleste prøveemner anses de beskrevne måle- og korrektionsmetoder dog for tilstrækkeligt nøjagtige. For tre ruder er g-værdien som funktion af strålingens indfaldsvinkel blevet målt i METSET-en. De optiske egenskaber for de tre ruder var meget forskellige, gående fra næsten ingen spektral følsomhed til meget markant spektral følsomhed, men alle tre ruder var plane og klare (ikke diffuserende) og deres g-værdier kunne således bestemmes ved hjælp af detaljerede beregningsmodeller. Herved er en sammenligning mellem målte og beregnede g-værdier mulig, idet det er anslået, at usikkerheden på beregningerne er ca 5%. En usikkerhedsanalyse på målingerne af g-værdier resulterede i en forventet

usikkerhed på de kalorimetriske målinger på ca 4-10% for de undersøgte ruder. De målte g-værdier lå i intervallet fra 0,29 til 0,75 og forskellene mellem beregnede og målte g-værdier lå i alle tilfælde indenfor de forventede usikkerheder (maksimal afvigelse var ca 7%). På denne baggrund synes de beskrevne måle- og korrektionsmetoder troværdige og det anses for eftervist, at kalorimetriske målinger - når måldata bliver behørigt korrigeret - giver meningsfulde resultater.

Resultater af integrerede transmittansmålinger for hhv. solsimulator spektrum og "rigtig" solspektrum kan i visse situationer anvendes ved spektrale korrektioner af g-værdier målt indendørs i METSET-en. Dette gælder især, hvis prøveemnet ikke kan beskrives termisk og optisk ved hjælp af en beregningsmodel (gælder f.x. mange optisk inhomogene materialer) eller hvis den spektrale fordeling af solsimulatorens stråling er usikker. Derfor er der konstrueret en udendørs måleopstilling til måling af den direkte soltransmittans. Opstillingen består af et skannende pyranometer monteret i en soltracker og muliggør måling af soltransmittansen for optisk inhomogene prøveemner under naturlig solstråling og under en vilkårlig indfaldsvinkel.

Ved at anvende det udstyr og de måle- og korrektionsmetoder, der er beskrevet i rapporten kan de fleste avancerede vinduer og ruder karakteriseres rimeligt præcist med hensyn til deres energimæssige ydeevne ved hjælp af målinger. Som eksempel på dette er de optiske og termiske karakteristika for fire aerogel prototype ruder bestemt ved hjælp af målinger.

1 Introduction

1.1 Aim of the project

The aim of the project was to enable a energy performance characterisation of advanced windows and glazing systems based on physical measurements and to gain confidence in the results. Energy performance of conventional windows and glazing systems can often be characterised by calculations. However as new materials, new designs and new applications are introduced in the production of windows the calculation models have to be modified, be expanded, be renewed or sometimes even given up. In the process of verifying existing or new calculation methods and in the process of characterising complex constructions that cannot be modelled results from measurements are essential.

Two key parameters describe the energy performance of windows: the thermal transmittance and the total solar energy transmittance of the window and the focus of the study has been on the development of the appropriate methods to quantify these two key parameters for advanced windows and glazings by means of measurements.

1.2 Methods

The working process of the project has involved:

- improvement of existing measuring equipment
- development and construction of new measuring equipment
- development of procedures for the measurements
- development of procedures for the treatment of data obtained from the measurements.

The methods developed in this study have been tested against

- measurements carried out in other laboratories using equipment designed to obtain the same results but not necessarily applying the same methods.
- calculations where these are considered being well documented and reliable.

In the latter case it may seem odd that measurements are being “verified” against calculations. However in the case of measurements of the total solar energy transmittance this can be accepted as long as comparisons between measurements and calculations are performed on samples that can be described by well documented theory.

The interlaboratory comparisons have been carried out by participation in the framework of IEA SHCP Task 18, in ISO/CEN working groups and in a Nordic co-operation funded by NORDTEST.

For especially the measurement of the total solar energy transmittance the work on the development of measuring procedures and data treatment cannot be considered concluded. However a number of significant problems have been identified and overcome and it has been demonstrated that measurements with good accuracy seems obtainable.

2 Background

During the last decades increasing interest has been shown to the thermal performance of buildings. The background for this interest is of course the fact that a high energy consumption in general has large negative effects on the environment and on the consumption of fossil fuels. A general reduction of the energy consumption is a very important step towards a sustainable energy situation and large improvements in the thermal insulation of buildings have been carried out. The building code in Denmark and in most other countries demands a certain level of thermal insulation of buildings. The demands for a high level of insulation has to cover all parts of the building including the windows. In the 1995 Danish building code (Bygningsreglement 1995) the maximum thermal transmittance of a window has been reduced to $1.8 \text{ W/m}^2\text{K}$ and though this represents a significant improvement of the thermal performance of windows the maximum U-value for windows is still at least six times the maximum U-value for an outer wall ($0.2 - 0.3 \text{ W/m}^2\text{K}$). Even though the windows represent a relatively small part of the building envelope, the impact of windows on the thermal performance of buildings is relatively large.

A very important factor in the heat balance of a window is the utilisation of solar radiation. The window is the only part of the building envelope that significantly can benefit from the sun, letting a large amount of the solar radiation penetrate into the building and in this way acting as a passive solar device. Indeed a high solar gain in combination with a low U-value can result in a window that gives a positive contribution to the energy balance in a house, i.e. instead of losing energy through the window in the heating season it is possible to achieve a net energy gain through the window. It is evident that the solar gain can have a very important impact on the net heating consumption in houses (Hutchins et al.) and the effect of solar gain will certainly be taken more into account in the near future. This is already taking place in several countries by means of window energy rating systems (USA, Canada, Australia) and a similar system has recently (2000) been introduced in Denmark.

In order to meet the increased demands to the thermal and optical performance of windows considerable development of highly insulating glazing and frame systems has taken place during the last decades and is still in progress. A number of new designs and materials have appeared on the market and it is very important to carry out optical and thermal characterisation of these. Some of the optical and thermal characterisations can be carried out by means of calculations but in many cases new designs and new materials (e.g. glazings with incorporated venetian blinds, vacuum glazings, glazings incorporation transparent insulation materials etc.) are not covered by standard calculation methods. In these cases the characterisation has to be supported by measurements. The measurements also play a very important role in the validation of new and existing calculation models.

A characterisation of fenestration products with respect to energy performance is very important for the following reasons:

- Windows have a major impact on the heat balance of buildings and on the indoor climate.
- A significant development in the thermal performance of windows has taken place over the last decades and is still continuing.
- Thermal and optical characterisations are important for the further development of high performance windows.
- Thermal and optical performances are a part of the product description, the energy rating and the competition parameters for windows.
- Thermal and optical performance data of windows are basic input to building energy simulation tools.

The present project has its main focus on the development and use of methods to characterise the thermal performance of windows by means of measurements. These measurements serve several purposes:

- To validate calculation models and programs
- To give input data to calculation models
- To characterise window types that are not covered by any standard calculation method
- To facilitate the further development of better performing windows and materials for window applications such as low emissivity coatings, transparent insulation materials, reflection free glass types etc.

3 Fundamental properties

In this chapter the definitions concerning the thermal transmittance, the solar transmittance and the total solar energy transmittance for a window or a glazing are given.

3.1 General

A window allows energy to pass in two different ways:

1. Transmittance of solar energy through the window
2. Heat transfer through the window caused by a temperature difference between the interior and the exterior environment.

The two energy flows may be in the same direction or the opposite depending on the conditions. During the heating season - which is the most interesting for residential buildings under Danish conditions - they will typically be opposite directed.

In order to describe the thermal properties of a window it is convenient to characterise the energy flows caused by solar energy and by temperature difference separately. The net energy gain of a window can be written as:

$$Q_{net} = Q_{solar} - Q_{\Delta T} \quad (3-1)$$

where Q_{solar} is the heat flow into the building caused by solar radiation on the window and $Q_{\Delta T}$ is the heat flow through the window caused by a temperature difference over the window. In order to minimise the energy consumption for heating Q_{solar} should be as large and $Q_{\Delta T}$ as small as possible preferably letting the window act as energy supplier instead of energy user during the heating season. This is possible for windows already on the market today as long as the windows are orientated southerly. The property that characterises the window with respect to solar energy gain is called the total solar energy transmittance or g-value of the window. The energy flow through the window caused by a temperature difference between inside and outside environment is characterised by the thermal transmittance or U-value of the window.

A convenient way of describing the net heat gain per unit area q_{net} through a window under steady state is:

$$q_{net} = g \cdot G - U \cdot \Delta T_n \quad (3-2)$$

where g is the total solar energy transmittance, G is the solar radiation level, U is the thermal transmittance of the window under the actual conditions but without solar

radiation and ΔT_n is the temperature difference between the inside and the outside environment.

3.2 Thermal transmittance, U-value

The thermal transmittance of a window here denoted the U_w -value is the most common energy performance parameter. The U_w -value can be derived from the knowledge of the U-value of each part of the window construction: glazing, edge and frame. The U_w -value is found by a weighting of the individual U-values. The weighting can be carried out in several ways.

In North America the following approach is being used (see figure 3.1) (ASHRAE Standard 142P):

$$U_{w,US} = \frac{U_{center} A_{center} + U_{edge} A_{edge} + U_{frame} A_{frame}}{A_w} \quad (3-3)$$

where U_{center} is the thermal transmittance of the glazing center. [W/m²K]
 A_{center} is the area of the glazing center
 U_{edge} is the thermal transmittance of the glazing edge (the area from the frame and 63.5 mm towards the center of glazing). [W/m²K]
 A_{edge} is the edge area [m²] [W/m²K]
 U_{frame} is the thermal transmittance of the frame. [W/m²K]
 A_{frame} is the projected area of the frame [m²]
 A_w is the projected area of the window [m²]

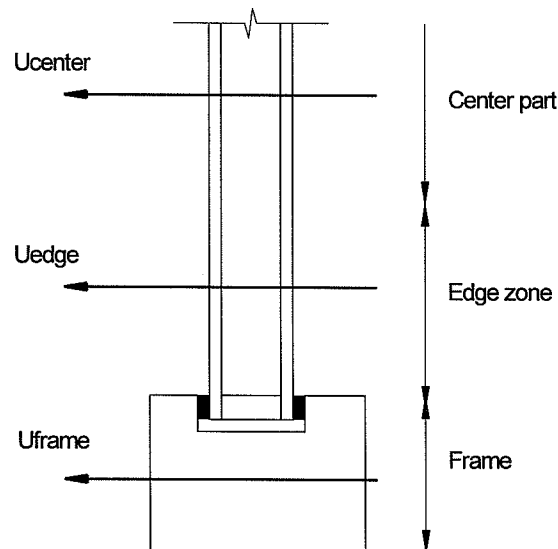


Figure 3.1 North American division of the window into areas of center, edge and frame.

In CEN-standards and draft standards (ex. EN10077-1) a different approach is used and this approach is also implemented in the Danish building code (by DS418, annex no.1) (see figure 3.2):

$$U_{w,CEN} = \frac{U_{center} A_g + U_{frame} A_{frame} + l_g \psi_g}{A_w} \quad (3-4)$$

where A_g is the glazing area [m^2]
 l_g is the glazing perimeter [m]
 ψ_g is the linear thermal transmittance due to the combined thermal effects of glazing, spacer and frame [W/mK]

Here l_g denotes the perimeter of the visible part of the glazing and ψ_g denotes the linear thermal transmittance that arises from the combined thermal effects of the spacer and the assembling details of the frame. ψ_g describes the thermal transmittance through the edge of glazing per meter of glazing perimeter and gives a quantification of the impact that the thermal bridge in the edge of glazing has on the thermal transmittance of the window.

The individual U-values and the ψ -value can be found either from literature and relevant standards, by use of simulation tools or by measurements.

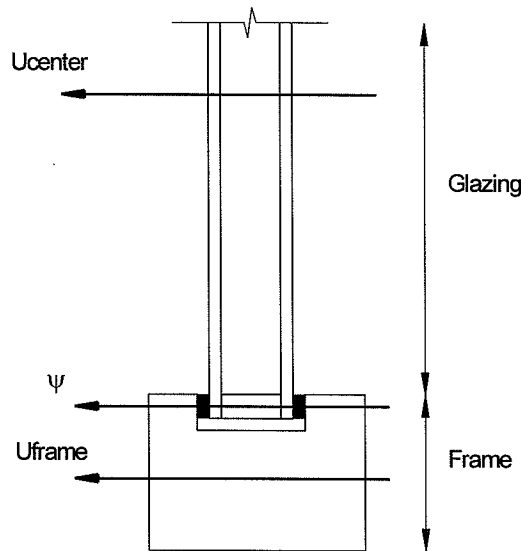


Figure 3.2 CEN division of the window into areas of glazing and frame.

3.3 Solar direct transmittance, τ_e

The solar direct transmittance of a glazing is defined as the ratio between solar radiation flux after and before the solar radiation has passed the glazing. The solar direct transmittance is the result of reflection, absorption and transmission in the glass. In figure 3.3 is shown the transmission of solar radiation in one sheet of glass.

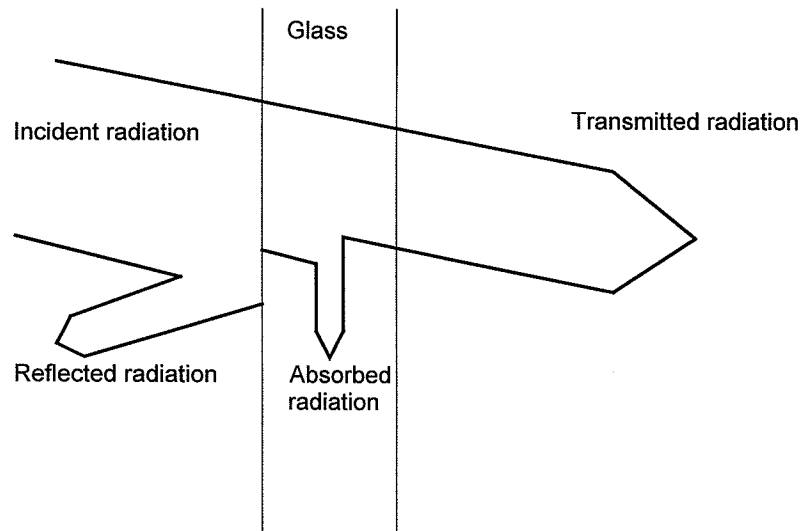


Figure 3.3 Radiation through glass sheet

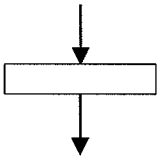
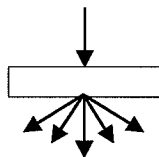
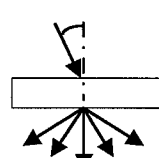
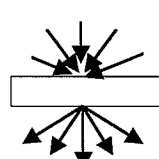
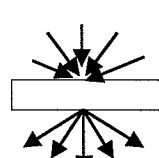
The amount of reflected, absorbed and transmitted radiation depends on the glass type and is characterised by the reflectance (ρ_e), absorptance (α_e) and transmittance (τ_e) of the glazing. Indices 'e' refer to optical properties for standard solar radiation. The relation between the three coefficients is:

$$\alpha_e + \rho_e + \tau_e = 1 \quad (3-5)$$

The solar direct transmittance is referred to a standard spectral distribution of solar radiation as laid down in CEN and ISO documents (EN 410 and ISO 9050).

For the further work with optical properties it is convenient to describe a number of definitions for different cases: (Hutchins et al.) Please note that the symbols for hemispherical-hemispherical and diffuse-hemispherical transmittances are identical. The difference between the two numbers is obtained by excluding all beam radiation in the diffuse-hemispherical transmittance, whereas in the hemispherical-hemispherical transmittance all radiation (beam and diffuse) is included.

Table 3.1 Definition of optical properties (Hutchins et al.)
Similar definitions apply for reflectance properties.

Sketch	Optical property
	τ^{nn} normal-normal transmittance
	τ^{nh} normal-hemispherical transmittance
	τ^{dh} directional-hemispherical transmittance
	τ^{hh} hemispherical-hemispherical transmittance
	τ^{dif-h} diffuse-hemispherical transmittance

3.4 Total solar energy transmittance, g-value

The total solar energy transmittance is also known as the g-value or the solar heat gain coefficient and describes the ratio between the total amount of solar energy that is transmitted through a component and the amount of solar energy that reaches the surface of the component. The total solar energy transmittance of a component consists of two parts:

$$g = \tau_e + q_i \quad (3-6)$$

where τ_e is the direct solar transmittance

q_i is the secondary heat transfer of the glazing towards the inside.

The direct solar transmittance is described in section 3.3. The secondary heat transfer towards the inside, q_i , arises from absorption of solar radiation in the component. The solar radiation that is absorbed in the component is transferred to the ambient by convection and IR-radiation. The secondary heat transfer towards the inside and outside is called q_i and q_o respectively and under steady state their sum equals the absorptance α_e of the component. In figure 3.4 is shown a sketch describing the total solar energy transmittance of a double glazed unit.

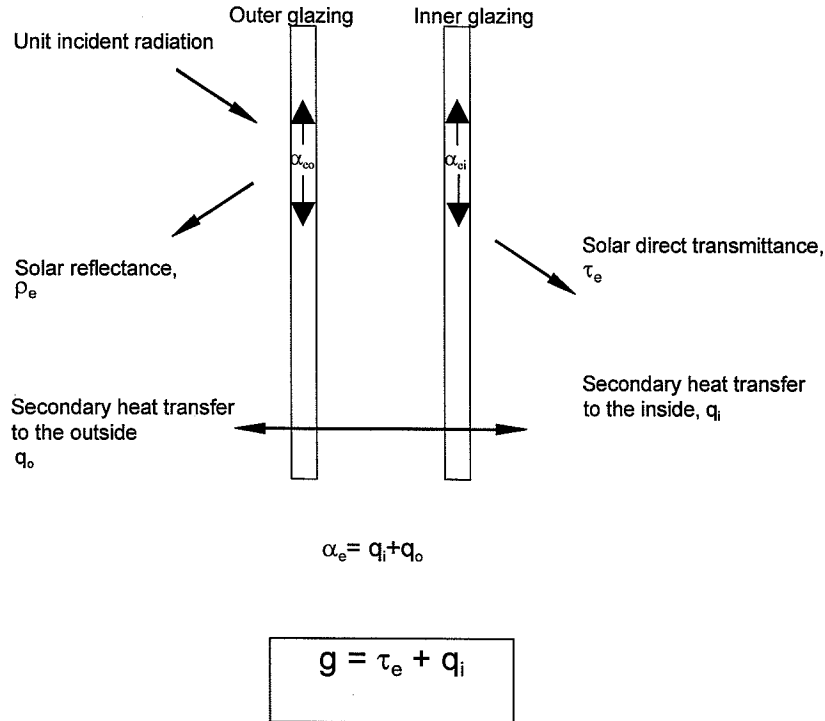


Figure 3.4 Total solar energy transmittance of a double glazed unit.

The ratio between q_i and q_o depends on the thermal resistance from each glazing layer to the inside and outside respectively. For a double glazed unit q_i can be calculated using the following expression (ISO 9050):

$$q_i = \left(\frac{\alpha_{eo} + \alpha_{ei}}{h_e} + \alpha_{ei} R_g \right) / \left(\frac{1}{h_i} + \frac{1}{h_e} + R_g \right) \quad (3-7)$$

where q_i is the the secondary heat transfer factor of the glazing towards the inside. q_i is non dimensional
 α_{eo} is the solar absorptance of the outer glass
 α_{ei} is the solar absorptance of the inner glass
 R_g is the thermal resistance between the inner and outer glass [$\text{m}^2\text{K}/\text{W}$]
 h_e is the heat transfer coefficient from the outer glazing to the outside [$\text{W}/\text{m}^2\text{K}$]
 h_i is the heat transfer coefficient from the inner glazing to the inside [$\text{W}/\text{m}^2\text{K}$]

The absorption of solar radiation is considered uniformly distributed in the glazing elements and the thermal resistance of the glass panes is neglected. The values of α_{eo} and α_{ei} include multiple reflection between the two glass panes.

4 Calculation methods

4.1 General

In many cases the thermal and optical properties of building components can be found by means of different calculation methods. This is especially true for many common windows already on the market and a number of calculation methods are covered by international standards and draft standards. Though detailed description of calculation of thermal and optical properties are outside the scope of this study some few aspects in the field of transmission of solar radiation in glazing will be described shortly. Main focus is on the present international standards with relatively simple models. The main reason for including these aspects is that some of the simple calculation methods will be useful for the treatment and correction of measured data for measurements of total solar energy transmittance described in chapter 6.

4.2 Solar transmittance in a multilayer glazing

The transmittance, reflectance and absorptance of a transparent material can be found from basic material data, extinction coefficient and refractive index (ex. Duffie, J.A.; Beckmann, W.A., 1991). Especially the refractive index is dependent on the spectral distribution of the incoming radiation. For many transparent materials the refractive index is known for sun light but when two or more panes are combined in a glazing the spectral distribution of the radiation will change each time it passes through a pane and the refractive index of pane no 2, 3, etc. will no longer be known. The change in spectral distribution is very dependent on the material the radiation passes through. Almost no change takes place when the material is low iron glass and a significant change takes place for glass with low emissivity coating. In figure 4.1 is shown two examples of the spectral transmittance of glass.

The solar direct transmittance at normal incidence can be calculated for a clear glazing in accordance to standard documents, (ISO 9050, EN 410). To perform this calculation the spectral reflectance $\rho(\lambda)$ and spectral transmittance $\tau(\lambda)$ in the wavelength range from 300 to 2500 nm must be available for each transparent element in the glazing.

For each wavelength the intensity of transmitted radiation is found as the product of the spectral transmittance of the glazing ($\tau_g(\lambda)$) and the radiation intensity at the specific wavelength. The energy intensity transmitted through the glazing for the solar spectrum is found by integrating the product over the solar spectrum.

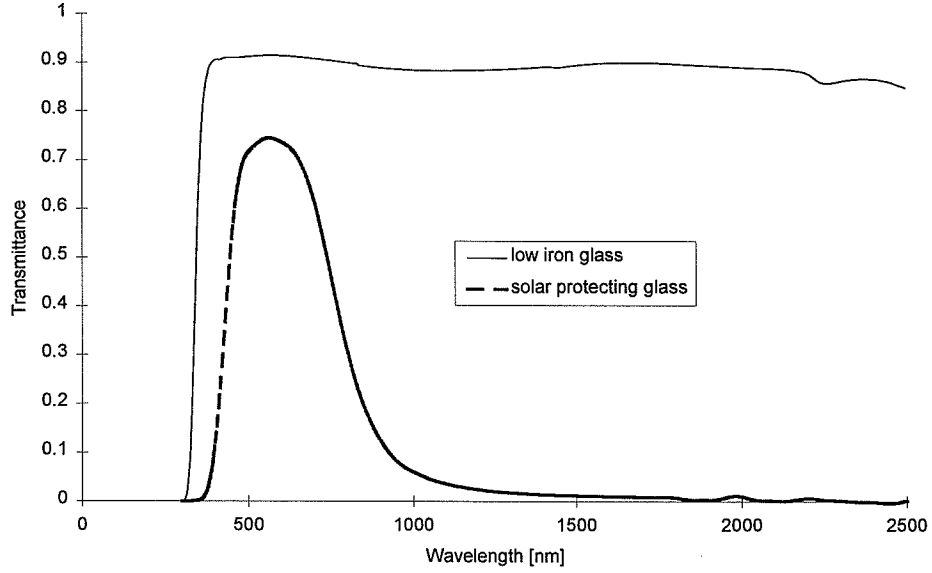


Figure 4.1 Spectral transmittance of two types of glass: glass with low content of iron oxide and float glass with solar protecting low emissivity coating.

The direct solar transmittance is found from the following expression (EN 410):

$$\tau_e = \frac{\int_{\lambda=0}^{\infty} (S_{\lambda} \cdot \tau_g(\lambda)) d\lambda}{\int_{\lambda=0}^{\infty} S_{\lambda} d\lambda} \quad (4-1)$$

where S_{λ} is the spectral distribution of the solar radiation
 $\tau_g(\lambda)$ is the spectral transmittance of the complete glazing.

For convenience equation 4-1 may be written as:

$$\tau_e = \frac{\sum_{\lambda=300}^{2500} S_{\lambda} \cdot \tau_g(\lambda) \cdot \Delta\lambda}{\sum_{\lambda=300}^{2500} S_{\lambda} \cdot \Delta\lambda} \quad (4-2)$$

where $\Delta\lambda$ is the wavelength step.

For double glazing units $\tau_g(\lambda)$ can be found from:

$$\tau_g(\lambda) = \frac{\tau_1(\lambda) \cdot \tau_2(\lambda)}{1 - \rho_1^b(\lambda) \cdot \rho_2(\lambda)} \quad (4-3)$$

where $\tau_1(\lambda)$ and $\tau_2(\lambda)$ are the spectral transmittance of outer and inner layer
 $\rho_1^b(\lambda)$ is the spectral reflectance of the backside of the outer layer
 $\rho_2(\lambda)$ is the spectral reflectance of the frontside of the inner layer.

The terms outer and inner is used under the assumption that the solar radiation travels from the outside to the inside. The expression for the spectral transmittance of a glazing can be expanded to three or more layers (ISO/FDIS 15099, ISO 9050, EN 410).

The spectral distribution of the solar radiation can be chosen from different sources; (Moon, P.1940; ASTM, ISO, CEN). In this study the solar curve presented in EN 410, Air Mass 1.0 Global will be chosen as reference spectrum. It is no problem to use a different spectrum as long as relevant data are available. Air Mass 1.0 is an expression telling how much atmosphere the beam solar radiation actually travels through in comparison to a path through the atmosphere perpendicular to the Earth.

4.3 Total solar energy transmittance

The g-value can be calculated after two different approaches:

- As part of an energy balance where the g-value is calculated for a fixed set of boundary conditions regardless of actual temperatures in the glazing. This approach is used in ISO 9050 and EN 410 and is in the following named “separate calculation of g”.
- As part of the resulting energy balance of a glazing exposed to actual solar radiation and bounding air temperatures.

The first approach is rather simple and may be carried out by using spread sheet calculations or simple computer code. However the resulting g-value is based on fixed “dark” properties of the glazing and does not include the effects of actual boundary conditions changing the thermal resistance network in the glazing.

The latter approach is more detailed and takes into account the actual temperatures of the glazing corresponding to different bounding temperatures and different levels of solar radiation. The method requires computer calculations as can be performed in WIS, WINDOW4.1 and other detailed calculation programs.

The two approaches result in different values – a short discussion of this is given later in this chapter.

4.3.1 Separate calculation of g

The separate calculation of g is convenient in many cases and the method gives a useful aid to the corrections of measured values that will be described in chapter 6.

In this calculation the g-value is defined as:

$$g = \tau_e + q_i \quad (4-4)$$

The solar direct transmittance, τ_e is found in accordance to section 4.2 or - in the case of a single glass sample - from basic material data of the glass. To calculate the secondary heat flow to the inside, q_{i1} , the amount of solar radiation absorbed in the panes has to be known along with the thermal resistances of each element in the glazing. That means that the thermal resistance of each pane and of each gap in the glazing must be known as well as the surface thermal resistances from the glazing to the exterior and interior respectively.

In figure 4.2 is shown a glazing with three glass layers. The amount of solar radiation absorbed in layer no 2 that is passed on to the interior depends on the ratio of the thermal resistance from layer 2 to the exterior and the total resistance of the glazing.

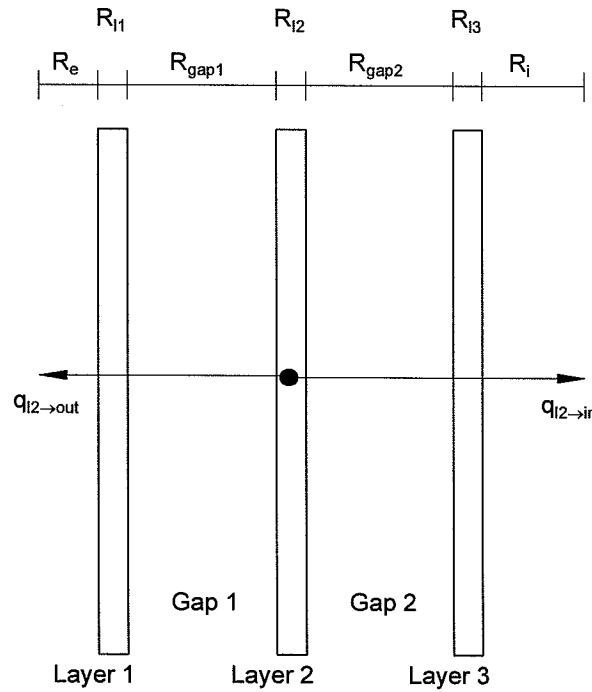


Figure 4.2 Division of absorbed radiation in layer 2 to the interior and exterior.

The fraction of energy first absorbed in layer 2 and subsequently transferred from layer 2 to the inside environment can be written as:

$$q_{I2 \rightarrow in} = \alpha_{e2} \frac{R_{out}}{R_{total}} \quad (4-5)$$

where α_{e2} is the solar absorptance in layer 2 including effects of reflection
 R_{out} is the thermal resistance from the absorption-location to the

exterior [W/m²K]
 R_{total} is the total thermal resistance of the glazing including surface resistances [W/m²K]

Similar considerations can be made for all layers in the glazing and q_i and q_o respectively can be found as:

$$q_i = q_{l1 \rightarrow in} + q_{l2 \rightarrow in} + q_{l3 \rightarrow in} \quad (4-6)$$

$$q_o = q_{l1 \rightarrow out} + q_{l2 \rightarrow out} + q_{l3 \rightarrow out} \quad (4-7)$$

The ratio between q_o and q_i depends on the thermal resistance from each glazing layer to the inside and outside respectively. For a double glazed unit q_i can be calculated using following expression (EN 410) (eq. 3-7 rewritten):

$$q_i = \frac{\alpha_{e1} \cdot R_e + \alpha_{e2} \cdot (R_e + R_g)}{R_e + R_g + R_i} \quad (4-8)$$

where q_i is the secondary heat transfer factor of the glazing towards the inside
 α_{e1} is the solar absorptance of the outer glass
 α_{e2} is the solar absorptance of the inner glass
 R_g is the surface to surface thermal resistance of the glazing [m²K/W]
 R_e is the thermal resistance from the outer glazing surface to the outside [m²K/W]
 R_i is the thermal resistance from the inner glazing surface to the inside [m²K/W]

The solar absorptances α_{e1} and α_{e2} can be found as the total solar absorptance in each layer including the effects of reflection between the layers in the glazing. For a double glazed unit the following expressions are valid (EN 410):

$$\alpha_{e1} = \frac{\sum_{\lambda=300}^{2500} S_{\lambda} \left(\alpha_1(\lambda) + \frac{\alpha_1^b(\lambda) \cdot \tau_1(\lambda) \cdot \rho_2(\lambda)}{1 - \rho_1^b(\lambda) \cdot \rho_2(\lambda)} \right) \Delta\lambda}{\sum_{\lambda=300}^{2500} S_{\lambda} \cdot \Delta\lambda} \quad (4-9)$$

$$\alpha_{e2} = \frac{\sum_{\lambda=300}^{2500} S_{\lambda} \left(\frac{\alpha_2(\lambda) \cdot \tau_1(\lambda)}{1 - \rho_1^b(\lambda) \cdot \rho_2(\lambda)} \right) \Delta\lambda}{\sum_{\lambda=300}^{2500} S_{\lambda} \cdot \Delta\lambda} \quad (4-10)$$

The equations 4-9 and 4-10 can be expanded to three or more layers in the glazing unit.

In the CEN document the following boundary conditions are fixed:

Table 4.1 Boundary conditions for EN 410

Property		
Outside glass surface temperature	2.5	°C
Inside glass surface temperature	17.5	°C
Mean temperature of gas space	10	°C
Outside heat transfer coefficient	23	W/m ² K
Inside heat transfer coefficient	8	W/m ² K
Radiation level	not included	

4.3.2 Determination of U and g by heat balance calculation

As mentioned in section 3.1 the net energy gain per unit area of a glazing can be described as $q_{net} = g \cdot G - U \cdot \Delta T_n$. The values g and U are depending on the boundary conditions under which the glazing is in operation. However most building simulation tools regard the two values as constant and the CEN standards EN410 and EN673 define the values for one specific set of boundary conditions. In this section the error introduced by using fixed values of g and U will be discussed.

In order to determine the g-value in a manner corresponding to the real conditions a detailed energy balance calculation of the glazing under specific boundary conditions must be carried out. To do this rather detailed energy balance equations of each element in the glazing must be set up in order to find the resulting temperatures of the elements.

The g-value is calculated in two steps: First the energy balance for the glazing is calculated for “dark” conditions (no solar radiation) and for the chosen pair of bounding temperatures - the result is the net energy flow $q_{net,dark}$. ($q_{net,dark}$ equals $U \cdot \Delta T_n$, where ΔT_n is the difference between the bounding environmental temperatures). Next the calculation is repeated with the same bounding temperatures but this time with a specific level of solar radiation, resulting in the net energy flow through the glazing for “solar” conditions ($q_{net,solar}$). In this calculation the effect of solar absorption in the panes is included. The g-value is now found as:

$$g = \frac{q_{net,solar} - q_{net,dark}}{G} \quad (4-11)$$

This procedure is different from the ISO 9050 and EN 410 procedure as a fixed set of boundary conditions is applied here and energy properties of the glazings are determined regardless of level of absorption of radiation.

The discrepancy in the g-values calculated according to the two different methods depends on the sample as well as the “real” boundary conditions. The discrepancy is related to the quantity of q_i as the solar transmittance part of the g-value is independent of temperature conditions. A glazing with a large value of q_i will be more sensitive to variations in the temperature or radiation level than samples with small values of q_i . To illustrate this U and g-values of three different glazings have been determined using the two different methods described above (called the “CEN approach” and the “detailed energy balance approach”). The calculations have been carried out in the WIS program. The glazings are designed to illustrate the impact of the calculation method on the calculated energy balance. The key properties of the glazings are shown in table 4.2.

Table 4.2 Key properties of three glazings.

No.	Outer pane	Inner pane	α_{e1}	α_{e2}	U W/m ² K	g	$\tau_{e,glazing}$	$\alpha_{e,glazing}$
1	Solar control	Float	0.33	0.07	~1.1	~0.4	0.34	0.36
2	Solar control	Float	0.78	0.09	~2.5	~0.2	0.12	0.79
3	Float	Low-e	0.07	0.13	~1.3	~0.7	0.58	0.18

For the “CEN-approach” the boundary conditions listed in table 4.1 have been applied. For the “detailed energy balance approach” two pairs of bounding temperatures have been chosen (temperature of outside environment/inside environment -10/20°C and 0/20°C respectively). For each of the temperature pairs the level of solar radiation has been varied between 100 W/m² and 1000 W/m². This gives a total of eight boundary conditions for each glazing, see table 4.3.

Table 4.3 Boundary conditions for detailed energy balance calculations

Property		
Inside air temperature	20	°C
Inside radiation temperature	20	°C
Inside convection coefficient	3	W/m ² K
Inside radiation coefficient	Calculated	
Outside air temperature	-10/0	°C
Outside radiation temperature	-10/0	°C
Outside convection coefficient	15	W/m ² K
Outside radiation coefficient	Calculated	
Solar irradiation level	100/250/500/1000	W/m ²

The resulting U and g-values are shown in Table 4.4. The U-values in table 4.4 are all calculated for “dark” conditions. For each glazing three different values are

obtained, depending on the temperature conditions. In the CEN calculation the thermal resistance of a glazing is determined from surface to surface and a standard surface heat resistance of $0.17 \text{ m}^2\text{K/W}$ is subsequently added to give the thermal resistance from inside to outside environment. In the detailed calculation the thermal resistance of the glazing is calculated from inside to outside environment and the surface heat resistance is part of this calculation. The convective part is considered constant and the radiative part is calculated, see table 4.3. That means that in the detailed calculation R_i and R_e depend on the surface temperatures of the glazing and hereby also on the U value of the glazing. The different handling of surface heat transfer has a relatively large impact on glazings with high U -values. Apart from the different surface heat resistances the mean temperatures of the glazings are different for the three sets of “dark” boundary conditions.

Table 4.4 U and g-values for three glazings calculated according to the “CEN approach” and “detailed energy balance approach”. Boundary conditions are shown as exterior environmental temperature/internal environmental temperature/irradiation level.

Calculation method	Boundary condition $T_{\text{ne}}/T_{\text{ni}}/G$	Glazing no 1		Glazing no 2		Glazing no 3	
		U	g	U	g	U	g
EN410/673	Table 4.1	1.061	0.366	2.620	0.226	1.287	0.678
Detailed energy balance	-10/20/0	1.186	-	2.430	-	1.363	-
	-10/20/100	1.186	0.375	2.430	0.232	1.363	0.672
	-10/20/250	1.186	0.375	2.430	0.232	1.363	0.672
	-10/20/500	1.186	0.374	2.430	0.234	1.363	0.672
	-10/20/1000	1.186	0.372	2.430	0.238	1.363	0.672
Detailed energy balance	0/20/0	1.067	-	2.497	-	1.268	-
	0/20/100	1.067	0.372	2.497	0.234	1.268	0.673
	0/20/250	1.067	0.372	2.497	0.235	1.268	0.673
	0/20/500	1.067	0.369	2.497	0.237	1.268	0.673
	0/20/1000	1.067	0.367	2.497	0.242	1.268	0.673
	$^{\circ}\text{C}/^{\circ}\text{C}/\text{Wm}^{-2}$	$\text{W}/\text{m}^2\text{K}$	-	$\text{W}/\text{m}^2\text{K}$	-	$\text{W}/\text{m}^2\text{K}$	-

The net gain for the three glazings obtained for the boundary conditions listed in table 4.3 are shown in the graphs in figure 4.3. The net gains are found both according to the CEN approach and by means of detailed energy balance calculations. Net gains are shown on the primary y axis and on the secondary y axis is shown the difference in net energy gain obtained according to the two methods.

The calculation method has minor influence on the net energy gain for glazing no. 1 and 3 but significant influence for the highly absorbing glazing no 2, where relative difference up to more than 12% is found. In other words:

The boundary conditions influence the U and g -values and the impact of this on the energy balance may be significant.

Using constant values for g and U is a simplification that may be acceptable for “ordinary” glazings with low U -values and relatively low solar absorptance but may lead to significant errors in the calculated energy gain for glazings with large solar absorptance.

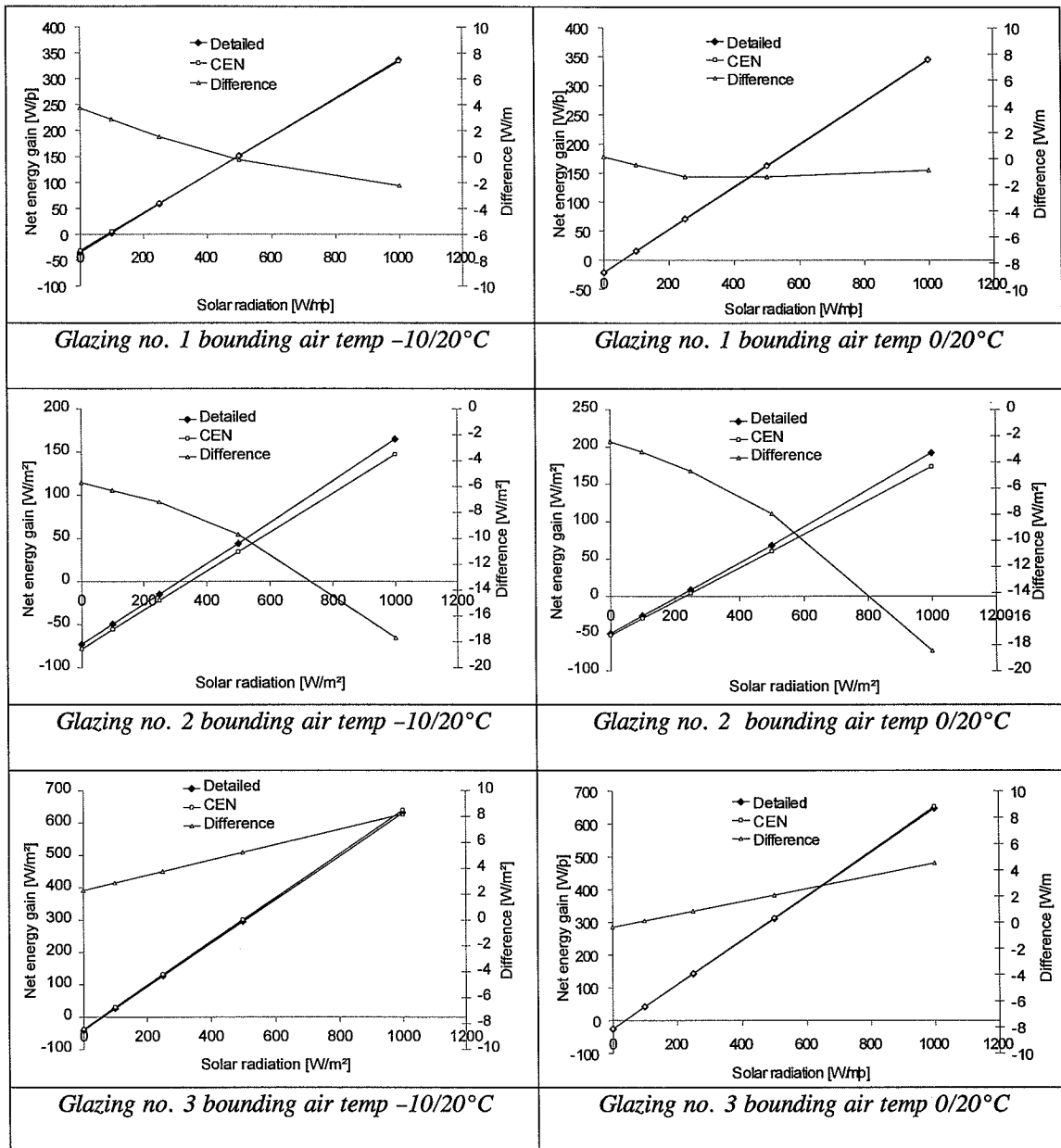


Figure 4.3. Net energy gain calculated respectively according to EN410/673 and by means of detailed energy balance (WIS). On the secondary y axis is shown the difference in energy gain obtained by the two methods.

5 Measurement of thermal transmittance, U-value

Abstract

Measurement of thermal transmittance of windows and other building components can be considered as a more or less standardised process. However experience has shown that the old standard measuring methods for windows lead to non-uniform results when identical windows are measured at different laboratories (Williams, R.). Thus new measuring procedures have been requested. Work on this field has been conducted within ISO and CEN working groups and The Department of Buildings and Energy is participating in this work. In this chapter the work carried out within this study is described concerning:

- development of measuring techniques
- update of measuring equipment
- uncertainty analysis
- investigations of the reliability of the measuring equipment by comparison with other reference (hot plate device)
- investigation of the reliability of the measuring techniques by inter laboratory comparisons of U-value measurements performed on identical windows
- comparison of calculated and measured values

A main result of the investigations is a high degree of confidence in the measuring equipment at the Department of Buildings and Energy as well as in the measuring procedures in general.

5.1 General

As previously mentioned it is in many cases possible to obtain the thermal properties of common marketed window products by means of calculations and a number of calculation methods are covered by international standards and draft standards (e.g. EN 673, prEN 10077, ISO/FDIS 15099). However when new materials, new designs and new applications are introduced in the window production the calculation models are not always adequate. In the process of verifying existing or new calculation methods and in the process of characterising complex constructions that cannot be simulated, results from measurements are essential. In this section the work carried out concerning development of methods for measuring the thermal transmittance of windows will be described. The work has been focused on measurements of thermal transmittance of glazings and windows with an emphasis on the development of the measuring technique and the measuring device.

5.2 Measurement of thermal transmittance and thermal resistance

For samples with no or little thermal inhomogeneities and with flat and parallel surfaces the thermal resistance can be measured by means of a hot-plate apparatus. By adding the surface thermal resistances (usually a total of $0.17 \text{ m}^2\text{K/W}$) to the measured component resistance the U-value is found as the inverted sum. Hot plate devices are covered by international standards (ISO8301, ISO8302) and are usually designed for a specimen size $< 1 \times 1 \text{ m}$. Measurements in a hot plate devices can be carried out with very good accuracy (usually an accuracy within $\pm 2\%$ can be obtained (ISO8301, ISO8302)) but the limitations in sample size and especially the demands for homogeneous samples with flat and parallel surfaces makes the hot plate devices unsuited for measurements on windows. For large inhomogeneous samples like windows and most other building components the thermal transmittance can be determined by means of the hot box methods. Two types of hot box devices are covered by international standards: Calibrated hot box and guarded hot box. Only the guarded hot box will be treated here.

5.3 Guarded hot box

In figure 5.1 is shown a sketch of the guarded hot box apparatus that is used at the Department of Civil Engineering for measurements on glazings and windows and in figure 5.2 is shown a photograph of the apparatus. The investigated sample is mounted in a surround panel between a warm side and a cold side. Standard sample size is $1.23 \times 1.48 \text{ m}$. The warm side is divided into two chambers, the metering box and the guard box. The metering box covers the aperture (with the sample) in the surround panel and by means of a heater in the metering box the temperature here is kept constant and the energy flow emitted by the heater is recorded. The temperature in the guard box is controlled in order to obtain a zero temperature difference across the metering box walls. Now all the energy delivered to the metering box is flowing through the specimen and through the surround panel to the cold side, where the temperature is kept at a constant (low) level. Fans on the cold side induce a controllable air flow across the specimen surface allowing a specific total surface thermal resistance to be obtained. Both the energy flow through the surround panel and the correct air flow across the specimen can be found from calibration measurements, see sections 5.4, 5.5 and 5.6.

Determination of thermal transmittance of inhomogeneous components is in general covered by the international standard ISO 8990. In this standard the general procedure for the operation of a hot box device is described together with some general requirements that a hot box apparatus must meet. However the standard is very general and working groups within the frame work of ISO (TC 163, SC 1, WG 14) and CEN (TC 89, WG 7) are elaborating procedures and guidelines with the scope of giving specific guidelines for the operation of hot boxes for U-value measurements on windows and doors (ISO 12567 and prEN 12412).

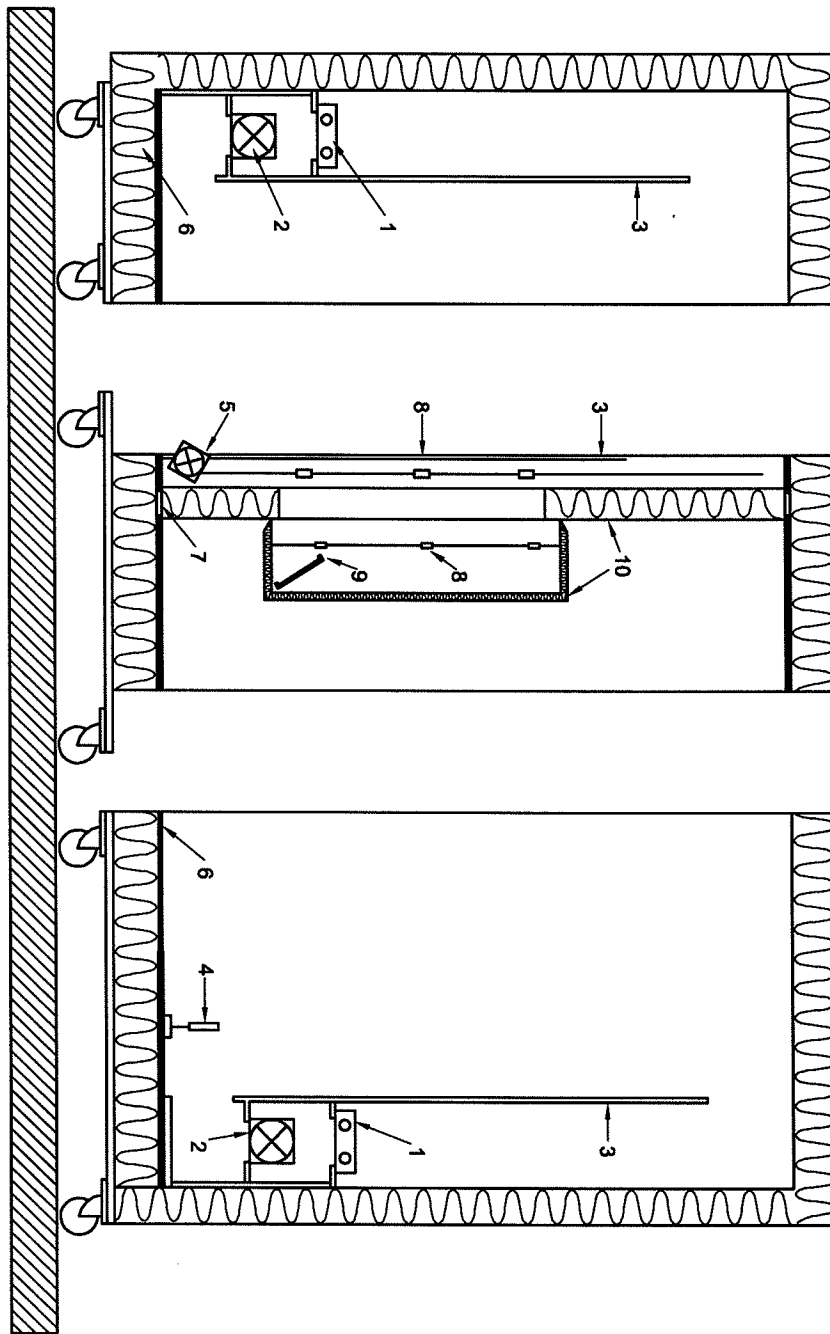


Figure 5.1 Sketch of the Guarded hot box at the Department of Buildings and Energy.

1: Cooling element. 2: Fan. 3: Baffle. 4: Guard box air temperature sensor. 5: Cold side wind simulator. 6: Sandwich element with polyurethane core. 7: Thermal break. 8: Air temperature sensors (warm and cold side). 9: Electrical heater in metering box. 10: Polystyrene (surround panel and metering box walls).

Maximum sample size (w x h): 1250 x 1500 mm. Surround panel thickness 170 mm (150 mm polystyrene + 20 mm plywood on cold side). Metering box aperture (w x h): 1350 x 1600 mm



Figure 5.2 Photograph of the guarded hot box.

In the old standard method the U-value measurements on windows and doors are based on the principle of surface to surface measurements. This means that the thermal resistance of a component is calculated as the average surface temperature difference [K] of the component divided by the heat flux density [W/m^2] through the specimen. The standard surface thermal resistance is subsequently added to the component thermal resistance and the U-value of the component is found as the inverted value of the sum. The advantage of this principle is that the surface thermal resistance is not included in the measurements itself. If the surface thermal resistance is included in the measurement it has to be found from calibrations and this will introduce an extra source of uncertainty. The disadvantage is that the average surface temperature of each side (warm and cold) of a component has to be found using a number of temperature sensors mounted on the surfaces of the component. The average surface temperature is found from area weighting of the temperatures of each individual sensor. In the case of inhomogeneous samples like windows this process involves a number of individual judgements, and rather non-uniform measurement results obtained for the same specimen but carried out by different laboratories have been seen. (Williams, R).

To overcome these problems the surface temperature measurements on the samples during U-value measurements should be avoided. This can be done by measuring the air to air thermal transmission of the sample in this way including the surface thermal resistance in the measured value. However this rises the problem that the heat transfer

from or to the surface of a sample consists of two parts: a convective and a radiative. The convective part relates to the difference between sample surface temperature and air temperature. The radiative part relates to the difference between sample surface temperature and the “mean temperature” of the surface “seen” by the sample. It means that the convective and the radiative parts of the surface heat transfer coefficient can not relate to neither air nor radiative temperature unless they are identical which in general is not the case. Instead the concept of environmental temperature difference is applied. The environmental temperature T_n is a weighted mix of air and radiant temperatures and can be calculated from:

$$T_n = \frac{h_c \cdot T_c + h_r \cdot T_r}{h_c + h_r}$$

where h_c and h_r is the convective and radiative part of the heat transfer coefficient [W/m²K]

T_c is the air temperature [K]

T_r is the mean radiant temperature of the surfaces “seen” by the sample [K].

The environmental temperature is the temperature of the surroundings to which both the convective and the radiative heat transfer components can be related. To calculate the radiative component, h_r , the temperature of the specimen surface and all surfaces “seen” by the specimen must be known along with all relevant emissivity factors and view factors. In the case of a guarded hot box the radiation exchange between sample surface, surround panel reveal and baffle must be calculated based on the individual surface temperatures, surface emissivities and view factors. When the total heat transfer through a sample is known together with the radiative heat transfer the convective part, h_c , can be deduced.

By performing calibrations of the hot box regarding surface thermal resistance prior to the U-value measurement (see sections 5.4-5.6), the environmental temperature concept facilitates that the surface thermal resistance can be a part of the measured value in a meaningful way.

This method opens the possibility of avoiding the individual judgements involved in the determination of the average surface temperature of the test specimen but introduces an uncertainty in the determination of the surface thermal resistance. However as the surface thermal resistance only forms a relatively small part of the total thermal resistance of modern windows (30% for a window with U-value = 1.8 W/m²K) and as the uncertainty in the surface thermal resistance is expected to be less than 10% (see section 5.9) the impact of this uncertainty on the overall U-value will be small.

5.4 Calibration of the guarded hot box

A key issue in the operation of a guarded hot box is the calibration of the apparatus that must be carried out prior to the actual *U*-value measurements. Prior to the actual *U*-value measurement the guarded hot box must be calibrated by measurements on two or more calibration panels with known thermal properties, see figure 5.3. For each panel measurements are carried out at three different temperature levels. The thermal resistances of the calibration panels should be chosen so they will cover the expected range of test specimen *U*-values (e.g. total panel thickness of 20 and 60 mm using a core of polystyrene sandwiched between two 4 mm glass sheets). The calibration must be carried out in order to establish the heat transfer through the surround panel and to establish the correct surface thermal resistance on the sample surface. During the first measurement using the thinner calibration panel the speed of the fan on the cold side is adjusted in order to obtain a specific total surface thermal resistance during the test. After the first test the voltage for the fan motor is kept constant in all subsequent measurements.

The interior and exterior surface thermal resistances ($R_{s,i}$ and $R_{s,e}$) are found from:

$$R_{s,i} = \frac{T_{ni,cal} - T_{si,cal}}{q_{cal}}$$

$$R_{s,e} = \frac{T_{ne,cal} - T_{se,cal}}{q_{cal}}$$

where $T_{ni,cal}$ is interior environmental temperature during calibration [K]
 $T_{ne,cal}$ is exterior environmental temperature during calibration [K]
 $T_{si,cal}$ is interior calibration panel surface temperature during calibration [K]
 $T_{se,cal}$ is exterior calibration panel surface temperature during calibration [K]
 q_{cal} is the heat flux density through the calibration panel [W/m²]

Apart from for the adjustment of the cold side fan the purposes of the calibrations are to establish:

- the heat flow through the surround panel as a function of specimen thickness and mean temperature of the surround panel.
- the total surface thermal resistance $R_{s,tot}$ as a function of the heat flux density through the specimen.
- the convective fractions of the internal ($F_{c,i}$) and external ($F_{c,e}$) surface heat transfer coefficients as a function of heat flux density through the specimen.

The convective fractions describe the ratio between convective and total surface heat transfers on warm and cold side respectively. The convective fractions are assumed to be solely dependent on the heat flux density through the specimen and this allows the

environmental temperature to be calculated during *U*-value measurements without measuring the surface temperatures of the sample:

$$T_n = F_c \cdot T_c + (1 - F_c) \cdot T_r$$

where T_c is the air temperature and T_r is the mean temperature of the surfaces “seen” by the sample.

Two different methods concerning the calibration have been considered of by the ISO and CEN working groups in the development of the new measuring standards ISO12567/EN12412:

1. Calibration solely by means of measurements
2. Calibration by a combination of measurements and numerical calculations.

In the first type each new specimen size requires a new set of calibrations (at least six measurements in the hot box) - this way of calibrating the hot box is denoted "measured calibration".

The second type requires only one set of calibrations (six measurements) of the hot box and all subsequent calibrations are replaced by numerical calculations in combination with the results of the six calibration measurements - this way of calibrating the hot box is denoted "combined calibration". Furthermore two cases of mounting of the calibration panels and test specimens are investigated. In the first case the specimen is mounted flush with the cold side surface of the surround panel. This mounting is investigated in the “measured calibration” case. In the second case the specimen is mounted flush with the warm side surface of the surround panel and this mounting is investigated in the “combined calibration” case.

In the following sections the two measuring methods for facade windows and a suggestion for a new measuring method for roof windows will be presented. The principle difference in the results obtained according to the two different calibration methods will be discussed as well.

5.5 Measured calibration

The calibration panels are mounted 25 mm from the surface of the cold side surround panel (see figure 5.3) and tested at three different mean temperatures resulting in a total of at least six calibration measurements. The position of the calibration panel corresponds to a typical position of the glazing part in a facade window.

The total surface thermal resistance and the convective fractions during calibrations are found as described in section 5.4. The heat flowing through the surround panel (Φ_{sur}) is found from the electrical input to the metering box (Φ_{in}), the heat flow through the metering box walls (Φ_{mb}) and the heat flow through the calibration panel (Φ_{cal}):

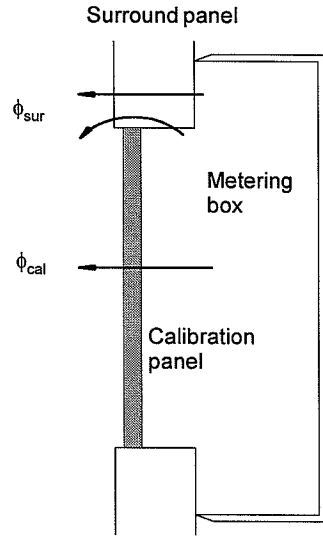


Figure 5.3 Heat flow through calibration panel and surround panel during calibrations. ϕ_{sur} and ϕ_{cal} denotes the heat flow through the surround panel and the calibration panel respectively.

$$\Phi_{sur} = \Phi_{in} - \Phi_{mb} - \Phi_{cal} = H_{sur} \cdot \Delta T_{sur} \quad (5-1)$$

where

$$\Phi_{cal} = \frac{\Delta T_{s,cal} \cdot A_{cal}}{R_{cal}}$$

where H_{sur} is the heat exchange coefficient of the surround panel [W/K]
 ΔT_{sur} is the average surface temperature difference across the surround panel [K]
 $\Delta T_{s,cal}$ is the average surface temperature difference across the calibration panel [K]
 A_{cal} is the area of the calibration panel [m²]
 R_{cal} is the thermal resistance of the calibration panel during measurement [m²K/W].
 and Φ_{mb} in general is 0 during the measurements.

From eq. 5-1 the heat exchange coefficient of the surround panel H_{sur} is found from:

$$H_{sur} = \frac{\Phi_{sur}}{\Delta T_{sur}} \quad (5-2)$$

H_{sur} includes the one dimensional as well as the two dimensional heat flow indicated in figure 5.3.

Examples of calibration curves can be seen in figure 5.4 and 5.5, where H_{sur} versus specimen thickness and surround panel mean temperature respectively $R_{s,total}$ ($=R_{s,i}+R_{s,e}$) versus heat flux density through the calibration panel are shown.

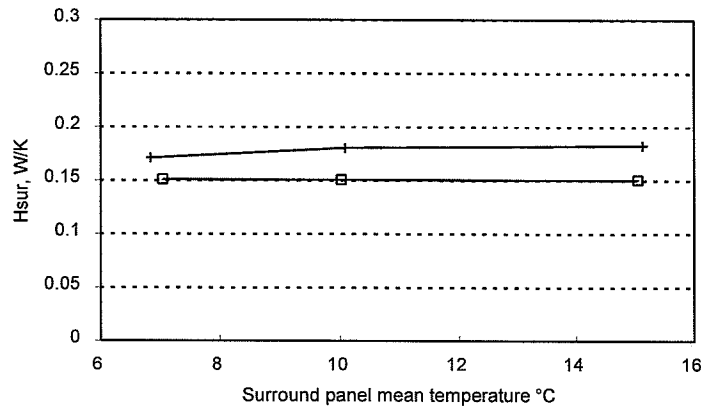


Figure 5.4 Example of surround panel heat exchange coefficient H_{sur} as function of specimen thickness and mean surround panel temperature. □ indicates 60 mm specimen thickness and + indicates 20 mm thickness. The varying surround panel mean temperatures are established during calibration by keeping the warm side at constant 20°C and obtaining steady state at three different cold side temperatures.

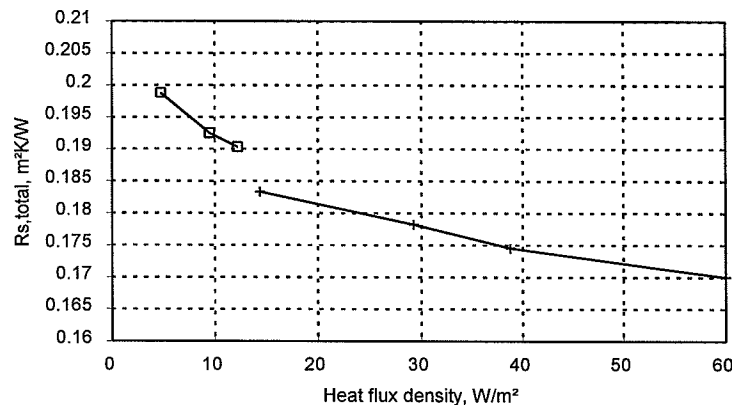


Figure 5.5 Total surface heat transfer resistance $R_{s,total}$ as function of heat flux density through calibration panels. □ indicates 60 mm specimen thickness and + indicates 20 mm thickness.

Calibrating the hot box solely by means of measurements makes it - to a certain extent - possible to include unrecognised systematic errors in the test setup in the surround panel heat exchange coefficient H_{sur} . This means that the subsequent U -value

measurements to a certain extent can be considered as relative measurements as long as they are covered by the calibration results. In other words the measurements are rather robust regarding unrecognised systematic errors in the test rig. However the calibration procedure outlined above is rather tedious and time consuming as it requires a new set of calibration measurements on the guarded hot box for each investigated window size. That means that for each U -value measurement on a new window size at least six calibration measurements must be carried out in advance. Investigations have also shown that the accuracy of the H_{sur} value in the departments Guarded Hot Box is rather poor (see section 5.9) but has only a small impact on the over all accuracy of the measurements. In other words a large effort is being done to calibrate the hot box regarding H_{sur} but the result is not very accurate and has only little importance for the final result. This has motivated a development of a different calibration procedure and a different approach is being elaborated by the CEN and ISO working groups. The principle is to combine physical calibrations with numerical calculations.

5.6 Combined calibration

Again at least six calibration measurements have to be carried out on at least two calibration panels with known thermal properties. During each calibration measurement the panel is mounted 40 mm from the warm side surface of the surround panel. The reason for moving the test specimen from the cold side surface of the surround panel towards the warm side surface is a wish to allow different surround panel thickness in the standard: The air temperature sensors on the warm side are fixed mid way between the warm side surface of the surround panel and the warm side baffle (prEN12412, ISO/DIS 12567). If the test specimen is mounted at the cold side surface of the surround panel the distance between the temperature sensors on the warm side and the specimen will depend on the surround panel thickness. For a large surround panel thickness the specimen will be mounted in a recessed position. This could cause problems for the natural convection on the warm side of the hot box and possibly introduce a layer of stagnant air between the temperature sensors and the specimen.

If instead the specimen is mounted close to the surface of the warm side surround panel the natural convection on the warm side will remain the same regardless of surround panel thickness. As the convection on the cold side is forced by fans even large surround panel thickness will not give reason for any stagnant air layer. So even though mounting a specimen in a recess on the cold side is not in agreement with most cases of window mounting in reality it is considered a less vulnerable position with regards to measurement accuracy in the hot box.

The fan speed on the cold side of the surround panel is adjusted during the first measurement using the thin calibration panel in such a way that a specific total surface thermal resistance is obtained (usually $0.17 \text{ m}^2\text{K/W}$). From the calibration measurements the total surface thermal resistance can be found as a function of heat flux density through the panels.

As it shows in figure 5.6 the heat flow through the surround panel can be divided into a one dimensional flow and a two dimensional flow.

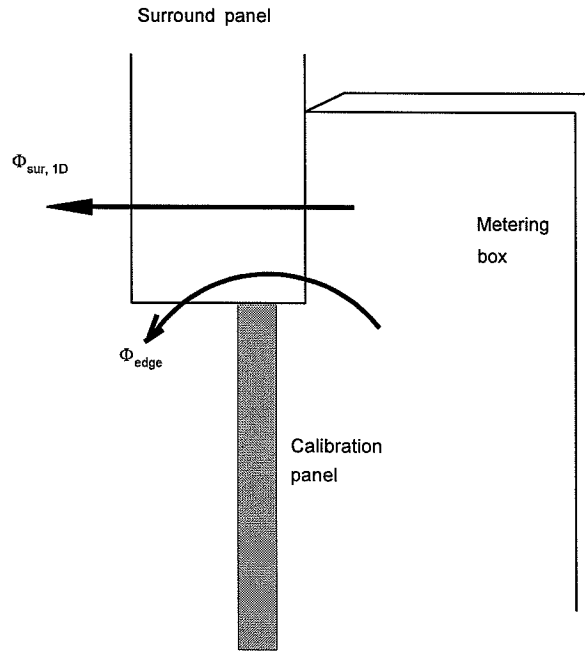


Figure 5.6 Heat flow through surround panel.

$$\Phi_{sur, 1D} = \frac{A_{sur} \cdot \Delta T_{sur}}{R_{sur}} \quad (5-3)$$

$$\Phi_{edge} = l_{edge} \cdot \psi_{edge} \cdot \Delta \theta_c \quad (5-4)$$

where A_{sur} is the area of the surround panel inside the metering box [m^2]
 R_{sur} is the thermal resistance of the surround panel [m^2K/W]
 l_{edge} is the perimeter of the calibration panel [m]
 ψ_{edge} is the linear thermal transmittance of the edge zone between calibration panel/sample and surround panel [W/mK]
 $\Delta \theta_c$ is the temperature difference between warm and cold side air [K]

From the calibration measurements with the thick panel the thermal resistance of the surround panel (R_{sur}) can be found on the basis of numerical calculations: From a known (or estimated) thermal conductivity of the surround panel material (λ_{sur}) and of the calibration panel material (λ_{cal}), the linear thermal transmittance, ψ_{edge} , can be found using the principle outlined in EN ISO 10211-1, Annex C and R_{sur} can be deduced. ψ_{edge} depends on the specimen thickness. To perform the calculation with a meaningful result the surround panel has to be constructed from a homogeneous material concerning thermal resistance. R_{sur} can now be found as a function of mean temperature of the

surround panel using the results from all three calibration measurements with the 60 mm panel.

An example of the calibration curve for R_{sur} versus surround panel mean temperature $\theta_{me,sur}$ can be seen in figure 5.7.

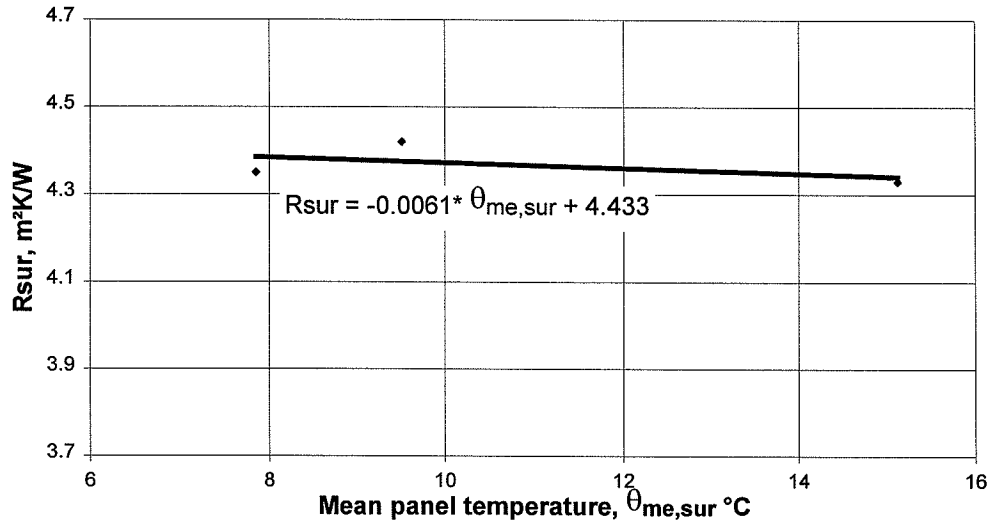


Figure 5.7 Thermal resistance of surround panel versus mean surround panel temperature $\theta_{me,sur}$.

The biggest advantage of the combined calibration procedure compared to the measured calibration is of course that only one set of calibrations will be needed for all subsequent U-value measurements regardless of specimen size. The main disadvantage is that the determination of R_{sur} and Ψ_{sur} will be based on numerical calculations under the assumption of known thermal properties of the surround panel. Furthermore all possible "unrecognised irregularities" in the hot box measurements will be accounted for in the R_{sur} -value found by calibration measurements and numerical calculations. When scaling the calibration results to a specimen size different from that of the calibration panel the "unrecognised irregularities" will also be scaled resulting in a possible error in the calibration result. However if the hot box is constructed and operated carefully the impact of calibration errors will be small.

5.7 Determination of the U-value

5.7.1 Boundary conditions

In the draft standards the boundary conditions have been set up: The measurements shall be performed at an average air temperature (warm and cold side) of approximately 10°C and at an environmental temperature difference of 20K ±2K. The U-value shall include the standard surface thermal resistance of 0.17 m²K/W and this can be obtained by correction of the measured U-value using the results from the calibrations ($R_{s,tot}$ versus heat flux density, figure 5.5).

5.7.2 The U-value measurement

The principle described below follows the descriptions given in ISO 8990, prEN 12412, ISO/DIS 12567. The heat flow density q_{sp} through a specimen during measurement is found by measuring the total electrical energy flow input to the metering box and subtracting the energy flow through the surround panel and through the metering box walls. By careful operation the latter energy flow can be considered zero. The measured U-value (U_m) can now be found from:

$$U_m = \frac{q_{sp}}{\Delta T_n} \quad (5-5)$$

where q_{sp} is the heat flow density through the specimen [W/m²]
 ΔT_n is the environmental temperature difference across the specimen [K]

Determination of q_{sp} depends on the calibration method.

For the measured calibration q_{sp} is found from:

$$q_{sp} = \frac{\Phi_{in} - H_{sur} \cdot \Delta T_{sur}}{A_{sp}} \quad (5-6)$$

where Φ_{in} is the (electrical) energy input to the metering box minus the heat flow through the metering box walls [W]
 A_{sp} is the projected area of the specimen [m²]
 H_{sur} is the surround panel heat exchange coefficient found from the calibration results for the actual specimen thickness and surround panel mean temperature [W/K]

For a window the specimen thickness will equal the thickness of the window frame and the actual value of H_{sur} can be found in figure 5.4 by interpolation. For thick specimens it is recommended to perform calibrations with calibration panel thickness corresponding to the specimen thickness.

For the combined calibration q_{sp} is found from:

$$q_{sp} = \frac{\Phi_{in} - \Phi_{sur} - \Phi_{edge}}{A_{sp}} \quad (5-7)$$

Φ_{sur} (the one dimensional heat flow rate through the surround panel) is found from the calibration results where R_{sur} was identified as a function of surround panel mean temperature (see figure 5.7).

Φ_{edge} is the two dimensional heat flow rate through the interface between the actual specimen and the surround panel. Φ_{edge} is calculated as shown in eq. 5-4 using the linear thermal transmittance of the edge zone that is valid for the actual specimen

thickness ($\psi_{\text{edge,sp}}$). This value can be found from numerical calculations similar to those carried out during the combined calibration procedure but now using the thickness of the actual specimen. In the calculation of $\psi_{\text{edge,sp}}$ a “real” window with wood frame is assumed to be mounted in the surround panel, see figure 5.8.

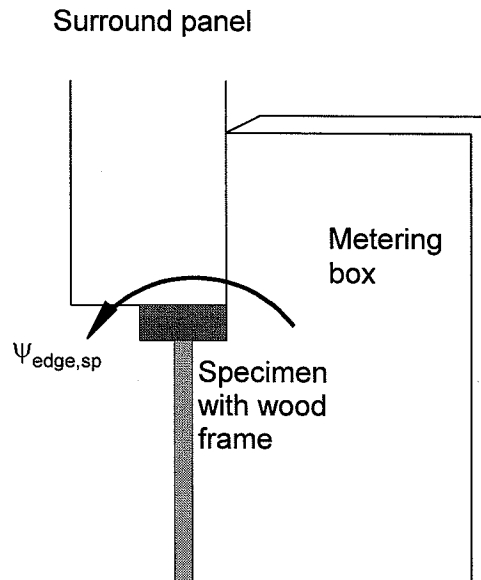


Figure 5.8 Geometric model for calculation of the linear thermal transmittance $\psi_{\text{edge,sp}}$ of the edge zone between specimen and surround panel.

5.7.3 Discussion of the two calibration principles

Apart from the mounting of the specimen, U-value measurements carried out on the basis of the two calibration methods differ in the treatment of the thermal interaction between the specimen frame and the surround panel.

When measuring the thermal transmittance of a sample after the measured calibration concept the thermal interaction between the sample and the surround panel is included in the specimen U-value. The reason for this is that the calibrations determining H_{sur} were carried out using unframed calibration panels made from insulation material. Thus the reference situation is an imaginary frame made from insulation material. When samples with frames (always of lower thermal resistance than the insulation material) are tested in the hot box the thermal interaction between sample and surround panel will “punish” the sample U-value.

When the U-value is based on the combined calibration procedure the reference situation from the calibrations and calculations is now a “real” wooden window. This means that the thermal interaction between the “wooden” frame and the surround panel is taken out of the U-value. Using a wooden window in the calculation of $\psi_{\text{edge,sp}}$

means that a wooden window is now the reference situation. If a window with different frame material is tested in the hot box the thermal interaction between the frame and the surround panel will be included in the U-value in such a way that thermally poor frames (e.g. metal frames with poor thermal break) will be “punished” while thermally good frames will be “rewarded”.

This means that U-values measured according to the combined calibration concept will be lower than U-values measured according to the measured calibration concept. In order to quantify this difference the value of $\psi_{\text{edge,sp}}$ has been calculated for a wooden window and for an insulation panel of same thickness as the window frame. Both specimen were calculated with a position at the warm side of the surround panel. The calculations showed that the difference in $\psi_{\text{edge,sp}}$ depends on the width of the frame/insulation panel and that the maximum difference was about 0.01 W/mK or 0.2 W pr meter of specimen perimeter in the standard measuring situation. For a 1 x 1 m² window with a U-value of 1.8 W/m²K this corresponds to a difference of maximum 2%. The difference is in other words not dramatic but a systematic difference in measured U-value will occur when using the two different calibration procedures.

The combined calibration procedure could be carried out corresponding to the measured calibration with regard to “frame” material. But using the combined calibration concept as described is an approach to characterise windows as components regardless of the thermal interaction between the window and the surrounding walls. Concerning the reference case with a wooden frame the thermal interaction between frame and surround panel has been cancelled corresponding to a situation where an adiabatic surface is introduced between the frame and the surround panel. This is in good agreement with the methods used when windows are modelled. Here an adiabatic surface is usually introduced at the boundary of the frame. However when using a different frame material than wood the interface between frame and surround panel still has an impact on the measured U-value of the window.

5.8 Roof windows

As a part of this study a proposal for a standardised U-value measurement on roof windows was elaborated. Roof windows represent a special problem for U-value measurements in a hot box for two reasons:

1. A large part of a roof window is usually exposed to the outside environment. If the results from the standard facade window calibrations are used this will result in incorrect values of especially the correction for energy flow through the edge zone between frame and surround panel as the roof window will be mounted quite differently from the facade window. Furthermore the total surface thermal resistance of the roof window will be different from the calibration situation as the wind speed on the cold side will be affected by the presence of the roof window. (See also figure 5.9 right).
2. Roof windows are in real life mounted with a varying slope and as the slope of a glazing has an impact on the convection inside a multilayer glazing and also on the surface thermal resistance the U-value will depend on the slope of the window. To

make an exhaustive characterisation of the roof window U-value measurements should be carried out at a number of different slopes and under varying surface thermal resistances. As only few hot-boxes world wide are capable of performing such measurements this does not seem applicable for a standardised test method and it is instead suggested to refer the U-value of roof windows to vertical mounting like facade windows even though this is not in correspondence to the real life physics.

In order to develop a method for measuring the thermal transmittance of roof windows a number of measurements on roof windows in the guarded hot box were carried out. Focus was especially set on the calibration procedure and three different approaches were investigated in order to develop a proper determination of the heat flow through the surround panel and of the surface thermal resistance during measurements (Duer,K. 1997; Duer,K. 1998, see also Appendix A and B where some details concerning the measurements are given):

1. A detailed calibration procedure using two calibration panels
2. A less detailed calibration procedure using only one calibration panel (simple calibration)
3. A less detailed calibration procedure using one calibration panel and numerical calculations (combined calibration).

5.8.1 Detailed calibration procedure

The calibration procedure is based solely on measurements and involves the following two steps:

1. Determination of the surround panel heat exchange coefficient H_{sur} by means of a calibration panel with known thermal resistance mounted flush with the cold side surface of the surround panel. The thickness of the panel corresponds to the distance that the roof window is entered into the surround panel. See figure 5.9 (left).
2. Adjustment of the total surface thermal resistance in the plane of the glazing in the roof window. This is done by mounting the roof window in the surround panel and performing a calibration measurement with a thin calibration panel with known thermal resistance mounted instead of the window glazing. See figure 5.9 (right). In this step the cold side fan speed is adjusted in order to obtain the desired total surface thermal resistance of $0.17 \text{ m}^2\text{K/W}$ for the glazing area. Measurements at three difference temperature levels on the cold side (-4°C , 0°C and $+10^\circ\text{C}$) are carried out.

From the first calibration step the value of H_{sur} corresponding to the physical dimensions of the roof window frame and the surround panel is found. From the second calibration step the total surface thermal resistance in the plane of the glazing of the roof window is found. Using the plane of the glazing as reference is an approximation as the roof window frame also is exposed to the cold side ambient.

However the approximation is reasonable as the area of the glazing in general is the dominant surface area also for roof windows.

5.8.2 Simple calibration procedure

Instead of performing a full calibration with regards to the surface thermal resistance focus was set on the cold side wind speed and assuming that a constant wind speed across the test sample results in a (reasonable) constant surface thermal resistance regardless of sample position. As the radiant heat exchange on the cold side is not affected by the position this is a reasonable assumption for the cold side surface thermal resistance (the sample surface can only “see” the cold side baffle in both the calibration and the U -value measurement situation). For the warm side the radiation exchange and the natural convection are assumed to be unchanged from the calibration to the U -value measurement even though the geometry is changed. Calculations have shown that this assumption is good for the radiation part (the radiative surface thermal resistance for the glazing part of a test sample changes about $0.003 \text{ m}^2\text{K/W}$ by moving the sample surface from calibration position to a measuring position 120 mm into the cold side environment). Whether or not the natural convection on the warm side changes due to a change in geometry is not easy to predict and has instead been investigated by measurements. An assumed fixed correlation between surface thermal resistance and wind speed means also that the impact of varying heat flux density through the sample on the total surface resistance has been neglected. (This impact on the over all U -value is considered small for modern insulating glazing units (Duer,K. 1997))

The calibration was carried out applying the following procedure:

The surround panel heat exchange coefficient H_{sur} was found using the calibration panel mounted flush with the surface of the cold side surround panel. See figure 5.9 (left). During the measurement the voltage for the wind simulator fan on the cold side was regulated in order to obtain the standard surface resistance in accordance to the standards. The wind speed and the fan speed was noted after steady state condition was reached. The wind speed was measured in front of the center of calibration panel in a fixed distance of 50 mm.

5.8.3 Combined calibration procedure

As is the case for the measured calibrations for facade window measurements the calibration procedures outlined in 5.8.1 and 5.8.2. require a new set of calibrations to be carried out for each new specimen size. Therefore the concept of combined calibration is investigated also for roof windows. Following the procedure described in section 5.6 calibration measurements are carried out using two calibration panels (e.g. 20 and 60 mm) with known thermal properties and mounted flush with the cold side surface of the surround panel. From these measurements the thermal resistance of the surround panel R_{sur} together with the total surface thermal resistance can be deduced.

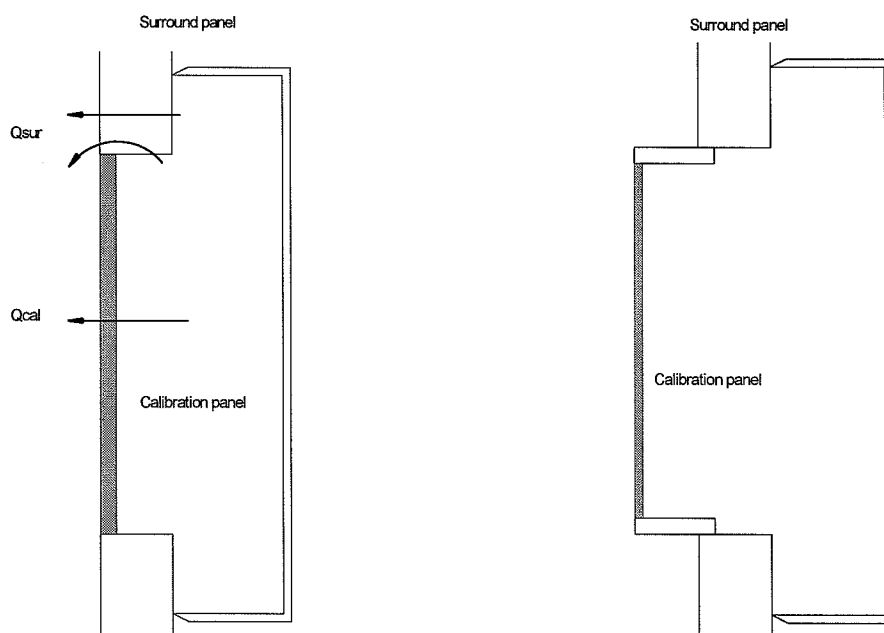


Figure 5.9 Calibration step 1 (left). Calibration step 2 (right)

From these data the energy flow through the surround panel during subsequent measurements can be found by numerical calculations regardless of the dimensions of the test specimen. But there are some problems related to the total surface thermal resistance. The total surface thermal resistance is found using a calibration panel mounted flush with the cold side surface of the surround panel. When a roof window is mounted in the surround panel the geometry of the “air channel” on the cold side of the hot box can be quite different from the geometry during calibration. A change of geometry has an impact on the wind speed across the window and thereby on the surface thermal resistance. How much the wind speed (and the surface thermal resistance) is changed depends on the individual design of the cold side of the hot box. An example of this is given in the next section.

5.8.4 Roof window measurements

To investigate the suitability of the different calibration approaches a number of measurements have been carried out in accordance to the three calibration procedures for roof windows. The results are summarised in table 5.1.

In figure 5.10 is shown curves for specific temperatures during one of the U -value measurements. No drift in temperatures take place after a relatively short period.

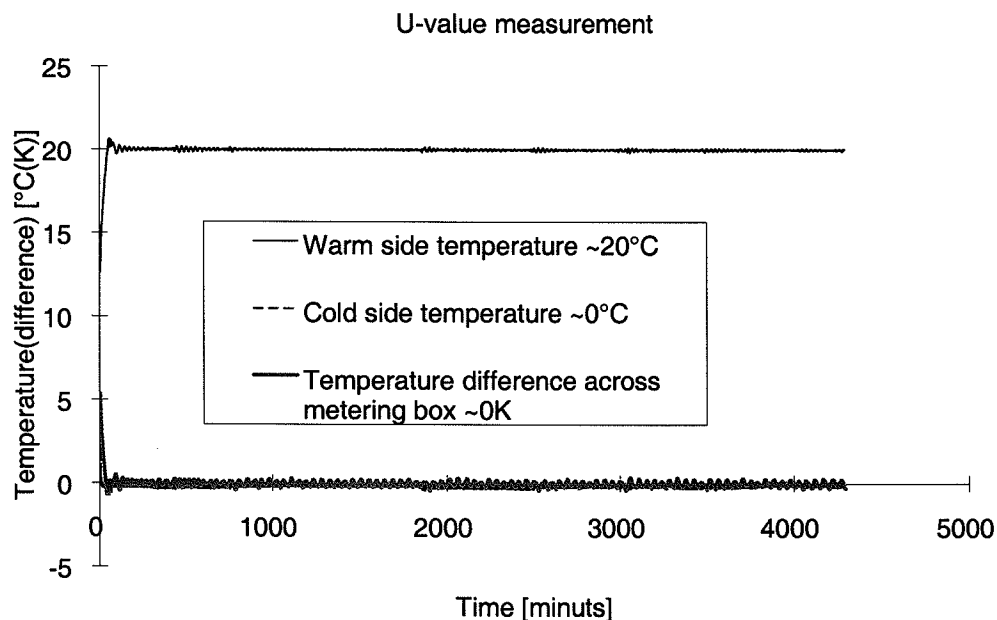


Figure 5.10 Curves of temperature difference across the metering box plus warm side and cold side temperatures during the U -value measurement.

Table 5.1 Measured U -value of a roof window depending on the calibration and measuring procedure.

Case no	Calibration type	Measured U -value	
1	Detailed calibration	1.85	$\text{W/m}^2\text{K}$
2	Simple calibration	1.82	$\text{W/m}^2\text{K}$
3	Combined calibration M1	1.81	$\text{W/m}^2\text{K}$
4	Combined calibration M2	1.78	$\text{W/m}^2\text{K}$
5	Combined calibration M3	1.83	$\text{W/m}^2\text{K}$

Here three different versions of the combined calibration procedure are shown:

- Combined calibration M1 denotes a U -value measurement where the fan speed on the cold side has been adjusted in order to obtain the same wind speed across the roof window glazing as was measured across the calibration panel during the calibration measurements. A calibration panel (without a frame) mounted in the surround panel has been used in the calculation of the linear thermal transmittance ψ_{edge} of the frame/surround panel interface. This method follows the principle in the simple calibration (section 5.8.2) both regarding the determination of the total surface thermal resistance for the glazing part of the roof window and regarding the energy flow through the surround panel. The latter has been found for same physical lay-out as used in section 5.8.2 but by means of numerical calculations instead of measurements. In this measurement the thermal interaction between the window frame and the surround panel is included in the final window U -value.
- Combined calibration M2 denotes a U -value measurement where the fan speed on the cold side has been adjusted in order to obtain the same wind speed across the

roof window glazing as was measured across the calibration panel during the calibration measurements (as in M1). The linear thermal transmittance ψ_{edge} of the frame/surround panel interface has been found by calculation using a “real” roof window with wooden frame mounted in the surround panel. Frame dimensions were 35 x 140 mm. This method follows the method outlined in section 5.8.3 except for the re-adjustment of the fan speed on the cold side. In this measurement the thermal interaction between the window frame and the surround panel is **not** included in the final window U-value.

- Combined calibration M3 denotes a measurement where the fan speed on the cold side during U-value measurement has remained unchanged compared to the adjustment carried out in the calibration measurement. The linear thermal transmittance ψ_{edge} of the frame/surround panel interface has been found by calculations using a “real” roof window with wooden frame mounted in the surround panel. Frame dimensions were 35 x 140 mm. This method follows exactly the method outlined in section 5.8.3. In this measurement the thermal interaction between the window frame and the surround panel is **not** included in the final window U-value.

Please note that in case 1, 2 and 3 in table 5.1 the thermal interaction between the window frame and the surround panel is included in the U-value. For the last two cases this interaction is **not** included. The result for the detailed calibration measurement in case 1 has been found for one complete calibration and measuring series. The results in cases 2, 3 and 4 in table 5.1 are derived from a second measuring series where the roof window has been removed from the surround panel, a new set of physical calibrations have been performed and the window has been remounted in the surround panel. The U-values in case 2, 3 and 4 are derived from the same measured data - the only difference between the three cases is the treatment of the correction for heat flow through the surround panel based on different calibration principles. The last case shows the result from the second measuring series but with a different adjustment of the cold side fan speed. In other words the first case represents measuring results from one mounting of the window and the next four cases represents results from a second set of physical measurements where the window has been remounted. In all five cases the window has been mounted in the same way inserted 20 mm into the surround panel.

All the results are within average $\pm 3\%$ and this is within the expected accuracy of the hot box measurements. Nevertheless some clear statements can be deduced:

- Using detailed and simple calibration gives results in good agreement. (Case 1 and 2 differs 1.6%)
- Using the measured or combined calibration procedure according to the simple calibration principle gives almost identical results. (Case 2 and 3 differs 0.5%)
- Using the combined calibration based on calculations with a “real” window results in a smaller U-value than using the similar calibration based on unframed calibration panel. (Case 3 and 4 differs 2%) This is a systematic difference due to the different handling of the frame/surround panel interface. Apart from this the results are alike.

- Using the same fan adjustment in the *U*-value measurement as was found in the calibration measurement leads in this case to an increase in *U*-value of 3%. (Case 4 and 5). This is due to the reduced surface thermal resistance that is a result of the increased wind speed across the window compared to the wind speed in the calibration measurement. This effect is dependent on the design of the cold side of the hot box.

5.8.5 Recommendations for *U*-value measurements on roof windows

In order to facilitate the calibrations also for *U*-value measurements on roof windows it is recommended to use the concept of combined calibration to establish the energy flow through the surround panel during measurements. However using the exact same procedure as outlined in section 5.8.3 (cold side fan speed adjustment remains unchanged from calibration to *U*-value measurement) may give more or less systematic errors in the results. This type of error depends as previously mentioned on the hot box design. In the present investigations the systematic error underestimates the total surface thermal resistance with about 0.015 m²K/W and for the investigated sample this corresponds to an overestimation of the *U*-value of 3%. Larger overestimation will occur for specimens with larger *U*-value and smaller overestimation for specimens with smaller *U*-value. The error in surface thermal resistance depends on the design of the “air channel” on the cold side: If the channel is narrow the surface thermal resistance will be underestimated like in the present case. If on the other hand the air channel is very wide and the distance between the sample surface and the cold side baffle is small opposite effects may be seen. I.e. the wind speed across the window is reduced resulting in an underestimation of the *U*-value. As the error tends to be systematic for the individual hot box design a larger discrepancy than 5% may occur for *U*-values measured in different hot boxes on identical roof window specimens.

Depending on the desired level of accuracy and comparability of results some guidelines to ways of quantifying that no significant change in surface thermal resistance takes place when mounting a test specimen in the surround panel should be given. If only the surface thermal resistance of the glass-part of the window is considered there is at least four ways to do this:

1. Measurement of the wind speed across the sample in a fixed distance from the sample. The wind speed should be (almost) the same during measurements as during calibrations. (Corresponds to case 3 in table 5.1)
2. Using a known center *U* value of the glazing in the window in combination with measured temperatures of the glass panes to verify the surface thermal resistance during measurements.
3. Using a calibration panel mounted instead of the glazing. (Corresponds to the second calibration step in case 1 in table 5.1)
4. Give geometrical guidelines to the design of the cold side of the hot box in order to reduce the impact of the specimen-mounting on the surface thermal resistance.

As the wind speed measurement on the cold side of the hot box is already a part of the standard measurement it is recommended to follow the first suggestion above.

5.9 Uncertainty of hot box measurements

In order to check the over all performance of the guarded hot box a measurement of the thermal transmittance of a well-defined calibration panel has been carried out. The panel consists of 40 mm polystyrene sandwiched between two 3 mm masonite plates. The dimensions of the panel was 1200 x 1200 mm. After a full measured calibration using 1200 x 1200 mm calibration panels of thickness 28 and 68 mm respectively (incl. glass) the thermal transmittance of the calibration panel was measured to $U_{\text{hot-box}} = 0.73 \text{ W/m}^2\text{K}$.

Subsequently the panel was cut in four pieces 600 x 600 mm and the thermal resistances of the four pieces were measured in a hot plate device based on the heat flow meter principle (ISO8301). The standard surface thermal resistance of $0.17 \text{ m}^2\text{K/W}$ was added to the average thermal resistance of the panel and the resulting thermal transmittance was found to $U_{\text{hot-plate}} = 0.74 \text{ W/m}^2\text{K}$. It should be noted that in the hot plate measurements the U -value corresponds to the one dimensional value. This is also the case in the hot box measurement as the hot box was calibrated using same kind of insulation material as was used in the test panel. This means that the thermal interaction between test sample and surround panel has been cancelled by the calibration. As the deviation between the two results is about 1% and as the expected uncertainty on the hot plate measurements is about 2% the result is very encouraging regarding the accuracy of the hot box measurements.

Nevertheless measurements in a guarded hot box imply a large number of potential sources of errors. The calibrations are carried out with quite a large relative error, particularly the measurement of the surround panel heat exchange coefficient (H_{sur}) involves relative errors of up to 50% depending very much on the surround panel area in the hot box. Fortunately the impact of this error on the final U -value is small as the energy flow through the surround panel in general is small compared to the heat flow through the test specimen. The relative error on the surface thermal resistance coefficient is typically less than 10%, but again the impact of this error is relatively small as the surface thermal resistance (for modern windows) only form a minor part of the total heat resistance of the construction.

Even though many uncertainties may be involved, hot box measurements can be performed with a high degree of accuracy if the hot box is designed and operated carefully. Work carried out in IEA SHCP Task 18 (Hutchins et al) on hot box error analysis showed that a relative uncertainty of about 5% can be obtained of course to a certain extend depending on the sample U -value and sample size. In appendix C the relative uncertainty for the measurement of a 1.2 x 1.2 m specimen with a U -value of 1.75 is calculated to about 6% using the measured calibration method. A similar uncertainty will occur for measurements carried out according to the combined calibration method.

In the next sections a few examples of measured and calculated thermal transmittance for different test samples will be given.

5.10 U-value, ISO round robin test, measured calibration

5.10.1 Introduction

As test specimen was chosen a PVC-window and the thermal transmittance of the window was measured by a number of laboratories in a so-called round robin test. The following laboratories have participated in the round robin measurements:

National Physical Laboratory (NPL), United Kingdom.

TNO Building and Construction Research, the Netherlands.

EMPA, Switzerland.

Institut für Fenstertechnik e.V. (IFT), Germany.

Forschungsinstitut für Wärmeschutz e.V. München (FIW), Germany

NRC-Institute for Research in Construction IRC, Canada

University of Massachusetts, United States of America

Swedish National Testing Institute (SP), Sweden

Technical University of Denmark (DTU), Denmark

The round robin test was carried out using the measured calibration procedure described in section 5.5 except for the measurement carried out by TNO who used a procedure corresponding to the combined calibration.

This section describes the results of the Danish part of the interlaboratory comparison of hot box measurements of a glazed window system using the procedures given in ISO/DIS 12567 version 09/1996 (Duer,K. 1997). An overview of the round robin results reported will be given.

5.10.2 Description of the window

The window is build from PVC frames and measures 1230 mm wide x 1480 mm high. The glazings are double glazed units (4-16-4 mm) with one float glass pane outermost and one Pilkington K-glass pane innermost (low e-coating in position 3). The gap between the glass panes is air filled and the spacer material is aluminium filled with desiccant.

The window is divided into three parts:

- one part contains a fixed glazing and measures 615 mm wide x 1480 mm high
- one part contains a side hung glazing and measures 615 mm wide x 1080 mm high
- one part contains a top hung glazing and measures 615 mm wide x 400 mm high

Details of the window construction can be seen in figure 5.11.

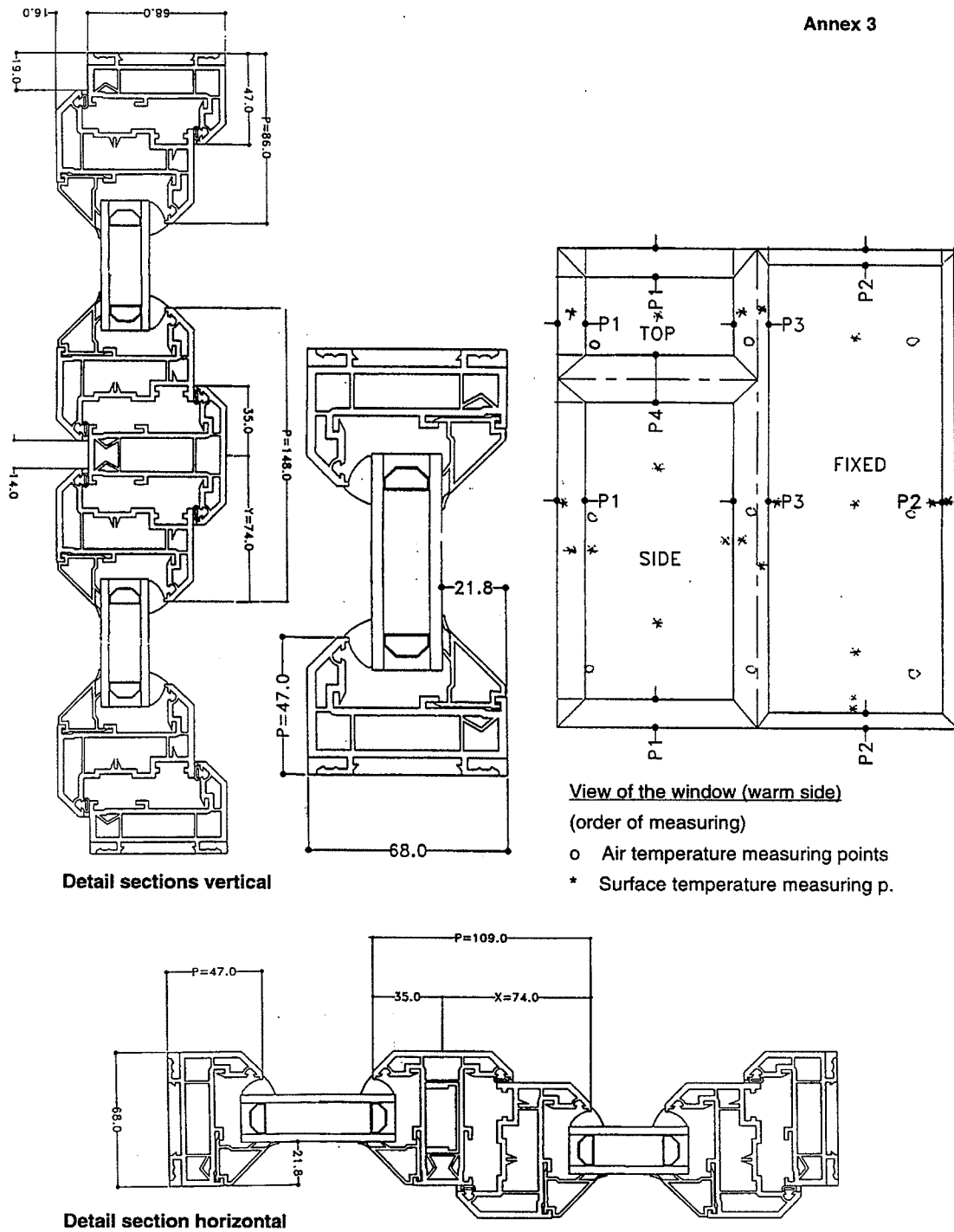


Figure 5.11 Details of the ISO round robin window

5.10.3 Calibration panels

Two calibration panels have been constructed in order to perform the hot box calibration procedure outlined in ISO/DIS 12567, using the measured calibration method described in section 5.5. The panels measure 1230 mm wide x 1480 mm high as the round robin window and have a total thickness of 28 mm and 68 mm respectively.

The core material is extruded polystyrene which prior to the assembling has been ground plane in order to avoid or at least reduce variations in the material thickness. The core thickness is 20 and 60 mm respectively. The glazings on both sides of the core are 4 mm float glass with normal emissivity. Prior to the assembling the polystyrene has been kept under laboratory conditions for seven weeks. The panels are assembled simply by means of heavy duty tape along the periphery of the panels, no glue has been used in this process.

The thermal conductivity λ of the core material has been measured for the two sample thickness, 20 mm and 60 mm. The measurements were performed in a hot plate device (ISO8301) and on the very same material samples that were used in the construction of the calibration panels.

The measurements were carried out at a mean temperature of 20°C and the results of the two measurements are:

20 mm polystyrene: $\lambda_{20} = 0.033 \text{ W/mK}$

60 mm polystyrene: $\lambda_{20} = 0.036 \text{ W/mK}$

The thermal conductivity was determined at only one mean temperature of the polystyrene, 20°C, and the λ -values at the relevant temperatures were found by assuming a change in the thermal conductivity as a function of temperature of 0.4%/K [VIK], using the following expression:

$$\lambda_{\theta} = \lambda_{20} - \frac{(20 - \theta_m) \cdot 0.4 \cdot \lambda_{20}}{100}$$

where θ_m is the actual mean temperature of the core material during calibrations.

5.10.4 Calibration measurements

The two calibration panels were both tested at three different air temperature levels on the cold side of the guarded hot box, -4°C, 0°C and 10°C. The air temperature on the warm side was kept constant at 20°C.

At the first calibration test the cold side temperature was 0°C and the wind speed on the cold side was adjusted in order to obtain a standard total surface resistance coefficient of $0.17 \text{ m}^2\text{K/W}$. After the first calibration the voltage for the wind simulator fan was kept constant for the rest of the measurements.

From the known thermal resistance of the calibration panels the surface resistance as a function of heat flux density through the panel as well as the surround panel heat exchange coefficient as a function of surround panel mean temperature can be found. The results are shown in figure 5.12 and 5.13.

In table 5.2 is shown the key results from the calibrations.

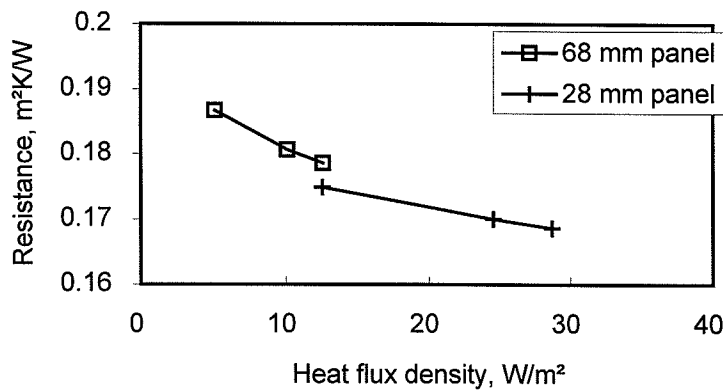


Figure 5.12 Total surface resistance versus heat flux density. From calibrations

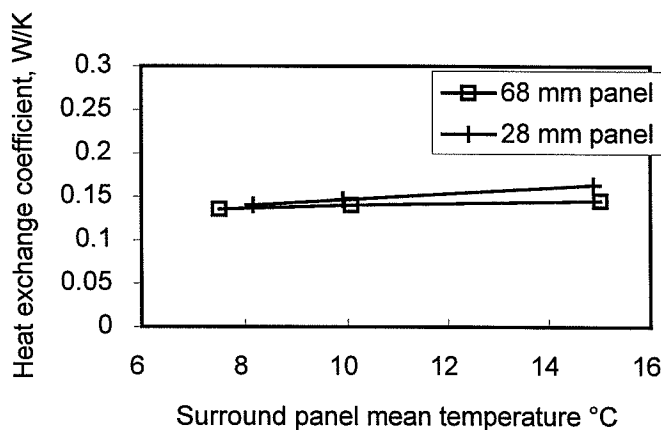


Figure 5.13 Surround panel heat exchange coefficient. From calibrations.

Table 5.2 Key results from calibrations

	28 mm	28 mm	28 mm	68 mm	68 mm	68 mm	
Panel mean temp	7.20	9.07	14.40	7.10	9.72	14.82	[°C]
ΔT_n	23.42	19.94	10.08	24.58	19.59	9.76	[K]
ΔT panel surface	18.57	15.77	7.88	22.34	17.76	8.81	[K]
Heat flux q_{cal}	28.72	24.56	12.54	12.57	10.11	5.12	[W/m ²]
Surf. resist.	0.169	0.170	0.175	0.179	0.181	0.187	[m ² K/W]
Power to box	55.47	47.55	24.43	26.11	21.05	10.68	[W]
ΔT_{Sur}	22.70	19.33	9.75	23.79	18.92	9.41	[K]
$\theta_{me,sur}$	8.16	9.92	14.88	7.50	10.08	15.02	[°C]
H_{sur}	0.140	0.147	0.164	0.136	0.140	0.146	[W/K]

5.10.5 U-value measurement

Mounting of the window

The window was mounted in the hot box aperture with the frame surface flush with the surface of the cold side of the surround panel.

The interface between the surround panel and the window was taped on both warm and cold side to secure that no air could penetrate the interface. The parts of the window that can be opened were taped on the warm side only.

Sensor locations

Nine thermocouples were mounted on each side of the window measuring the surface temperature of the glazing parts of the window.

Results

Key results from the U-value measurement are shown in table 5.3. Due to the relatively large thickness of the smallest calibration panel the R_s curve in figure 5.12 does not cover the actual heat flux density from the U-value measurement. However the slope of the curve is decreasing with increasing heat flux density and from an extrapolation of the curve in figure 5.12 the total surface resistance coefficient during the U-value measurement is estimated to:

$$R_{s,tot} = 0.165 \text{ m}^2\text{K/W}$$

Now the standard U-value can be found from the following expression:

$$U_{st} = [1/U_m + 0.17 - R_{s,tot}]^{-1}$$

$$U_{st} = 1.90 \text{ W/m}^2\text{K}$$

Table 5.3 Key results from U-value measurement, ISO round robin window

	Warm	Cold	
Air temperature	20.00	0.08	[°C]
Baffle temperature	19.57	0.28	[°C]
Glazing temperature	15.50	1.97	[°C]
Reveal temperature	18.29	0.63	[°C]
Environment. temp	19.69	0.12	[°C]
ΔT_{sur}	18.85		[K]
Heat flow through surround panel	2.71		[W]
Electrical input	70.96		[W]
$\Delta T_{\text{metering box}}$	0.00		[K]
ΔT_n	19.57		[K]
U_m	1.92		[W/m²K]

5.10.6 Interlaboratory comparison

Not all results have been reported from the participating laboratories but the seven European laboratories have reported the results given in table 5.4:

Table 5.4 Summary of round robin U-value measurement. European laboratories. Standard U-value includes the surface thermal resistance of 0.17 m²K/W. (Williams and Hall, 1998). Measured U-value is directly measured value not yet corrected for deviation between surface thermal resistance in hot box and the standard value.

Laboratory	Heat flux through window [W/m²]	Warm side environmental temperature [°C]	Cold side environmental temperature [°C]	Measured U-value [W/m²K]	Standard U-value [W/m²K]
NPL, UK	37.47	22.04	2.30	1.90	1.90
TNO, NL	34.52	19.68	0.58	1.81	1.80
EMPA, CH	39.52	21.12	0.56	1.92	1.93
IFT, D	39.46	23.85	2.96	1.89	1.94
FIW, D	37.39	20.21	0.89	1.93	1.94
SP, S	36.84	19.87	0.20	1.87	1.90
DTU, DK	37.49	19.69	0.12	1.92	1.90

As it shows from table 5.4 the results are within the range of 1.80 to 1.94 W/m²K with an overweight of results very close to 1.90 W/m²K. The average of the measurements is 1.89 W/m²K and all measurement results are within $\pm 5\%$ of the average result corresponding to the expected uncertainty of the measurements. The good agreement between the results indicate that the method described in the draft standards is very applicable. It must be noted that the TNO-measurement did not follow the same calibration procedure as the other participating laboratories. TNO transferred the calibration results from one specimen size to the actual window size by

calculations in a process similar to the combined calibration procedure. All other laboratories performed calibration measurements on calibration panels of exactly the same size (height x width) as the investigated window. When comparing between laboratories performing the measurements according to the same calibration procedure the average result is 1.91 and the spreading of results $\pm 2\%$.

5.11 Nordic round robin test, combined calibration

A second round robin exercise carried out utilising the concept of combined calibrations has been conducted with the participation of the following laboratories:

Norwegian Building Research Institute, NBI
Swedish National Testing and Research Institute, SP
Technical Research Centre of Finland, VTT
Technical University of Denmark, DTU

Two windows with approximate U -values of $1 \text{ W/m}^2\text{K}$ and $2.5 \text{ W/m}^2\text{K}$ have been tested. Due to limited time it was decided that instead of circulating the same two windows to all participants four pairs of windows (eight windows in total) were all tested at SP to check the uniformity of the U -values and subsequently the windows were distributed to the participants.

5.11.1 Description of the windows

Window type A is a wooden window with one double glazed unit (DGU) (4-15-4 mm) with no coatings or noble gas filling. Expected U -value about $2.5 \text{ W/m}^2\text{K}$.

Window type B is a wooden window having one sealed DGU with low emissivity coating mounted in the inner casement. A single glass pane with an inward facing hard low emissivity coating is mounted in the outer casement. Expected U -value about $1 \text{ W/m}^2\text{K}$.

Both windows measure $1185 \times 1185 \text{ mm}$.

5.11.2 Calibration panels

Two calibration panels were constructed from the same material as was used for the ISO round robin exercise, but with a thickness of 12 and 50 mm polystyrene resulting in total calibration panel thickness of 20 and 58 mm respectively. The calibration panels were constructed in accordance to (Williams and Hall, 1997) in a process where the glass panes were glued to the insulation material by silicone glue. Very much care was taken in measuring the average thickness of the calibration panels in order to reduce the uncertainty in the resulting thermal resistance of the panels.

The thermal conductivity of the polystyrene panes was found after the same principles as was used in the ISO round robin test and also on the very same material as was used in the calibration panels.

5.11.3 Calibration measurements

The calibrations were carried out following the combined calibration procedure described in section 5.6 by all laboratories except VTT who used the measured calibration procedure (section 5.5). The calibration curves resulting from the Danish calibrations are shown in figure 5.14 to 5.16.

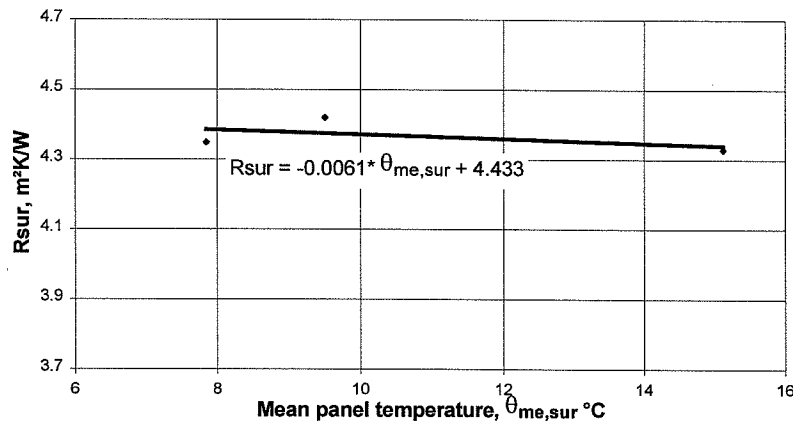


Figure 5.14 Thermal resistance R_{sur} of the surround panel vs. surround panel mean temperature $\theta_{me,sur}$.

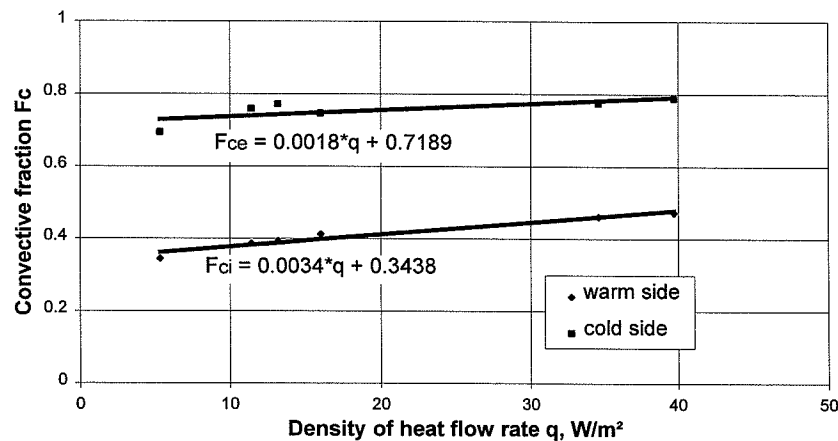


Figure 5.15 Convective fractions F_c for warm and cold side vs. density of heat flow rate through the specimen.

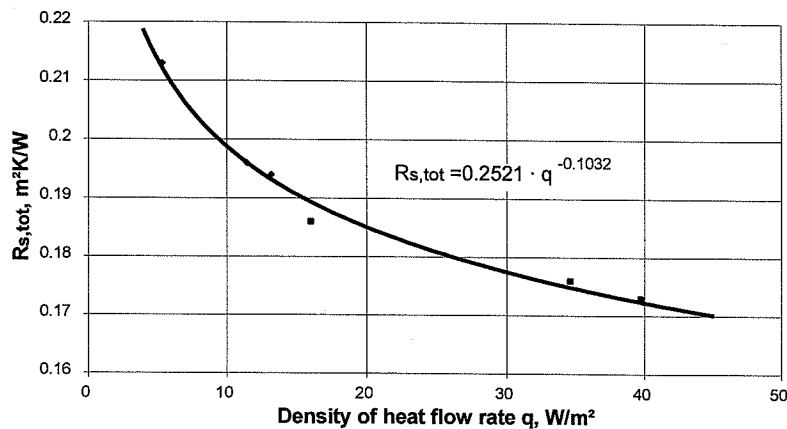


Figure 5.16 Total surface resistance $R_{s,tot}$ of specimen vs. density of heat flow rate through the specimen.

5.11.4 U-value measurements

Mounting of the windows

The windows were mounted in the hot box aperture with the frame surface flush with the surface of the warm side of the surround panel. The interface between the surround panel and the window was taped on both warm and cold side to secure that no air could penetrate the interface. The part of the window that can be opened was taped on the warm side only.

Results

The results from the U-value measurements are listed in table 5.7. The presentation is slightly different from the one used for the ISO round robin results, partly due to the different calibration procedure.

Table 5.7 Key results from U-value measurements. Nordic round robin.

Term		Type A	Type B
$\theta_{me,cal}$	mean temp. of sur.panel °C	9.49	9.34
R_{sur}	surround panel resistance ¹ m ² K/W	4.375	4.376
$\Delta\theta_{s,cal}$	temp.difference of sur.panel K	18.16	18.40
$\Delta\theta_c$	air temp.difference K	19.85	20.15
Φ_{in}	heat input to hot box W	69.93	33.22
Φ_{sur}	surround panel heat flow W	3.07	3.11
Φ_{edge}	edge zone heat flow W	0.54	0.54
q_{sp}	heat flow density of specimen W/m ²	47.25	21.06
F_{ci}	convective fraction - warm ² -	0.504	0.415
F_{ce}	convective fraction - cold ³ -	0.804	0.757
$R_{s,tot}$	total surface resistance ⁴ m ² K/W	0.169	0.184
θ_{ri}	radiant temp. - warm °C	19.19	19.51
θ_{re}	radiant temp. - cold °C	0.43	0.04
θ_{ni}	environmental temp. - warm °C	19.60	19.71
θ_{ne}	environmental temp. - cold °C	0.20	-0.10
$\Delta\theta_n$	environmental temp.difference K	19.40	19.81
U_m	measured U-value W/(m ² K)	2.44	1.06
ΔU_m	uncertainty of the measurement W/(m ² K)	±0.12	±0.08
U_{st}	standardised U-value W/(m²K)	2.44	1.08

$$^1 R_{sur} = -0.0072 \cdot \theta_{me,sur} + 4.2875$$

$$^2 F_{ci} = 0.0034 \cdot q_{sp} + 0.3438$$

$$^3 F_{ce} = 0.0018 \cdot q_{sp} + 0.7189$$

$$^4 R_{s,tot} = 0.2521 \cdot q_{sp}^{-0.1032}$$

5.11.5 Interlaboratory comparison, Nordic countries

The results from the four laboratories are shown in table 5.8 (window type A) and table 5.9 (window type B).

Table 5.8 U-value for window type A. Nordic round robin.

Laboratory	Heat flux through window [W/m ²]	Warm side environmental temperature [°C]	Cold side environmental temperature [°C]	Measured U- value [W/m ² K]	Standard U- value [W/m ² K]
NBI	47.97	19.73	-0.10	2.42	2.45
SP	50.68	19.60	-0.18	2.56	2.58
VTT	53.61	19.48	-0.48	2.69	2.66
DTU	47.25	19.60	0.20	2.44	2.44

Table 5.9 *U-value for window type B. Nordic round robin.*

Laboratory	Heat flux through window [W/m ²]	Warm side environmental temperature [°C]	Cold side environmental temperature [°C]	Measured U- value [W/m ² K]	Standard U- value [W/m ² K]
NBI	21.48	20.14	0.44	1.09	1.11
SP	23.01	20.18	-0.25	1.13	1.14
VTT	24.04	19.78	-0.26	1.20	1.20
DTU	21.06	19.71	-0.10	1.06	1.08

The average U-value for type A is 2.53 W/m²K and all results are within average $\pm 5\%$. For type B average U-value is 1.13 W/m²K and all results are within average $\pm 6\%$. The spreading of the results corresponds to the expected uncertainty of the measurements. It must be noted however that the VTT measurements have been performed with the measured calibration procedure and this leads to systematically larger U-values than the combined calibration procedure (see section 5.7.1). When comparing the three laboratories performing the measurements after the combined calibration principle the average U-value for type A window is 2.49 and the three results are within $\pm 4\%$ of average. For window type B the corresponding value is 1.11 W/m²K $\pm 3\%$.

5.12 Comparison of calculated and measured values

Appendix D is an article submitted to the official journal of the International Solar Energy Society "Solar Energy". The abstract from the paper is given below – for full description reference is given to Appendix D.

Abstract – The influence of windows on the energy consumption in buildings is well known and in order to encourage the development and the appropriate use of high performance glazings and windows in Denmark an Energy Labelling and Rating system is being developed. During this work a need for establishing a common and well defined method to characterise the performance of glazings and windows on the Danish market has been recognised. This paper gives a short description of the Danish Energy Labelling and Rating system for glazings and windows introduced in year 2000. Furthermore the results of a comparison between measured and calculated thermal transmittance for five different window types are given. The calculations on the glazing part have been performed in five different programmes (WIS, WINDOW, VISION, CALUMEN and GLAD99). The calculations on the frame part have been performed in three different programmes (FRAME, THERM and WinIso). The comparison indicates that all investigated programmes are qualified for calculating energy labelling data for glazings and windows.

5.13 Conclusions

The design, operation procedure and data treatment associated to the guarded hot box at the Department of Buildings and Energy has been updated and all the measuring equipment (temperature sensors, thermopiles, Watt-meter, Voltmeter) has been calibrated in order to meet the demands for accurate measurements of the thermal transmittance of windows.

The operation and the accuracy of the guarded hot box was examined in three steps:

- First a system performance test was carried out in which the thermal transmittance of a well-defined calibration panel was measured in the hot box as well as in a hot plate device. Excellent agreement between the two results was obtained (discrepancy about 1% for a U-value of 0.75 W/m²K).
- Next a round robin test was conducted with the participation of seven European countries. The obtained results for the six measurements that were based on the same calibration procedure (measured calibration) showed excellent agreement (1.91 W/m²K ±2%).
- Finally a second round robin test on two windows with the participation of four Nordic countries was carried out. Again good agreement between the results was obtained and for the three measurements that were based on the same calibration procedure (combined calibration) the reported results were 2.49 W/m²K ±4% and 1.11 W/m²K ±3% respectively.

A proposal for the measurement of roof window thermal transmittance was elaborated in order to facilitate such measurements and to bring them in accordance with the general concept in the draft proposals prEN12412 and ISO/DIS12567.

A comparison of calculated and measured U-values for five different windows resulted in good agreement between the results obtained.

On the basis of the investigations on hot box measurements a high degree of confidence in the measurement accuracy of the guarded hot box at the Department of Buildings and Energy has been obtained. At the same time the testing procedure outlined in the draft standards has proven to be reliable giving good agreement between results for identical samples measured in different devices.

6 Calorimetric measurement of total solar energy transmittance, g-value

Abstract

The measurement of the total solar energy transmittance is far from a standardised process. In this study work has been done to facilitate a physical correct and at the same time feasible way to measure the value. This has involved the development of:

- measuring equipment
- measuring procedures
- correction procedures

Especially the correction procedures draw attention. Corrections are necessary as the measurements are performed indoor under boundary conditions that differ from “real life” or a fixed reference situation.

As the measuring and corrections techniques are under development it has been essential to perform an evaluation of results obtained from measurements utilising the developed techniques. This can not be done in general as there is no general reference to compare the obtained results with. However for most conventional glazings (clear non diffusing glazings with known optical and thermal properties) the total solar energy transmittance can be calculated with good accuracy using well established thermal and optical theory. Even though it is a bit “the other way around” the calculations have been used to verify the results obtained from measurements and corrections. Three glazings have been investigated and an analysis of the expected uncertainty in the measurements has been carried out. Though the samples investigated are all clear glazings that can be modelled the scope of the work has been to develop a measuring and data treatment technique that will apply for complex samples that can not be modelled.

6.1 General

The total solar energy transmittance (g-value) consists of two parts: the directly transmitted solar radiation τ and the secondary heat transfer towards the inside q_i . The latter originates from radiation first absorbed in the samples and subsequently transmitted partly to the outside (q_o) and partly to the inside (q_i) by convection and radiation. However in a situation with mixed solar gain and heat loss through a window the above definition is not very clear. A more useful definition is based on the heat balance approach described in section 4: The g-value is determined as:

$$g = \frac{q_{net,solar} - q_{net,dark}}{G}$$

where $q_{\text{net,solar}}$ is the net energy gain of the window at a specific set of boundary conditions (including solar radiation) and $q_{\text{net,dark}}$ is the net energy gain of the window for the same set of boundary conditions, but without the solar radiation.

For many cases the g-value of a window/glazing can be calculated using calculation models and this is especially true for many non-diffusing glazings, see also section 4. However when the geometry of the investigated sample is complex or when materials or constructions with unknown optical or thermal properties are used the calculations have to be supported by measurements.

Several different ways of measuring the g-value of a transparent sample have been described in literature e.g. (Petersen, E. 1966) and (Harrison, S.J. 1990) but no international standards or draft standards for the direct calorimetric measurement of g-values have yet been developed and seem still far away. The principle in the calorimetric measurements is to mount the sample in an insulated box equipped with an absorber (the metering box). Next the sample (in the metering box) is exposed to solar radiation and the amount of energy collected in the box is measured. The idea is in other words to collect all the energy that penetrates the sample (i.e. $\tau_e + q_i$) by means of an absorber. The collected energy may be measured by means of an absorber cooled by circulating fluid or by means of heat flux sensors. The experimental g-value is then calculated as the ratio between the net energy flux in to the box (q_{net} , [W/m²]) and the energy flux in the solar radiation (G , [W/m²]) that reaches the sample surface when a zero temperature difference is obtained between the inside and outside environment. If a temperature difference ΔT_n between inside and outside environment occurs the g_{exp} is found from eq. 6-1.

$$g_{\text{exp}} = \frac{q_{\text{net}} + U_{\text{exp}} \cdot \Delta T_n}{G} \quad (6-1)$$

where U_{exp} is the specimen U-value for the experimental conditions. The term experimental conditions covers the actual boundary conditions during the measurement, in this case the laboratory conditions.

In practice a number of circumstances makes the measurements quite a lot more difficult than it sounds:

- At least in Denmark the sun is not very reliable, which makes it more convenient to perform the measurements indoor in a solar simulator. Unfortunately the spectral distribution of a solar simulator will differ from that of the real sun (or from a radiation with a standardised spectrum) and for most coated glazings the impact of differences in radiation spectra on the g-value is not negligible. Furthermore will different coatings have different impacts on the g-value.
- No absorber can absorb all the radiation that reaches it, i.e. even the best absorber will reflect some radiation. Some of the radiation that is reflected from the absorber will be send back from the sample towards the absorber depending on the backside reflectance of the sample. In other words the impact of the absorber reflectance depends also on the sample.
- Internal and external surface heat resistance shall be tuned in order to represent reality or standard conditions. The secondary heat transfer coefficient q_i depends on the surface

resistances and the impact of mis-tuned surface resistances depends on the glazing type: The g-value for an absorbing glazing with a relatively large value of q_i is of course more dependent on the surface resistances than the g-value of a glazing with low absorptance and a corresponding low q_i .

- Temperature difference between inside and outside environment or across the metering box walls will induce energy flows that must be accounted for.
- Edge effects due to the mounting of the sample must be avoided. Two types of edge effects occur: 1) When measuring the g-value of a thick diffusing glazing at oblique angles of incidence radiation can be trapped in the glazing edge resulting in an underestimation of the g-value. 2) If the center of glazing g-value is required the thermal bridge effect of a spacer profile in a multiple layer sample will induce unintended heat flow through the spacer profile.

6.2 Reference conditions

As mentioned in section 4 the g-value depends on the boundary conditions. In the present study it is a goal to develop a method to determine the g-value of glazings and windows at a specific set of boundary conditions. The method can then be used at any set of boundary conditions that can be established in the laboratory. No international standard is yet defined on calorimetric measurements of g-value and it follows of course that neither are the reference boundary conditions for such measurements defined. However standards describing the calculation of g-value for clear glazings at normal incidence on the basis of optical and thermal data do exist (EN410, ISO9050) and it would be natural to define reference conditions for measurements in correspondence with these standards. The reference boundary conditions from the calculation standards are listed in table 6.1. The reference conditions concerning temperature levels correspond to the standard situation for the determination of thermal transmittance, where the inside environment is at about 20°C and the outside environment at about 0°C.

Table 6.1 Reference boundary conditions for determination of g-value by calculation according to EN410.

Property	Reference condition
Solar spectrum	AM1.0 Global
External surface heat transfer h_e	23 W/m ² K
Internal surface heat transfer h_i ¹⁾	$3.6 + 4.4 \cdot \varepsilon_i / 0.837$ W/m ² K
Sample U-value determined at	10°C
Temperature difference between bounding glass surfaces	15 K

¹⁾In the most common cases (uncoated inner glass surface of the sample, $\varepsilon_i=0.837$) this corresponds to $h_i=8.0$ W/m²K also used in ISO/DIS12567, EN673 etc. for determination of window U-values.

Unfortunately in the case of calorimetric measurements of g-value significant problems occur if the boundary conditions in table 6.1 are to be met during the measurements.

- A solar simulator will not be able to radiate a pre-defined spectral distribution like AM 1.0 Global or any other standard spectrum.

- To obtain a surface-to-surface temperature difference of 15 K across the sample will not be applicable for the chosen measuring method as absorption takes place in the sample and the surface temperature will therefor depend on the individual sample. A temperature difference between inside and outside environment of about 20 K could be obtained but is not applicable either as this will result in a relatively large thermal loss through the sample leading to an expected increase in the measurement uncertainty (eq. 6-1). Furthermore establishing a low external temperature will require the construction of an air conditioned box simulating external weather conditions. This can of course be done but at a rather large expense.
- The heat transfer coefficients can in some cases be difficult to control during measurements.

Instead of performing the g-value measurements under conditions corresponding to the reference boundary conditions the physical measurements may be carried out under controlled and known experimental boundary conditions. Subsequently the measured value can be corrected for discrepancies between experimental and reference conditions in order to obtain the reference g-value. It means that for each of the items in the reference conditions list it must be evaluated whether or not the experimental boundary conditions meet the reference requirements and - if not - a correction of the experimental value must be performed. The corrections and the problems involved in performing these corrections are discussed in section 6.7.

In order to perform the physical measurements under conditions as close to the chosen reference conditions as possible it was decided to refer the final g-value to a situation where there is a zero temperature difference between the inside and outside environment. For the solar spectrum it was decided to use the AM1.0 Global as this spectrum is chosen in EN410. For clarity reasons the chosen reference boundary conditions are listed in table 6.2:

Table 6.2 Reference boundary conditions for determination of g-value by calorimetric measurements.

Property	Reference condition
Solar spectrum	AM1.0 Global
External surface heat transfer h_e	23 W/m ² K
Internal surface heat transfer h_i	8 W/m ² K
Sample U-value determined at	Lab. temp. (25-28°C)
Temp. difference between inside and outside environment	0 K

6.3 Measuring devices

When deciding on the design and the operation of a calorimetric test cell a number of parameters must be considered. A few but important parameters are discussed in this section.

6.3.1 Collection of the transmitted energy

Two different approaches for the collection of energy transmitted through a sample into the absorber in the metering box of a calorimetric measuring device apply:

- Heat flux sensors
- Fluid cooled absorber

In the case of heat flux sensors these are mounted in order to measure the energy transfer from a black absorber in the metering box to a thermostatically controlled environment behind the absorber (usually a fluid with a controlled and uniform temperature). By using a number of heat flux sensors local heat fluxes may be detected.

In the case of a fluid cooled absorber the energy collected by the absorber can be determined from measured values of fluid flow rate and temperature difference between the fluid outlet and inlet provided that the heat capacity of the fluid is known. Only integrated values for the whole sample can be obtained. The principle corresponds to that of a solar collector.

6.3.2 Solar simulator

The solar simulator is not a direct part of the calorimetric device but has a large impact on the results directly measured by the device. For solar simulators the following must be considered:

- Spectral distribution of the lamps. As no lamps have a spectral distribution corresponding to the reference spectrum at least the spectral distribution of the lamps should be known in order to facilitate spectral corrections of the measured g-values. Furthermore the simulator spectrum should cover the whole spectrum of the “real” sun i.e. there shall not be any (significant) cut-offs in the spectral interval 300 to 2500 nm. The closer the simulator spectrum is to the reference spectrum the smaller will the necessary spectral correction be.
- Divergence of the radiation from a solar simulator. The radiation from all solar simulator lamps tend to be divergent but there are large differences between different types of lamps and it is possible to (partly) collimate the light by using lenses or special filters in front of the lamps. The impact of solar divergence depends strongly on the sample type: For most plane samples like conventional glazings the impact is small but for more complex types like glazings with incorporated blinds the impact may be significant for some blind positions.

- Variations in the radiation level on the sample. If the radiation level is not constant across the sample surface local and unintended lateral heat flows may occur. Furthermore the density of the energy flux reaching the absorber in the metering box will also be varying and the impact of such local variations on the measured g-value depends especially on the way the transmitted energy is measured. If local heat fluxes are measured (heat flow meters) variations in radiation level can induce errors while integral measurements (fluid cooled absorber) are less sensitive to variations in radiation level.

6.3.3 Surface heat transfer

The external and internal surface heat transfers during measurements should be as close as possible to the reference situation listed in table 6.2. For the external of the sample the heat transfer depends mainly on the convective conditions, on sample surface temperature and sample emissivity and on the “sky” temperature in the laboratory. By generating a wind across the sample the external heat transfer can be controlled.

For the internal of the sample a value of the heat transfer coefficient close to the reference value can be obtained in several ways:

- By designing the metering box with a relatively large room separating the sample and the absorber natural convection will take place inside the metering box. If the absorber emissivity is high the internal heat transfer coefficient will be reasonably close to the reference value. If additional fans inside the metering box are installed the convection here can be controlled allowing low emissivity absorbers to be used but care must be taken to measure the energy input to the fans.
- By using a plane absorber and plane test specimens a small and constant air gap between absorber and sample can be obtained. From known emissivities of the sample and of the absorber, and from known thermal properties of the air the thermal resistance of the gap can be found and the width of the gap adjusted to obtain a specific resistance between the sample and absorber.

In the next section the test facility for g-value measurements that is constructed and used at the Department of Buildings and Energy is described.

6.4 The METSET

The METSET (Measuring Equipment for Total Solar Energy Transmittance) is an experimental device for the determination of total solar energy transmittance (g-value) for transparent materials (see fig. 6.1). The equipment was ready for the first measurements in 1994. Until the start of the present study only uncorrected g-values were measured in the METSET. As a part of this study the facility and the operation of it has been improved in several ways in accordance to the experience obtained.

The METSET can be placed indoors in a solar simulator as well as outdoors in the sun but so far it has only been used indoors. Many types of samples can be tested e.g. glazings, windows, solar shading devices, solar collector covers or transparent glazing systems for solar walls. In figure 6.2 is shown a photograph of the METSET mounted in the indoor solar simulator.

The system consists of an insulated metering box surrounded by an insulated guard box. Inside the metering box five black water cooled absorber plates absorb most of the energy coming through the sample. In a hydraulic loop the fluid temperature and the fluid flow rate are controlled and the inlet and outlet fluid temperatures are measured, as well as the flow rate to determine the absorbed energy. In the solar simulator, different angles of incidence can be obtained by rotating the box around a vertical axis. The ambient temperature is about 25-28°C and cannot be controlled, but five fans can generate airflow with a speed up to 8 m/s parallel to the sample being tested. The preferred (and biggest) size of the sample is 1250 mm × 1500 mm, but smaller samples can also be measured. During measurements the temperature in the inside environment (metering box) is kept at the same level as the outside environment (laboratory) in order to reduce energy flow across the sample with other origin than the radiation from the solar simulator.

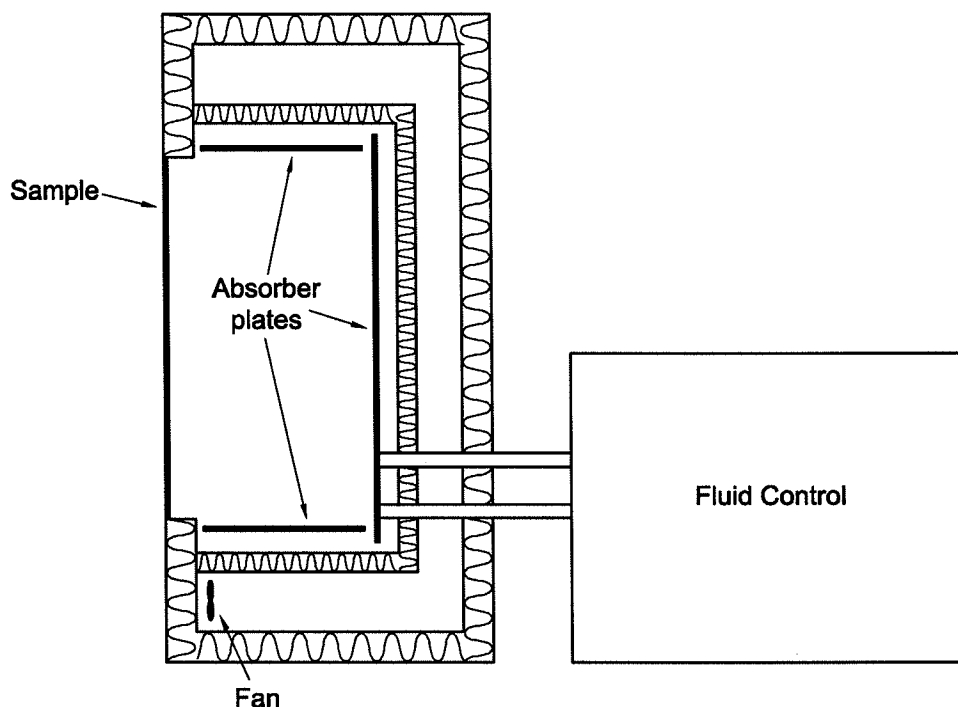


Figure 6.1 Schematic view of the METSET.

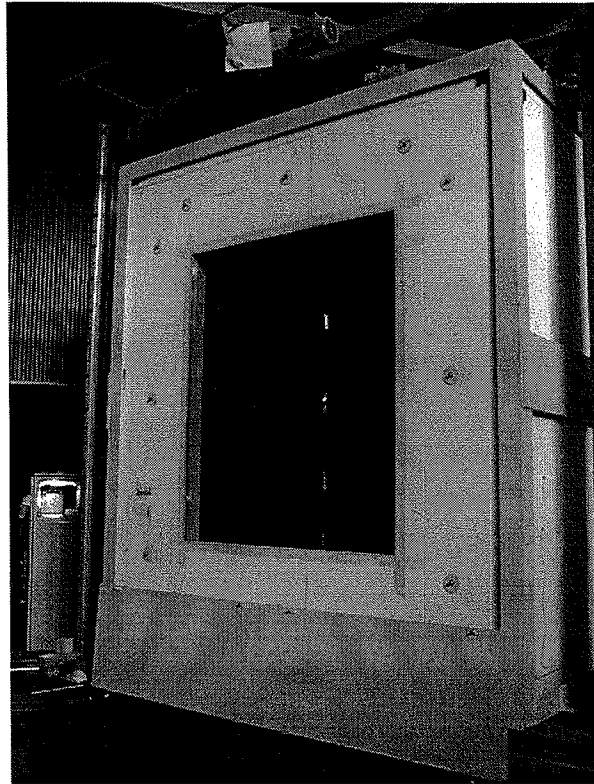


Figure 6.2 *The METSET mounted in the indoor solar simulator.*

6.4.1 Solar simulator

The solar simulator consists of 64 General Electric/Thorn Compact Source Iodide (CSI) 1 kW lamps with no lenses, but clear front glass. In figure 6.3 is shown a front photograph of the solar simulator seen from the sample position.

The overall illuminated test area is 3.0 m × 3.0 m. Within the test area the uniformity of radiation is within $\pm 15\%$ of mean. The array beam divergence half angle is 15° for 91% of the irradiance. The irradiance level is about 800 W/m² measured in the plane of the METSET sample position.

The solar simulator was originally designed for measurement of solar collector performance and for most solar collectors the divergence of the CSI lamps was not considered a problem. (CSI lamps are used in many laboratories for measurements on solar collectors.) However for *g*-value measurements the divergence may be a problem depending on the sample characteristics. For special types of samples like glazings with incorporated micro-lamellas for solar protection the solar transmittance is very dependent on the incidence angle (can drop to zero for an angular change of a few degrees) and special care must be taken when measuring such samples.

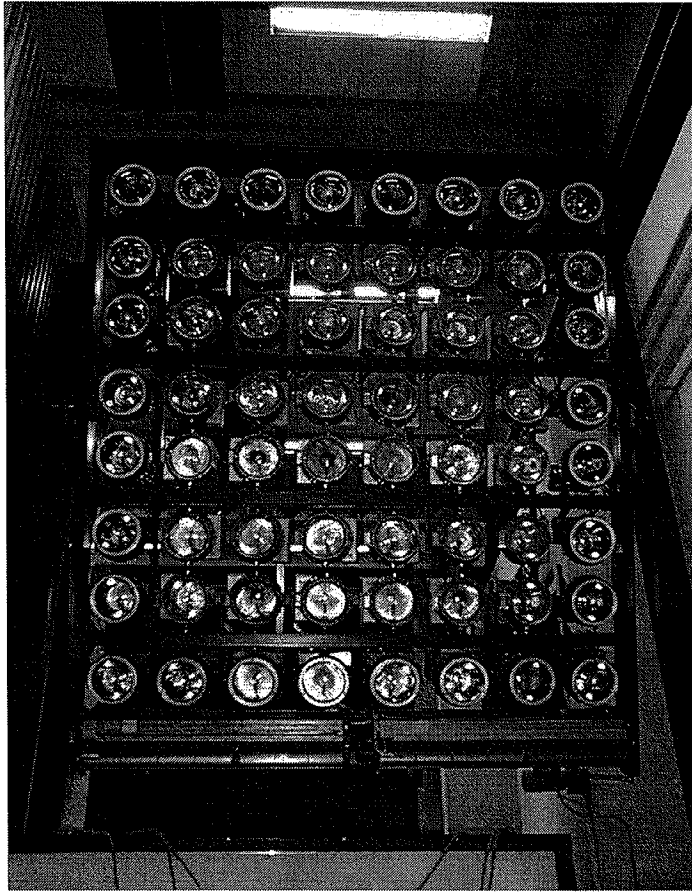


Figure 6.3 Solar simulator, 64 CSI-lamps.

As for other types of solar simulator lamps the spectral distribution varies for each CSI lamp or at least the spectrum varies for lamps with individual age. In order to account for the differences in spectral distribution of the CSI lamps the average spectrum of three CSI lamps with different ages has been measured over the spectral range of 250-1800 nm at the University of Wales, Cardiff. The measured range corresponds to more than 96% of the energy in the solar spectrum. Even though the average of three lamps is considered as a reasonably good approximation to the total simulator spectrum some discrepancies can be expected. As it until now not has been possible to perform in situ measurements of the simulator spectrum over the solar range, the average spectrum measured at Cardiff has been chosen to represent the simulator spectrum at the Department of Buildings and Energy.

The average spectral distribution of the three CSI lamps is compared to the AM1.0 spectrum in fig. 6.4. Spectra shown are normalised.

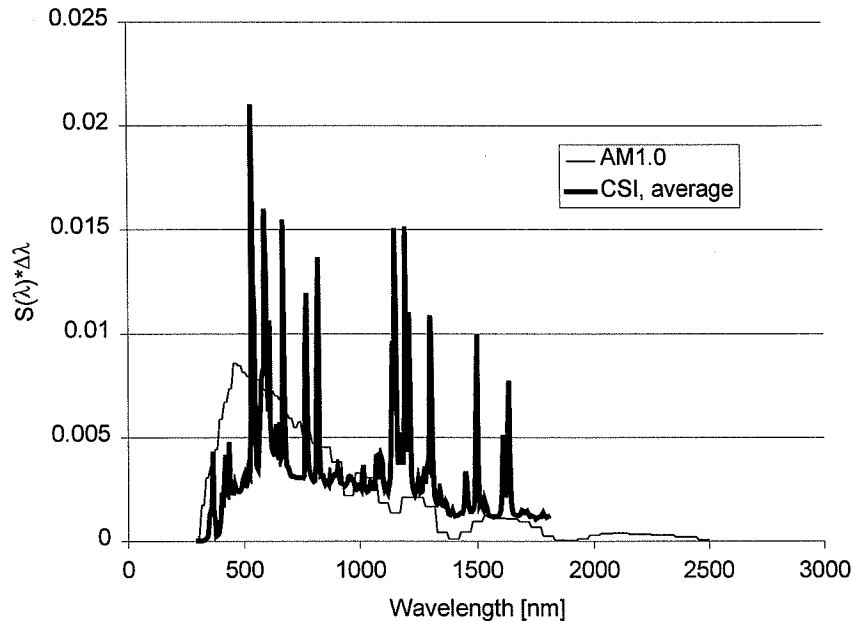


Figure 6.4 Average spectrum of three aged CSI-lamp compared to AM 1.0 (EN 410). CSI lamps measured at University of Wales, Cardiff.

6.4.2 Metering box

The metering box is constructed from 80 mm PUR-elements sandwiched between two 0.5 mm steel plates. As it is desired to allow g-value measurements on samples with non planar surfaces (like windows including frames) the internal surface heat transfer can not be controlled using a fixed distance between sample and absorber (see section 6.3). Instead the metering box has been designed to facilitate natural convection inside the box. The internal dimensions are (height x width x depth) 1800 mm x 1500 mm x 600 mm.

An absorber is installed inside the metering box to cool the air in the box but no fans or heaters are installed. By controlling the fluid inlet temperature to the absorber the air temperature in the metering box is controlled. The temperature difference across the metering box walls is measured by means of thermopiles, each covering equivalent area. The air temperature in the metering box is measured in three levels with thermocouple type T.

Measuring the air temperature under solar irradiation creates the problem of absorption of radiation in the measuring point and in the wires of the thermocouple. In order to choose a measuring technique that shows only little sensitivity to solar radiation five different techniques have been investigated experimentally:

- Thermocouples in vertical single radiation shield tubes made from aluminium
- Thermocouples in vertical double radiation shield tubes made from aluminium
- Thermocouples in vertical single or double radiation shield tubes covered with highly reflecting tape
- Un-shielded thermocouples made from different wire thickness
- Un-shielded thermocouples made from stripped wire of different thickness

The air temperature was measured applying the five different techniques in side-by-side tests under a radiation level of 850 W/m^2 in the indoors solar simulator. The sensors were all mounted inside the metering box of the METSET during g-value measurements on a conventional float glass DGU.

The “most correct” technique is considered to be the one leading to the lowest measured temperature as absorption in the wires and the measuring point of the thermocouple of course will increase the measured temperature. The result was that a thin un-shielded thermocouple with at least 100 mm naked wire gave the most correct result. The thickness of the chosen wire type is 0.1 mm. The worst type (no 1 on the list) measured temperatures up to 5 K higher than the best type. Due to absorption in the aluminium shield the temperature of the shield will raise above the temperature of the surrounding air. Apparently the air-exchange inside the radiation shield tubes is insufficient to remove all the absorbed solar radiation leading to a significant increase in the measured temperature. Wallentén, P., 1998 made similar investigations and came to same conclusion.

An additional advantage of not having the radiation shield tubes is that the solar reflections from the bright shields is avoided. Such reflections result in an underestimation of the g-value, as a (small) part of the incoming radiation never reaches the absorber.

Air temperature in the metering box is measured at three locations in a vertical array. Due to the uniform absorber temperature (see next section) there is only little temperature stratification in the metering box and the readings from the three sensors are within average $\pm 0.5^\circ\text{C}$.

6.4.3 Absorber

The main part of the radiation transmitted through the sample in the metering box is absorbed by the five black absorber elements, based on aluminium plates with integrated copper tubes. The fluid cooled absorber type is chosen as integral values are preferred when measuring g-values of non-planar samples with opaque parts (like windows). Furthermore the integral measurement is less sensitive than heat flux meters to variations in the solar intensity on the sample area. This is relevant as the uniformity of radiation from the solar simulator on the sample is only within $\pm 15\%$ of mean.

The absorber is constructed from a number of solar collector elements from Sunstrip connected in series and painted black using paint with normal high emissivity. The high emissivity is chosen, as the internal surface resistance of the samples should represent reality

during measurements without the use of any fans in the metering box. The fins of the absorber strips are bend towards the back side of the metering box, hereby reducing the absorber fin to 26 mm. The surface temperature of the absorber is measured on the backside (shadow side) by using thermocouples kept in position by means of tape. The number of sensors on the absorber is 16 equally distributed over the total absorber area. During operation a high fluid flow through the absorber is maintained in order to keep the absorber surface at a uniform temperature and to avoid temperature stratification in the metering box. During measurements the absorber temperature is within average temperature $\pm 1^\circ\text{C}$

As the surface of the absorber is rather uneven radiation reflected from the absorber can be considered as diffuse. The shape of the absorber resembles a box with one side left open for the sample. This design improves the solar absorption of the absorber: some of the radiation that is reflected from the absorber surface will be reflected towards other parts of the absorber and absorbed here. The effective reflectance from the absorber is only 2% measured as a mean value across the aperture in the metering box, measured at normal incidence. The absorptance is assumed independent of spectral distribution of irradiance and it is assumed that the reflectance is independent of incidence angle due to the absorber shape but this still remains to be verified.

6.4.4 Guard box

The guard box encloses the metering box and is constructed from 120 mm PUR-elements sandwiched between two 0.5 mm steel plates. The purpose of the guard box is to enable a zero degree temperature difference across the metering box walls. In the design of the guard box it was considered unlikely that the guard box temperature should ever be less than the ambient air temperature. For this reason it is only possible to increase the temperature in the guard box by means of an electrical fan, no cooling device is mounted. However, it has shown that the inside surface temperature of the metering box walls during measurements sometimes is smaller than the air temperature in the guard box. The reason for this is the fact that the absorber temperature has to be less than the air temperature in the metering box - especially for high g-values - and energy is transferred from the metering box walls to the absorber. However as the temperature difference over the walls in general is small $\sim 2\text{K}$ and as the heat exchange coefficient of the metering box furthermore is known from calibrations (4.0 W/K, see section 6.6.2), the energy flow across the metering box walls can be corrected for. For this reason it has not been considered worth installing a cooling device in the guard box.

6.4.5 Measurement of the collected energy

The dominant part of the transmitted energy is absorbed by the five black absorber elements, based on aluminium plates and copper tubes. To determine the amount of absorbed energy the temperature difference between outlet and inlet fluid is measured by means of a calibrated thermopile with ten elements. The mass flow rate is measured directly by means of a very accurate Danfoss MASS1000 or MASS2100 mass flowmeter depending on the actual flow rate. From the measurements the energy collected by the absorber can be calculated from:

$$q_{abs} = \frac{m \cdot \Delta T_f \cdot c_f}{A_{sp}} \quad (6-2)$$

where q_{abs} is the absorbed energy [W/m²]
 m is the mass flow rate [kg/s]
 ΔT_f is the temperature difference between fluid outlet and inlet [K]
 c_f is the specific heat capacity of the fluid at mean fluid temperature [J/kgK]
 A_{sp} is the projected specimen area [m²]

6.4.6 Auxiliary equipment

Five fans are placed in front of the METSET in order to generate a wind parallel to the sample. The maximum wind speed is 8 m/s.

After the *g*-value measurement has been completed the radiation level on the sample surface is automatically measured by three Kipp & Zonen CM11 pyranometers in a grid of 100 mm × 100 mm. By moving the METSET away from the solar simulator, the radiation level can be measured in the same position as the front of the sample had during the *g*-value measurement.

As the solar simulator was originally designed for efficiency measurements on solar collectors it is placed in an elevated rig, see figure 6.5. The windows are tested in vertical position and consequently the minimum angle of incidence is 22.5°, corresponding to a solar height of 22.5° and an azimuth of 0°. Higher angles of incidence can be obtained by rotating the METSET around a vertical axis, corresponding to different values of azimuth and a constant solar height of 22.5°.

Solar simulator

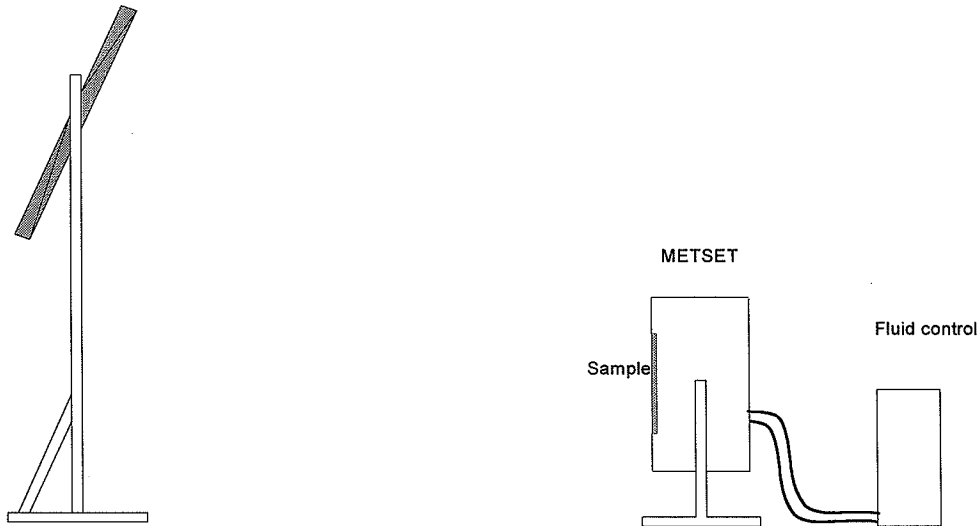


Figure 6.5 Schematic view of the METSET placed in the solar simulator

6.4.7 Technical Characteristics Summary

Solar simulator:

Type of lamp:	General Electric/Thorn CSI 1000 C
Number of lamps:	64
Average lamp lifetime:	1000 hours
Irradiance level:	800 W/m ²
Uniformity:	±15% of mean
Collimation:	91% of incident radiation within ±15° semiangle
Test area:	3.0 m × 3.0 m

Calorimeter

Max sample size:	1250 mm x 1500 mm
Preferred sample size:	1250 mm x 1500 mm
Air speed	0 - 8 m/s
Ambient temperature	not controlled, about 25-28°C
Absorber plates	modified Sunstrip with fin width 26 mm
Coating	black painting, high emissivity

Main instrumentation:

Global radiation	Kipp & Zonen pyranometer CM11
Air temperatures	unshielded 0.1 mm thermocouples type T
Outlet - inlet	thermopiles
Water flow rate	Danfoss MASS 1000 or 2100 mass flowmeter
Air speed	Vane probe anemometer

6.5 Measuring procedure, METSET

The test sample is placed in the METSET and the test rig is exposed to solar radiation in the indoors solar simulator. The absorber in the METSET is connected to the fluid control system. This system serves two purposes:

1. it circulates fluid through the absorber in the METSET extracting and measuring the energy that is absorbed by the absorber
2. by controlling the fluid temperature at the inlet to the absorber it controls the temperature of the environment in the METSET metering box. The inlet temperature can be controlled manually or automatically by a computer

During the test, the temperatures in the metering box and in the guard box are controlled in order to avoid or at least reduce the heat flow across the test sample and across the metering box walls.

Once every minute all measurements are carried out and recorded by a computer.

The directly measured *g*-value (g_m) is found from the measured energy input, q_{abs} [W/m²]:

$$g_m = \frac{q_{abs}}{G} = \frac{m \cdot \Delta T_f \cdot c_f}{G \cdot A_{sp}} \quad (6-3)$$

where A_{sp} is the sample area.

$g_m = q_{abs}/G$ is not the final g-value for the test sample. Several corrections of the value have to be carried out, and depending on the type of sample and measuring conditions some or all of the following factors have to be accounted for:

- Heat flow across the test sample due to temperature difference between inside and outside environment
- Heat flow across the metering box walls
- Heat flow through the edge zone of the sample. (If the g-value for the center of sample is requested, a correction for the energy flow through the edge of sample must be carried out).

After correcting for these three factors the experimental value for the total solar energy transmittance (g_{exp}) is obtained. g_{exp} refers to the total solar energy transmittance obtained under the experimental conditions in the laboratory. In order to relate the g-value to reference conditions the following factors must be accounted for:

- Difference in the spectral distribution between the standard solar radiation (AM1.0 Global) and the solar simulator (CSI-lamps)
- Reflection from the absorber in the METSET
- Difference in the surface heat transfer coefficients h_i and h_e from the standard coefficients ($h_i = 8$ and $h_e = 23$ W/m²K)
- Difference in sample resistance for experimental and reference conditions

In sections 6.6 and 6.7 the correction to experimental and to reference conditions are described.

6.6 Determination of the g-value for experimental conditions (g_{exp})

Reduction of the directly measured data to useful experimental results involves the correction for three unintended heat flows during the measurements:

- Heat flow through the sample due to a temperature difference between inside and outside environment. (In practice a temperature difference will occur even if efforts are done to prevent this). This heat flow is a function of specimen U-value (U_{sp}) and temperature difference between inside and outside environment (ΔT_n).
- Heat flow through the metering box walls. This heat flow is due to a temperature difference across the metering box walls and depends on the heat exchange coefficient of the metering box (H_{mb}) and the temperature difference across the wall (ΔT_{mb}). The temperature difference can be controlled and kept very close to zero if the guard box is air-conditioned.
- Heat flow through the edge of the glazing (Q_{edge} , [W])). Measuring the integrated energy transmitted through a multilayer sample with a cold bridge effect in the edge zone means that edge effects will be included in the result.

g_{exp} is found from:

$$g_{exp} = \frac{m \cdot c_f \cdot \Delta T_f + U_{sp} \cdot A_{sp} \cdot \Delta T_n + H_{mb} \cdot \Delta T_{mb} + Q_{edge}}{G \cdot A_{sp}} \quad (6-4)$$

In the next three sections the procedures for these corrections are discussed

6.6.1 Correction for heat flow across the test sample

To make this correction the U-value of the test sample has to be known for the experimental conditions. I.e. the U-value must be known for the actual temperature difference between inside and outside environment and at the mean value of these temperatures. As “sky” temperature and air temperature are generally different during the g-value measurement the environmental temperature must be applied (see also section 5.3 or 6.7.4). As the U value describes the thermal property of the sample under “dark” conditions the U value of the sample must be determined for conditions corresponding to the experimental conditions but without solar radiation.

The U-value of the specimen can be found from calculations if a physical model describing the heat flow through the sample is available. If no model is available the thermal transmittance can be measured using a hot box device or a hot plate device depending on the sample type. In this case it may be difficult to obtain the U-value for conditions corresponding to the experimental conditions in the g-value measurement. However as the temperature difference between the inside and outside environments can be held close to zero during the tests the correction is in general small and the precise U-value for the specimen is not critical as the following example shows:

If a measurement on a 1.25x1.5 m sample with a U-value of 3 W/m²K and a g-value of 0.5 is carried out in the METSET with a temperature difference between inside and outside environment of 2K the energy input coming through the test sample will be in the range from 420 W to 750 W depending on the angle of incidence. (The radiation level at an incidence angle of 60° is roughly 450 W/m² and 800 W/m²K at an incidence angle of 22.5°). The energy flow through the test specimen induced by the temperature imbalance will be 11 W or between 1% and 3% of the energy input from the solar simulator. That means that even if the correction is carried out with large uncertainty the impact on the final result is small.

6.6.2 Correction for heat flow across the metering box walls

The heat exchange coefficient of the metering box (H_{mb}) has been found by calibrations under “dark” conditions:

First a calibration sample with large and known thermal resistance was mounted in the METSET. Next the metering box was heated up by means of the hydraulic loop until a condition of steady state was reached. The energy input to the metering box from the hydraulic loop was known together with the heat flow through the calibration sample and now the heat flow through the metering box walls can be deduced. The energy input from the hydraulic loop was about 75 W, the energy flow across the calibration sample roughly 20 W and the remaining 55 W was the heat loss through the metering box walls, leading to a heat exchange coefficient of 4.0 W/K.

As the temperature difference over the metering box walls in general is small (~2K) and since the heat transfer coefficient is well known the impact of temperature imbalance across the metering box walls on the final g-value is very small.

6.6.3 Correction for heat flow through the sample edge

The edge-construction in a glazing consisting of two or more layers separated by a spacer profile has an impact on the g-value of the glazing, measured directly by a calorimetric device like the METSET. This is due to the integral measurement of transmitted energy in the fluid cooled absorber. In some cases it is the center g-value of a glazing that is desired and the energy flow through the spacer should in such cases be avoided. The energy flow through the edge of the sample can be avoided or at least significantly reduced by mounting insulation on the glazing edges inside and outside during the measurement. However by doing so the aperture in the glazing will be reduced resulting in a reduced energy flow into the metering box. Especially if no insulation is applied on the glazing edges (inside and outside) during measurements, heat will be transferred by conduction through the glass panes and through the spacer. The amount of energy transferred and the direction of the energy flow depend on the construction of the glazing (types of glass, coatings, gas and spacer) and on the interior and exterior boundary conditions during the measurements. Depending on the situation the g-value for the center part of a sample may be requested and if so the heat flow through the spacer profile is a source of error. The present section gives a way to quantify the thermal bridge effect due to the spacer in a double glazed unit (DGU). An evaluation of

the amount of energy transferred through the spacer in two different glazings is also given in order to establish the maximum error that will result if no insulation is applied on the edge of glazing during measurements.

Equations

The heat flow through the spacer can be calculated by treating each glass pane as a fin with base at the spacer and by using a number of assumptions. In figure 6.6 is shown the heat flow through the edge construction in a DGU where the outer glazing is warmer than the inner.

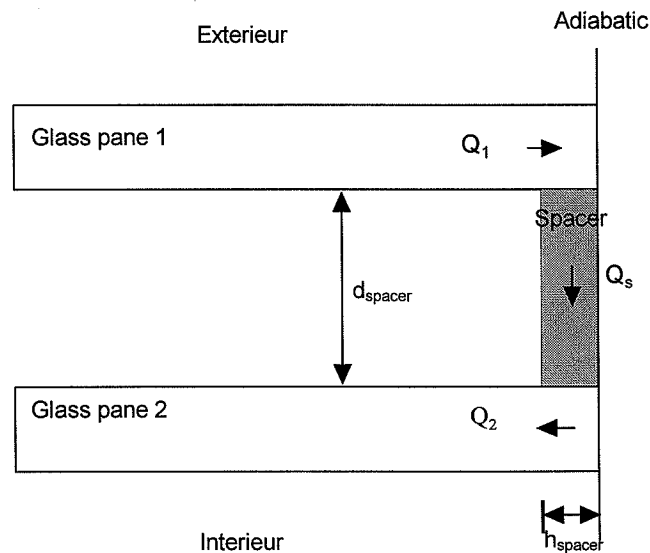


Figure 6.6 Heat flow through edge of glazing. Q_1 , Q_2 and Q_s denotes the heat flow [W] in glass pane 1 and 2 and through the spacer respectively.

The assumptions are:

- There is no “horizontal” heat flow through the spacer in figure 6.6
- There is no “vertical” temperature gradient across the two glass panes.
- The space between the glass panes is replaced by a solid material with an equivalent thermal conductivity (corresponding to the method in prEN10077-2)
- The external and internal heat transfer coefficients h_e and h_i are both constant
- There exist a plane halfway between the glass panes where the temperature is constant θ_m
- $Q_1 = Q_2 = Q_s$ (see figure 6.6)

In figure 6.7 is shown the heat balance for a segment of the outer glass pane.

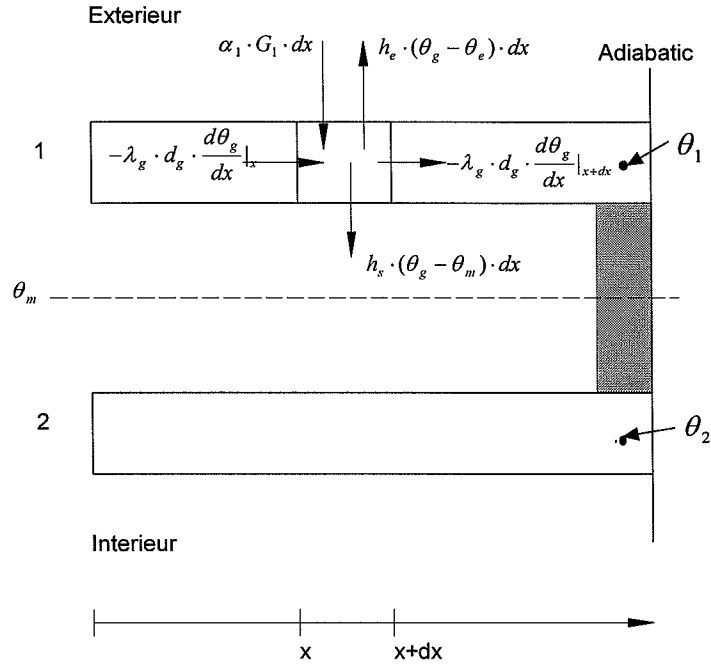


Figure 6.7 Heat balance of a segment in a glass fin. θ_1 and θ_2 represents the temperatures at the base of the fins

The energy balance for the segment in figure 6.7 can be written as:

$$\alpha_1 \cdot G_1 \cdot dx - h_e (\theta_g - \theta_e) \cdot dx - h_s \cdot (\theta_g - \theta_m) \cdot dx + (-\lambda_g \cdot d_g \cdot \frac{d\theta_g}{dx} | _x) - (-\lambda_g \cdot d_g \cdot \frac{d\theta_g}{dx} | _{x+dx}) = 0 \quad (6-5)$$

where α_1 is the solar absorptance of pane 1
 G_1 is the solar irradiance on pane 1 [W/m²]
 h_e is the outside surface heat transfer coefficient [W/m²K]
 h_s is the heat transfer coefficient from the outer glass pane to the plane halfway between the glass panes [W/m²K]
 θ_g , θ_e and θ_m are respectively the temperatures of the glazing segment, the outside environment and the plane between the glass panes [°C]
 λ_g is the thermal conductivity of the glass [W/mK]
 d_g is the thickness of the glass [m]

On the basis of eq. 6-5 Q_1 , Q_2 and Q_s can be found in appendix E.

Examples

Two different examples have been calculated for conditions similar to the experimental conditions in the METSET. The two examples are imaginary and are both describing clear (non-diffusing) DGU's with the optical properties shown in table 6.3 (example 1) and table

6.4 (example 2) (index 'exp' denotes optical properties for CSI solar spectrum). Other parameters used in the calculations are shown in table 6.5.

Table 6.3 Optical properties of example 1, solar absorbing coating in position 2.

	Outer pane (g1)	Inner pane (g2)
τ_{exp}	0.4	0.84
ρ_{exp}	0.3	0.08
α_{exp}	0.3	0.08

Table 6.4 Optical properties of example 2, solar absorbing coating in position 3.

	Outer pane (g1)	Inner pane (g2)
τ_{exp}	0.84	0.4
ρ_{exp}	0.08	0.3
α_{exp}	0.08	0.3

The two examples have been chosen, as they will result in relatively large heat flows through the spacers due to the large difference in solar absorptance in the two glass layers. In figure 6.8 is shown the calculated heat flow through the spacer as a function of the spacer conductance. The spacer conductance Λ_s is calculated from:

$$\Lambda_s = \frac{\lambda_{\text{spacer}}}{d_{\text{spacer}}} \cdot h_{\text{spacer}}$$

where λ_{spacer} , h_{spacer} and d_{spacer} are the equivalent thermal conductivity, the height and the width of the edge profile including the spacer.

Heat flow is calculated per meter periphery of the glazing.

It appears that for spacer conductance larger than 1 W/mK only small increase in the heat flow occurs. The reason for this is that for a small spacer resistance the resistance in the glass fins will be dominant. Note that for example 1 the heat flow through the spacer results in an overestimation of the g-value, for example 2 the opposite is the case.

Of course the resulting error in g-value depends very much on the sample size and for a spacer conductance of 2 W/mK the relative error as function of sample size has been drawn in figure 6.9 for the two investigated examples. A spacer conductance of 2 W/mK corresponds to a typical edge construction with aluminium spacer.

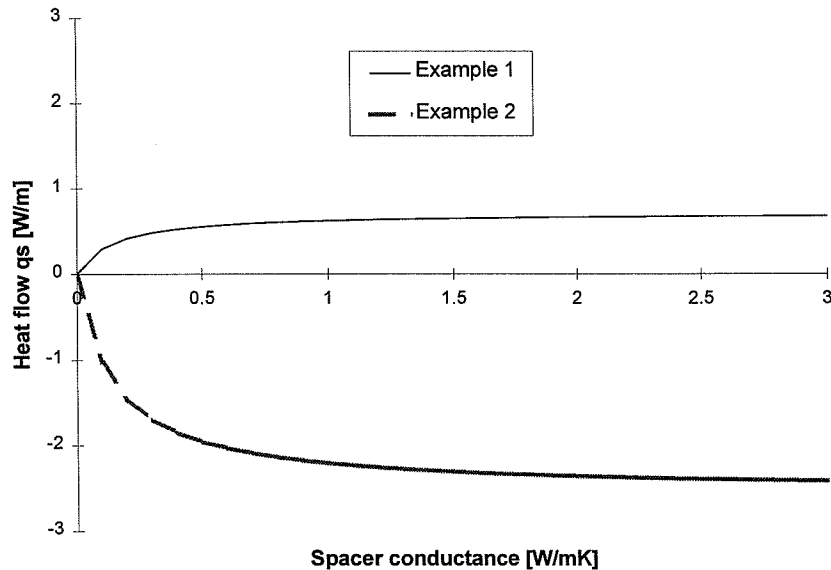
Table 6.5 Other parameters for the calculations of example 1 and 2. Indices 1 and 2 indicate glazing layer, e.g. G_1 is irradiance on layer 1

	Example 1	Example 2
d_{g1}	6 mm	4 mm
d_{g2}	4 mm	6 mm
g-value ¹⁾	0.38	0.56
U_{center}	1.5 W/m ² K	1.5 W/m ² K
h_s	4 W/m ² K	4 W/m ² K
h_i	7.7 W/m ² K	7.7 W/m ² K
h_e	23 W/m ² K	23 W/m ² K
G_1	800 W/m ²	800 W/m ²
G_2 ²⁾	320 W/m ²	672 W/m ²
θ_i	25°C	25°C
θ_e	25°C	25°C
W ³⁾	1.25 m	1.25 m
d_{spacer}	16 mm	16 mm
h_{spacer}	10 mm	10 mm
λ_g	1 W/mK	1 W/mK

¹⁾ g-value is the center of glazing value calculated in WINDOW 4.1.

²⁾ G_2 is calculated simple as $\tau_1 * G_1$, not taking reflections between the glass panes into account.

³⁾ The width (W) of the sample is here 1.25 m corresponding to the maximum sample size.



The calculations are not very sensitive to the value of W.

Figure 6.8 Heat flow through spacer vs. spacer conductance for two glazing examples. Heat flow is calculated as Watt per meter of glazing periphery and for the conditions listed in table 6.5

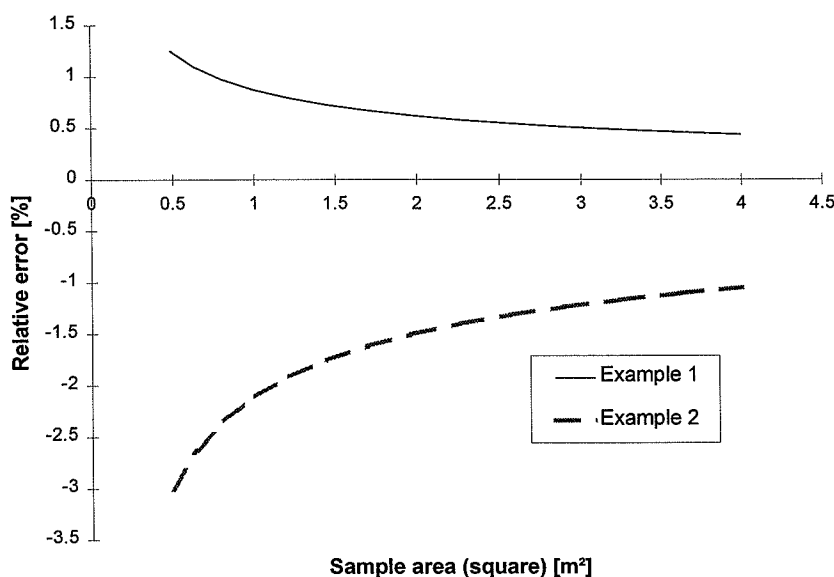


Figure 6.9. Relative error in g-value vs. sample size for examples 1 and 2 for the conditions listed in table 6.5. Spacer conductance is 2 W/mK.

Discussion

If the center of glazing g-value is desired, the calculations carried out here show a relative error in the order of 1-2% due to heat flow through the spacer when the edge of a 1x1 m DGU is exposed during measurements. The calculations are based on several assumptions but indicate that the thermal effects of the sample edge only introduce minor errors in the final center of sample g-value. For samples including materials or design with unknown thermal and optical properties the correction may have to be based on further assumptions. This is acceptable, as the correction is not critical for the final g-value.

The examples shown here are more critical for errors than conventional DGU's with or without low-e coatings, but glazings constructed from glass panes with even larger difference in solar absorptances may occur and the potential error in g-value for these glazings will of course increase. Nevertheless it seems that the error in general is small and may be corrected for by calculation following the procedure outlined in this section.

6.7 Determination of the g-value for reference conditions (g_{ref})

6.7.1 General

If a physical model of the solar and thermal transmittance through the sample is available corrections can be performed in accordance to model calculations using the relevant boundary

conditions. (ISO9050 and EN410 include a model describing clear glazings for normal incidence). Input for such models include optical and thermal data for all parts in the sample. For each sample the correction can be found from:

$$\text{Correction}(\text{sample}) = g(\text{reference}) - g(\text{experimental})$$

where $g(\dots)$ denotes the g-value of the sample calculated with the model for reference and experimental boundary conditions respectively. The correction can be divided into four parts corresponding to the parameters that need to be corrected for: Absorber reflectance, solar spectrum, surface heat transfer coefficients and sample resistance. The solar spectrum has an impact on both the τ part and the q_i part of the g-value and it may be useful to analyse these two quantities separately. As an example the correction of the direct solar transmittance part can be written: (index 'ref' is for standard solar spectrum (table 6.2), index 'exp' is for simulator spectrum)

$$\text{Correction}(\tau) = \tau_{\text{ref}} - \tau_{\text{exp}}$$

In other words the difference between solar transmittance for reference and for experimental conditions is calculated and this value denotes the spectral correction of the solar transmittance. If a physical model describing the sample is available it may be of limited interest to perform measurements especially since the calculations have to be performed for the corrections. However in some cases (e.g. if the optical data measured by spectrometer are more uncertain than the calorimetric determination of g_{exp}) the accuracy in the g-value determination can be improved by performing calorimetric measurement and correct these afterwards using the physical model. In this study the emphasis is put on the case where no physical model is available since this is the general case for complex samples.

If no physical model for solar and thermal transmittance is available the reduction of experimental results to reference results may be based on simplified models using assumptions for unknown elements. In order to evaluate such simplified models with regards to correction of g-value measurements it is very valuable to know which elements of the measurements introduce large needs for corrections and which elements are less critical.

It must also be kept in mind that the outcome of a successful g-value measurement describes the sum $g = \tau_e + q_i$. The direct solar transmittance τ_e can in far the most cases be found from optical measurements. Even for complex glazings this can be done in several ways: Spectrophotometer equipped with a (large) integrating sphere, photo goniometer performing spectral measurements or - most simple - out-door broadband measurements (the latter does not give the transmittance for a specific solar spectrum). That means that when large effort is put into the calorimetric measuring of the g-value it is actually the secondary heat transfer towards the inside (q_i) we are trying to measure. q_i depends on the solar absorption and the thermal resistance network in the sample together with the surface heat resistances. Instead of the expression for q_i used in the EN410 and ISO9050 (see also section 4.4) q_i may be written in a general form as (Rosenfeld, 1996):

$$q_i = \frac{(R_e + \gamma \cdot R_g) \cdot \alpha_g}{R_t} \quad (6-6)$$

where R_e , R_g , and R_t are external heat resistance, resistance of the sample and total air to air resistance of the sample

γ is a non dimensional number between 0 and 1 indicating the plane in the sample at which all solar absorption could be referred to, resulting in the same heat flows and temperature gradients in the model sample as in the physical sample.

α_g is the solar absorptance of the complete sample.

If all required data are available the number γ can be calculated directly corresponding to EN410 or ISO9050 but a large force of the formalism in eq. 6-6 is that also with knowledge to only parts of the data meaningful estimates of γ may be made.

In the next three sections correction procedures intended to reduce experimental values to reference results are presented.

6.7.2 Correction to reference boundary conditions

The radiation from the solar simulator has a spectral distribution that differs from that of the standard AM 1.0. The impact of this difference depends on the type of material that is used in the test sample. If the sample is a window made of low iron glass without any coatings the impact is very small. If the sample is a window with solar protection or other coatings with selective properties the impact may be rather large.

The solar spectrum has influence on both the τ part and the q_i part of the g-value and the two quantities have to be treated separately. For most cases the transmittance part will be dominant and the correction of the solar transmittance part is:

$$Correction(\tau) = \tau_{ref} - \tau_{exp}$$

τ_{ref} is the solar transmittance for the reference solar spectrum and τ_{exp} is the transmittance for the solar simulator spectrum (experimental conditions). If a model describing the optical properties of the sample is available together with relevant optical data (transmittance and reflectance for all elements in the sample) τ_{ref} and τ_{exp} can be calculated directly. If no model is available the correction of τ has to be based on optical measurements on the sample as described in section 6.7.1 and chapter 7.

The quantity of q_i is more complex as q_i depends on both optical and thermal properties of the sample plus the interior and exterior heat transfer coefficients. A model capable of describing optical as well as thermal transmission through the sample is needed to perform a correction from $q_{i,exp}$ to $q_{i,ref}$. If such a physical model is available the correction of q_i can be calculated directly provided that the relevant optical and thermal data are available.

For complex samples more empirical methods have to be considered and the formalism described by (Rosenfeld, 1996) (eq. 6-6) is useful in this approach. In eq. 6-6 all quantities except γ can usually be found by measurements and γ can be deduced by rewriting 6-6:

$$\gamma = \frac{q_i \cdot (R_e + R_g + R_i)}{\alpha_g \cdot R_g} - \frac{R_e}{R_g} \quad (6-7)$$

The ideal absorber has an absorptance $\alpha = 1$. However it is difficult to obtain an absorptance above 0.95-0.97 and since there is no transmittance of radiation through the absorber, 3-5% of the radiation that reaches the absorber is reflected. Some of the reflected radiation is trapped in the metering box (due to the geometry of the absorber as well as of the metering box) and measurements carried out on the METSET show that about 2% of the radiation that reaches the absorber is reflected through the aperture of the METSET. Of these 2% some radiation will through multiple reflections be re-reflected into the metering box because of the reflectance of the test sample, some will be absorbed in the test sample and partly transferred to the metering box as secondary heat gain and finally some will be transmitted through the test sample. This means that during the calorimetric measurements the amount of reflected radiation that is absorbed in the sample will result in an overestimation of the g-value. On the other hand the amount of radiation that is transmitted through the sample will result in an underestimation of the g-value. The correction must take into account all parts. As the radiation reflected from the absorber is considered diffuse the optical properties for diffuse radiation (transmittance and reflectance) on the backside of the sample must be known. In order to perform the proper correction the resulting transmittance ($\tau_{exp,res}$) and resulting absorptance ($\alpha_{exp,res}$) including the effects of the multiple reflections between sample and absorber must be calculated for experimental conditions:

$$\tau_{exp,res} = \frac{\tau_{exp}}{1 - \rho_{exp,dif}^b \cdot (1 - \alpha_{exp,abs})}$$

$$\alpha_{g,exp,res} = \alpha_{g,exp} + \tau_{exp,res} \cdot (1 - \alpha_{exp,abs}) \cdot (1 - \tau_{exp,dif} - \rho_{exp,dif}^b)$$

where $\alpha_{exp,abs}$ is the absorptance of the absorber in the METSET (= 0.98)

$\rho_{exp,dif}^b$ is the backside diffuse reflectance of the sample

$\tau_{exp,dif}$ is the diffuse transmittance of the sample

All for experimental boundary conditions

For experimental conditions γ_{exp} can now be found from:

$$\gamma_{exp} = \frac{q_{i,exp,res} \cdot (R_{e,exp} + R_{g,exp} + R_{i,exp})}{\alpha_{g,exp,res} \cdot R_{g,exp}} - \frac{R_{e,exp}}{R_{g,exp}}$$

where

$$q_{i,exp,res} = g_{exp} - \tau_{exp,res} \cdot \alpha_{exp,abs}$$

If no other (more precise) models of the sample are available a useful - but physically incorrect - approach is to assume that the value of γ is the same for reference as for experimental boundary conditions. The secondary heat transfer coefficient for reference conditions ($q_{i,ref}$) can then be calculated by means of eq. 6-6 using the experimental value for γ and the reference values for the other parameters in the equation. It must be stressed out that this is not correct from a physical point of view as γ is a function of solar spectrum, of the thermal resistance network in the sample and of the surface heat transfer coefficients. However by keeping the internal and external heat transfer coefficients close to the reference values during measurements some of the errors introduced by the simplified correction method can be eliminated.

6.7.3 Effect of the surface heat transfer coefficients

The surface heat transfer coefficients (h_i and h_e) have an influence on the secondary heat transfer factor q_i . If the panes in the test specimen are non-absorbing or with only little absorptance q_i is relatively small and therefor also the impact of h_i and h_e on the final g-value is small. Objects with no or only small absorptance include a number of transparent plastic materials, low iron glass and to a certain extend also ordinary float glass. If on the other hand an absorbing layer is included in the construction, the impact of h_i and h_e on the final g-value may be significant. This will be the case when a glazing includes a low emissivity coating and especially if the glazing is a solar control type with relative high absorptance in the outer layer and a low g-value. By using the calculation method from ISO9050, EN410 the impact of h_i and h_e on the final g-value has been investigated for three glazing types:

- a conventional float glass DGU without coatings or gas filling
- a double glazed unit of solar control type with an absorbing glass layer with low solar transmittance placed outermost in an Argon-filled glazing.
- a double glazed unit with low-e coating in position 3 and Argon filling

The three glazings are imaginary but with properties considered “typical” for the different types. Key parameters for the three investigated glazings are given in table 6.6

Table 6.6 Key parameters for three glazing examples. U-values calculated in WINDOW 4.1, τ and g calculated by ISO9050.

	Float glass DGU	Solar control DGU	Low-e coated DGU
$\tau_{\text{layer 1}}$	0.84	0.40	0.84
$\tau_{\text{layer 2}}$	0.84	0.84	0.60
$\rho_{\text{layer 1}}$	0.08	0.30	0.08
$\rho_{\text{backside, layer 1}}$	0.08	0.30	0.08
$\rho_{\text{layer 2}}$	0.08	0.08	0.20
$\alpha_{\text{layer 1}}$	0.08	0.30	0.08
$\alpha_{\text{layer 2}}$	0.08	0.08	0.20
U_{center} [W/m ² K]	2.9	1.5	1.5
τ_{glazing}	0.71	0.34	0.51
g_{glazing}	0.77	0.43	0.68

In figure 6.10 is for each of the three glazing types shown the calculated g-value as function of h_e and h_i respectively. Also shown in the figure are the relative errors connected to a mis-tuning of the surface coefficient relative to the standard coefficients. The largest potential errors are very dependent on the glazing type and the largest errors occur not surprisingly in situations where a layer with high absorptance is involved in the construction and especially where the surface heat transfer coefficient adjacent to this layer is mis-tuned. This means that the surface heat transfer coefficient adjacent to an absorbing layer is more critical than the surface heat transfer coefficient adjacent to a layer with little solar absorptance.

From figure 6.10 it also shows that for the same absolute errors in surface coefficients the error in g-value is larger in cases where the surface coefficients are too small than in cases where they are too large. In other words rather a surface heat transfer coefficient that is too large than too small.

Though the calculations presented here are performed for relative simple samples, the conclusions stated do also apply for more complex samples.

External heat transfer h_e in the METSET

The external heat transfer coefficient h_e during the measurements is the result of convective and radiative heat transfer components. The wind speed, the sample surface temperature, the sample surface emissivity and the indoor sky temperature determine h_e . As the solar simulator surface is heated well above the ambient air temperature the resulting indoor sky temperature in the laboratory is higher than the air temperature and in general much higher than the outdoor sky temperature. The indoor sky temperature in the laboratory during operation of the solar simulator has been measured and found to 32-34°C (Espersen & Weibøl, 1994). The air temperature in the laboratory is in the range of 25-28°C depending on the season (warm in the summertime). The surface heat transfer from the sample surface to the ambient consists of a radiative and a convective part. The former relates to the temperature difference between the sample surface and the sky temperature and the latter relates to the temperature difference between sample surface and air temperature.

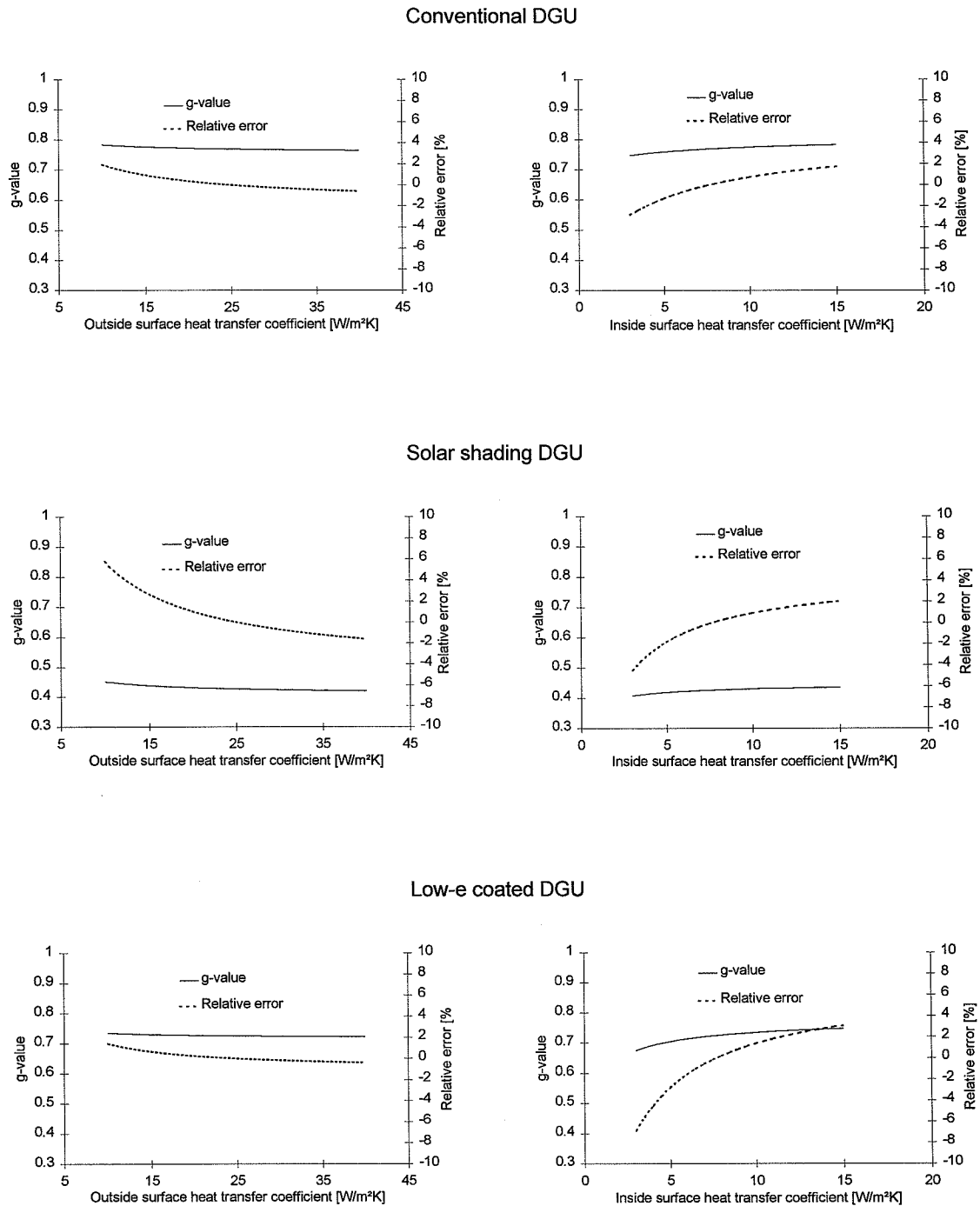


Figure 6.10

Calculated g-value versus outside and inside surface heat resistance (primary axis). Also shown is the relative error in g-value that results from mis-tuned surface heat resistances (secondary axis). Calculations performed in accordance to ISO 9050. Reference values of h_e and h_i are $23W/m^2K$ and $8W/m^2K$ respectively.

As the indoor sky temperature is different from the air temperature the two heat transfer parts cannot both be referred to neither air nor indoor sky temperature. Instead the environmental temperature T_n can be used:

$$T_n = \frac{h_c \cdot T_c + h_r \cdot T_r}{h_c + h_r} \quad (6-8)$$

where h_c and h_r are the convective and radiative part of the heat transfer coefficient [W/m²K]
 T_c is the air temperature [K]
 T_r is the mean radiant temperature of the surfaces “seen” by the sample [K]

h_r can be found analytically from known surface temperatures and emissivities and h_c can be found from empirical expressions or by experiments.

The external convective heat transfer coefficient $h_{c,e}$ for the test conditions in the METSET has been found by calibration measurements: A measurement with a calibration panel mounted in the METSET has been performed under dark conditions (no sun). Warm fluid is circulated through the absorber in the metering box until a steady state situation (where the temperature inside the metering box is above the laboratory temperature) is reached. It is assumed that the surface temperature of the surroundings “seen” by the sample surface equals the air temperature as the calibration is performed under dark conditions. From the known thermal resistance of the calibration sample, the surface temperatures of the sample and the air temperature the total external heat transfer coefficient can be found. The air speed across the external surface of the sample is adjusted to ~5.5 m/s and the convective heat transfer coefficient is calculated to 17 W/m²K. This value is assumed to be constant even under solar conditions as the convective heat transfer mainly is dependent on the air speed. Under solar conditions the indoor sky temperature has been measured to about 33°C. Using the procedure given above the external radiative heat transfer coefficient $h_{r,e}$ and the external environmental temperature $T_{n,e}$ can be found from measurement of sample surface temperature $T_{s,e}$ during measurements, leading to the over all external heat transfer coefficient h_e :

$$h_e = (q_r + q_c) / (T_{s,e} - T_{n,e})$$

where q_r and q_c are radiant and convective heat flow [W/m²]

This value relates to the difference between sample surface temperature and external environmental temperature. The quantity of h_e during the measurements depends on the specific conditions but is in the region of 22-23 W/m²K.

The two main sources of error to this value is 1) the measured surface temperature of the sample under radiation and 2) the measured indoor sky temperature. As the indoor sky temperature is included in the calculation of both the radiative heat transfer and the calculation of the environmental temperature even large uncertainty in this number will not

affect the final h_e value greatly. The resulting uncertainty in h_i is therefore mainly dependent on the measurement of sample surface temperature.

Internal heat transfer coefficient h_i in the METSET

h_i is calculated as a convective and radiative part, $h_{c,i}$ and $h_{r,i}$. As natural convection takes place inside the metering box the value of $h_{c,i}$ depends on the temperature of the sample during measurements and the results from the calibrations are not generally valid. Instead the convective heat transfer may be found by an empirical correlation found for vertical plates: (Incropera and de Witt, 1990 p.500 with data for atmospheric air)

$$h_{c,i} = q_c / (T_{s,i} - T_{c,i}) \approx 1.47 * (\Delta T / l)^{0.25}$$

where q_c is the convective heat flux [W/m²]
 ΔT is the temperature difference between sample surface and air temperature [K]
 l is the sample height [m]

This empirical correlation is found for laminar flow. For some samples with high absorptance in the inner layer a shift to turbulent flow may occur if the sample height is more than 1 m. The effect of such a shift has not been evaluated in the present study but it is expected that the uncertainty in the correlation used later will cover the effect.

The radiative heat flux q_r is calculated under the assumption that the inside sample surface can see nothing but the absorber.

$$h_{r,i} = q_r / (A_{sp} * (T_{s,i} - T_{absorber}))$$

On the basis of $h_{r,i}$ and $h_{c,i}$ the inside environmental temperature $T_{n,i}$ is found using the same approach as described above for $T_{n,e}$ (eq. 6-8).

The summarised internal heat transfer h_i is calculated as

$$h_i = (q_r + q_c) / (T_{s,i} - T_{n,i})$$

The final h_i -value during measurements depends on the conditions but varies in the range from 6 to 8 W/m²K. Only the center part of the sample is considered as this represents about 80% of sample area for the standard sample size.

The main sources of error to the h_i value are concentrated on the measurements of sample surface temperatures and on the correlation for calculating h_c . The uncertainty in the calculation of h_c is more or less unknown. q_c is about 20-30% of the total surface heat transfer flow and if an uncertainty in q_c of 50% is assumed this error will be the dominant error resulting in an uncertainty of 10-15% in the internal heat transfer coefficient.

6.8 Calibration measurements

In order to carry out a performance check of the testing facility and the data manipulation outlined in section 6.6 and 6.7 a number of “calibration” measurements have been carried out on three different glazings. The three samples were all tested in the METSET at three different angles of incidence (22.5°, 45° and 60°).

The aim of the calibration exercise was to make a comparison between the measured (and corrected) results and the corresponding calculated values assuming that the calculated values are correct. As all three glazings are plane and non-diffusing they can be modelled for normal incidence using e.g. the calculation programme [WIS] provided that spectral data for all glass panes are available together with the thermal resistance of each layer in the glazings. For oblique angles of incidence the calculations have in general to be based on transmittance and reflectance data measured for each angle of incidence. However for uncoated glass panes the angular properties can be found from basic material data on the glass (extinction coefficient and refractive index) or from a set of normal-hemispherical transmittance and reflectance measurements (Duffie and Beckman, 1991).

All calculated values are found using the detailed energy balance calculation in WIS. Input data are angular spectral properties and surface emissivities for all glass panes. The optical properties of the glass panes of the three samples were measured at laboratories in Germany (Fraunhofer Institut für Solare Energiesysteme, Freiburg), France (CSTB, Grenoble) and in the UK (Oxford Brookes University). Unfortunately data for incidence angle of 22.5° are missing and as an approximation data for 30° angle of incidence are used instead.

The accuracy of the calculated values depend of course strongly on the reliability of especially the optical data on the glass panes and especially for higher angles of incidence some uncertainty in the spectral data has to be expected. It is assumed that the g-value for the glazings can be determined by calculation with an uncertainty of about 5%. (This number is based on the variation in spectral transmittance and reflectance measurements carried out by different laboratories on the same type of samples.)

The three tested glazings are all clear (non diffusing) double glazed units but with very different optical and thermal properties:

1. Float glass DGU consisting of 2 x 5 mm float glass showing little spectral selectivity. Thermal transmittance: Center of glazing 2.8 and total 2.9 W/m²K.
2. Low emissivity DGU with a 6 mm glass pane with an inward facing low emissivity hard coating outermost and a 6 mm float glass pane innermost. Coating in position 2, thermal transmittance: Center of glazing 1.7 and total 1.9 W/m²K. This unit shows significant spectral selectivity.
3. Solar control DGU with a 6 mm glass pane with an inward facing solar controlling low emissivity coating outermost and a 4 mm float glass pane innermost. Coating in position 2, thermal transmittance: Center of glazing 1.1 and total 1.4 W/m²K. This unit is extremely spectral selective.

The optical properties (solar transmittance, τ and solar absorptance, α) for all three samples have been calculated by means of the spectral properties of the glazings. Experimental and

reference optical values are found using the spectra of the solar simulator and the AM1.0 Global in figure 6.4. The method applied for the optical calculations corresponds to EN410 and ISO9050.

The normal-hemispherical spectral transmittances for the three glazings are shown in figure 6.11. It appears that especially the solar control unit is spectrally selective and this type of glazing makes heavy demands on the spectral corrections of the measured data.

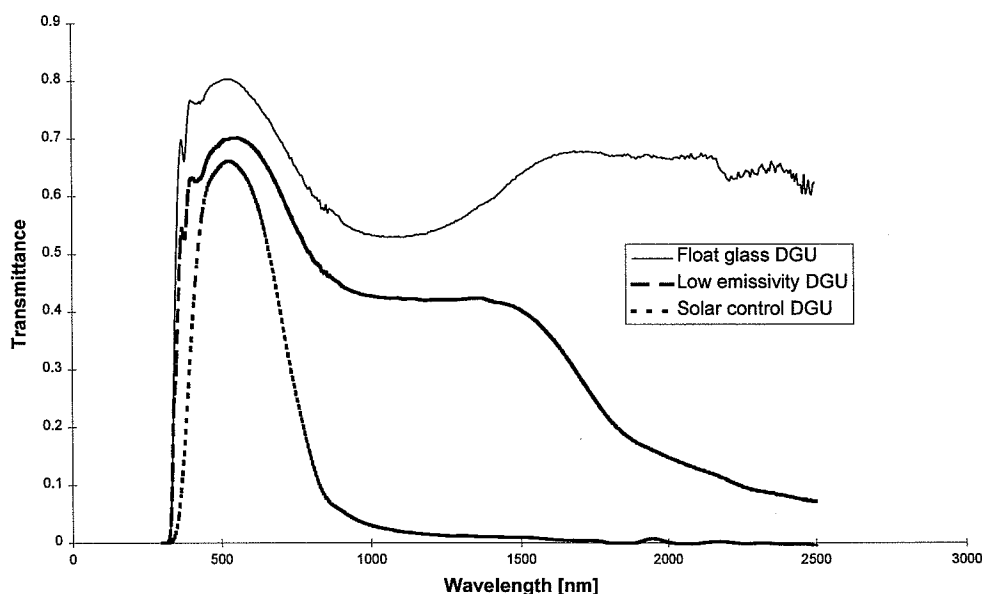


Figure 6.11 Spectral transmittances for the three calibration glazings.

Figure 6.12 illustrates the course of a typical g-value measurement carried out in the METSET. The measurement period is in total at least 4 hours and a period with no drift in temperatures or absorbed energy is selected to calculate average values of temperatures and absorbed energy. As it shows from figure 6.12 the ambient temperature (the lab temperature) keeps increasing throughout the measurement period. This is due to the large amount of heat released from the solar simulator and the fact that no air conditioning system is installed in the lab. However the increase in ambient temperature happens at a slow rate and as the heat capacity of the system (METSET + sample) is relatively small the effect of this temperature drift is small. The resulting g-value calculated from the data in figure 6.12 changes less than 0.5% if the selected period is changed from minute number 100-200 to minute number 200-238.

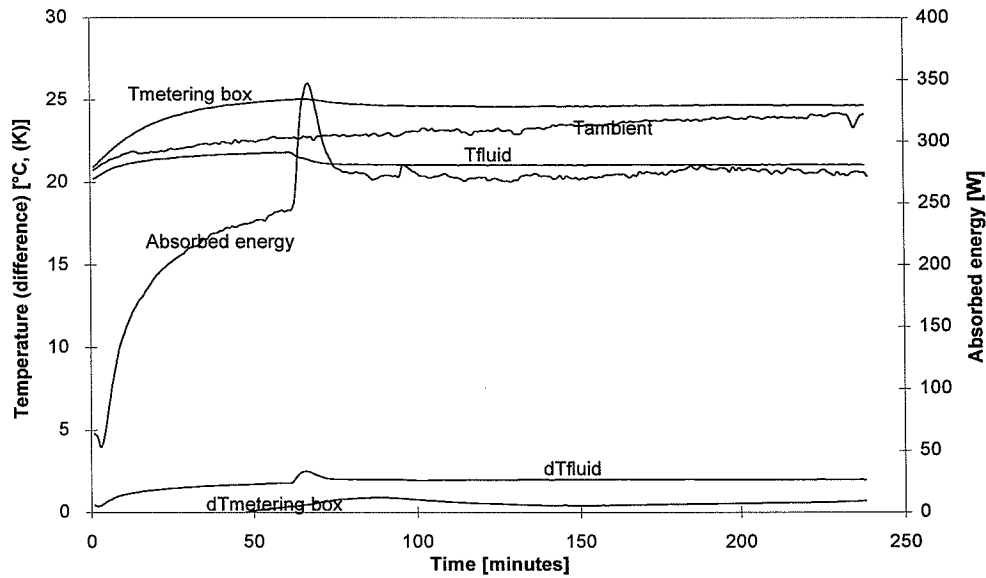


Figure 6.12 Example of measured data during g-value measurement in the METSET. Temperatures for metering box air, ambient air and fluid at the absorber inlet are shown in the upper three curves. Absorbed energy relates to the secondary y-axis. Temperature difference between absorber outlet and inlet (dT_{fluid}) and temperature difference across the metering box surfaces ($dT_{\text{metering box}}$) are shown in the two lower curves.

6.8.1 Float glass DGU

In order to check the reproducibility of the testing method and to allow a sample to be cut into pieces for optical investigations two identical units were measured in the METSET. The first unit was only measured at an angle of incidence of 22.5° ; the second unit was measured at 22.5° , 45° and 60° angles of incidence. The measuring conditions are listed in table 6.7 together with the directly measured (uncorrected) energy absorbed by the absorber (q_{abs}) in the METSET.

Table 6.7 Measuring conditions for float glass DGU. Two samples were tested at an incidence angle of 22.5° .

i	Radiation G	Outside air temp $\theta_{c,e}$	Inside air temp $\theta_{c,i}$	Outside env. temp $T_{n,e}$	Inside env. temp $T_{n,i}$	External heat transfer h_e	Internal heat transfer h_i	q_{abs}
22.5	820	26.7	24.8	301.4	293.9	22.5	7.3	628
22.5	810	26.1	23.9	300.9	293.8	22.5	7.4	613
45	620	25.5	25.1	300.5	294.8	22.4	7.0	449
60	442	26.2	25.4	301.0	295.5	22.3	6.6	297
[°]	[W/m ²]	[°C]	[°C]	[K]	[K]	[W/m ² K]	[W/m ² K]	[W/m ²]

In table 6.8 the directly measured data are reduced to experimental boundary conditions yielding g_{exp} .

The corrections are calculated as energy flows per m² of sample and are performed as:

- Correction for temperature difference between inside and outside environment (denoted " $q_{\Delta T_{\text{sample}}}$ " in the table).
- Correction for temperature difference across the external and internal surfaces of the metering box walls (denoted " $q_{\Delta T_{\text{metering box}}}$ " in the table)
- Correction for energy flow through the spacer profile (denoted " $q_{\text{edge conduct.}}$ " in the table).

Uncertainties in g_{exp} are found on the basis of section 6.8.5.

Table 6.8 *Reduction of measured data to experimental boundary conditions. Float glass DGU. The energy flows corresponding to the four input types are shown pr. m² of sample area. Otherwise g_{exp} is calculated according to eq. 6-4.*

i	q_{abs}	$q_{\Delta T_{\text{sample}}}$	$q_{\Delta T_{\text{metering box}}}$	$q_{\text{edge conduct.}}$	g_{exp}
22.5	628	22.1	8.0	0.3	0.73±0.03
22.5	613	20.9	6.2	0.3	0.72±0.03
45	449	16.5	5.1	0.3	0.69±0.03
60	297	15.3	5.7	0.3	0.62±0.03
[°]	[W/m ²]	[W/m ²]	[W/m ²]	[W/m ²]	

In table 6.9 the values have been corrected to reference boundary conditions according to section 6.7 yielding the final g-value g_{ref} . The corrected values are compared to g-values calculated in WIS (g_{calc}).

- Difference in the spectral distribution between the reference solar radiation and the solar simulator (CSI-lamps)
- Reflection from the absorber in the METSET
- Difference in the surface heat transfer coefficients h_i and h_e from the standard coefficients ($h_i = 8$ and $h_e = 23$ W/m²K)
- Difference in sample resistance for experimental and reference conditions

In figure 6.13 the measured and calculated g-values are shown as function of incidence angle.

Table 6.9 *Reduction of experimental data to reference boundary conditions Float glass DGU. g_{ref} given with uncertainty corresponding to section 6.8.5.*

i	τ_{exp}	τ_{ref}	α_{exp}	α_{ref}	γ_{exp}	$q_{i,\text{exp}}$	$q_{i,\text{ref}}$	g_{ref}	g_{scale}
22.5 ¹⁾	0.649	0.675	0.230	0.196	0.55	0.090	0.079	0.75±0.03	0.75 ²⁾
22.5 ¹⁾	0.649	0.675	0.230	0.196	0.50	0.084	0.073	0.75±0.03	0.74 ³⁾
45°	0.624	0.651	0.240	0.204	0.40	0.075	0.067	0.72±0.03	0.72
60°	0.554	0.583	0.233	0.198	0.46	0.077	0.070	0.65±0.03	0.66

¹⁾Spectrally corrected using data for 30° incidence angle.

²⁾Incidence angle = 0°

³⁾Incidence angle = 30°

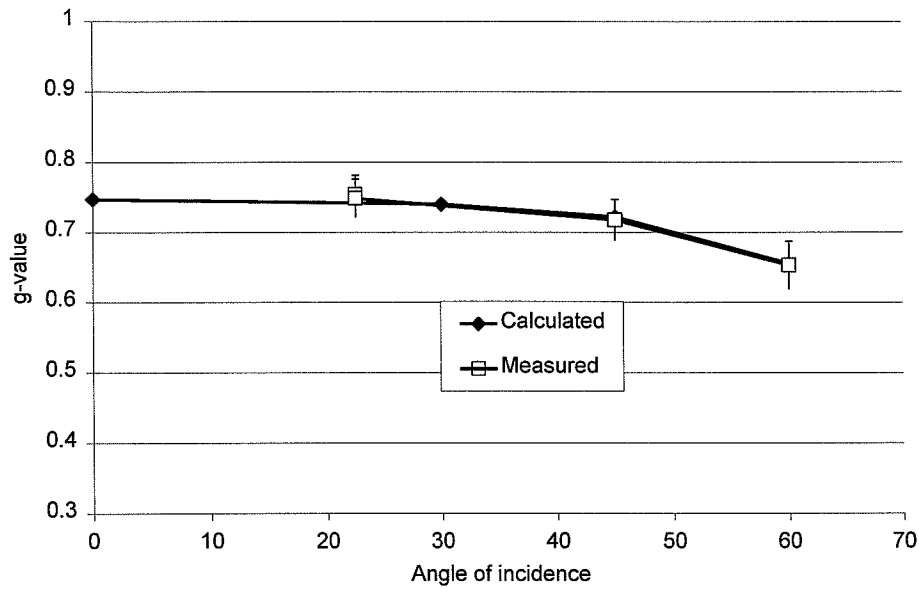


Figure 6.13 Measured and calculated g-value versus angle of incidence for float-glass DGU.

6.8.2 Low emissivity DGU

Again two units were measured in the METSET: One at 22.5° incidence and the other at 22.5, 45 and 60° incidence. The measuring conditions are listed in table 6.10 together with the directly measured (uncorrected) energy absorbed by the absorber (q_{abs}) in the METSET.

Table 6.10 Measuring conditions for low emissivity DGU. Low-e coating in position 2. Two samples were tested at an incidence angle of 22.5°.

i	Radiation G	Outside air temp $\theta_{c,e}$	Inside air temp $\theta_{c,i}$	Outside env. temp $T_{n,e}$	Inside env. temp $T_{n,i}$	External heat transfer h_e	Internal heat transfer h_i	q_{abs}
22.5	829	26.9	26.3	301.5	295.7	22.5	7.3	490
22.5	826	26.4	25.3	301.2	294.9	22.5	7.4	485
45	621	25.9	26.5	300.8	295.5	22.5	7.0	342
60	459	26.5	25.8	301.2	296.1	22.4	7.1	228
[°]	[W/m ²]	[°C]	[°C]	[K]	[K]	[W/m ² K]	[W/m ² K]	[W/m ²]

In table 6.11 the measured data are corrected for unintended heat flows in order to obtain the g-value for experimental boundary conditions.

The corrections are performed as in section 6.8.1.

Table 6.11 *Reduction of measured data to experimental boundary conditions. Low emissivity DGU. The energy flows corresponding to the four input types are shown pr. m² of sample area. Otherwise g_{exp} is calculated according to eq. 6-4.*

i	q_{abs}	$q_{\Delta T sample}$	$q_{\Delta T metering\ box}$	$q_{edge\ conduct.}$	g_{exp}
22.5	490	9.2	5.6	2.9	0.57±0.02
22.5	485	10.8	5.7	2.9	0.56±0.02
45	342	9.1	5.6	2.5	0.52±0.02
60	228	8.0	5.6	2.3	0.46±0.02
[°]	[W/m ²]	[W/m ²]	[W/m ²]	[W/m ²]	

In table 6.12 the values have been corrected to reference boundary conditions yielding the final g-value g_{ref} as in section 6.8.1. The corrected values are compared to the g-values calculated in WIS (g_{calc}). In figure 6.14 the measured and calculated g-values are shown as function of incidence angle.

Table 6.12 *Reduction of experimental data to reference boundary conditions Low emissivity DGU with coating in position 2. g_{ref} given with uncertainty corresponding to section 6.8.5.*

i	τ_{exp}	τ_{ref}	α_{exp}	α_{ref}	γ_{exp}	$q_{i,exp}$	$q_{i,ref}$	g_{ref}	g_{calc}
22.5° ¹⁾	0.484	0.530	0.410	0.355	0.22	0.093	0.081	0.61±0.03	0.62 ²⁾
22.5° ¹⁾	0.484	0.530	0.410	0.355	0.20	0.088	0.077	0.61±0.03	0.61 ³⁾
45°	0.455	0.502	0.430	0.374	0.15	0.075	0.067	0.57±0.03	0.59
60°	0.395	0.442	0.443	0.385	0.13	0.073	0.064	0.51±0.03	0.53

¹⁾Spectrally corrected using data for 30° incidence angle.

²⁾Incidence angle = 0°

³⁾Incidence angle = 30°

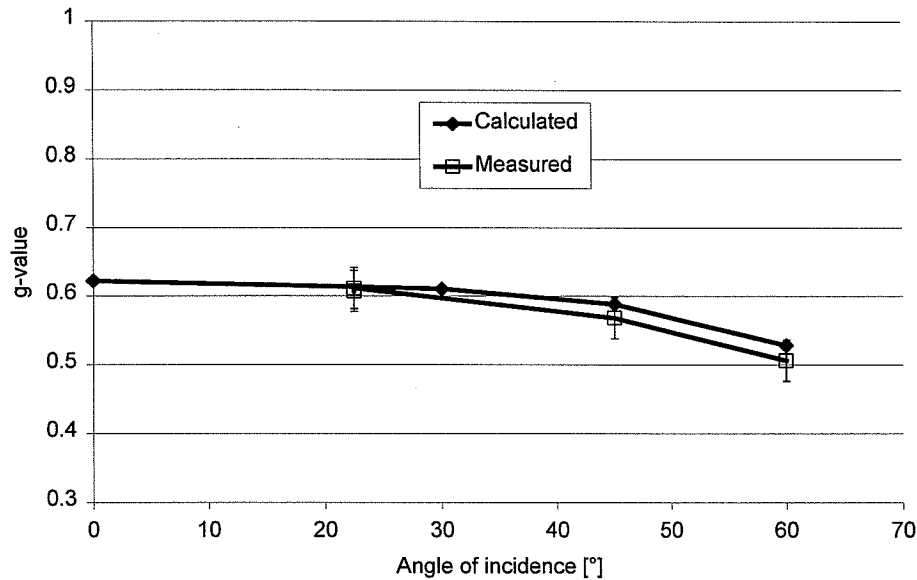


Figure 6.14 Measured and calculated g-value versus angle of incidence for low emissivity DGU. Low-e coating in position 2.

6.8.3 Solar control DGU

A single solar control unit was measured at three angles of incidence: 22.5°, 45° and 60°. The measuring conditions are listed in table 6.13 together with the directly measured (uncorrected) energy absorbed by the absorber (q_{abs}) in the METSET.

Table 6.13 Measuring conditions for solar control DGU

i	Radiation G	Outside air temp $\theta_{\text{c,e}}$	Inside air temp $\theta_{\text{c,i}}$	Outside env. temp $T_{\text{n,e}}$	Inside env. temp $T_{\text{n,i}}$	External heat transfer h_{e}	Internal heat transfer h_{i}	q_{abs}
22.5	813	24.2	23.0	299.5	294.7	22.5	6.8	209
45	619	23.6	23.8	299.0	295.5	22.4	6.5	150
60	451	25.2	24.0	300.2	295.9	22.4	6.3	101
[°]	[W/m ²]	[°C]	[°C]	[K]	[K]	[W/m ² K]	[W/m ² K]	

In table 6.14 the measured data are corrected for unintended heat flows in order to obtain the g-value for experimental boundary conditions. The corrections are performed as in section 6.8.1.

Table 6.14 Reduction of measured data to experimental boundary conditions.
Solar control DGU. The energy flows corresponding to the four input types are shown pr. m² of sample area. Otherwise g_{exp} is calculated according to eq. 6-4.

i	q_{abs}	$q_{\Delta T sample}$	$q_{\Delta T metering\ box}$	$q_{edge\ conduct.}$	g_{exp}
22.5	209	7.4	0.9	1.8	0.24±0.01
45	150	5.5	1.1	1.4	0.23±0.01
60	101	6.7	2.9	1.5	0.20±0.02
[°]	[W/m ²]	[W/m ²]	[W/m ²]	[W/m ²]	

In table 6.15 the values have been corrected to reference boundary conditions yielding the final g-value g_{ref} as in section 6.8.1. The corrected values are compared to the g-values calculated in WIS (g_{calc}). In figure 6.15 the measured and calculated g-values are shown as function of incidence angle.

Table 6.15 Reduction of experimental data to reference boundary conditions
Solar control DGU with coating in position 2. g_{ref} given with uncertainty corresponding to section 6.8.5.

i	τ_{exp}	τ_{ref}	α_{exp}	α_{ref}	γ_{exp}	$q_{i,exp}$	$q_{i,ref}$	g_{ref}	g_{calc}
22.5° ¹⁾	0.215	0.312	0.182	0.269	0.15	0.032	0.049	0.36±0.03	0.36/0.34 ²⁾
45°	0.204	0.295	0.206	0.297	0.10	0.028	0.041	0.34±0.03	0.33
60°	0.168	0.240	0.178	0.277	0.17	0.033	0.053	0.29±0.03	0.27

¹⁾Spectrally corrected using data for 30° incidence angle.

²⁾For incidence angle = 0° and 30° respectively

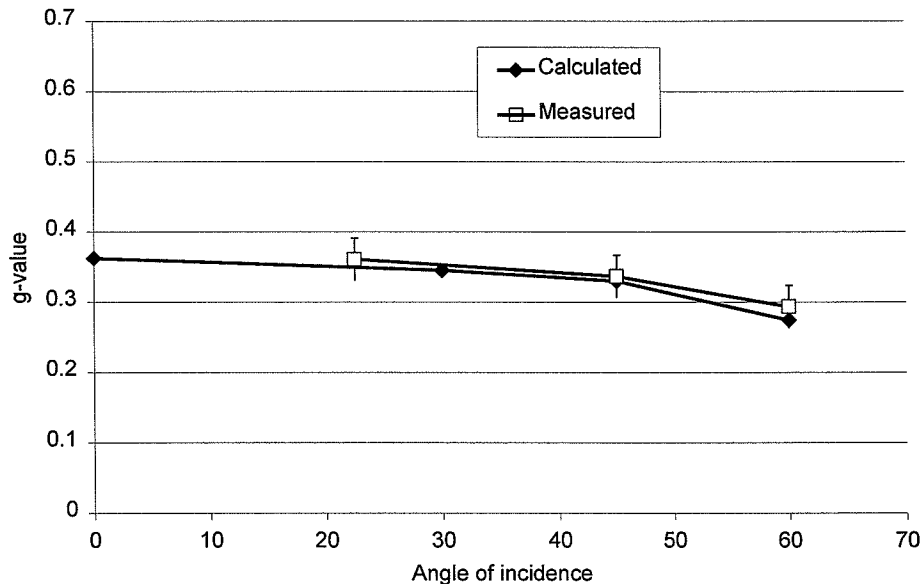


Figure 6.15 Measured and calculated g-value versus angle of incidence for solar control DGU.

Discussion

A good correspondence between measured and theoretical g-values has been found for all three calibration samples and for all angles of incidence. The discrepancies are in all cases smaller than the expected uncertainty of the measured values. There is a tendency to increased discrepancy at relatively high angles of incidence. One reason for this may be the uncertainty in the actual angle of incidence during the measurement. The actual angle of incidence is established by rotating the METSET around its vertical axis and this is done using simple mechanical means. An uncertainty in actual angle of incidence is also present in the spectral measurements (which form the basis for the theoretical values).

The corrections on the measured data were performed using detailed optical and thermal data on each layer in the glazings. This method was chosen for convenience as all relevant data were available. The method may in general not be applicable as such data can only be achieved by detailed measurements (the sample has to be taken apart and each part has to be characterised) and the data can only be used if a model describing the optical properties of the complete sample is available. Instead the same relevant optical data for the samples could be achieved by measuring the spectral transmittance and reflectance of the complete samples as discussed earlier. Provided that such measurements are performed with same accuracy as the measurements used here the final measured g-values (g_{ref}) after corrections would be identical to the results presented in the previous three sections.

In the examples previously treated all relevant optical and thermal data were available. This may not be the situation in general and a major force of the described correction method is the low sensitivity to lacking input data. Key parameters in the correction procedure are the ratios between experimental and reference transmittance and absorptance ($\tau_{\text{exp}}/\tau_{\text{ref}}$ and $\alpha_{\text{exp}}/\alpha_{\text{ref}}$). The absolute values of these four parameters have only second order effects on the final result – it is their ratios that influence the corrections and these ratios only show a slight dependency of incidence angle. Taking the three examples previously treated and assuming that only data for normal incidence were available for each sample all corrections would have to be based on these normal incidence data. In figure 6.16 is shown the final g-values determined by performing corrections based on normal incidence optical data for each sample. For comparison is also shown the g-values corrected with the full data set.

As it shows in figure 6.16 the normal incidence data set leads to almost same results as the full data set. Performing reliable measurement of the normal transmittance for experimental and reference conditions is in most cases possible as discussed earlier. More complicated is the measurement of reflectance data for complex samples which may include diffusing, scattering, reflecting and other elements with special optical properties. Again we should remember that it is the ratio between the experimental and reference reflectances that really matters – not the absolute magnitude of the two numbers – and some types of systematic errors in the optical measurements do not greatly influence the corrections performed in this study

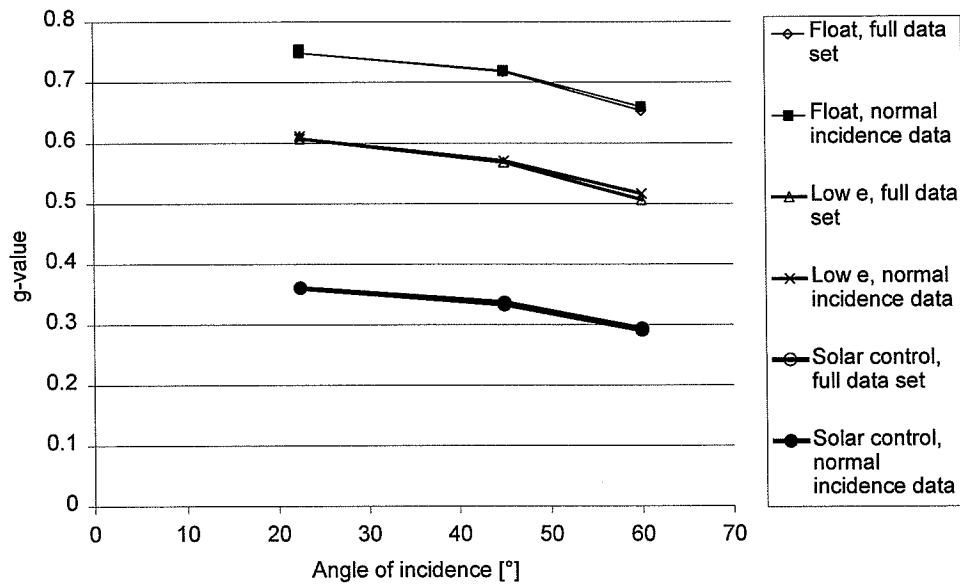


Figure 6.16 Measured g-values for Float glass DGU, Low emissivity DGU and Solar control DGU. Corrections from experimental to reference conditions are performed using full data set and normal incidence data respectively.

To illustrate the impact of errors in the $\alpha_{\text{exp}}/\alpha_{\text{ref}}$ ratio on the resulting g-value the normalised g-values at 22.5° incidence for the three calibration samples are shown versus the $\alpha_{\text{exp}}/\alpha_{\text{ref}}$ ratio in figure 6.17. The g_{ref} -values at 22.5° incidence in tables 6.9, 6.12 and 6.15 are used as reference values for the normalisation and for each sample is shown the position of the reference value. Relatively large errors may be the result when using “extremely wrong” values of $\alpha_{\text{exp}}/\alpha_{\text{ref}}$ (up to 17% for the low-e DGU in the investigated range). On the other hand errors in $\alpha_{\text{exp}}/\alpha_{\text{ref}}$ ratio up to say 0.2 has only limited influence on the result for the investigated samples. The reason for this is of course the fact that the ratio only influences the correction of q_i which in most cases is relatively small. For samples with very small solar transmittance and very high absorptance in the innermost glass pane q_i will be dominating and the influence of the $\alpha_{\text{exp}}/\alpha_{\text{ref}}$ ratio on the final g-value will be relatively large.

In the investigated cases far the dominant corrections are on the transmittance part and even though the transmittance of the solar control glazing is low more extreme samples with very low solar transmittance and high solar absorptance may be found. Such samples will result in a different ratio between τ and q_i and the more difficult correction on the q_i term will be more critical. For any given sample the worst possible case occurs if γ_{exp} is 0 and γ_{ref} also is assumed to be 0, but in reality is 1 or vice versa. Of course this situation will not occur, but if the absorptance of the sample is very selective and if panes with different selectivity are incorporated in the sample, significant difference between γ_{exp} and γ_{ref} may result and the correction method will be increasingly inaccurate with increasing difference between γ_{exp} and γ_{ref} .

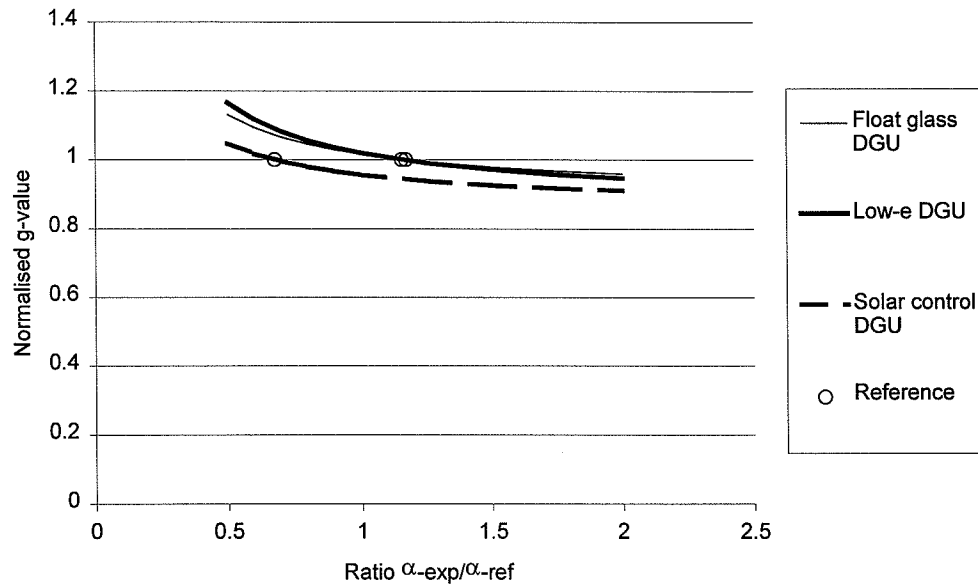


Figure 6.17 Normalised g-value at 22.5° incidence for three samples. Shown as functions of the $\alpha_{exp}/\alpha_{ref}$ ratio.

6.8.4 Simple correction data

As the solar control unit is the most sensitive of the three units regarding boundary conditions a correction from experimental to reference conditions has been carried out without the use of detailed optical data. This corresponds to a more general situation where no model describing the optical and thermal properties of the sample is available, where only data for the complete sample can be found and where relatively simple optical measuring equipment is available.

The correction of the transmittance term in eq. 4-4 can simply be done by measuring the broadband transmittance of the sample - first in the CSI solar simulator and subsequently outdoor. The correction in the transmittance part is the difference between the two measured quantities. Of course the outdoor measurement will not result in exactly the transmittance for the reference solar spectrum but the value will be much closer to the standard value than the result from the indoor measurement. More sophisticated measurements of the solar transmittance can be performed as described in section 6.7.1 using special optical equipment. However such specialised equipment tends to be very expensive, and as the results will show acceptable accuracy seems to be obtainable by more simple means.

The correction of the q_i term in eq. 4-15 can be done by means of eq. 6-6 and 6-7. Necessary input data are all the quantities in eq. 6-7 for experimental as well as reference boundary conditions. Instead of utilising the spectral optical data already available a more simple approach has been used to achieve transmittance τ and absorptance α for the sample for both sets of boundary conditions. As reference values the broadband transmittance and reflectance of the glazing has been measured outdoor. (In the Solar Tracker, see also chapter 7). As experimental values the broadband transmittance and reflectance have been measured indoor

in the CSI solar simulator. The measurements have only been carried out for the incidence angle 22.5° . The measured values are listed in table 6.16.

*Table 6.16 Measured optical properties of the solar control glazing.
Angle of incidence is 22.5° , broadband measurements.*

	Transmittance	Reflectance
Indoor (experimental spectrum)	23	58
Outdoor	31	44
	%	%

For comparison the calculated solar transmittance of the glazing for reference solar spectrum is 31.2% which is in very good agreement with the result of the outdoor measurement. The corresponding calculated transmittance using the CSI spectrum shown in figure 6.4 is 21.5%. The expected instrumental uncertainty of the indoor broadband measurements is less than 2%. This could indicate that the expected CSI spectrum in figure 6.4 is somewhat erroneous. However also the spectrum of the real solar radiation and the spectral data for the solar control DGU may differ from the expected values.

The experimental values for inside and outside surface heat resistances are listed in table 6.13 and the $R_{g,exp}$ is found from the total U-value of the glazing ($1.4 \text{ W/m}^2\text{K}$).

Starting from the measured value, g_m , all the corrections listed in section 6.5 can be carried out on the basis of the available data. The correction for the cold bridge effect in the edge of the glazing is carried out by assuming equal absorptance and transmittance in the two glass layers. This could be done more detailed on the basis of γ_{exp} but the inaccuracy will still be large and the impact on the g-value small.

The reduction of measured data to experimental boundary conditions is shown in table 6.17.

*Table 6.17 Simplified reduction of measured data to experimental conditions.
Solar control DGU with coating in position 2.*

i	q_{abs}	$q_{\Delta T sample}$	$q_{\Delta T metering \text{ box}}$	$q_{edge \text{ conduct.}}$	g_{exp}
22.5	209	6.7	0.9	0.3	0.25 ± 0.01
[$^\circ$]	[W/m^2]	[W/m^2]	[W/m^2]	[W/m^2]	

The reduction of experimental g-value to reference value is shown in table. 6.18. The procedure is similar to the procedure previously used – only the input data to the correction have been obtained in a different way..

Table 6.18 *Reduction of experimental data to reference boundary conditions using simple optical input data. Solar control DGU with coating in position 2.*

i	τ_{exp}	τ_{ref}	α_{exp}	α_{ref}	γ_{exp}	$q_{\text{i,exp}}$	$q_{\text{i,ref}}$	g_{ref}	g_{calc}
22.5°	0.23	0.31	0.19	0.25	0.06	0.020	0.027	0.34±0.03	0.36/34 ¹⁾

¹⁾For incidence angle = 0° and 30° respectively

Again the measured and calculated g-values are in very good agreement and within the expected uncertainty of the measurement.

6.8.5 Uncertainty of the g-value measurements

The uncertainty of the corrected g-value, g_{ref} , depends on the sample and on the necessary corrections especially from experimental to reference conditions. The measurement of g_{m} is based on simple and accurate technique, measuring temperature difference, mass flow rate and solar radiation. In the correction to experimental conditions additional sources of errors are introduced. The sources of error and their associated uncertainties are listed in table 6.19. Uncertainties in temperatures, mass flow rate and solar radiation level are found from calibration of temperature sensors, flow meter and pyranometers. For the temperature difference of absorber fluid a relative uncertainty of 2% is used as this was the maximum uncertainty obtained during calibration. (Tested temperature differences 1 – 5K). Uncertainty in heat capacity of fluid is the difference between the regression used in the calculations and tabulated values for water. Uncertainty in thermal transmission through window is a conservative value estimated to cover situations where only limited knowledge about the sample U-value is available (for simple samples the uncertainty is smaller than 15%). Uncertainties in metering box heat exchange coefficient, environmental temperature difference, temperature difference across metering box walls and heat flow through edge of glazing are rough estimates which are considered conservative. Uncertainty in height and width measures are based on practical experience.

Table 6.19 *Estimated uncertainties in parameters determining g_{exp}*

Property	Estimated uncertainty	
Temperature difference of absorber fluid	2	%
Mass flow rate	0.3	%
Solar radiation level	1.5	%
Heat capacity of the fluid	1	%
Thermal transmittance, window	15	%
Heat exchange coefficient metering box	15	%
Environmental temperature difference	4	K
Temperature diff. metering box walls	1	K
Heat flow through edge of glazing	20	%
Height and width measures	0.002	m

From the expression for g_{exp} in eq. 6-4 the total uncertainty of the value can be calculated on the basis of the uncertainties listed in table 6.20. For the three investigated glazings the results and their corresponding uncertainties are listed in table 6.20:

Table 6.20 g_{exp} and corresponding uncertainty for the measurements on three glazings.

Sample	Angle of incidence	g_{exp}	uncertainty
Float glass DGU	22.5	0.72	4
	45	0.68	4
	60	0.61	5
Low emissivity DGU	22.5	0.56	3
	45	0.52	4
	60	0.46	4
Solar control DGU	22.5	0.24	5
	45	0.23	5
	60	0.20	8
	[°]		[%]

Conducting the next corrections to obtain g_{ref} involves new potential errors: absorptance of absorber, solar simulator spectrum, optical and thermal data for the sample. Some are very difficult to quantify, such as confidence in solar simulator spectrum and reliability of spectral data. However some very simple considerations concerning the accuracy of the corrections can be done. The solar simulator spectrum is for especially the solar control sample a source of error. For this sample a difference in the τ_{exp}/τ_{ref} ratio of about 7% was found when using the calculated and the measured experimental transmittance respectively. Assuming that this difference can be taken as an expression for the effect of the uncertainty in the solar simulator spectrum a rough estimate of the uncertainty in the corrections may be done. The influence of this uncertainty on the g-value of the solar control unit is also about 7%. As the uncertainty in the τ_{exp}/τ_{ref} ratio only influences the correction from g_{exp} to g_{ref} it is reasonable to refer the uncertainty in the solar simulator spectrum to the correction part and here the effect of the uncertainty will be about 20%. As described previously the influence of uncertainty in the $\alpha_{exp}/\alpha_{ref}$ has relatively small effect on the g-value (at least for the investigated samples) and the observed difference in the $\alpha_{exp}/\alpha_{ref}$ ratio found from calculated and measured (broadband) data corresponds to an uncertainty of about 5% in the correction for the solar control glazing. An estimated uncertainty in the absorber absorptance of 3% leads to an uncertainty in the correction part of about 5% for the solar control unit. In other words the estimated uncertainty in the solar simulator spectrum is dominating for the solar control unit. This leads to the rough estimate that the correction from g_{exp} to g_{ref} is performed with an uncertainty on the correction of about 25% for the solar control unit. Similar considerations have been performed for the other two samples. For these samples correction in the transmittance term is relatively small and the uncertainty in the absorber absorptance is dominating corresponding to uncertainties in the correction part of 50% and 25% for the float glass DGU

and the low-e DGU respectively. These uncertainties are included in the results previously presented.

For the correction procedure an uncertainty is also related to the assumption that γ_{exp} equals γ_{ref} . If this assumption is wrong and if significant absorption takes places in the sample critical errors will result.

The examples have shown that g_{exp} can be determined with only small expected uncertainty. However the resulting uncertainty on g_{ref} will be larger depending on the sample, on the correction procedure and on the magnitude of the corrections for boundary conditions needed.

6.8.6 Conclusions and discussion

The METSET and the associated equipment (solar simulator, environmental conditions, data logging equipment, measuring systems etc.) have been characterised, improved and calibrated. A number of problems regarding calorimetric measurement of g-value have been identified and (to a certain extend) solved. These include:

- Solar simulator spectrum
- Solar simulator divergence
- Absorber reflectance
- Internal and external heat transfer coefficients
- Unintended heat flows through sample and metering box walls
- Specimen mounting in the METSET

A number of decisions of "definition character" had to be taken in the process in order to facilitate the calorimetric measurements and the subsequent corrections. These include choice of reference boundary conditions such as solar spectrum as well as internal and external heat transfer coefficients. For the latter it was decided to refer the g-value to the standard coefficients (8 and 23 W/m²K) and that these values should be valid for all samples even though this may not be the case in "real life" where the coefficients will be affected by the specific sample design such as surface emissivity, fins and other protruding elements with relatively high convective heat transfer.

Procedures for performing the measurements in the METSET have been developed together with procedures for the subsequent corrections of the measured results. The method has been designed to be applicable also for complex samples which can not be modelled. However the corrections of the q_i -part of the g-value is still object for further development. This is especially true for specimens with low solar transmittance, large solar absorption in the inner part of the sample and spectral selective absorptance in the layers. For less extreme cases the procedures outlined in this chapter are considered sufficiently accurate.

The g-value as function of incidence angle for three different glazings have been measured in the METSET. The glazings had very different optical and thermal properties but were all clear (non diffusing) glazings covered by well established optical and heat transfer theory. This enabled a

comparison between measured and calculated g-values. For two of the glazings measurements were performed on an additional sample in order to investigate the reproducibility of the measurements. The additional measurements showed that the reproducibility in the g-value measurement was better than 1% provided that the glazings can be considered identical two by two.

For the investigated samples good agreement was found between theoretical and measured g-values and all discrepancies were within the expected uncertainties of the measurements.

For the solar control DGU a correction utilising simple optical input data was applied with good result.

An error analysis of the measurements showed that the expected relative uncertainty for g_{exp} is between 3% and 8%. Roughly estimated uncertainties in the correction from experimental to reference boundary conditions brings the relative uncertainty on g_{ref} up to about 4 to 10% for the investigated samples, largest numbers for samples with low g-value. This uncertainty is of the same magnitude as the expected uncertainty in the model calculations using detailed optical and thermal data.

The dominant correction is related to the transmittance term and of course this correction is very sensitive to the spectral distribution of the solar simulator. Even though the spectrum for the solar simulator was measured as an average of three lamps, it is evident that the spectral distribution of the solar simulator in reality may be different from the data-set used for the detailed spectral corrections. By using corrections based on indoor and outdoor broadband measurements the impact of an erroneous CSI spectrum is reduced, but at the same time is introduced the uncertainty of the reference spectrum (which is not exactly the same as the solar spectrum during the outdoor measurements).

7 Measurement of direct solar transmittance, τ_e

7.1 General

The reason for showing interest in the direct solar transmittance (τ_e) is mainly that it is relevant to the total solar energy transmittance (g-value). From a thermal point of view the solar transmittance alone is not very interesting as it only covers a part of the total amount of solar energy that penetrates a window. However as the solar transmittance in general is the largest element of the total solar energy transmittance the solar transmittance can be used as an indication of the g-value that can be expected for a certain specimen. Furthermore the solar transmittance can be used to perform corrections of g-value measurements performed under indoor solar simulator conditions. As it appeared from chapter 6 it is not always possible to perform the spectral correction based on spectral data of elements in a sample and in these cases a correction by means of the direct solar transmittance of the complete sample may be the only option. Finally measurement of direct solar transmittance is also of interest when characterising other solar components than windows (such as solar collector covers).

7.2 Measuring principles

The direct solar transmittance can be obtained in several ways. The most detailed procedure is to carry out spectral measurements over the solar spectrum range on all layers in a sample by means of a suitable spectrophotometer. The result of the measurements will be the spectral transmittance, $\tau(\lambda)$, and spectral reflectance, $\rho(\lambda)$, of each transparent layer in the investigated construction and from the known spectral distribution of the sun the direct solar transmittance can be found by means of a suitable optical model if such a model exists (e.g ISO9050, EN410 for clear glazings at normal incidence). By performing measurements on a complete multilayer sample the spectral transmittance of the sample can be found directly by means of a spectrophotometer. However when dealing with samples that are optically inhomogeneous or show diffusing properties (or maybe both) the measurements will be increasingly difficult to perform, resulting in high demands to the optical equipment and the operation of it. A large integrating sphere or a photogoniometer is necessary to perform detailed optical measurements on optically complex samples. It can be done - it is not always easy but always expensive.

Less detailed but well suited for the purpose outlined in section 7.1 is the broadband measurement where the measurement is carried out under outdoor solar conditions over the whole solar spectrum by means of pyranometers. Again we have the problem of stability of the solar radiation in Denmark, but as a measurement of solar transmittance can be carried out in a few minutes the problem is not critical.

7.3 Solar tracker

To facilitate the outdoor broadband measurements of direct solar transmittance mentioned above a solar tracking device with relevant measuring equipment has been constructed. The solar tracker has a three-fold purpose:

- To perform outdoor measurement of broadband solar transmittance of transparent materials under different angles of incidence
- To prepare a test rig for outdoor measurements of g-values of windows using the METSET
- To prepare a test rig for outdoor measurements of solar collector performance.

Only the first item has been tested so far.

The solar tracker is shown in figure 7.1, where the measuring plane can be seen in the pictures (a grid of wooden laths). The tracker is operated and controlled by a computer where also the recording of measured data takes place.

The tracker allows the measuring plane to follow the arc of the sun under a chosen angle of incidence. By rotating the measuring plane around two axes (a vertical and a horizontal) the angle of incidence can be controlled by the computer. The rotation around the vertical axis includes the whole test rig while the rotation around the horizontal axis only involves the measuring plane.

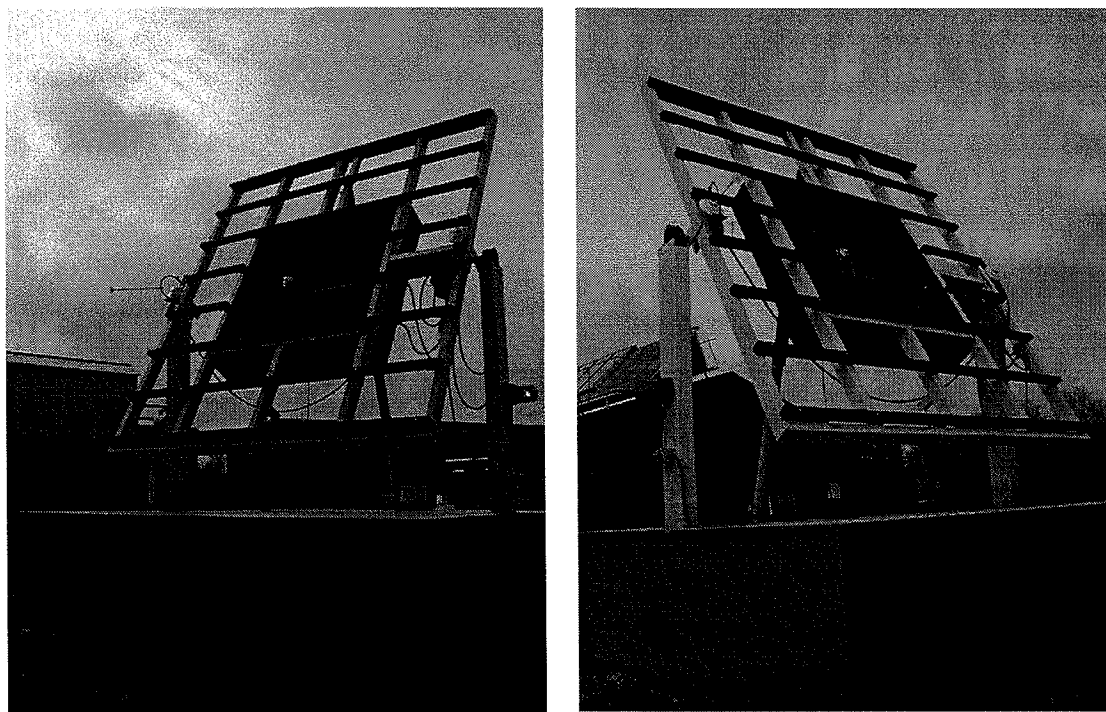


Figure 7.1 The solar tracker. The measuring plane is the grid of wooden laths.

On the basis of the date, time of the day and the geographical position of the solar tracker the apparent position of the sun on the sky can be calculated using the approach given in (Duffie and Beckmann, 1991). The output of the calculations is the solar height and the solar azimuth. The solar height is defined as the angle between a straight line from the observer to the sun and the horizontal projection of the line. The solar azimuth is defined as the angle between the south direction and the horizontal projection of a straight line from the observer to the sun.

The tracking algorithms have been developed using the following geometrical approach: Two planes perpendicular to each other and to the measuring plane are defined and named plane 1 and plane 2. See figure 7.2. A unity vector with origin in the measuring plane at the crossing of plane 1 and 2 and pointing towards the sun is defined as the solar vector. The projection of the solar vector on plane 1 is defined as trace 1 and the projection of the solar vector on plane 2 is defined as trace 2, see figure 7.2.

Depending on the position of the measuring plane relative to the sun, four different situations can now occur:

- If the length of both trace 1 and trace 2 is unity this means that the solar vector and the surface normal to the measuring plane are congruent and the angle of incidence is zero
- If only the length of trace 1 is unity this means that the slope of the measuring plane equals the solar height but the azimuth of the measuring plane is different from the solar azimuth. The angle of incidence can be found from the trace of the solar vector in plane 2 (ΔAz in figure 7.2).
- If only the length of trace 2 is unity this means that the azimuth of the measuring plane equals the solar azimuth but the slope of the measuring plane is different from the solar height. The angle of incidence can be found from the trace of the solar vector in plane 1 (Δh in figure 7.2).
- If the length of neither trace 1 nor trace 2 is unity the incidence angle is different from zero and appears as a result of simultaneous displacements in height/slope and azimuth. The displacements relative to height/slope and azimuth can be found from trace 1 and trace 2, see figure 7.2. The resulting angle of incidence can be found from the surface normal and the solar vector.

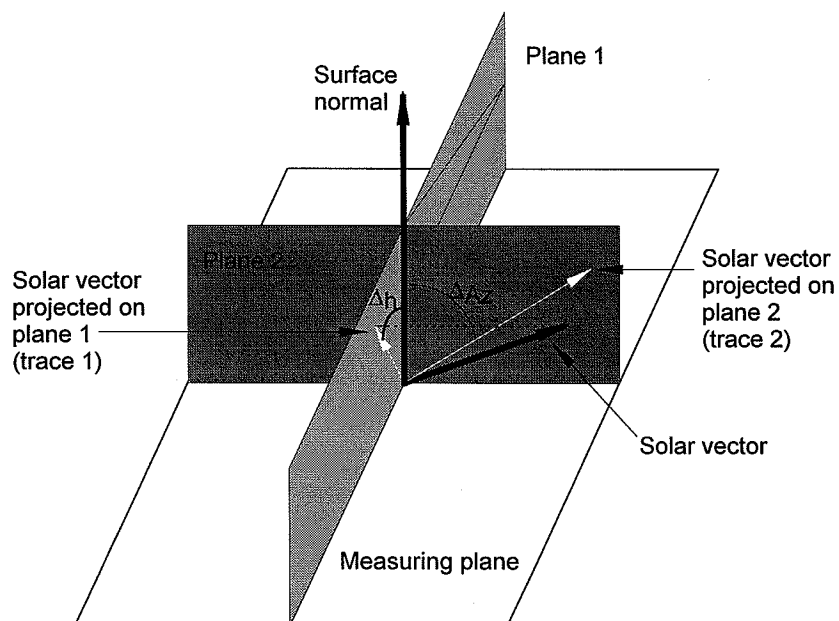


Figure 7.2 Definition of geometry. Plane 1 and 2 are tools used to control and evaluate the positioning of the measuring plane. ΔAz is the angular displacement of the azimuth of the measuring plane relative to the solar azimuth. Δh is the angular displacement of the slope of the measuring plane relative to the solar height.

The movement of the measuring plane can be controlled to result in the following options:

- a chosen angular displacement between solar height and slope of the measuring plane, combined with a zero displacement between solar and measuring plane azimuths
- a chosen angular displacement between solar azimuth and the azimuth of the measuring plane, combined with a zero displacement between solar height and measuring plane slope
- a free combination of the two angular displacements
- a fixed position of the measuring plane
- rotation around only one of the two axes.

Option one and two above are used in order to allow measurements on inhomogeneous specimens that are symmetrical around only one axis.

By performing the positioning as described it is in principle possible to obtain any combination of angular displacements relative to the solar azimuth and solar height. However it may not always be possible to obtain very high angles of displacement relative to the solar height alone as the measuring plane can only be tilted in the range of 0-90°. This means that high angles can only be obtained when the solar height is low.

The solar tracker is controlled by a computer and the operator can (under the above considerations) freely choose the combination of angular displacements that is relevant. Two AC motors enable the physical motion of the measuring plane, one motor for tilting and one motor for turning around the vertical axis. Each rotation of the motors correspond to specific movements of the measuring plane.

By letting the measuring plane start at a well defined position and afterwards keeping track of the number of rotations of the two rotation motors the actual position of the measuring plane can be found.

The system is designed to allow a difference between the desired angle of incidence and the actual calculated angle of incidence of $\pm 1^\circ$. This is done because:

- the same computer performs the control of the solar tracker and the control of the measuring devices mounted on the tracker (see next section)
- the computer is operating as a “single task” computer
- the physical positioning of the measuring plane is rather slow

7.4 Broadband measurements, SolTrans

In order to perform the broadband measurements the solar tracker has been equipped with a measuring device consisting of three pyranometers, the SolTrans: One pyranometer measures the total solar radiation, a second measures the diffuse radiation and the third pyranometer measures the radiation transmitted through a test sample, see figure 7.3. As many interesting materials are inhomogeneous the third pyranometer is mounted on a motor-driven actuator enabling the pyranometer to be moved during measurements (scanning pyranometer). This feature allows the measurement of solar transmittance of materials with scattering and inhomogeneous transmittance properties. The pyranometer can be moved either continuously or in stepmode over a maximum scanning width of 200 mm. When the scanner is in step-mode the step size and the time between each measurement step (step pause) can be chosen freely under consideration to the time constant of the pyranometer and to the type of test specimen. Minimum step size is 0.5 mm.

Samples should be of a size sufficiently large to allow edge effects to be neglected. For diffusing and scattering samples a minimum size of 1 m x 1 m is recommended. Maximum sample size is 3 m x 3 m but the metering aperture in the measuring plane is only 1.25 m x 1.25 m.

The diffuse solar radiation is measured by a pyranometer with a shadow disk, 52 mm in diameter and mounted in a distance of 520 mm from the pyranometer in the direction towards the sun. By keeping the area of the shadow disk in this position the amount of diffuse radiation excluded by the shadow disk can be neglected (Hunt et al 1980). The shadow disk is painted black on the side facing the pyranometer and white on the

opposite side. The shadow disk can be positioned in all relevant positions but this must be done manually.

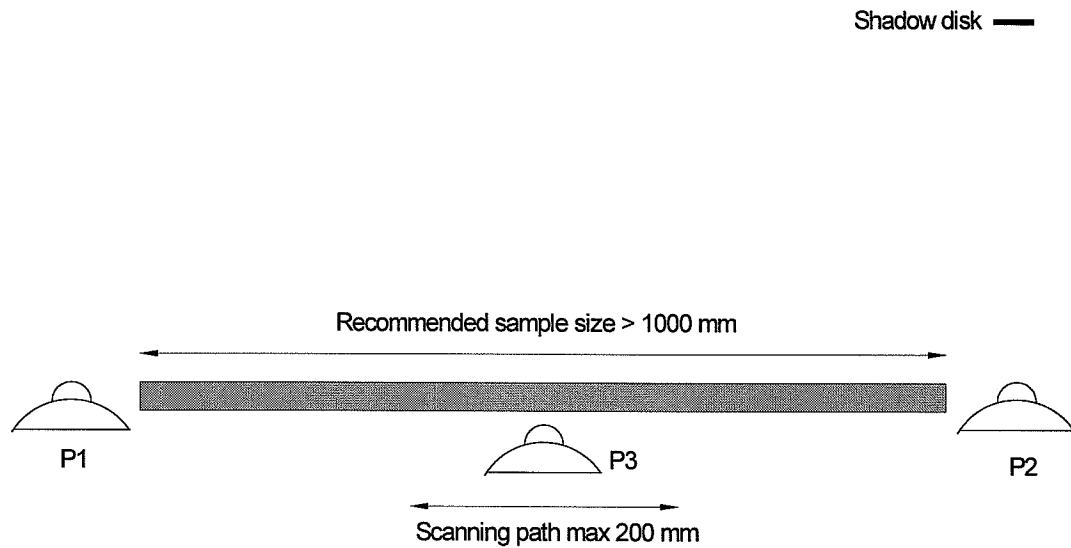


Figure 7.3 Sketch of measuring principle in SolTrans. Pyranometer P1 measures total solar radiation, P2 measures diffuse radiation by means of the shadow disk, P3 measures the transmitted radiation. The scanning path must be considerably smaller than sample size to reduce edge effects.

After the solar radiation is transmitted through the test sample it enters a box where the scanning pyranometer is located. The box is painted black inside in order to avoid backside reflections on the test sample. A fan is installed in the box wall to ensure that sufficient ventilation takes place in order to avoid temperature related disturbance of the scanning pyranometer. Figure 7.4 shows a photograph of the scanning pyranometer in the black box and of the pyranometer that measures the diffuse radiation.

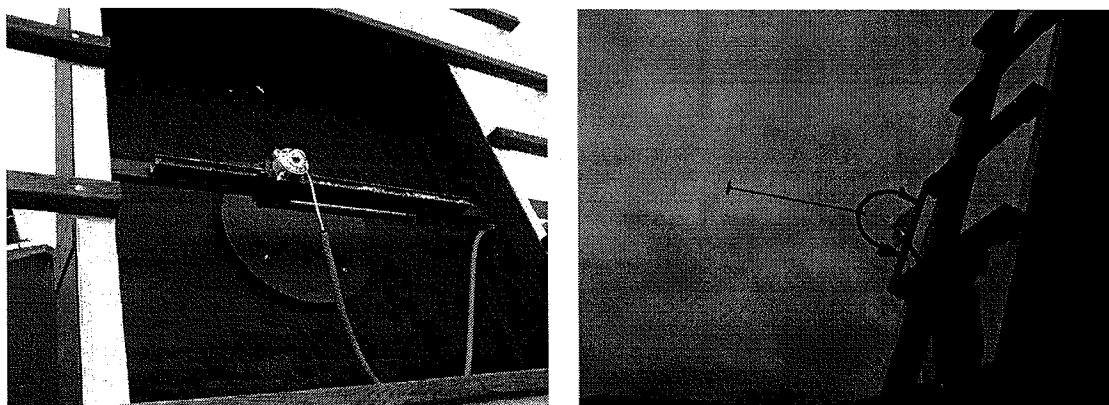


Figure 7.4 Photograph of SolTrans. Left the scanning pyranometer and right the shadow disk for diffuse measurement.

The motion of the scanning pyranometer is controlled by the same computer that controls the solar tracker and the computer also records the measured data.

Stored data include general information about the chosen control parameters and for each measurement step:

- the position of the scanning pyranometer
- the output from the three pyranometers
- the angle of incidence

7.4.1 Measuring the solar transmittance

The measurement is carried out by mounting the test sample on the measuring plane of the solar tracker. Next the measuring parameters must be given to the controlling computer program and the measurement will now be carried out automatically except for the positioning of the shadow disk.

Measuring parameters include:

- Scanning rate (continuous or step. If step is chosen also the step size and the step pause must be given)
- Scanning path (maximum scanning path is 200 mm)
- Tracking type (fixed measuring plane, rotation around vertical axis, rotation around horizontal axis, rotation around both axes. If no rotation or only one axis of rotation is chosen the fixed orientations must be given. If any rotation is chosen also the angular displacements relative to solar azimuth and/or solar height must be given)
- Number of scanings to be performed with the above chosen parameters

When deciding on the scanning path the type of sample must be considered. It is important that the path is long enough to cover a number of representative sections of the test sample. On the other hand the scanning path must be considerably shorter than the extension of the test sample in order to avoid edge effects. In other words large samples are preferred as they will be less critical to edge effects and the length of the scanning path.

For each measurement step the output of the three pyranometers are given together with the actual position of the scanning pyranometer. From these data the hemispherical-hemispherical transmittance (τ^{hh}) for the actual radiation conditions can be calculated as the ratio between transmitted radiation and total radiation. However this number is not very useful as different values of τ^{hh} will be measured under different radiation conditions. The amount of diffuse radiation has an impact on the τ^{hh} and a more convenient number for the solar transmittance is the directional-hemispherical transmittance τ^{dh} . In this number the effect of diffuse radiation has been excluded and the number can be found from the following expression:

$$G_{total} \cdot \tau^{hh} = G_{direct} \cdot \tau^{dh} + G_{diffuse} \cdot \tau^{dif-h} \quad (7-1)$$

which can be rewritten as:

$$\tau^{dh} = \frac{G_{total} \cdot \tau^{hh} - G_{diffuse} \cdot \tau^{dif-h}}{G_{direct}} \quad (7-2)$$

where G_{total} is the total solar radiation [W/m²]

$G_{diffuse}$ is the diffuse part of the radiation [W/m²]

G_{direct} is the direct (beam) part of the radiation ($G_{total} - G_{diffuse}$) [W/m²]

τ^{hh} is the hemispherical-hemispherical solar transmittance

τ^{dh} is the directional-hemispherical solar transmittance

τ^{dif-h} is the diffuse-hemispherical solar transmittance

Now the only number missing is the diffuse-hemispherical transmittance τ^{dif-h} . For plane samples like glass and other optically homogeneous materials a commonly used assumption (Duffie and Beckman, 1991) is that the transmittance for isotropic diffuse radiation is equivalent to the transmittance for direct radiation (beam radiation) with an incidence angle of 60° and this value can be measured by means of the solar tracker.

However the above assumption is not true for most inhomogeneous materials and as the SolTrans was essentially build in order to perform measurements on this type of materials a different approach must be used. As the measurements of τ^{dh} shall be carried out under clear sky conditions the diffuse part of the radiation can be considered relatively small (~10% of total) resulting in only minor difference between τ^{hh} and τ^{dh} . It means that even if the τ^{dif-h} value is known with large uncertainty, only small errors in the τ^{dh} value will occur. Thus the τ^{dif-h} -value can be measured with sufficient accuracy after one of the following two procedures:

- Measure the hemispherical-hemispherical transmittance of the test sample on a day with over cast sky (of which there are plenty in Denmark) under the assumption that the resulting radiation can be considered isotropic diffuse
- Measure the hemispherical-hemispherical transmittance of the test sample by pointing the measuring plane away from the sun in this way avoiding that any direct solar radiation reaches the instruments or the sample. Again the assumption is that the resulting radiation can be considered isotropic diffuse.

The result of either of the two measurement-methods described above will be a useful τ^{dif-h} -value.

7.4.2 Accuracy of the measurements

The measurement is very simple and as long as edge effects are avoided the only uncertainties involved are related to the pyranometers, to the measurement of $\tau^{\text{dif-h}}$ and to the digital voltmeter measuring the voltage from the pyranometers.

The pyranometers are Kipp & Zonen CM11 with an expected measuring error of less than $\pm 1.5\%$.

The digital voltmeter is a Hewlett Packard instrument which according to calibrations have a measuring error less than $\pm 0.1\%$ in the relevant voltage range.

The uncertainty on the $\tau^{\text{dif-h}}$ -value is mainly depending on how reliable the assumptions regarding diffuse isotropic radiation are. In general the difference between $\tau^{\text{dif-h}}$ and $\tau^{\text{n-h}}$ is less than 20% and as the measurement of $\tau^{\text{dif-h}}$ is not totally wrong the uncertainty on $\tau^{\text{dif-h}}$ is estimated to $\pm 10\%$.

Using eq. 7-2 rewritten as:

$$\tau^{\text{dh}} = \frac{G_{\text{transmitted}} - G_{\text{diffuse}} \cdot \tau^{\text{dif-h}}}{G_{\text{total}} - G_{\text{diffuse}}} \quad (7-3)$$

will allow the expected uncertainty to be calculated. In section 7.5 measured results and their associated uncertainties are presented.

7.4.3 Test example

With the purpose of investigating the impact of the step pattern (step size and step pause) on the over all test result, a number of transmittance measurements have been carried out on an inhomogeneous sample. The sample was a rib-framed two-layer polycarbonate solar collector cover. The test sample is shown in figure 7.5 where it is mounted in the solar tracker. The sample consists of two layers of polycarbonate separated with rib-frames in 10 mm's interval. This kind of sample results in a transmittance pattern with large variations depending on whether the solar radiation passes a rib-frame or not. In other words large differences in solar transmittance can be expected over the scanning path and this is critical for the measuring technique.

A number of different scanning rates were tested on the same specimen under constant solar radiation and under constant angle of incidence = 0° . First a series of measurements was carried out with a constant scanning step of 1 mm and step pauses in the range from 1 to 15 seconds. As the step pause is important for the total measuring time the pause should be as small as possible without causing inaccuracies due to the time constant of the pyranometer. By scanning over the maximum distance (200 mm), the total scanning duration will vary from about 250 seconds to about 3050 seconds by using step pauses between 1 and 15 seconds. A long measuring time should be avoided partly because the intensity of the solar radiation varies over time and partly because the measurements have to be watched by the operator.

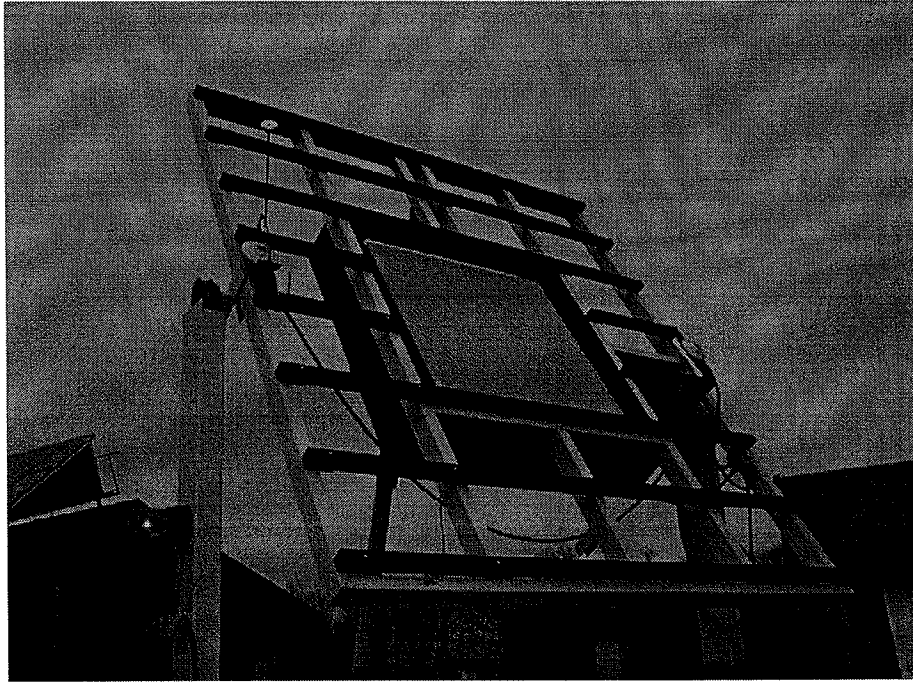


Figure 7.5 Photograph of test sample mounted in the solar tracker.

For the two extreme step pauses 1 and 15 seconds the scanning results are shown in figure 7.6. The curve for the 1 second step pause measurements (dashed curve) has been displaced 10 mm in order to be able to distinguish between the two curves in the figure.

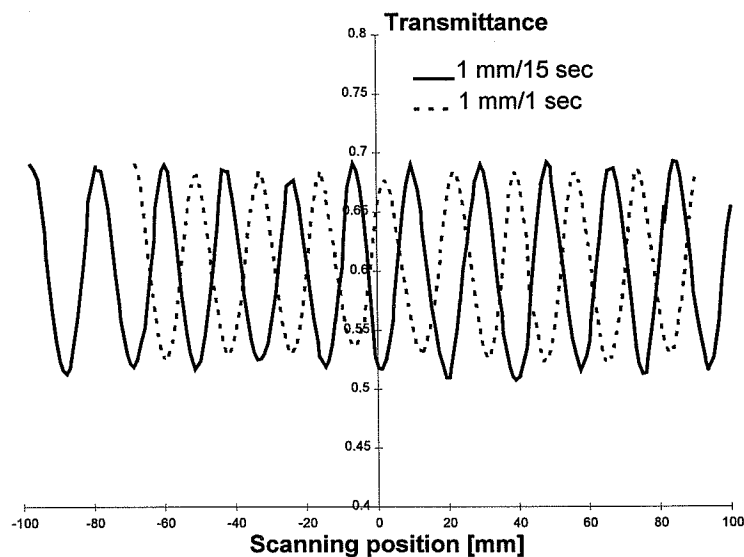


Figure 7.6 Transmittance as function of scanning position for polycarbonate cover. Results of scanings with constant step size and different step pauses. 1mm/15sec and 1mm/1sec denotes a step size of 1mm and step pauses of 15 and 1 second respectively. The 1mm/1sec curve (dashed) has been displaced 10 mm in order to distinguish between the two curves.

The next test series was carried out with a constant step pause of 4 seconds and a step size in the range of 1 to 7 mm. The results of the scanings with 1 and 7 mm step size are shown in figure 7.7 Not surprisingly quite a big difference in the transmittance patterns can be observed. The reason for the difference is the rather large distance between inhomogenities in the test sample resulting in large and abrupt changes in transmittance over the scanning path. (If the inhomogenities had been much closer together the sensor in the pyranometer would not have been able to distinguish between areas with a high solar transmittance and areas with a low transmittance).

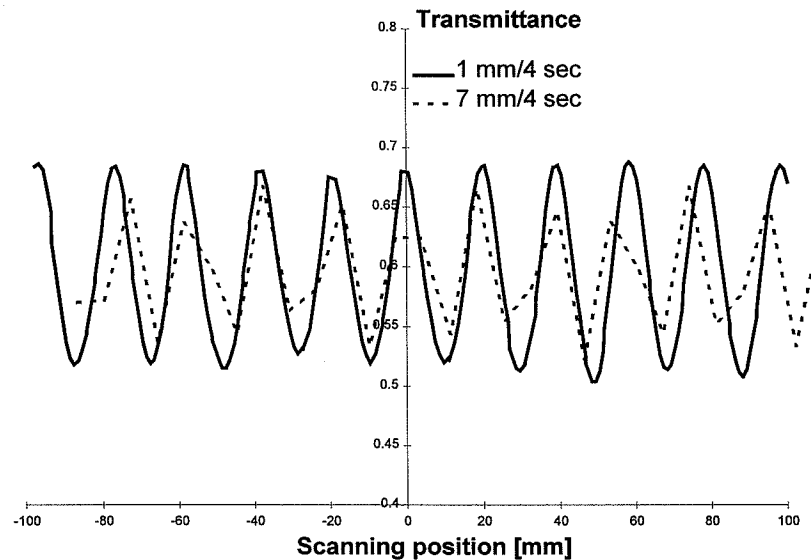


Figure 7.7 Transmittance as function of scanning position for polycarbonate cover. Results of scanings with constant step pause and different step sizes. 1mm/4sec and 7mm/4sec denotes a step pause of 4 seconds and step sizes of 1 and 7 mm respectively.

The measured average hemispherical-hemispherical solar transmittances (τ^{hh}) are listed in table 7.1 together with the solar conditions during each measurement. The total radiation level and the diffuse part of the radiation are almost constant for all measurements and the comparison of results can be performed directly on the τ^{hh} -value.

Table 7.1 Measured solar transmittances under different scanning rates. The total solar radiation level for all measurements is 1010 to 1040 W/m².

Step size	Step pause	Diffuse/Total radiation-ratio	τ^{hh}
1 mm	1 sec	0.09	0.60
1 mm	2 sec	0.09	0.60
1 mm	4 sec	0.08	0.60
1 mm	15 sec	0.09	0.60
2 mm	4 sec	0.08	0.60
3 mm	4 sec	0.08	0.59
4 mm	4 sec	0.08	0.59
5 mm	4 sec	0.08	0.59
6 mm	4 sec	0.08	0.60
7 mm	4 sec	0.08	0.60

Within the expected accuracy of the measurements all results are in concordance which leads to the conclusion that the scanning rate does not have significant influence on the integrated value of τ as long as the scanning path covers a representative part of the geometry of the test sample. However the step size has a rather large influence on the measured transmittance pattern as shown in figure 7.7 and it is recommended to use a combination of small step size and small step pause rather than larger step size and larger step pause even though the total scanning duration may be the same for the two scanning rates.

7.5 Measurement of τ^{dh} for three samples

The directional-hemispherical solar transmittance τ^{dh} of three samples with diffusing/scattering properties have been measured in the SolTrans for different angles of incidence. The results have been compared to measurements on similar samples carried out using indoor optical equipment by other European laboratories.

7.5.1 Description of the samples

Three samples have been tested:

- 50 mm transparent insulation (ISOFLEX) sandwiched between two acrylic sheets
- 40 mm transparent insulation (OKALUX) sandwiched between two 6 mm float glass sheets
- A sheet of diffusing PTFE-01 foil (diffusing Teflon film).

The size of the ISOFLEX and the OKALUX samples was 1250x1500 mm, the size of the tested PTFE-foil was 500x500 mm.

7.5.2 Measurements

The measurements have been performed as broadband transmittance measurements under natural solar radiation in the SolTrans. All presented results are from step-wise scanning, the ISOFLEX and the OKALUX samples were scanned over 100 mm and the PTFE-foil over 10 mm (as the foil can be considered homogeneous).

The measurement for each sample was carried out in two steps:

First the hemispherical-hemispherical transmittance τ^{hh} is measured under clear sky conditions and for the incidence angles that are of interest. Next the diffuse-hemispherical transmittance τ^{diff-h} is measured under cloudy sky condition. The diffusivity of the radiation is checked by comparing the measured total and diffuse radiation.

Now the direct-hemispherical transmittance can be found from eq. 7-2.

7.5.3 Results

The results from the measurements are shown in table 7.2, 7.3 and 7.4 below:

Table 7.2 Broadband measurements of solar transmittance for 50 mm ISOFLEX

i	G_{total}	$G_{diffuse}$	$G_{transmitted}$	τ^{hh}	τ^{diff-h}	τ^{dh}	Uncertainty
0	713	31	437	0.61	0.51	0.62	2
45	523	34	279	0.53	0.51	0.54	2
60	382	35	161	0.42	0.51	0.41	3
[°]	[W/m ²]	[W/m ²]	[W/m ²]	-	-	-	[%]

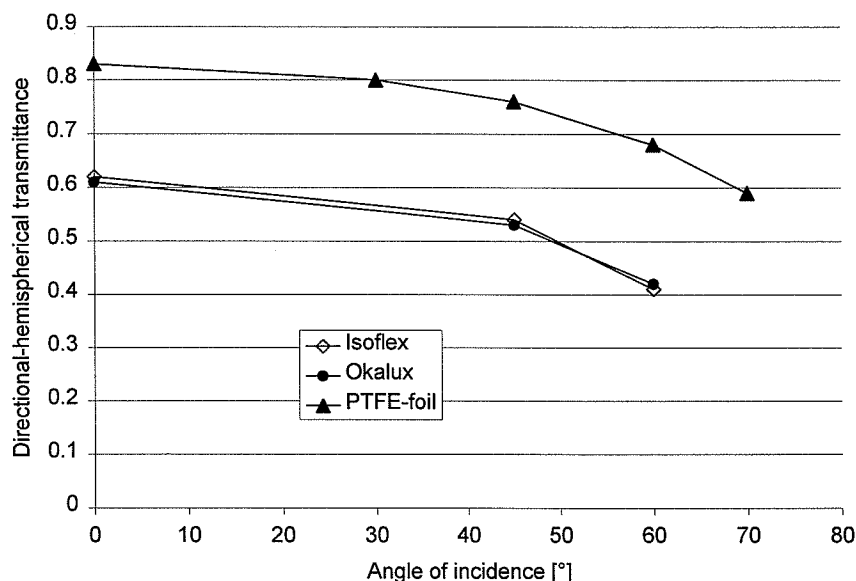
Table 7.3 Broadband measurements of solar transmittance for 40 mm OKALUX

i	G_{total}	$G_{diffuse}$	$G_{transmitted}$	τ^{hh}	τ^{diff-h}	τ^{dh}	Uncertainty
0	739	43	447	0.60	0.51	0.61	2
45	544	38	286	0.53	0.51	0.53	2
60	400	36	171	0.43	0.51	0.42	3
[°]	[W/m ²]	[W/m ²]	[W/m ²]	-	-	-	[%]

Table 7.4 Broadband measurements of solar transmittance for PTFE-foil

i	G_{total}	G_{diffuse}	$G_{\text{transmitted}}$	τ^{hh}	$\tau^{\text{diff-h}}$	τ^{dh}	Uncertainty
0	834	147	673	0.81	0.71	0.83	3
30	800	126	630	0.79	0.71	0.80	3
45	668	109	501	0.75	0.71	0.76	3
60	474	84	324	0.68	0.71	0.68	4
70	348	112	219	0.63	0.71	0.59	7
[°]	[W/m ²]	[W/m ²]	[W/m ²]	-	-	-	[%]

The results are also shown in figure 7.8. Please note that the results for ISOFLEX and OKALUX are almost identical.

Figure 7.8 Directional-hemispherical transmittance τ^{dh} for the investigated samples.

7.5.4 Interlaboratory comparison

Optical investigations on samples similar to the three test samples described here have been conducted in other European countries as part of the IEA SHCP Task 18 project. The methods used by the different countries differ quite a lot and the methods can be divided into two groups: 1) spectral measurements and 2) broadband measurements. Within both groups differences in measuring equipment is reported, e.g. detector sensitivity range (both groups) and light source spectrum (broadband measurements). All laboratories except the Danish performed the measurements indoor using integrating spheres and for the broadband measurements a collimated solar simulator lamp as light source. The aim for all participating countries in this exercise was the same: to establish reliable optical data on the test samples. In this study the focus is set on the directional-

hemispherical transmittance of the samples for radiation conditions corresponding to the reference solar spectrum. Besides Denmark (DK) the participating countries were France (FRA), Germany (D), Italy (IT), the Netherlands (NL) and the United Kingdom (UK). For full details see (Hutchins et al).

In table 7.5 is shown the measured data for the ISOFLEX sample and figure 7.9 is a graphical interpretation of the results. Similar data for the OKALUX and the PTFE sample are shown in table 7.6/figure 7.10 and table 7.7/figure 7.11 respectively. For the ISOFLEX sample a reasonably good agreement between the reported measurements is obtained, especially for lower angles of incidence. For the two other samples significant differences between reported results is observed also for small angles of incidence. The Danish results from the SolTrans measurements have their largest relative deviation (-5%) from average values for the normal-hemispherical transmittance measurement on the OKALUX sample. For the results on the other samples the Danish data are within $\pm 3\%$ of average. Relative deviations up to +15% from average is reported (OKALUX sample) indicating that optical measurements on diffusing or scattering materials must be performed with great care. The average values should not be taken as the "truth" but are included in the tables just to show the spreading of the reported results. Except for the fact that the investigated samples may be different, many sources of errors are involved in especially the indoor measurements. Such errors include light source spectrum, light source collimation, design of integrating sphere and that the sensitivity range for the detectors not in all cases cover the complete solar spectrum. In (Hutchins et al) a number of recommendations for the measurement procedure utilizing an integrating sphere has been given on the basis of these and other optical investigations.

Table 7.5 Directional-hemispherical transmittance τ^{dh} of ISOFLEX sample.

Incidence angle	FRA ¹	D ²	DK ²	Average
0	0.62	0.625	0.62	0.622
45	0.52	0.53	0.54	0.53
60	0.36	0.43	0.41	0.40
70		0.33		0.33

¹ Spectral measurements

² Broadband measurements

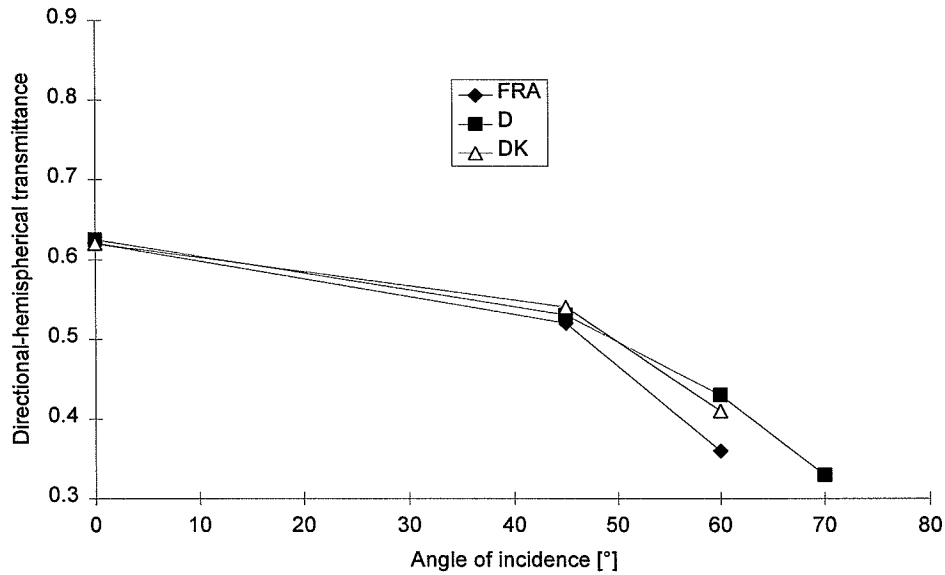


Figure 7.9 Directional-hemispherical transmittance τ^{dh} for ISO FLEX sample.

Table 7.6 Directional-hemispherical transmittance τ^{dh} of OKALUX sample

Incidence angle	NL ²	D ²	UK ¹	DK ²	Average
0	0.629	0.662	0.675	0.61	0.644
45	0.565	0.581	0.532	0.53	0.552
60	0.383	0.473	0.418	0.42	0.424
70	0.229	0.304	0.262	-	0.265

¹ Spectral measurements

² Broadband measurements

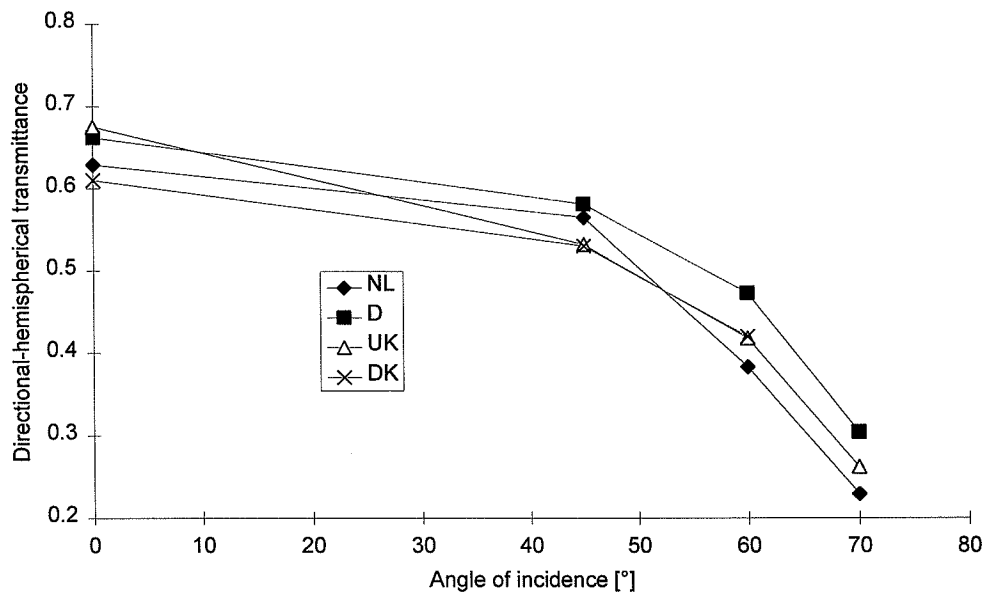
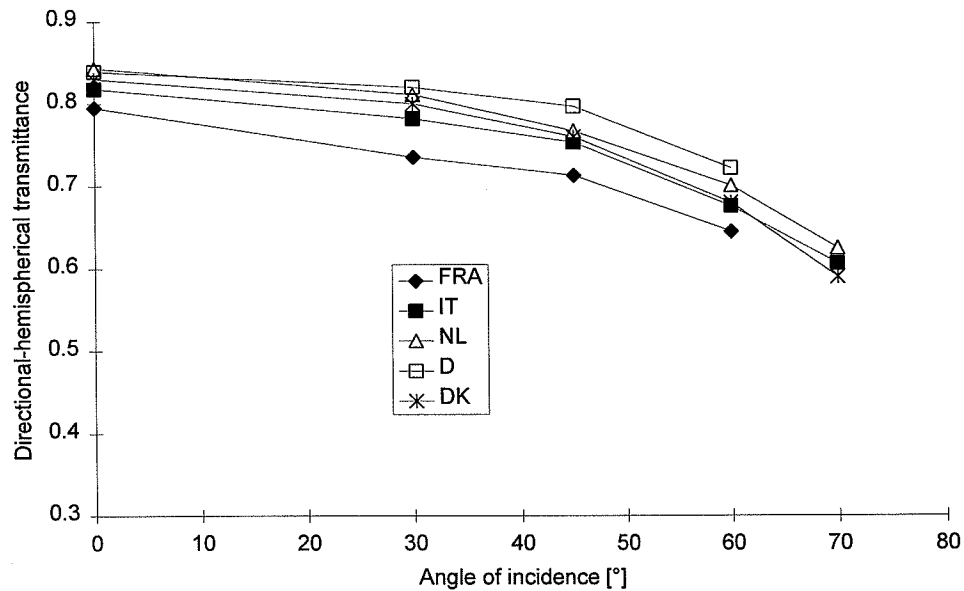


Figure 7.10 Directional-hemispherical transmittance τ^{dh} for OKALUX sample.

Table 7.6 Directional-hemispherical transmittance τ^{dh} of PTFE sample.

Incidence angle	FRA ¹	IT ¹	NL ²	D ¹	D ²	DK ²	Average
0	0.795	0.818	0.843	0.80	0.839	0.83	0.821
30	0.735	0.782	0.811	-	0.82	0.8	0.79
45	0.713	0.753	0.767	-	0.797	0.76	0.758
60	0.645	0.676	0.701	-	0.722	0.68	0.669
70	-	0.606	0.625	-	-	0.59	0.607

¹ Spectral measurements² Broadband measurementsFigure 7.11 Directional-hemispherical transmittance τ^{dh} for PTFE sample.

7.6 Conclusion

A solar tracking device has been constructed with a tracking algorithm based on date, time of the day and the geographical position of the tracker. On the basis of these parameters the apparent position of the sun on the sky is calculated and the tracker can be positioned in relation to this position. The tracker is controlled by a computer on the basis of input describing the desired angular displacements of the measuring plane of the tracker relative to the position of the sun. Any desired angular displacement can be chosen provided that the resulting tilt angle of the measuring plane is within the range of 0-90°.

A scanning pyranometer - SolTrans - has been constructed for outdoor measurements of solar transmittance of especially inhomogeneous transparent material. The SolTrans can be mounted in the tracker and the solar transmittance of transparent materials can now

be determined for any angle of incidence as long as the tilt angle is within 0-90°. The instrumental uncertainty of the transmittance measurement is small but a significant uncertainty has been estimated on the measurements of diffuse transmittance. Depending on the radiation conditions and the transmittance value of the sample the expected uncertainty is about 3%.

An interlaboratory comparison of the angular-dependent solar transmittance of three diffusing or scattering samples has been conducted within the frame of IEA SHCP Task 18. The reported results were rather varying - differences from average value up to 15% were seen. The large discrepancies are believed to be due to differences in measuring techniques and a number of erroneous elements in especially the indoor measurements utilising integrating spheres and (for the indoor broadband measurements) solar simulator lamps were identified. In spite of the not very congruent results from the different laboratories it seems reasonable to keep a high level of confidence in the measuring results from the SolTrans device. The reason for this is the simplicity of the SolTrans measurements and the fact that the measurements have been carried out on large samples under natural solar radiation. This can eliminate some of the classical problems of optical measurements on diffusing or scattering materials using an integrating sphere and (for broadband measurements) a solar simulator lamp. Only broadband values for the solar transmittances can be obtained by the SolTrans measurements and for diffusing or scattering samples it is essential that the sample size is large compared with the path of the scanning pyranometer to avoid edge effects. Furthermore will the solar spectrum neither be completely constant not completely identical to the reference spectrum.

8 Monolithic silica aerogel in glazings

In this chapter an example of optical and thermal characterisation of an advanced glazing is given in the form of a summary of an article accepted for publishing in the official journal of the International Solar Energy Society "Solar Energy". For full details reference is given to annex F.

8.1 Abstract

Silica aerogel is an open-pored porous transparent material with optical and thermal properties that makes the material very interesting as an insulation material in windows. A number of different aerogels have been investigated for their optical and thermal performance. High thermal resistance of aerogel was found for all the investigated samples and the samples showed very high solar as well as light transmittance. However all the investigated aerogel samples showed a tendency to scatter the transmitted light resulting in a reduced optical quality when the aerogels are integrated in glazings. This phenomenon is considered being the main obstacle to incorporate the material in clear glazings but a significant improvement of the optical quality of aerogel has been observed during the last five years. A number of prototypical evacuated 500x500x28 mm aerogel double glazed units employing a new edge seal technique were manufactured and characterised for their optical and thermal properties. As expected the same scattering of light was found in the aerogel glazings as in the aerogel samples, but excellent thermal performance was found, indicating a glazing type that from a thermal point of view is without competition in heating dominated climates.

8.2 Introduction

The work on which the presented results are based has been carried out in the aerogel project within the IEA SHCP Task 18 project. The scope of the aerogel project was to perform an evaluation of the aerogel material in order to identify some of the strengths and weaknesses that can be expected of aerogel as a material for window applications.

The main goals of the aerogel project were to carry out an optical and thermal characterisation of the aerogel and to show that it will be possible to construct a glazing with a U-value below 0.5 W/m²K and at the same time achieve a total solar energy transmittance (g-value) above 0.75.

8.3 Measurements

The optical and the thermal properties of the aerogel have been investigated. Five samples have been selected to give a good picture of the range of especially optical properties that are characteristic for different aerogel materials. Key parameters for the five samples are described in table 8.1.

Table 8.1 Key parameters of test specimen

	JAP1	NOR1	SWE1	FRA1	JAP2
Type	Aerogel	Xerogel	Aerogel	Carbogel	Aerogel
Density	90 kg/m ³	500 kg/m ³	150 kg/m ³	173 kg/m ³	116 kg/m ³
Thickness	12 mm	9 mm	7 mm	11 mm	9 mm

8.3.1 Measured solar and visible properties

The spectral normal-normal transmittance (τ_{λ}^{nn}) and the spectral normal hemispherical transmittance (τ_{λ}^{nh}) have been obtained in the spectral range from 300 to 2500 nm, using when necessary an integrating sphere.

From the measured spectra the integrated transmittance values have been calculated using standard documents (ASTM - E891; Pr EN 410). Table 8.2 shows the solar properties indicated with subscript e and table 8.3 shows the visible light properties indicated with subscript v. TR is the Transparency Ratio (Elaloui et al., 1992), expressed as the ratio:

$$TR = \frac{\tau_v^{nn}}{\tau_v^{nh}} \quad (8-1)$$

where subscript v indicates visible light parameters. For explanation of the quantities in eq. 8-1 reference is given to section 3.3. TR is expected to be as high as possible to guarantee a good transparency and vision quality.

Table 8.2 Solar properties

	JAP1	SWE1	NOR1	FRA1	JAP2
Type	Aerogel	Aerogel	Xerogel	Carbogel	Aerogel
τ_e^{nh} [%]	87.3	89.7	86.0	86.7	92.1
τ_e^{nn} [%]	68.4	73.6	80.5	76.1	89.0
τ_e^{n-dif} [%]	20.9	16.3	5.5	-	3.1
ρ_e^{nh} [%]	2.9	3.8	3.3	-	1.9

Table 8.3 Light properties

	JAP1	SWE1	NOR1	FRA1	JAP2
Type	Aerogel	Aerogel	Xerogel	Carbogel	Aerogel
τ_v^{nh} [%]	84.1	87.2	86.7	89.9	92.1
τ_v^m [%]	65.3	65.4	79.6	77.4	88.0
τ_v^{n-dif} [%]	18.8	21.8	7.1	-	4.0
ρ_v^{nh} [%]	4.0	4.8	4.6	-	2.8
TR	0.78	0.75	0.92	0.86	0.96

As shown in table 8.2 and 8.3 the samples are found to have high transmittance (84-92%) for radiation in the solar spectrum as well as in the visible part of the solar spectrum. These values are about the same as for conventional clear glass. However, part of the solar radiation is being diffused when transmitted through the material. Measurements have shown that the scattering is taking place mainly at shorter wavelength i.e. in the visible part of the solar spectrum. This means that the aerogel is the reason for more or less hazy pictures when objects are viewed through the material.

The scattering $S(\lambda)$ can be expressed by the following model (Hutchins et al.):

$$S(\lambda) = S_{\text{bulk}}(\lambda) + S_{\text{surface}} \quad (8-2)$$

where $S_{\text{bulk}}(\lambda)$ is the wavelength dependent bulk scattering and S_{surface} is the wavelength independent surface scattering. By reducing the typical dimension of pores, cavities and silicon oxide particles in the aerogel it may be possible to push the scattering towards shorter wavelength into the ultraviolet and thereby out of the visible, resulting in less visible scattering (Hutchins et al.). The value of the Transparency Ratio TR is a simple way of quantifying the scattering phenomenon. For the sake of comparison ordinary float glass has a TR value of about 0.99, where the TR value for the investigated samples were in the range of 0.75 to 0.96. It is worth noticing that the JAP2 sample has a lower visible scattering (~4%) and at the same time a higher solar and visible transmittance than all other investigated samples in this way showing a significant improvement in especially the visible properties of the aerogel.

8.3.2 Measured thermal properties

Depending on the density of the aerogel the non-evacuated and evacuated thermal conductivity for the samples investigated have been measured to 0.015-0.017 W/mK and 0.009-0.011 W/mK respectively. The xerogels showed higher thermal conductivity in non-evacuated condition (0.025 W/mK) but the same thermal conductivity as aerogels in evacuated state (Hutchins et al.).

8.4 Aerogel double glazed unit

8.4.1 Production of an aerogel glazing

An aerogel glazing can be constructed as a sandwich by inserting a 20 mm thick aerogel disk between two glass panes, sealing the unit and evacuating the interior of the aerogel glazing to a level below 5000 Pa. Of course this is much easier said than done.

To maintain a low U_{center} of the evacuated glazing it is essential that the edge sealing is sufficiently vapour and air tight during the expected lifetime of the glazing. The ideal edge seal for an evacuated aerogel glazing should be airtight, vapour tight and resulting in no or only little thermal bridge effect.

In a recent work a promising edge seal for an evacuated aerogel glazing has been described (Jensen et al., 1996). The principle of the edge seal is very simple: Instead of the stainless steel that so far has been used, a special plastic laminate with glass dust is used in the sealing in combination with butyl and polysulfide.

As the sealing is about 1.6 mm thick (including plastic foil, butyl and polysulfide) it results only in small cold bridge effect in the final edge seal. In table 8.4 is shown calculated U-values for aerogel glazings (20 mm aerogel sheet) of different sizes, all using the described edge seal. Values are including the effect of the butyl and polysulfide layers.

Table 8.4 Calculated total U-values (U_{2D}) for different sizes of aerogel glazings with rim seal of 0.1 mm laminated plastic foil and 0.5 mm of butyl protected with a 1 mm polysulfide sealant. (Jensen et al., 1996)

Spacer material	Glazing size	Perimeter	Area	Equivalent thermal conductivity	U_{centre}	U_{2D}
	m × m	m	m ²	W/mK	W/m ² K	W/m ² K
Plastic foil	0.5 × 0.5	2.0	0.25	0.20	0.40	0.44
	1.0 × 1.0	4.0	1.00			0.42
	1.5 × 1.5	6.0	2.25			0.41

Four evacuated aerogel double glazed units in small scale have been constructed at the Department of Buildings and Energy, all using the basic principle of the edge seal described above. Four glazings were manufactured in order to allow investigations in four different laboratories in Europe. Each glazing was made of a 20 mm thick Swedish Airglass disk and two 4 mm low iron hardened glass panes. The overall size of each unit was 500x500x28 mm with an aperture of about 450x450 mm.

8.4.2 Measurement of key performance parameters

The key performance parameters (U-value, g-value, solar transmittance τ_e^{nh} and light transmittance τ_v^{nh}), have been measured at different laboratories. The results of the measurements are shown in table 8.5. The optical results shown are integrated values of normal-hemispherical transmittance in the solar and visible spectrum respectively, i.e. τ_e^{nh} and τ_v^{nh} . U-value measurements were carried out using hot-plate devices and the results are shown for a mean temperature of the glazing of 10°C and including total surface resistance of 0.17 m²K/W. The g-value was measured in the METSET using the indoor solar simulator (CSI-lamps).

Table 8.5 Key performance parameters for aerogel glazing

Laboratory	FIN	FRA	FRG	DK	
U _{center}	0.42	-	0.41	0.47	[W/m ² K]
τ_e^{nh}	78.0	74.1	75.0	-	[%]
τ_v^{nh}	73.7	71.7	72.0	-	[%]
g	-	-	-	0.79 ¹	-

¹ Incidence angle = 22.5°

As it shows in table 8.5 the measurements indicates that the aerogel glazings that have been tested exhibit very high thermal resistance as well as very high solar and visible transmittance. The goal initially set (U < 0.5 W/m²K and g > 0.75) seem to be reached.

8.5 Conclusion

Several candidate materials of the aerogel type have been investigated from an optical and thermal point of view. The expected high thermal resistance of aerogel was found for all the investigated samples and the samples showed very high values for the transmittance of radiation in the solar spectrum as well as in the visible part of the solar spectrum. As expected the measurements showed that the investigated materials all have a tendency to scatter the transmitted light resulting in a hazy picture when objects are viewed through the material. This phenomenon is considered to be one of the major problems for the use of aerogel-type materials in clear windows. However the sample labelled JAP2 represents a significant improvement of the visible properties of aerogel and must clearly be seen as a step towards an aerogel suitable for window applications from an optical as well as thermal point of view.

The measurements of the thermal key parameters of the aerogel glazings showed that very high values for thermal resistance and total solar energy transmittance were reached, resulting in a glazing type that from a thermal point of view is without competition for especially heating dominated climates.

9 Conclusion

The aim of the project was to enable an energy performance characterisation of advanced windows and glazing systems based on physical measurements and to gain confidence in the measured results.

Two key parameters describe the thermal performance of windows: The thermal transmittance and the total solar energy transmittance and the focus of the study has been set on the development of appropriate methods to determine these two key parameters for advanced windows and glazings by means of measurements.

To reach the objective techniques for measuring the thermal transmittance, the total solar energy transmittance and the direct solar transmittance for windows and glazings were investigated and developed. This process included the improvement of existing equipment and existing measuring methods as well as the development of new measuring equipment and new measuring and data treatment methods.

Measurements of thermal transmittance by means of a guarded hot box have been investigated. The accuracy of the guarded hot box measurement was confirmed by a system performance test in which the thermal transmittance of a well-defined calibration panel was measured in the hot box as well as in a hot plate device.

The reliability and robustness of the calibration and measuring procedures were confirmed through analytical investigations and physical round robin tests on three different windows. The window U-values were ranging from 1.1 W/m²K to 2.5 W/m²K. Good agreement between the reported results was obtained and the differences in measured U-values were in all cases within the expected uncertainties of the measurements.

A proposal for the measurement of roof window thermal transmittance was elaborated in order to facilitate such measurements and to bring them in accordance with the general concept in the draft proposals prEN12412 and ISO/DIS12567.

On the basis of the investigations of hot box measurements a high degree of confidence in the measurement accuracy of the guarded hot box at the Department of Buildings and Energy has been obtained. At the same time the testing procedure outlined in the draft standards has proven to be reliable giving good agreement between results for identical samples measured in different hot box devices.

Indoor g-value measurements in a calorimetric test facility (the METSET) mounted in a solar simulator has been investigated.

Procedures for performing the g-value measurements in the METSET have been developed together with procedures for the subsequent corrections of the measured results. Corrections of the measured results are necessary as the measurements are carried

out under conditions different from the defined reference conditions. A very robust correction method has been applied covering most types of samples. However for samples with very low solar transmittance, large solar absorption in the inner part of the sample and spectral selective absorptance in the layers, the corrections of the q_i -part of the g-value is still object to further development. For less extreme cases the procedures outlined in this report are considered sufficiently accurate.

The g-value as function of incidence angle for three calibration glazings have been measured in the METSET. The glazings had very different optical and thermal properties but were all clear glazings. This enabled a comparison between measurements and detailed calculations assuming that the uncertainty in the calculated values is $\pm 5\%$. For two of the glazings, measurements were performed on additional samples in order to investigate the reproducibility of the measurements which showed to be better than 1%.

An error analysis of the measurements showed that the expected uncertainty for the final measured g-value, g_{ref} , is about 0.03 or a relative uncertainty of 4-10% for the investigated samples. This uncertainty is of the same magnitude as the expected uncertainty in the model calculations.

The dominant correction is related to the transmittance part of the g-value and of course this correction is very sensitive to the spectral distribution of the solar simulator. Even though the spectrum for the solar simulator was measured as an average of three lamps it is evident that the spectral distribution of the solar simulator in reality may be different from the data-set used for the detailed spectral corrections. By using corrections based on indoor and outdoor broadband measurements the impact of an erroneous solar simulator spectrum is reduced but at the same time is introduced the uncertainty of the reference spectrum (which is not exactly the same as the solar spectrum during the outdoor measurements).

The results of the investigations give good reason to increase the confidence in the method used to obtain the measured g-values and shows that the calorimetric measurements - when properly corrected - give meaningful results.

An outdoor solar tracking device has been constructed with a tracking algorithm based on date, time of the day and the geographical position of the tracker. On the basis of these parameters the apparent position of the sun on the sky is calculated and the tracker can be positioned in relation to this position.

A scanning pyranometer - SolTrans - has been constructed for outdoor measurements of solar transmittance of especially transparent materials with inhomogeneous optical properties. The SolTrans can be mounted in the tracker and the solar transmittance of transparent materials can now be determined for any angle of incidence. Three different types of material have been tested and depending on the radiation conditions and the transmittance value of the samples the expected relative uncertainties of the measurements in SolTrans were about 2-7%.

An interlaboratory comparison of the angular-dependent solar transmittance of three diffusing or scattering samples has been conducted within the frame of IEA SHCP Task 18. The reported results were rather varying – relative differences from average value up to 15% were seen. The large discrepancies are believed to be due to differences in measuring techniques and a number of erroneous elements in especially the indoor measurements utilising integrating spheres and (for the indoor broadband measurements) solar simulator lamps were identified. In spite of the not very congruent results from the different laboratories it seems reasonable to keep trust in the measuring results from the SolTrans device. The reason for this is the simplicity of the SolTrans measurements and the fact that the measurements have been carried out on large samples under natural solar radiation. This can eliminate some of the classical problems of optical measurements on diffusing or scattering materials using an integrating sphere and (for broadband measurements) a solar simulator lamp. Of course only integrated values for the solar transmittances can be obtained by the SolTrans measurements and for diffusing or scattering samples it is essential that the sample size is large compared with the path of the scanning pyranometer. Furthermore will the solar spectrum neither be completely constant not completely identical to the reference spectrum.

Utilising the equipment and the procedures for measurements and data treatment described in this report will in most cases allow a full characterisation of energy performance data for advanced windows and glazings to be carried out by measurements and with good accuracy. As an example of this the thermal and optical properties of four prototypical aerogel glazing have been determined in chapter 8.

9.1 Outlook

In far the most cases the measurement of the thermal transmittance of a specimen is considered covered by the presented methods. However this is not always the case for the measurement of the total solar energy transmittance: Even though the presented methods can be utilised to measure the g-value of many interesting and advanced window and glazing designs not all possible design cases are covered by the presented procedures. Especially two categories of specimens will cause problems for the g-value measurements:

1. samples with very low solar transmittance and very high spectrally selective absorptance in especially the inner part of the sample
2. samples with very angular selective optical properties

For the first category the problem occurs if there is no optical and thermal model valid for the sample or if the simulator spectrum is very uncertain. The problem is related to the spectral difference between solar simulator and reference solar spectrum: The q_i part of the g-value will not be proper spectrally corrected by the model suggested in chapter 6 if the sample shows a high degree of spectral selective

absorptance in the inner part of the sample. A further development of correction models is needed.

For the second category the problem is related to the divergence of the solar simulator: As the radiation from the simulator is not collimated (like the real sun) part of the radiation reaches the sample surface under incidence angles different from the expected angle. For samples that are very angular selective this may result in errors in the transmittance part of the g-value. The problem can be partly solved by using different solar simulator lamps facilitating lenses for the collimation of the light or the problem can be completely solved by performing the measurements outdoor. The basic equipment for performing the measurements outdoor (the METSET and the Solar Tracker) is now available and hopefully a chance will come to carry out the work necessary to facilitate future outdoor measurements.

SYMBOLS

A	Area	[m ²]
Az	Azimuth	[°]
c	Specific heat capacity	[J/kgK]
d	Thickness, width	[m]
D(λ)	Spectral distribution difference between reference solar spectrum and simulator.	
F	View factor	
F _c	Convective fraction	
g	Total solar energy transmittance	
G	Solar radiation level	[W/m ²]
h	Solar height, slope	[°]
h	Surface heat exchange coefficient	[W/m ² K]
H	Heat exchange coefficient	[W/K]
l	Length, perimeter	[m]
m	mass flow rate	[kg/s]
q	Energy flux, heat flow rate, heat flux density	[W/m ²]
q _i	Secondary heat transfer coefficient towards the inside	
q _o	Secondary heat transfer coefficient towards the outside	
Q	Energy flow, heat flow	[W]
R	Thermal resistance, surface thermal resistance	[m ² K/W]
S(λ)	Spectral scattering	
S _{λ}	Spectral distribution	
T	Temperature	[K]
TR	Transparency Ratio	
U	Thermal transmittance	[W/m ² K]
α	Absorptance	
$\alpha(\lambda)$	Spectral absorptance	
γ	Non dimensional number between 0 and 1 indicating the plane in a sample at which all solar absorption could be referred to, resulting in the same heat flows and temperature gradients in a model sample as in the physical sample	
Δ	Difference, step	
ε	Hemispherical emissivity	
θ	Temperature	[°C]
λ	Thermal conductivity	[W/mK]
λ	Wavelength	[nm]
ρ	Reflectance	

$\rho(\lambda)$	Spectral reflectance	
τ	Transmittance	
$\tau(\lambda)$	Spectral transmittance	
Φ	Heat flow	[W]
Ψ	Linear thermal transmittance	[W/mK]

Subscripts

c	Convective, air property
cal	Calibration panel
dark	Measuring condition without solar radiation
e	Reference solar condition (optical)
e	Exterior
edge	Edge of glazing, edge zone
exp	Experimental
f	Fluid
g	Glazing, glass
i	Interior, inner, inwards
in	Input
m	Mean, measured, mid
mb	Metering box
me	Mean
n	Environmental
net	Net
o	Outer, outwards
r	Radiative property
ref	Reference condition
s	Surface
solar	Solar condition
sp	Specimen, sample
st	Standardised
sur	Surround panel
t	Total
v	Visible property (optical)
λ	Spectral property (optical)

Superscripts

nn	Normal-normal
nh	Normal-hemispherical
dh	Directional-hemispherical
hh	Hemispherical-hemispherical

dif-h	Diffuse-hemispherical
n-dif	Normal-diffuse
b	Backside property

References

Litterature:

- Bygge- og Boligstyrelsen: *Bygningsreglementet (Danish Building Code)*
1. april 1995
- Duer, K.: *U-value measurements on Roof Window*
Department of Buildings and Energy, Technical University of Denmark
Report SR 97-17, 1997
- Duer, K.: *U-value measurements on ISO Round Robin Window*
Department of Buildings and Energy, Technical University of Denmark
Report SR 97-20, 1997
- Duer, K.: *U-value measurements on Roof Window, Second study*
Department of Buildings and Energy, Technical University of Denmark
Report SR 98-09, 1998.
- Duffie, J.A.; Beckman, W.A.: *Solar Engineering of Thermal Processes*.
Second edition. John Wiley & Sons, Inc. 1991
- Elaloui, E.; Achard, P.; Chevalier, B.; Chevalier, J.L.; Durant, M.; Pajonk, G.M.:
Improved monolithic aerogel for transparent glass spacer in innovative windows.
Proceedings of SPIE v 1727 p. 402-417, 1992.
- Espersen, A.M.; Weibøl, C.: *Metoder til Effektivitetsprøvning af Solfangere*.
(Methods
for determining solar collector performance)
Department of Buildings and Energy, 1994
- Harrison, P.E; Dubrous, F.M.: *Determination of Window Thermal Characteristics using Solar-simulator-based Test Method*.
ASHRAE Transactions V. 96 pt. 1. 1990
- Heinemann, U.; Hümmer, E.; Büttner, D.; Caps, R.; Fricke, J.:
Silica aerogel - a light-transmitting thermal superinsulator.
High Temperatures High Pressures v 18
n5 1986 p. 517-526

- Hunt, A.J.; Grether, D.F.; Wahlig, M.: *The Measurement of Circumsolar Radiation. An Introduction to Meteorological Measurements and Data Handling for Solar Energy Applications*.
IEA Task iV - Development of an Insolation Handbook and Instrument Package. DOE/ER-0084.
U.S. Department of Energy 1980.
- Hunt, Arlon J.; Martin, Marlo: *Scaling up production of silica aerogel using the CO₂ substitution method*.
Proceedings of International Symposium on Aerogels. Sept. 30 - Oct. 2, 1991
- Hutchins, M.G.; Aschehoug, O.; Ballinger, J. (eds): *International Energy Agency Solar Heating & Cooling Programme Task 18, Advanced Glazing Materials, Technical Reports of Subtask A and Subtask B*.
To be published.
- Incropera, F.P.; DeWitt, D.P.: *Introduction to heat transfer*. Second edition
John Wiley & Sons, 1990
- Jensen, K.I.: *Højisolerende transparente dæklag. (Highly insulating transparent covers)*
Department of Buildings and Energy, Technical University of Denmark
Report no. 49, 1989
- Jensen, K.I.; Schultz, J.M.; Svendsen, S. (eds): *Development and investigation of evacuated windows based on monolithic silica aerogel spacers*.
EU-contract JOU2-CT92-0192. (1992-1995).
- Jensen, K.I.: *Passive solar component based on evacuated monolithic silica aerogel..*
J. of Non-Crystalline Solids v 145 n 1-3 Aug 1, p237-239. 1992
- Kistler, S.S.: *Nature* 127.
1931
- Kistler, S.S.: *J. Phys. Chem* 39.
1935
- Kistler, S.S.: *J. Phys. Chem* 46.
1942

- Maccari, A.: *Spectral Distribution Error Analysis*
IEA SHCP Task 18 working document T18/B12/IT6/95
Italian Agency for New Technology, Energy and Environment.
Energy Department. ENEA, Rome, Italy. 1995
- Moon, P.: *Proposed Standard Solar -radiation Curves for Engineering Use.*
The Journal of the Franklin Institute.
November 1940
- Petersen, E.: *Solindfald Gennem Vinduer. (Solar Heat Gain Through Windows)*
Department of Buildings and Energy, Technical University of Denmark.
Meddelelse nr. 13. 1966.
- Rosenfeld, J.L.J.: *On the Calculation of the Total Solar Energy Transmittance for Complex Glazing Systems.*
Paper presented at 8th International Meeting on Transparent Insulation,
Freiburg Germany. 1996.
- Rubin, M.; Lampert, C.M.: *Transparent Silica Aerogels for Window.*
Insulation Solar Energy Materials 7 (1983) 393-400.
- VIK: Varmeisoleringskontrollen i Danmark. *Personal communication with Mogens R. Byberg*
- Wallentén, P.: *Heat Flow in Full Scale Room Exposed to Natural Climate.*
Department of Building Science, Lund Institute of Technology,
Lund University. Sweden.
Report TABK-98/3051. 1998.
- Williams, R.: *Personal communication based on the following two reports:*
1. *Synthesis report on the results of the laboratories who participate in the Comparison on Thermal Measurements on double glazed units.* 1989
2. *Intercomparison of thermal measurements on double glazed windows: Synthesis Report.* 1994. Project MTR – 105
Both by N. König, Fraunhofer Institut für Bauphysik - Stuttgart
- Williams, R.; Hall, D.: *Design and Validation of Glazed Calibration Panels Required for the Measurement of Thermal Transmittance of Glazed Assemblies. Final Summary Report.*
EU Contract MATI-CT 940063, SMT Project 3032
National Physical Laboratory UK
NPL Report CBTM 2. 1997.
- Williams, R.; Hall, D.: *Laboratory Intercomparison of Hot Box Measurements of a Glazed Window System using the measurement procedures given in ISO/DIS*

12567 and prEN12412-1 standards
National Physical Laboratory UK
NPL Report CBTM 5. 1998.

Calculation programs:

WIS *Advanced Windows Information System.*
TNO Building and Construction
Research, The Netherlands, 1996.

THERM: *A PC Program for Analysing Two-Dimensional Heat Transfer Through Building Products.*
Window and Daylighting Group, Building Technologies Program
Lawrence Berkely National Laboratory.
Berkely, CA 94720 USA.

WINDOW 4.1: *A PC Program for Analyzing The Thermal Performance of Fenestration Products.*
Window and Daylighting Group, Building Technologies Program
Lawrence Berkely National Laboratory.
Berkely, CA 94720 USA.

International (draft) standards:

ASHRAE Standard 142P. *Standard Method for Determining and Expressing the Heat Transfer and Total Optical Properties of Fenestration Products, Public Review Draft, October 1996, American Society of Heating, Refrigerating and Air-Conditioning Engineers, Inc., Atlanta, GA.*

DS 418 Annex 1 *Beregning af bygningers varmetab. Tillæg omhandlende vinduer og yderdøre. (Calculation of heat loss in buildings. Annex 1 regarding windows and doors).* 1997

EN 410. *Glass in Building - Determination of light transmittance, solar direct transmittance, total solar energy transmittance, ultraviolet transmittance and related glazing characteristics.* April 1998

EN 673. *Glass in Building - Determination of thermal transmittance (U value) - Calculation method.* November 1997

prEN 1077. *Windows, doors and shutters - Calculation of thermal transmittance.*
10.10.1997/29.02.2000

- prEN 12412. *Windows and doors - Thermal transmittance - calibrated and guarded hot box method*. Same as ISO/DIS12567
- EN ISO 10211-1. *Thermal bridges in building constructions - Heat flows and surface temperatures*. October 1995.
- ISO 8301. *Thermal insulation - Determination of steady-state thermal resistance and related properties - Heat flow meter apparatus*.
- ISO 8302. *Thermal insulation - Determination of steady-state thermal resistance and related properties - Guarded hot plate apparatus*.
- ISO 8990. *Thermal insulation - Determination of steady-state thermal transmission properties - Calibrated and guarded hot box*. 1994.
- ISO 9050. *Glass in Building - Determination of light transmittance, solar direct transmittance, total solar energy transmittance and ultraviolet transmittance and related glazing factors*. 1990
- ISO 9845. *Solar energy - Reference solar spectral irradiance at the ground at different receiving conditions*. 1992
- ISO/DIS 12567. *Thermal performance of doors and windows - Determination of thermal transmittance by hot box method*. Versions 1996/09 and 1998/07.
- ISO/CD 15099. *Thermal Performance of Windows, Doors and Shading Devices – Detailed Calculations*.

APPENDIX A

1 INTRODUCTION

This report describes the results of the U-value measurements performed on a roof window.

The measurements have been performed using the procedures given in CEN prEN 12412:1996 with a few modifications especially concerning the calibration procedure. The measurements were carried out at the Technical University of Denmark, Department of Buildings and Energy.

2 DESCRIPTION OF THE WINDOW

The window is a wooden roof window and measures 1400 mm high x 1140 mm wide. The glazing is 4-16-4 mm with one hardened glass pane outermost and one soft-coated glass pane innermost (low e-coating in position 3). The gap between the glass panes is Argon filled and the spacer material is aluminium.

3 CALIBRATION PANELS

Two calibration panels have been constructed in order to carry out the hot box calibration procedure. The panels measure 1400mm high x 1140mm wide and 1215mm high x 990mm wide respectively and have both a total thickness of 28 mm.

The core material is polyurethane which prior to the assembling has been ground plane in order to avoid or at least reduce variations in the material thickness. The core thickness is 20 mm.

The glazings on both sides of the core are 4 mm hardened glass with normal emissivity.

The panels are assembled simply by means of heavy duty tape, no glue has been used in this process.

The thermal conductivity λ has been measured for the sample thicknesses of 20 mm. The measurements were performed on material samples produced in the same batch as the material samples that were used in the calibration panels.

The thermal conductivity was determined at three mean temperatures of the polyurethane: 16, 21 and 26°C. A linear temperature dependency for the thermal conductivity of the polyurethane was found in this range and it is assumed that the same linear change in the thermal conductivity as a function of temperature can be used also outside the measured range. The λ -values at the relevant temperatures during calibrations were found using the following expression:

$$\lambda_t = \lambda_{21} - \frac{(21 - t) \cdot \Delta\lambda \cdot \lambda_{21}}{100}$$

where t is the actual temperature of the core material during calibrations and $\Delta\lambda$ is the temperature dependency of the thermal conductivity of polyurethane.

The results of the measurements are:

$$\lambda_{21} = 0.0294 \text{ W/mK}$$

$$\Delta\lambda = 0.3 \text{ \%/K}$$

4 GUARDED HOT BOX

The hot box measurements were performed in a guarded hot box. Maximum sample size is 1500 x 1250 mm and the metering box measures 1600 x 1350 mm inside. The guarded hot box is build and the measurements are performed in accordance to ISO 8990, CEN prEN 12412:1996 and the ISO/CD12567 proposal with the following exceptions:

- No wind speed measurements are carried out during measurements but the windspeed on the cold side has previously been measured to ensure that the windspeed here is at least 2 m/s.
- Due to limitations in the cooling system it has not been possible to obtain a cold side temperature below -8°C during calibration.
- The calibration panel is >20 mm.
- The calibration procedure has been changed as explained in section 5.

Prior to each calibration or U-value measurement the metering box is tested for air tightness in order to assure that no air will be exchanged between hot and cold side.

5 CALIBRATION MEASUREMENTS

As the roof window was going to be measured with 22 mm of the frame mounted in the surround panel reveal and the rest of the construction exposed to the cold side ambient, the calibration procedure differed from the procedure outlined in CEN prEN12412:1996. The calibration was carried out in two steps using the following procedure:

1. First the surround panel heat exchange coefficient H_{sur} was found using the 1400x1140x28 mm calibration panel.
The calibration panel was mounted flush with the face of the cold side surround panel. See figure 2. Three measurements were carried out with 20°C on the warm side and 0°C, -5°C and +10°C respectively on the cold side. During the first measurement the voltage for the wind simulator fan on the cold side was regulated in order to obtain the standard surface resistance in accordance to the CEN standard.
2. Next the window with the second calibration panel was mounted in the surround panel. See figure 3. Four series of measurements were carried out:

2a. One measurement with the calibration panel mounted with tape and performing the measurement with the same wind simulator voltage as in 1.

$T_{\text{warm}} = 20^{\circ}\text{C}$ and $T_{\text{cold}} = 0^{\circ}\text{C}$.

The purpose of this measurement was merely to observe the change in surface resistance when mounting the window.

2b. Three measurements were carried out with 20°C on the warm side and 0°C , -8°C and $+10^{\circ}\text{C}$ respectively on the cold side. During the first measurement the voltage for the wind simulator fan on the cold side was regulated again in order to obtain the standard surface resistance in the new glazing plane.

2c. One measurement with the calibration panel mounted with the alu-profiles from the window, wind speed from 2b. $T_{\text{warm}} = 20^{\circ}\text{C}$ and $T_{\text{cold}} = 0^{\circ}\text{C}$

2d. One measurement with the calibration panel mounted with the alu-profiles and all metal covering mounted on the cold side, wind speed from 2b. $T_{\text{warm}} = 20^{\circ}\text{C}$ and $T_{\text{cold}} = 0^{\circ}\text{C}$.

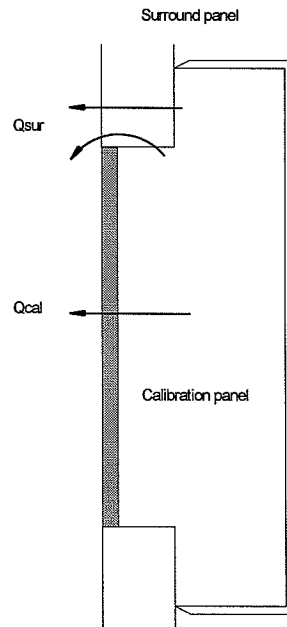


Figure 2. Mounting of calibration panel 1 (calibration step 1).

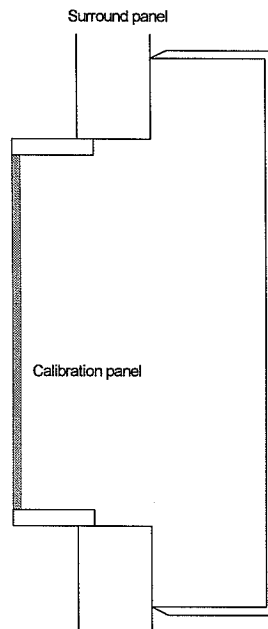


Figure 3. Mounting of calibration panel 2 (calibration step 2).

From the known thermal resistance of the calibration panels it is now possible to find the surround panel heat exchange coefficient H_{sur} as a function of surround panel mean temperature as well as the surface resistance R_s as a function of heat flux density through the calibration panel. The results are shown in figure 4 and 5. In Annex A is shown the key results from all calibrations.

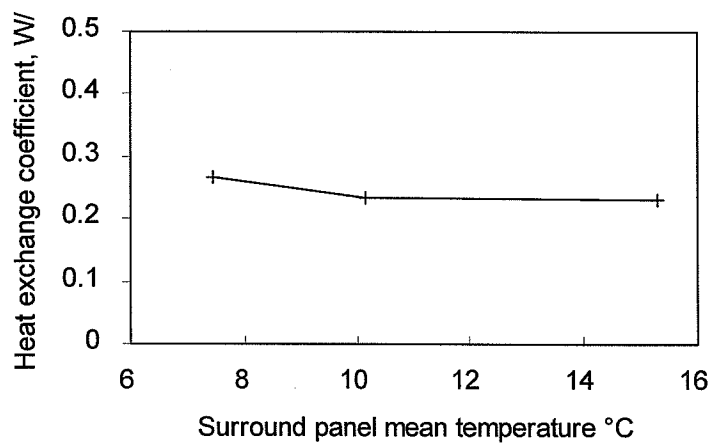


Figure 4. Surround panel heat exchange coefficient. From calibration step 1.

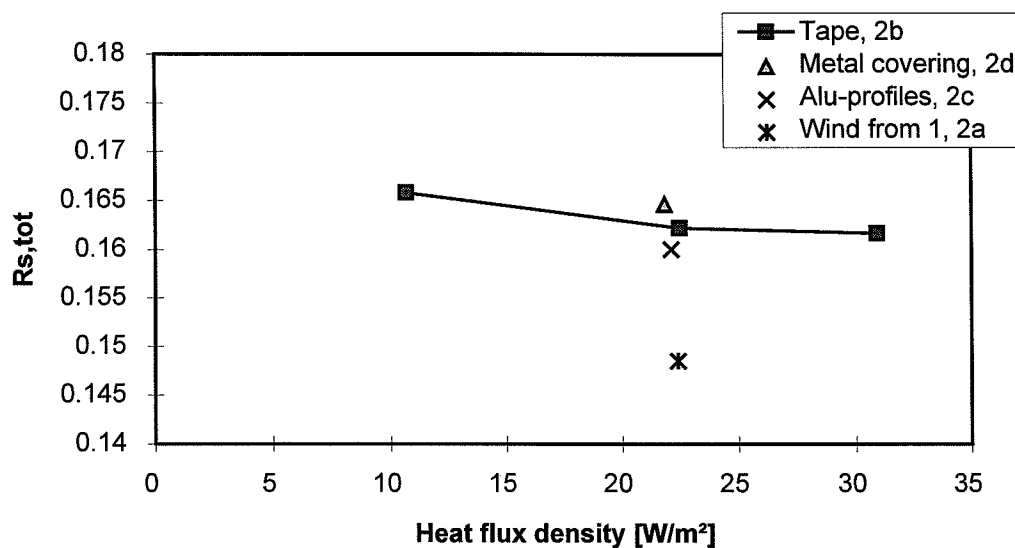


Figure 5. Total surface resistance versus heat flux density. Calibration step 2.

6 U-VALUE MEASUREMENTS

6.1 Mounting of the window

The window was mounted in the hot box aperture with the frame inserted 22 mm into the surround panel and the rest of the window exposed to the cold side ambient. The interface between the surround panel and the window was taped on both warm and cold side to secure that no air could penetrate the interface. The parts of the window that can be opened were taped on the warm side only. The U-value of the window was found with the metal covering mounted on the cold side.

6.2 Sensor locations

Nine thermocouples were mounted on each side of the window measuring the surface temperature of the glazing part of the window and additional seven sensors were used to measure the surface temperature of the warm side of the wooden frame.

6.3 Results

The following results were obtained from the U-value measurement:
(See also annex B)

Warm side:

Air temperature $\vartheta_{a,i,me}$ 20.00°C
 Baffle temperature $\vartheta_{b,i,me}$ 19.77°C
 Reveal temperature $\vartheta_{p,i,me}$ 18.43°C
 Glazing temperature: 16.51°C
 Average frame surface: 14.81°C

Cold side:

Air temperature $\vartheta_{a,e,me}$ -0.13°C
 Baffle temperature $\vartheta_{b,e,me}$ 0.07°C
 $\Delta T_{\text{surround panel}}$ 18.52°C
 Glazing temperature: 1.40°C

Electrical input to warm side heater: 63.93 W

Heat flux through surround panel: 4.33 W

$$q_c = 37.3 \text{ W/m}^2$$

$$\Delta T_n = 19.82 \text{ K}$$

$$U_m = 1.88 \text{ W/m}^2.$$

ΔT_n has been calculated in accordance to ISO 12567 Annex A using the mean surface temperature of the glazing in the window as the sample surface temperature.

Due to the relatively large thermal resistance of the calibration panel the R_s -curve in figure 5 does not cover the actual heat flux density from the U-value measurement. However the slope of the curve is decreasing with increasing heat flux density and from an extrapolation of the curve in figure 5, the total surface resistance coefficient during the U-value measurement is estimated to:

$$R_{s,tot} = 0.161 \text{ m}^2\text{K/W}$$

Now the standard U-value can be found from the following expression:

$$U_{st} = [1/U_m + 0.17 - R_{s,tot}]^{-1}$$

$$U_{st} = 1.85 \text{ W/m}^2\text{K}$$

ANNEX A

Calibrations

Appendix A U-value measurements on a roof window

Air warm	Air cold	Panel warm	Panel cold	Baffle warm	Baffle cold	Reveal warm	Reveal cold	Temp.dif surround
20.00	0.28	17.30	1.55	19.73	0.44	18.67	0.83	18.63
Power input		Panel temperature		9.42				
39.53		Panel resistance:		0.71				Therm. properties of calib. panel:
		Dimensions in m:		Reveal warm	Reveal cold			lambda at [°C]
		Height	Width					0.029
		1.40	1.14	0.14	0.00			21.00
Results:								panthick
R si	R se	R s,tot	H sur	qc	Tm,surr			0.02
0.11	0.06	0.17	0.23	22.04	10.14			dIamd/dT
								0.30
First calibration in step 1								

Air warm 20.00	Air cold -5.12	Panel warm 16.61	Panel cold -3.50	Baffle warm 19.67	Baffle cold -4.91	Reveal warm 18.36	Reveal cold -4.43	Temp.dif surround 23.73
Power input 50.84	Panel temperature Panel resistance:			6.56 °C 0.72 m2K/W		Therm. properties of calib. panel:		
Results:		Dimensions in m:		Reveal	Reveal	lambda		
		Height	Width	warm	cold	at [°C]		
		1.40	1.14	0.14	0.00	panthick		
R si	R se	R s,tot	H sur	qc	Tm,surr	dlamd/dT		
0.11	0.06	0.17	0.27	27.89	7.44	0.029		
						21.00		
						0.02		
						0.30		
Second calibration in step 1								

Air warm 20.00	Air cold 10.59	Panel warm 18.61	Panel cold 11.22	Baffle warm 19.83	Baffle cold 10.71	Reveal warm 19.27	Reveal cold 10.87	Temp.dif surround 8.86
Power input 18.84	Panel temperature Panel resistance:			14.92 0.70	Therm. properties of calib. panel:			
	Dimensions in m:			Reveal	Reveal	lambda		
		Height	Width	warm	cold	at [°C]		
		1.40	1.14	0.14	0.00	panthick		
Results:						dlamd/dT		
R si 0.12	R se 0.06	R s,tot 0.17	H sur 0.23	qc 10.52	Tm,surr 15.30			
Third calibration in step 1								

Air warm	Air cold	Panel warm	Panel cold	Baffle warm	Baffle cold	Reveal warm	Reveal cold	Temp.dif surround
20.00	-0.31	17.04	0.81	19.78	-0.17	16.98	0.21	19.27
Power input	Panel temperature			8.93 °C		Therm. properties of calib. panel:		
59.33	Panel resistance:			0.72 m2K/W		lambda 0.029		
	Dimensions in m:			Reveal warm	Reveal cold	at [°C] 21.00		
		Height	Width			panthick 0.02		
		1.22	0.99	0.37	0.00	dlamd/dT 0.30		
Results:								
R si	R se	R s,tot	H sur	qc	Tm,surr			
0.10	0.05	0.15	1.66	22.68	9.84			
Calibration 2a (step 2)								

Appendix A U-value measurements on a roof window

Air warm 20.00	Air cold -0.33	Panel warm 17.06	Panel cold 0.98	Baffle warm 19.78	Baffle cold -0.17	Reveal warm 17.00	Reveal cold 0.29	Temp.dif surround 19.18
Power input 58.30		Panel temperature Panel resistance:		9.02 0.72 m2K/W		Therm. properties of calib. panel:		
		Dimensions in m:		Reveal warm	Reveal cold	lambda at [°C]		
		Height 1.40	Width 1.14	0.26	0.00	panthick dlamd/dT		
Results:								
R si 0.11	R se 0.06	R s,tot 0.16	H sur 1.17	qc 22.48	Tm,surr 9.88			
First calibration in calibration serie 2b (step 2) (obtaining correct surface resistance)								

Air warm 20.00	Air cold -8.22	Panel warm 16.02	Panel cold -6.38	Baffle warm 19.72	Baffle cold -8.03	Reveal warm 15.64	Reveal cold -7.39	Temp.dif surround 26.64
Power input 81.57		Panel temperature Panel resistance:		4.82 °C 0.72 m2K/W		Therm. properties of calib. panel:		
		Dimensions in m:		Reveal warm	Reveal cold	lambda at [°C]		
		Height 1.40	Width 1.14	0.26	0.00	panthick dlamd/dT		
Results:								
R si 0.10	R se 0.06	R s,tot 0.16	H sur 1.21	qc 30.90	Tm,surr 5.93			
Second calibration in calibration serie 2b (step 2)								

Appendix A U-value measurements on a roof window

Air warm 20.00	Air cold 10.39	Panel warm 18.51	Panel cold 11.02	Baffle warm 19.87	Baffle cold 10.50	Reveal warm 18.35	Reveal cold 10.69	Temp.dif surround 9.08
Power input 27.27		Panel temperature Panel resistance:		14.77 0.70 m2K/W		Therm. properties of calib. panel:		
		Dimensions in m:		Reveal warm	Reveal cold	lambda at [°C]		
		Height 1.40	Width 1.14	0.26	0.00	panthick dlamd/dT		
Results:								
R si 0.11	R se 0.06	R s,tot 0.17	H sur 1.13	qc 10.65	Tm,surr 15.23			
Third calibration in calibration serie 2b (step 2)								

Air warm 20.00	Air cold 0.06	Panel warm 17.10	Panel cold 1.30	Baffle warm 19.79	Baffle cold 0.21	Reveal warm 17.00	Reveal cold 0.68	Temp.dif surround 18.81
Power input 57.49		Panel temperature Panel resistance:		9.20 0.72 m2K/W				Therm. properties of calib. panel:
		Dimensions in m:		Reveal	Reveal			lambda
		Height	Width	warm	cold			at [°C]
		1.40	1.14	0.26	0.00			panthick
Results:								dIamd/dT
R si	R se	R s,tot	H sur	qc	Tm,surr			
0.11	0.05	0.16	1.18	22.10	10.08			
Calibration 2c (step 2)								

Air warm 20.00	Air cold 0.20	Panel warm 17.11	Panel cold 1.50	Baffle warm 19.81	Baffle cold 0.37	Reveal warm 17.03	Reveal cold 1.25	Temp.dif surround 18.23
Power input 53.75		Panel temperature Panel resistance:		9.30 0.71 m2K/W		Therm. properties of calib. panel:		
		Dimensions in m:		Reveal	Reveal	lambda		
		Height	Width	warm	cold	at [°C]		
		1.40	1.14	0.26	0.00	panthick		
Results:						dlamd/dT		
R si	R se	R s,tot	H sur	qc	Tm,surr			
0.11	0.06	0.16	1.04	21.84	10.37			
Calibration 2d (step 2)								

ANNEX B

U-value measurement

U-value measurement

25 |

APPENDIX B

1 INTRODUCTION

This report describes the results of the U-value measurements performed on a roof window.

The measurements have been performed using the procedures given in ISO 12567 draft version 1998-03-02 with a few modifications especially concerning the calibration procedure. The measurements were carried out at the Technical University of Denmark, Department of Buildings and Energy.

2 DESCRIPTION OF THE WINDOW

The window is a wooden roof window and measures 1400 mm high x 1140 mm wide. The glazings are 4-16-4 mm with one hardened glass pane outermost and one soft-coated glass pane innermost (low e-coating in position 3). The gap between the glass panes is Argon filled and the spacer material is aluminium.

3 CALIBRATION PANELS

A single calibration panel has been constructed in order to carry out a hot box calibration procedure. The panel measure 1400mm high x 1140mm wide and has a total thickness of 28 mm.

The core material is polyurethane which prior to the assembling has been ground plane in order to avoid or at least reduce variations in the material thickness. The core thickness is 20 mm.

The glazings on both sides of the core are 4 mm hardened glass with normal emissivity.

The panels are assembled simply by means of heavy duty tape, no glue has been used in this process.

The thermal conductivity λ has been measured for the sample thicknesses of 20 mm. The measurements were performed on material samples produced in the same batch as the material samples that were used in the calibration panels.

The thermal conductivity was determined at three mean temperatures of the polyurethane: 16, 21 and 26°C. A linear temperature dependency for the thermal conductivity of the polyurethane was found in this range and it is assumed that the same linear change in the thermal conductivity as a function of temperature can be used also outside the measured range. The λ -values at the relevant temperatures during calibrations were found using the following expression:

$$\lambda_t = \lambda_{21} - \frac{(21 - t) \cdot \Delta\lambda \cdot \lambda_{21}}{100}$$

where t is the actual temperature of the core material during calibrations and $\Delta\lambda$ is the temperature dependency of the thermal conductivity of polyurethane.

The results of the measurements are:

$$\lambda_{21} = 0.0294 \text{ W/mK}$$

$$\Delta\lambda = 0.3 \text{ \%/K}$$

4 GUARDED HOT BOX

The hot box measurements were performed in a guarded hot box. Maximum sample size is 1500 x 1250 mm and the meeting box measures 1600 x 1350 mm inside. The guarded hot box is built and the measurements are performed in accordance to ISO 8990, CEN prEN 12412:1996 and the ISO/CD12567 proposal with the following exception:

- The calibration procedure has been changed as explained in section 5.

Prior to each calibration or U-value measurement the meeting box is tested for air tightness in order to assure that no air will be exchanged between hot and cold side.

5 CALIBRATION MEASUREMENTS

Instead of performing a full calibration with regards to the surface resistance it is suggested to focus on the cold side wind speed and use the assumption that a constant wind speed across the test sample results in a (reasonable) constant surface resistance regardless of sample position. That means that for simplicity reasons the impact of varying heat flux density through the sample on the total surface resistance has been neglected. (This impact on the overall U-value is considered small for modern insulating glazing units)

The calibration was carried out in two steps using the following procedure:

1. First the surround panel heat exchange coefficient H_{sur} was found using the 1400x1140x28 mm calibration panel mounted flush with the face of the cold side surround panel. See figure 1. A single measurement was carried out with 20°C on the warm side and 0°C on the cold side. During the measurement the voltage for the wind simulator fan on the cold side was regulated in order to obtain the standard surface resistance in accordance to the CEN standard. The wind speed and the fan speed was noted after steady state condition was reached. The wind speed was measured in front of the center of glazing in a fixed distance of 50 mm.
2. Next the surround panel heat exchange coefficient H_{sur} was found using the 1400x1140x28 mm calibration panel mounted 40 mm from the face of the warm side surround panel. See figure 2. A single measurement was carried out with 20°C on the warm side and 0°C on the cold side. During the measurement the voltage for the wind simulator fan on the cold side was regulated in order to

obtain the standard surface resistance in accordance to the CEN standard. The wind speed and the fan speed was noted after steady state condition was reached. The wind speed was measured in front of the center of glazing in a fixed distance of 50 mm.

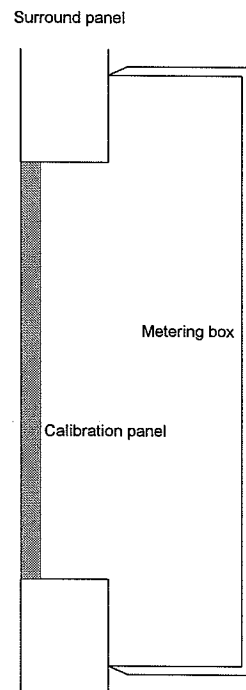


Figure 1. Mounting of calibration panel 1 (calibration step 1).

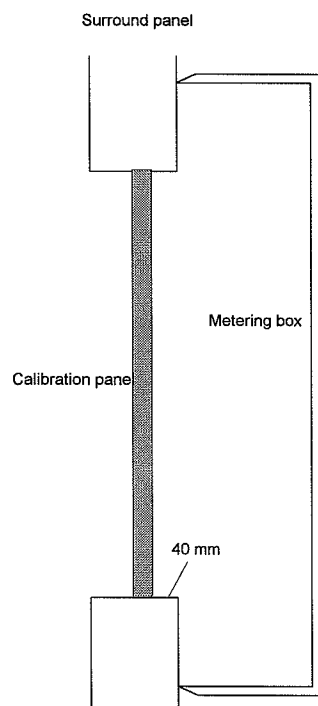


Figure 2. Mounting of calibration panel 2 (calibration step 2).

From the known thermal resistance of the calibration panel it is now possible to find the surround panel heat exchange coefficient H_{sur} for the two investigated cases and the correlation between windspeed and total surface heat transfer coefficient has been found for the two investigated cases, see table 1.

Table 1. Results from the two calibrations

Calibration	H_{sur}	$R_{s, total}$	Vind speed	Fan speed
1	0.256	0.168	2.1	4.57
2	0.182	0.173	2.2	10
	[W/K]	[m ² K/W]	[m/s]	[Volt]

In a previous investigation carried out on the same calibration panel and the same window but using a different calibration procedure H_{sur} was found to 0.233 W/K (Duer, 1997) in a situation corresponding to calibration 1.

In Annex A is shown the key results from all calibrations.

6 U-VALUE MEASUREMENTS

6.1 Mounting of the window

Four cases were investigated (see figure 3):

1. The window mounted in the hot box aperture with the frame inserted 20 mm into the surround panel and the rest of the window exposed to the cold side ambient. The wind speed across the glazing part of the window was corresponding to the windspeed in calibration 1 (2.1 m/s). The purpose of this measurement was first of all to check that the measured U-value using the more simple calibration process is in accordance to a more detailed investigation carried out previously (Duer, 1997).
2. The window mounted in the hot box aperture with the frame inserted 50 mm into the surround panel and the rest of the window exposed to the cold side ambient. The wind speed across the glazing part of the window was corresponding to the windspeed in calibration 1 (2.1 m/s).
3. The window mounted in the hot box aperture with the outer part of the window frame flush with the cold side surround panel. The wind speed across the glazing part was similar to the windspeed in calibration 2 (2.2 m/s).
4. The window mounted in the hot box aperture with the outer part of the window frame flush with the cold side surround panel. The fan speed setting was similar to the fan speed in calibration 2 (10 Volt), resulting in a wind speed of 2.85 m/s.

The interface between the surround panel and the window was taped on both warm and cold side to secure that no air could penetrate the interface. The parts of the window that can be opened were taped on the warm side only. The U-value of the window was found with the metal covering mounted on the cold side.

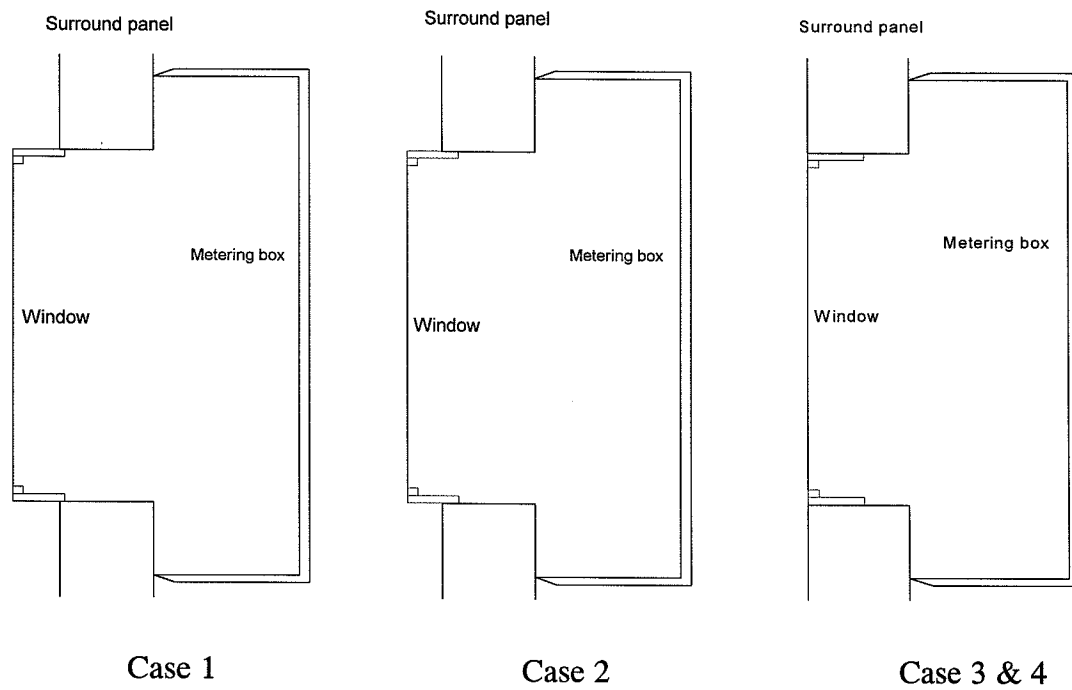


Figure 3. Mounting of the window in the surround panel for the four cases.

6.2 Sensor locations

Nine thermocouples were mounted on each side of the window measuring the surface temperature of the glazing part of the window and additional eight sensors were used to measure the surface temperature of the warm side of the wooden frame.

6.3 Results

The following results were obtained from the U-value measurements:

Table 2. Results from U-value measurements. Four different cases have been investigated using calibration results from a previously performed test (Duer, 1997), from the first calibration (calibration panel mounted flush cold side surround panel) and from the second calibration (calibration panel mounted 40 mm from warm side surround panel).

Case no.	Mounting of the window	Previous calibration	First calibration	Second calibration
1.	20 mm in surround panel	1.83	1.82	1.86
2.	50 mm in surround panel	1.72	1.71	1.75
3.	Frame flush cold side, wind speed as in calibration 2	1.54	1.53	1.57
4.	Frame flush cold side, fan speed as in calibration 2	1.58	1.56	1.61
		[W/m ² K]	[W/m ² K]	[W/m ² K]

In the more detailed study previously carried out the U-value of the same window mounted 20 mm in the surround panel (corresponding to case 1) was found to 1.85 W/m²K including standard surface resistance of 0.17 m²K/W (Duer, 1997). The results in the present study are in good agreement with this number indicating that the simplified calibration procedure gives acceptable accuracy.

What happens if the fan setting is kept constant from the calibration measurement to the U-value measurement regardless that the geometry of the roof window is very different from that of the calibration panel? For case 3 and 4 in table 2 it is investigated how big influence the wind speed has on the U-value. For case 3 the **wind** speed was adjusted in order to obtain the same wind speed as was obtained in calibration 2, resulting in a wind speed of 2.2 m/s. For case 4 the **fan** speed was adjusted to the same setting as in calibration 2, resulting in a wind speed of 2.85 m/s. The change in wind speed changes of course the total surface resistance and changes the U-value about 0.04 W/m²K. This change depends to a certain extend on the design of the cold side of the hot box. In the Danish hot box the wind is flowing in a

closed channel along the test specimen and the wind speed in the channel is rather sensitive to changes in the geometry of the channel. If for example the roof window is mounted as in case 1 and the fan speed setting is kept constant after calibration 1 the wind speed across the test specimen increases from 2.1 m/s (calibration 1) to more than 4 m/s (case 1). The reason is of course that the window is blocking a relatively large part of the air channel. In the previous study the U-value of the window measured with the same fan speed setting as in calibration 1 (wind speed > 4 m/s) was found to 1.92 W/m²K where the value using the correct surface resistance was 1.85 W/m²K.

REFERENCES

Draft ISO/DIS 12567 version 1998-03-02

Duer, Karsten: U-value measurements on roof window, Department of Buildings and Energy, Technical University of Denmark, Report S 97-17, 1997.

ANNEX A

Calibrations

Air warm 20.00	Air cold 0.17	Panel warm 17.17	Panel cold 1.37	Baffle warm 19.72	Baffle cold 0.31	Reveal warm 18.55	Reveal cold 0.75	Temp.dif surround 18.53
Power input 40.03		Panel temperature Panel resistance:		9.27 0.71		Therm. properties of calib. panel:		
		Dimensions in m:		Reveal	Reveal	lambda		
		Height	Width	warm	cold	at [°C]		
		1.40	1.14	0.14	0.00	panthick		
Results:					dlamd/dT			0.30
R si	R se	R s,tot	H sur	qc	Tm,surr			
0.12	0.05	0.17	0.26	22.10	10.01			
First calibration Flush cold side								

0.39								
Air warm 20.00	Air cold 0.16	Panel warm 16.92	Panel cold 1.22	Baffle warm 19.52	Baffle cold 0.29	Reveal warm 18.23	Reveal cold 0.40	Temp.dif surround 18.24
Power input 38.35		Panel temperature Panel resistance:		9.07 0.72	Therm. properties of calib. panel:			
		Dimensions in m:		Reveal	Reveal	lambda		
		Height	Width	warm	cold	at [°C]		
		1.40	1.14	0.04	0.10	panthick		
Results:					dlamd/dT			0.30
R si	R se	R s,tot	H sur	qc	Tm,surr			
0.13	0.05	0.17	0.18	21.94	9.52			
Second calibration, flush warm minus 40 mm								

ANNEX B

U-value measurement

Measured average temperatures:									
Air warm	Air cold	Glazing warm	Glazing cold	Baffle warm	Baffle cold	Reveal warm	Reveal cold	Temp.dif surround	
20.00	0.24	16.50	1.81	19.75	0.41	18.41	1.56	17.85	
		Heat flux through surround panel is (in W)						4.58	
Power input	Hsur (W/K)=			0.26					
61.04	Dimensions in m								
		Height	Width	Reveal varm	Reveal cold	Total Height	Total Width		
		1.40	1.14	0.26	0.00	1.40	1.14		
Results:									
diff.Tn	Um								
19.43	1.82								
Hsur in accordance to calibration 1 (flush cold side)									
U-VALUE Case 1, window mounted 20 mm in surround panel									
Wind speed adjusted corresponding to calibration 1									
Resulting wind speed 2.1 m/s									

Measured average temperatures:									
Air warm	Air cold	Glazing warm	Glazing cold	Baffle warm	Baffle cold	Reveal warm	Reveal cold	Temp.dif surround	
20.00	0.24	16.50	1.81	19.75	0.41	18.41	1.56	17.85	
Heat flux through surround panel is (in W)							3.25		
Power input	Hsur (W/K)=			0.18					
61.04	Dimensions in m								
	Height	Width	Reveal varm	Reveal cold	Total Height	Total Width			
	1.40	1.14	0.26	0.00	1.40	1.14			
Results:									
diff.Tn	Um								
19.44	1.86								
Hsur in accordance to calibration 2 (40 mm from warm side)									
U-VALUE, Case 1, window mounted 20 mm in surround panel									
Wind speed adjusted corresponding to calibration 1									
Resulting wind speed 2.1 m/s									

Measured average temperatures:								
Air warm	Air cold	Glazing warm	Glazing cold	Baffle warm	Baffle cold	Reveal warm	Reveal cold	Temp.dif surround
20.00	0.11	16.45	1.49	19.74	0.27	18.59	1.08	18.32
Heat flux through surround panel is (in W)							4.70	
Power input	Hsur (W/K)=			0.26				
58.08	Dimensions in m							
	Height	Width	Reveal warm	Reveal cold	Total Height	Total Width		
	1.40	1.14	0.23	0.00	1.40	1.14		
Results:								
diff.Tn	Um							
19.58	1.71							
Hsur in accordance to calibration 1 (flush cold side)								
U-VALUE, Case 2 window mounted 50 mm in surround panel								
Wind speed adjusted corresponding to calibration 1								
Resulting wind speed 2.1 m/s								

Measured average temperatures:								
Air warm	Air cold	Glazing warm	Glazing cold	Baffle warm	Baffle cold	Reveal warm	Reveal cold	Temp.dif surround
20.00	0.11	16.45	1.49	19.74	0.27	18.59	1.08	18.32
Heat flux through surround panel is (in W)							4.28	
Power input	Hsur (W/K)=			0.23				
58.08				Dimensions in m				
	Height	Width		Reveal varm	Reveal cold	Total Height	Total Width	
	1.40	1.14		0.23	0.00	1.40	1.14	
Results:								
diff.Tn	Um							
19.59	1.72							
Hsur in accordance to calibration 2 (40 mm from warm side)								
U-VALUE, Case 2 window mounted 50 mm in surround panel								
Wind speed adjusted corresponding to calibration 1								
Resulting wind speed 2.1 m/s								

Measured average temperatures:								
Air warm	Air cold	Glazing warm	Glazing cold	Baffle warm	Baffle cold	Reveal warm	Reveal cold	Temp.dif surround
20.00	0.11	16.38	1.46	19.64	0.27	18.83	0.52	18.63
Heat flux through surround panel is (in W)							4.78	
Power input	Hsur (W/K)=			0.26				
52.64				Dimensions in m				
	Height	Width		Reveal varm	Reveal cold	Total Height	Total Width	
	1.40	1.14		0.05	0.00	1.40	1.14	
Results:								
diff.Tn	Um							
19.64	1.53							
Hsur in accordance to calibration 1 (flush cold side)								
U-VALUE, Case 3 window mounted flush cold side								
Wind speed adjusted corresponding to calibration 2								
Resulting wind speed 2.2 m/s								

Measured average temperatures:								
Air warm	Air cold	Glazing warm	Glazing cold	Baffle warm	Baffle cold	Reveal warm	Reveal cold	Temp.dif surround
20.00	0.11	16.38	1.46	19.64	0.27	18.83	0.52	18.63
Heat flux through surround panel is (in W)							3.40	
Power input	Hsur (W/K)=			0.18				
52.64				Dimensions in m				
	Height	Width		Reveal warm	Reveal cold	Total Height	Total Width	
	1.40	1.14		0.05	0.00	1.40	1.14	
Results:								
diff.Tn	Um							
19.65	1.57							
Hsur in accordance to calibration 2 (flush cold side)								
U-VALUE, Case 3 window mounted flush cold side								
Wind speed adjusted corresponding to calibration 2								
Resulting wind speed 2.2 m/s								

Measured average temperatures:

Air warm	Air cold	Glazing warm	Glazing cold	Baffle warm	Baffle cold	Reveal warm	Reveal cold	Temp.dif surround
20.00	0.05	16.35	1.26	19.63	0.19	18.82	0.42	18.73
Heat flux through surround panel is (in W)								4.80
Power input	Hsur (W/K) =			0.26				
54.02				Dimensions in m				
				Reveal warm	Reveal cold	Total Height	Total Width	
	Height	Width		0.05	0.00	1.40	1.14	
	1.40	1.14						
Results:								
diff.Tn	Um							
19.71	1.56							

Hsur in accordance to calibration 1 (flush cold side)

U-VALUE, Case 4 window mounted flush cold side

Windsimulator adjustment corresponding to calibration 2

Resulting windspeed 2.84-2.87 m/s

APPENDIX C

UNCERTAINTY IN GUARDED HOT BOX MEASUREMENT

Procedure for window hot box test evaluation including error analysis IEA 18, project B14

In the following is given an example of the total expected error in the U-value measured in the guarded hot box on a double glazed unit with a U-value of about 1.8 W/m²K. The results include:

- Detailed results from all together six calibration measurements performed on two calibration panels
- Detailed results from U-value measurement on a double glazed unit
- Estimated measurement errors
- Expected uncertainties in the calibration measurements
- Expected over-all uncertainty in the measured U-value

All absolute temperatures are measured by means of thin thermocouple type T wire and temperature differences are measured by means of thermopiles made from same wire type. The power input to the DC heater element in the metering box is measured by measuring the voltage drops across a reference resistance and across the heater element. The first voltage drop allows us to calculate the current in the circuit provided that the resistance is known. The second voltage drop allows us to calculate the power input to the DC heater with a high precision.

The estimated measurement errors are found from careful calibrations of temperature sensors, voltmeter and resistances mounted in the electrical power circuit to the heater element.

DETAILED CALIBRATION

RESULTS:

	first calibration panel: ident.: 28 mm			second calibration panel: ident.: 68 mm			
	test 1	test 2	test 3	test 1	test 2	test 3	
Internal:							
temperatures:							
air: $\theta_{a,i}$	19.91	20.00	20.00	20.01	19.99	20.20	°C
baffle: $\theta_{b,i}$	19.68	19.69	19.90	19.90	19.83	20.17	°C
reveal: $\theta_{p,i}$	18.70	18.70	18.70	19.10	18.80	19.80	°C
calib. panel: $\theta_{c,i}$	16.93	16.19	18.45	18.73	18.28	19.56	°C
surr. panel: $\theta_{sur,i}$	19.52	19.52	19.82	19.64	19.48	20.04	°C
emiss. calib.panel,i ec	0.90	0.90	0.90 estimated	0.92	0.92	0.92 estimated	
emiss. baffle,i eb	0.95	0.95	0.95 estimated	0.95	0.95	0.95 estimated	
emiss. reveal ep	0.95	0.95	0.95 estimated	0.95	0.95	0.95 estimated	
view factor cal->baf fcb	0.84	0.84	0.84	0.89	0.89	0.89	
view factor sur->sur fpp	0.13	0.13	0.13	0.09	0.09	0.09	
view factor cal->sur fcp	0.16	0.16	0.16	0.11	0.11	0.11	
view factor sur->baf fpb	0.44	0.44	0.44	0.46	0.46	0.46	
rad.factor cal->baf acb	0.72	0.72	0.72	0.78	0.78	0.78	
rad.factor cal->sur acp	0.15	0.15	0.15	0.11	0.11	0.11	
rad.heat transf. coef.cal->baf hcb	5.61	5.59	5.66	5.66	5.65	5.70	W/m ² K
rad.heat transf. coef.cal->sur hcp	5.58	5.56	5.62	5.64	5.62	5.69	W/m ² K
rad.heat transfer coef. hr,i	4.90	4.88	4.94	5.06	5.05	5.09	W/m ² K
rad.temp. $\theta_{r,i}$	19.51	19.52	19.69	19.80	19.70	20.12	°C
rad. heat flux qr,i	12.62	16.24	6.13	5.41	7.17	2.87	W
conv. heat transfer coef. ha,i	3.96	3.82	4.35	3.29	3.12	3.65	W/m ² K
conv. heat flux qc,i	11.79	14.55	6.75	4.21	5.34	2.34	W
air fraction	0.45	0.44	0.47	0.39	0.38	0.42	
env. temp. $\theta_{-env,i}$:	19.69	19.73	19.84	19.88	19.81	20.16	°C
External:							
temperatures:							
air: $\theta_{a,e}$	-0.09	-5.51	9.79	0.05	-6.94	9.63	°C
baffle: $\theta_{b,e}$	0.04	-5.31	9.82	0.10	-6.88	9.65	°C
reveal: $\theta_{p,e}$	0.90	-4.70	10.25	0.59	-6.35	9.98	°C
calib: $\theta_{c,e}$	1.28	-3.93	10.40	0.58	-6.24	9.92	°C
surr: $\theta_{sur,e}$	0.38	-4.91	10.10	0.60	-6.51	10.05	°C
emiss. calib.panel ,e ec	0.92	0.92	0.92	0.92	0.92	0.92	
emiss. baffle ,e eb	0.95	0.95	0.95	0.95	0.95	0.95	
emiss. reveal ep	0.95	0.95	0.95	0.95	0.95	0.95	
view factor cal->baf fcb	0.96	0.96	0.96	0.96	0.96	0.96	
view factor sur->sur fpp	0.04	0.04	0.04	0.04	0.04	0.04	
view factor cal->sur fcp	0.04	0.04	0.04	0.04	0.04	0.04	
view factor sur->baf fpb	0.48	0.48	0.48	0.48	0.48	0.48	

rad. factor acb	0.84	0.84	0.84	0.84	0.84	0.84	
rad. factor acp	0.06	0.06	0.06	0.06	0.06	0.06	
rad. heat transf. coef. cal->baf hcb	4.65	4.38	5.15	4.63	4.29	5.13	W/m ² K
rad. heat transf. coef. cal->sur hcp	4.67	4.40	5.16	4.64	4.30	5.14	W/m ² K
rad.heat transfer coef. hr,e	4.13	3.92	4.61	4.15	3.84	4.59	W/m ² K
rad.temp. $\theta_{r,e}$	0.09	-5.27	9.85	0.13	-6.85	9.67	°C
rad. heat flux qr,e	4.94	5.27	2.55	1.86	2.33	1.15	W
conv. heat transfer coef. ha,e	14.22	16.15	16.93	14.63	14.53	14.00	W/m ² K
conv. heat flux qc,e	19.48	25.52	10.33	7.75	10.17	4.06	W
air fraction	0.77	0.80	0.79	0.78	0.79	0.75	
env. temp. $\theta_{-env,e}$:	-0.05	-5.46	9.80	0.07	-6.92	9.64	°C
Temp. differences:							
mean envir. temp.diff.: d θ_{env}	19.74	25.19	10.03	19.81	26.73	10.52	K
mean surf. temp.diff.: d $\theta_{cal,s}$	15.65	20.12	8.05	18.15	24.52	9.64	K
mean panel temp. $\theta_{cal,m}$:	9.11	6.13	14.43	9.66	6.02	14.74	°C
conductance Hcal at $\theta_{cal,m}$:	1.56	1.53	1.60	0.53	0.51	0.54	W/m ² K
flux through cal.panel: qcal	24.41	30.78	12.88	9.62	12.51	5.21	W/m ²
sum of surf. resistances Rtc:	0.167	0.165	0.154	0.17	0.18	0.17	m ² K/W
interior surf. resistance hi:	8.86	8.70	9.30	8.35	8.17	8.75	m ² K/W
exterior surf. resistance he:	18.38	20.07	21.54	18.78	18.37	18.59	m ² K/W
panel area Acal:	1.44	1.44	1.44	1.44	1.44	1.44	m ²
flow thr. panel: Qcal	35.16	44.33	18.55	13.85	18.01	7.50	W
injected power: Qel	39.23	49.81	20.16	16.80	23.56	8.83	W
Metering box:							
temp. diff. over metering box	0.00	0.00	0.00	0.00	0.00	0.00	K
conductance metering box: Hmb	0.70	0.70	0.70	0.70	0.70	0.70	W/K
heat flow thr. met.box: Q3	0.00	0.00	0.00	0.00	0.00	0.00	W
heat flow to cold box: Qin	39.23	49.81	20.16	16.80	23.56	8.83	W
Surround panel:							
heat flow thr. sur.panel: Qsur	4.07	5.48	1.61	2.95	5.55	1.33	W
mean surface temp. diff.: d $\theta_{sur,s}$	19.14	24.43	9.72	19.04	25.99	9.99	K
conductance sur.panel, Hsur (at given thickness and $\theta_{sur,mn}$)	0.21	0.22	0.17	0.15	0.21	0.13	W/K
mean sur.panel temp. $\theta_{sur,mn}$	9.95	7.31	14.96	10.12	6.49	15.05	°C

DETAILED U-VALUE MEASUREMENT RESULTS:

ident.: Double glazed unit

interpolated value for Hsur:

based on thickness and $\theta_{sur,mn}$

mean sur.panel temp. $\theta_{sur,mn}$	10.20	°C
conductance sur.panel Hsur,m	0.19	W/K

Internal:

temperatures:

air: $\theta_{a,i}$	20.00	°C
baffle: $\theta_{b,i}$	19.69	°C
surr: $\theta_{sur,i}$	19.53	°C

External:

temperatures:

air: $\theta_{a,e}$	0.30	°C
baffle: $\theta_{b,e}$	0.52	°C
surr: $\theta_{sur,e}$	0.86	°C

surround panel:

mean surface temp. difference:	18.67	K
heat flow thr. sur.panel, $Q_{sur,m}$	3.55	W

injected power Q_{el} :	53.03	W
---------------------------	-------	---

Metering box:

temp. diff. over metering box:	0.00	K
Hmeter.box:	0.70	W/K
heat flow thr. met.box Q_3 :	0.00	W

heat flow to cold box: Q_{in} :	53.03	W
-----------------------------------	-------	---

heat flow thr. sample Q_m	49.48	W
sample area $A_m = A_{cal}$	1.44	m ²
heat flux thr. sample q_m	34.36	W/m ²

internal:

air fraction	0.80	
mean environmental temp.: $\theta_{-env,i}$:	19.94	°C

external:

air fraction	0.44	
mean environmental temp. $\theta_{-env,e}$:	0.42	°C

mean env. temp. diff.:	19.58	K
------------------------	-------	---

interpolated value for R_{tc} :

based on flow q_m :	34.36	W/m ²
-----------------------	-------	------------------

$R_{tc,m}$	0.167	m ² K/W
------------	-------	--------------------

Ust ($R_{tc,st}=0.170$ m²K/W)	1.75	W/m²K
------------------------------------------------------------	-------------	-------------------------

ERROR ANALYSIS:

ESTIMATED MEASUREMENT UNCERTAINTIES:

	absolute (unit)	+	relative (%)
env.temp.dif $e(d\theta_{env})$:	0.2 K		0 %
cal.panel temp.dif. $e(d\theta_{cal})$:	0.2 K		0 %
conductance $e(1/R_{cal})$, panel 1	0 W/m ² K		4 %
conductance $e(1/R_{cal})$, panel 2	0 W/m ² K		4 %
power input $e(Q_{el})$	0.1 W		0 %
heat thr. met. box $e(Q_3)$	0.1 W		0 %
cal.panel area $e(A_{cal})$	0 m ²		0.12 %
sur.panel temp.dif. $e(d\theta_{sur})$	0.2 K		0 %
sample area $e(A_m)$	0 m ²		0.12 %

PROPAGATED ERRORS:

CALIBRATION PANEL 1:

first calibration panel: 28 mm
test 1 test 2 test 3

uncertainty in R_{tc} :			
env.temp.dif $d\theta_{env}$	0.008	0.006	0.016
cal.panel temp.dif $d\theta_{cal}$	0.010	0.008	0.019
conductance $1/R_{cal}$	0.001	0.001	0.001
root of squared sum	0.013	0.010	0.025
relative (%):	7.9	6.3	16.1

uncertainty in H_{sur} :

power input Q_{el}	0.005	0.004	0.010
heat thr. met. box Q_3	0.005	0.004	0.010
cal.panel area A_{cal}	0.002	0.002	0.002
conductance $1/R_{cal}$	0.073	0.073	0.076
cal.panel temp.dif $d\theta_{cal}$	0.023	0.018	0.047
sur.panel temp.dif. $d\theta_{sur}$	0.002	0.002	0.003
root of squared sum	0.078	0.075	0.091
relative (%):	36.4	33.5	54.9

TEST SAMPLE:

double glazed unit

uncertainty in heat through sample:

power input Q_{el}	0.005
heat thr. met. box Q_3	0.005
sur. panel heat transfc. H_{sur}	0.074
sur.panel temp.dif. $d\theta_{sur}$	0.002
env.temp.dif $d\theta_{env}$	0.026
root of squared sum	0.079
relative (%):	3.1

uncertainty in U_{st}

sample area A_m	0.002
heat through sample H_m	0.054
surface resistance R_{tc}	0.040
root of squared sum	0.096
relative (%):	5.5

ENERGY LABELLING OF GLAZINGS AND WINDOWS IN DENMARK

Karsten Duer, Svend Svendsen, Morten Moller Mogensen

Department of Buildings and Energy, Technical University of Denmark, Building 118, 2800 Kgs. Lyngby, Denmark,
Phone +4545251867, Fax +4545934430, kd@ibe.dtu.dk

Abstract – The influence of windows on the energy consumption in buildings is well known and in order to encourage the development and the appropriate use of high performance glazings and windows in Denmark an Energy Labelling and Rating system is being developed. During this work a need for establishing a common and well defined method to characterise the performance of glazings and windows on the Danish market has been recognised. This paper gives a short description of the Danish Energy Labelling and Rating system for glazings and windows which is expected to be put into operation during this year (2000). Furthermore the results of a comparison between measured and calculated thermal transmittance for five different window types are given. The calculations on the glazing part have been performed in five different programmes (WIS, WINDOW, VISION, CALUMEN and GLAD99). The calculations on the frame part have been performed in three different programmes (FRAME, THERM and WinIso). The comparison indicates that all investigated programmes are qualified for calculating energy labelling data for glazings and windows..

1 INTRODUCTION

In the Danish governments action plan on energy one of the activities to stimulate energy savings is focused on the development of products with a better energy performance. Due to the large potential on energy savings by use of glazings and windows with improved energy performance they are included in this activity. In order to stimulate the use of glazings and windows with better energy performance and to improve the competition on the energy performance of glazings and windows an energy labelling and rating system for these products has been established and is being put into operation during this year (2000). In the following the Danish energy labelling and rating is described shortly. Furthermore the paper gives the results of comparisons carried out between measured and calculated U values for five Danish window designs.

2 ENERGY LABELLING AND RATING DATA FOR GLAZINGS AND WINDOWS

2.1 Energy labelling data

The energy performance of glazings and windows is based on the characteristic values shown in table 1. Most of the data are traditionally used for characterising the energy performance of glazings and windows.

The data are defined in the listed standards and need no explanation here. However the equivalent thermal conductivity of the edge construction of glazings is added in order to make it easy to compare this important detail of glazings. This is defined as the thermal conductivity of an imaginary solid material that is identical to the edge construction (spacer and seal) with respect to dimensions and heat flow.

The energy labelling data can be found by use of calculations or tests. In order to make it easy for manufacturers to document the characteristic data for their products a number of detailed programs have been compared with tests of a number of typical Danish windows. The results are summarised in section 3 and 4. Based on this general validation it is allowed the manufacturers to use the investigated programs for documenting the energy labelling data for glazings and windows without testing.

2.2 Energy rating data for glazings

In order to characterise the energy performance of glazings and windows it is necessary to include both U value and g-value. To make it easy for private consumers to compare products to be used in heating dominated houses the net energy gain during the heating season can be used.

Table 1. Energy labelling data for glazings and windows.

	Data	Reference
Glazing	Thermal transmission coefficient, center value	EN 673
	Visible transmittance, center value	EN 410
	Total solar energy transmittance, center value	EN 410
	Equivalent thermal conductivity of edge construction	
Windows	Thermal transmission coefficient based on total area	prEN ISO 10077-1 prEN ISO 10077-2
	Visible transmittance based on total area	ISO DIS 15099
	Total solar energy transmittance based on total area	ISO DIS 15099

By using typical climatic data for Denmark and by choosing a reference building the relative areas for the main orientations of the windows can be used in calculating the net energy gain as a function of the U value and the g-value of the glazing.

The description of the method and the assumptions used to generalise the angular dependence of the total solar transmittance glazings can be found in (Nielsen and Svendsen, 2000). The net energy gain can be found for specific glazings from the equation:

$$E_{\text{net energy gain}} = 196.4 \cdot g - 90.46 \cdot U \text{ [kWh/m}^2\text{]}$$

Only glazings with positive net energy gain are classified:

- A : net energy gain of more than 20 kWh/m²
 B : net energy gain between 10 and 20 kWh/m²
 C : net energy gain between 0 and 10 kWh/m²

The classification will of course depend on the climatic data used and the reference house and is only meant to give the private consumer an easy way to compare products.

Only glazings are given a rating.

2.3 Information on the energy labelling and rating of products

The energy labelling and rating system is open to all manufacturers and has been accepted by the European Commission.

The manufacturers participating in the system have to provide information on their products as follows:

The four energy labelling data for glazings must be available on paper or electronically

The energy rating class (if any) for glazings must be given in the spacer profile

The three energy labelling data for the windows must be available for each window based on the actual dimensions on paper or electronically.

3 CALCULATED THERMAL TRANSMITTANCE

The calculations of energy labelling data for glazings and windows have been carried out by means of a number of relevant calculation programs. Distinctions are made between programs for determination of data for the glazing part and programs for determination of data for the frame part. The investigated programs are listed in Table 1 and

Table 2.

Table 1 Outline of programs for glazing calculations

Program	Distributor
WIS	TNO, Netherland
WINDOW4.1	Lawrence Berkeley National Laboratory, USA
VISION4	Enermodal Engineering, Canada
CALUMEN	Saint Gobain
GLAD99	EuroGlass

Table 2 Outline of programs for frame calculations

Program	Distributor
FRAME	Enermodal Engineering, Canada
THERM2.0	Lawrence Berkeley National Laboratory, USA
WinIso	Sommer Informatik, Germany

3.1 Calculations of energy properties of glazings

The five calculation programs listed in Table 1 above have been tested by means of calculations on a total of 9 different glazings.

For each glazing the U value, the total solar energy transmittance (g-value) and the light transmittance were calculated.

Table 3 specifies the composition of glazing, gas type and width of space between the panes that were computed. Three types of coatings were investigated: Hard low e-coating, soft low-e coating and solar protecting low e-coating – the latter always in position 2.

Table 3 Composition of glazings.

Glazing No.	No. of glass panes	Coating position	Gas filling	Width of space (mm)
1	2	3	1*	12
2	2	3	1*	12
3	2	2	1*	12
4	2	2 + 3	2*	12
5	2	2 + 3	1*	6
6	2	2 + 3	1*	12
7	2	2 + 3	1*	18
8	2	2 + 3	3*	12
9	3	2 + 5	1*	12

*Legend: 1: Air/Argon, 10/90%

2: Air, 100%

3: Air/Krypton, 10/90%

The glazings have been compiled in order to make demands on the accuracy of the calculation programs

rather than to represent glazings that have typical applications.

Therefore the glazings Nos. 4-8 are equipped with two low-emission coatings even though this would normally not be relevant in double glazed units.

The calculated solar transmittances (not shown in this paper) were independent of the calculation programme and the calculated g-values (not shown) were within ± 0.01 of mean values. The calculated U values are shown in Table 4.

3.2 Discussion

There is in general a good consistency between the calculated results. It should be noted, however, that as to glazing No. 7 in Table 4 there is a significant deviation between the obtained results. The deviations are due to the applied calculation models. The programs WIS, CALUMEN and GLAD99 apply a model, corresponding to EN673, whereas the programs WINDOW4.1 and VISION4 apply a more detailed model. At present analyses are in progress in the relevant ISO and CEN working groups, partly investigating the differences in the results of the different models and partly investigating which models represent the actual conditions best. Provisional results indicate that the EN673-model gives too low U values compared with measurements for glass distances larger than 12 mm and in fact this corresponds to the results in Table 4.

3.3 Description of the five test windows

Five different typical frame designs, of wood, aluminium covered wood, plastic, metal and mixed materials, have been selected. The designs of the five frame profiles are shown in section 4. All the windows measure about 1.48 x 1.23 m (height x width) and are equipped with a double glazed unit composed of: 4 mm clear float glass – 10/90% Air/Argon-filled space – 4 mm glass with soft low emissivity coating in position 3. The glass pane distance varies from window to window, but glass types and gas filling are the same for all five windows.

Calculation of the window U value

The calculations are divided up into three elements:

- Centre U value for the glazing, U_g [W/m²K]
- The U value of the frame design, U_r [W/m²K]
- The linear thermal transmittance for jointing of glazing and frame, Ψ_g [W/mK]

The calculation of U_g has been carried out in consistency with EN673. The calculation of U_r and Ψ_g has been carried out in accordance with prEN10077-2. For a detailed description of the calculations carried out and the assumptions applied, reference is made to (Duer and Svendsen, 2000).

The results of the total window U value calculations are shown in Table 5.

Table 5 Calculated total U values for five windows. The frame part calculated with FRAME, THERM2.0 and WinIso respectively. Glazing part calculated with GLAS98.

Window No.	1	2	3	4	5	
FRAME	1.75	1.47	1.49	1.78	1.56	[W/m ² K]
THERM	1.73	1.46	1.46	1.76	1.56	[W/m ² K]
WinIso	1.74	1.47	1.49	1.74	1.56	[W/m ² K]
Mean	1.74	1.47	1.48	1.76	1.56	[W/m ² K]

As appears from Table 5, by and large the same total U value is achieved for a specific window irrespective of which calculation program is chosen. The deviation from average is 1% at the maximum.

3.4 Measurements

Measurements of the total U values for the five windows have been carried out in a guarded hot box in consistency with the relevant draft standards (prEN12412-1 and ISO/DIS12567). (The two documents describe identical procedures). Also the centre U values of the glazings and selected temperatures of the frame profiles and the glazings have been measured.

The centre U values of the glazings have been measured by mounting a window (incl. glazing) in the hot box and by attaching a sheet of polystyrene foam with a known thermal resistance on the glazing. The temperatures in the hot box were controlled so that the surface temperatures of the glazing came close to the surface temperatures that appeared during the U value measurement of the current window. These temperatures also correspond to the boundary conditions demanded in EN673.

Table 4 Comparison between calculated centre U values for nine glazings

Glazing No.	1	2	3	4	5	6	7	8	9	
WIS	1.64	1.26	1.46	1.59	1.99	1.24	1.09	1.02	0.77	[W/m ² K]
WINDOW4.1	1.65	1.29	1.48	1.58	2.00	1.27	1.21	1.08	0.77	[W/m ² K]
VISION4	1.65	1.28	1.47	1.60	1.97	1.26	1.19	1.05	0.77	[W/m ² K]
CALUMEN	1.64	1.26	1.47	1.59	1.99	1.24	1.14	1.02	0.77	[W/m ² K]
GLAD99	1.68	1.28	1.50	1.60	2.00	1.26	1.08	1.04	0.78	[W/m ² K]
MEAN	1.65	1.27	1.48	1.59	1.99	1.25	1.14	1.04	0.77	[W/m ² K]

By measuring the temperature difference across the polystyrene sheet the heat flow through the glazing can be determined, and by measuring the temperature difference across the glazing the thermal resistance of the glazing, and with that the U value of the glazing, can be determined under conditions corresponding to the total U value measurement and also corresponding to the standard boundary conditions in EN673.

4 COMPARISONS BETWEEN CALCULATED AND MEASURED RESULTS FOR THE FIVE WINDOWS

By the comparison between measured and calculated total U values the mean values of the calculated quantities given in Table 5 were used to represent the calculated window U values.

Apart from the U values comparisons are also made on calculated and measured values of selected temperatures. Temperatures were calculated in THERM. A comparison between measured and calculated surface temperatures should be made with care, as there are not necessarily exactly the same boundary conditions in measurements as in calculations.

In the present investigations a comparison between measured and calculated temperatures is therefore not expected to be carried out with a greater accuracy than $\pm 1^\circ\text{C}$ (Duer and Svendsen, 2000). It is still estimated, however, that the comparisons of the temperatures will enable an evaluation of the validity of the calculated results.

In the following a comparison has been made for each window between measured and calculated U values and surface temperatures and in two cases the temperature of a slightly ventilated cavity. The positions of temperature sensors are shown on a sketch for each window. Surface temperatures on the warm side of the glazings were measured from the sash and 100 mm into the glazing. The results are not included in this paper but for all five windows the course of the temperature over the glazing agrees well, measured and calculated and the discrepancy between measured and calculated temperatures were in all cases less than 1°C (Duer and Svendsen, 2000).

4.1 Window No. 1

The frames in window No. 1 are made from massive wood. As appears from Table 6 there is a fine consistency between measured and calculated values for U values as well as for surface temperatures.

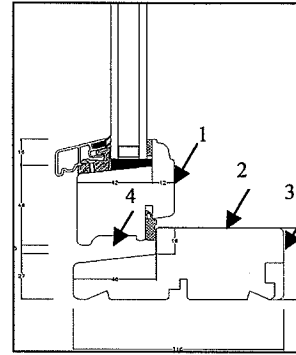


Figure 1 Locations of temperature sensors

Table 6 Measured and calculated values. Window No. 1

	Measured	Calculated	
U centre	1.18 ± 0.07	1.16	[W/m ² K]
U total	1.72 ± 0.09	1.74	[W/m ² K]
Temp. 1	14.6	13.9	[°C]
Temp. 2	17.4	17.6	[°C]
Temp. 3	18.6	18.9	[°C]
Temp. 4	4.1	4.9	[°C]

4.2 Window No. 2

The frames in window No. 2 are made from aluminium clad wood. Again there is a fine consistency between measured and calculated window U value as well as calculated and measured surface temperatures, see Table 7. The glazing in window no. 4 has a glass spacing of 24 mm. Following the discussion in section 3.2 a calculation of the center U value according to EN673 would lead to an underestimation of the center U value and the biggest deviation between measured and calculated values is indeed found for this glazing. However the calculated and measured center U values are within the expected tolerance of the measurement and more accurate measurements will have to be performed to investigate this matter.

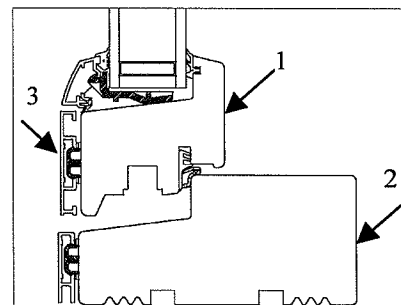


Figure 2 Locations of temperaturesensors

Table 7 Measured and calculated values. Window No. 2

	Measured	Calculated	
U centre	1.25±0.08	1.18	[W/m²K]
U total	1.50±0.08	1.47	[W/m²K]
Temp. 1	14.8	15.0	[°C]
Temp. 2	18.5	18.5	[°C]
Temp. 3	1.9	1.5	[°C]

4.3 Window No. 3

The frames in window No. 3 are made from plastic with two steel reinforcements. As appears from Table 8 there is a fine consistency between measured and calculated values for U values as well as for surface temperatures.

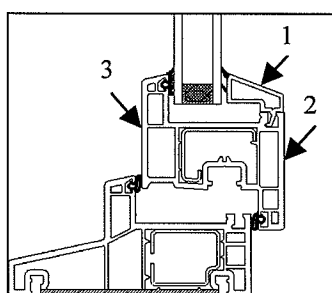


Figure 3 Locations of temperature sensors

Table 8 Measured and calculated values. Window No. 3

	Measured	Calculated	
U centre	1.17±0.07	1.13	[W/m²K]
U total	1.41±0.07	1.48	[W/m²K]
Temp. 1	15.0	14.5	[°C]
Temp. 2	16.3	16.4	[°C]
Temp. 3	2.6	1.8	[°C]

4.4 Window No. 4

The frames in window No. 4 are made from aluminium with thermal break. For window No. 4 there is a discrepancy between measured and calculated total U value which lies outside the uncertainty of the U value measurement – see Table 9.

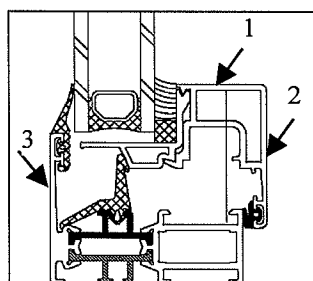


Figure 4 Locations of temperature sensors

Table 9 Measured and calculated values. Window No. 4

	Measured	Calculated	
U centre	1.18±0.07	1.14	[W/m²K]
U total	1.65±0.08	1.76	[W/m²K]
Temp. 1	14.3	11.8	[°C]
Temp. 2	14.3	11.8	[°C]
Temp. 3	3.7	3.2	[°C]

Apart from this there is a significant difference between the measured and the calculated surface temperatures on the hot side of the frame (temperatures 1 and 2). As there is a good agreement between measured and calculated centre U value for the glazing and as the course of the temperature over the glazing agrees well, measured and calculated, it indicates that there is an error in the calculated U value of the frame part (U_r) and/or the linear thermal transmittance of the spacer profile of the glazing (Ψ_g).

Window No. 4 is built of aluminium profiles with thermal break of synthetic material. In the frame profile the heat transfer is depending on the thermal resistance of the thermal break and the air gap indicated on Figure 5 below.

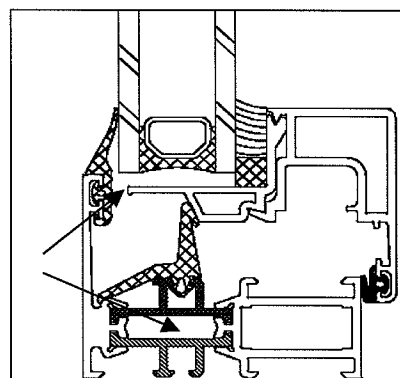


Figure 5 Critical thermal resistance in window No. 4

In the calculation of the U value of the frame profile the cavity to the left in Figure 5 is calculated as one large cavity even though the cavity is partly divided at the upper arrow. The gap at the arrow is smaller than 10 mm and taking prEN10077-2 as a starting point arguments can be put forward for dividing up the cavity into two parts as shown in Figure 6.

By calculating the situation illustrated in Figure 6 U_r is found at 3.1 W/m²K and ψ_g at 0.082 W/mK. (Calculations performed with THERM2.0. Equivalent values with one large cavity are 3.4 W/m²K and 0.093 W/mK). The corresponding total window U value and surface temperature is shown in Table 10.

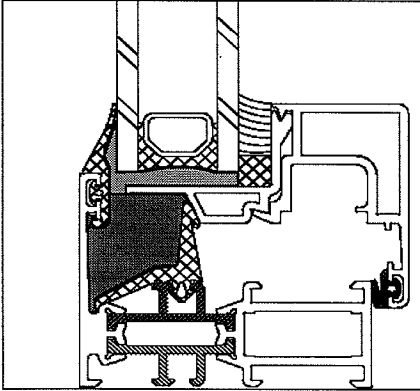


Figure 6 Division of cavity into two parts.

Table 10 Measured and calculated values. Window No. 4. Divided cavity.

	Measured	Calculated	
Centre U value	1.18 ± 0.07	1.14	[W/m ² K]
Total U value	1.65 ± 0.08	1.70	[W/m ² K]
Temp. frame, hot	14.3	12.5	[°C]

As appears from Table 10 there is a better consistency between measured and calculated total U value, but there is still a relatively large deviation between measured and calculated surface temperatures on the hot side of the frame. There are several possible reasons for this:

- In the calculations a firmly defined geometry is used corresponding to the sketches provided by the manufacturer. Even a small variation of the size of the critical air gap in Figure 5 is of significance to the calculation result.
- In the calculations there is assumed a perfect metal-metal contact between the window frame and the clipped on glazing supports. Experience from e.g. metal absorbers in solar collectors has shown that a thermal contact resistance can occur between two metal parts that are clipped together. If a contact resistance is introduced into the calculations, the calculated U value of the frame profile will fall and the calculated surface temperature on the hot side of the frame will rise. The contact resistance can be determined through detailed measurements but this is not done in the present study.

Thus the fact can be established that especially for frame profiles of metal it is important to be careful even about small details.

4.5 Window No. 5

In window No. 5 the frame part is made from solid wood and the sash part is aluminium (outermost) and PVC (innermost). As appears from Table 11 there is a fine

agreement between measured and calculated values for U values as well as for surface temperatures.

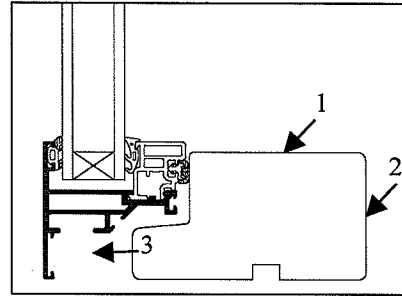


Figure 7 Locations of temperature sensors

Table 11 Measured and calculated values. Window No. 5

	Measured	Calculated	
U centre	1.16 ± 0.07	1.13	[W/m ² K]
U total	1.57 ± 0.08	1.56	[W/m ² K]
Temp. 1	16.8	16.4	[°C]
Temp. 2	18.4	18.4	[°C]
Temp. 3	2.7	3.0	[°C]

However it is open to discussion whether the cavity between the aluminium profile and the frame should be divided into three cavities, c.f. the discussion under window No. 4. According to the same argumentation as applied for window 4 the cavity for window 5 can be divided as stated in Figure 8. The cavity indicated as point 3 in Figure 7 is regarded a slightly ventilated cavity as the gap between the aluminium sash and the surrounding wall is less than 10 mm.

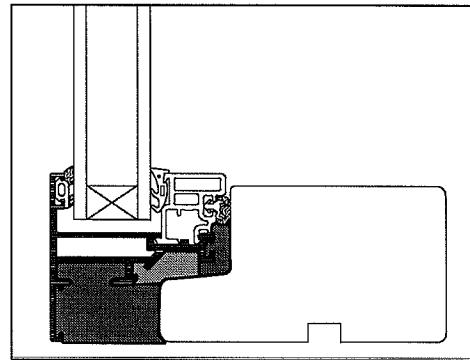


Figure 8 Window No. 5 with divided cavity

By calculating the situation illustrated in Figure 8 with Therm 2.0 U_f is found at 2.8 W/m²K and ψ_g at 0.051 W/mK. (Corresponding values with one large cavity are 3.0 W/m²K and 0.050 W/mK). By this the following values are found:

Table 12 Measured and calculated values. Window No. 5

	Measured	Calculated	
U total	1.57±0.08	1.53	[W/m²K]
Temp. 1	16.8	16.7	[°C]
Temp. 2	18.4	18.4	[°C]
Temp. 3	2.7	2.9	[°C]

The calculated total U value will only be slightly affected by dividing the cavity in the calculation. This is due to the fact that the reduction of the U value of the frame profile is by and large corresponding to the increase of the linear transmittance, Ψ_g . On the other hand it appears that the measured and calculated surface temperatures agree better with a calculation based on divided cavity. For both situations, however, the measured and calculated values clearly fall within the anticipated tolerances.

5 CONCLUSION

Investigations have been carried out for comparison of the results of different calculation programs, mutually and with measurements.

Following the discussion in section 3.2 some discrepancy between calculated results for glazing U value according to the EN673-model and more detailed models is observed for large glass spacing. Though this may be considered a second order effect it does call for further work in developing, investigating and harmonising the calculation models in the calculation standard.

The comparisons between calculated and measured thermal transmittance for especially the aluminium window (No. 4) shows that care must be taken when modelling profiles with critical thermal resistances like thermal breaks and (air)gaps between highly conducting parts. It is recommended that unventilated and slightly ventilated cavities are subdivided according to the comments in section 4.4

All in all a good consistency has been found between the calculated results irrespective of which calculation program was used and it may be concluded that all the investigated programs can be used for calculation of energy labelling data for glazings and windows.

References

Duer K. and Svendsen S. (2000). Analysis of calculated and measured energy properties of windows, SR-0010. Department of Buildings and Energy, Technical University of Denmark.

Nielsen T.R and Svendsen S. (2000). Determination of net energy gain from glazings and windows. *To be presented at Eurosun 2000, Copenhagen.*

prEN12412-1 Windows and doors – Thermal transmittance – calibrated and guarded hot box method.

ISO/DIS12567 Thermal performance of doors and windows – Determination of thermal transmittance by hot box method. Final draft version, July 1998.

EN410 Glass in building – Determination of luminous and solar characteristics of glazing, April 1998

EN673 Glass in building – Determination of thermal transmittance (U value) Calculation method, November 1997

prEN ISO10077-2 Thermal performance of windows, doors and shutters - Calculation of thermal transmittance - Part 2: Numerical methods for frames, February 2000.

APPENDIX E

CORRECTION FOR HEAT FLOW THROUGH EDGE OF SAMPLE

1. Introduction

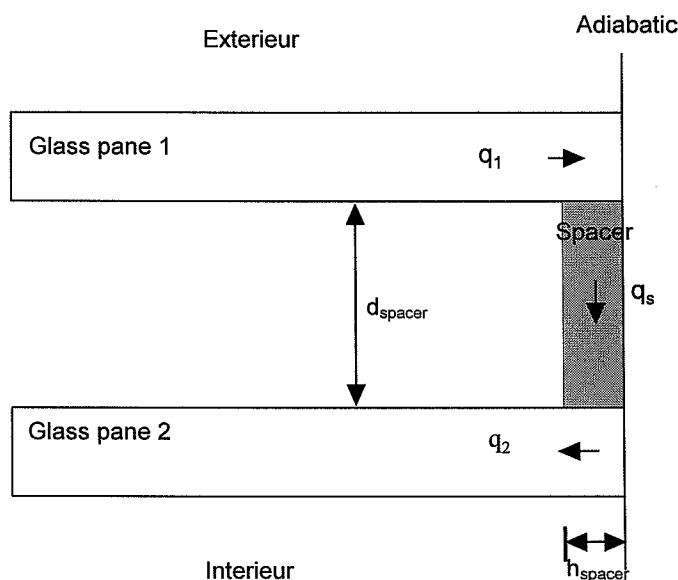
The edge-construction of a glazing has an impact on the g-value of the glazing, measured by calorimetric devices. If no insulation is applied on the glazing edges (inside and outside) during measurements, heat will be transferred by conduction through the glass panes and through the spacer. The amount of energy transferred and the direction of the energy flow depends on the construction of the glazing (types of glass, coatings and spacer) and on the interior and exterior temperatures during the measurements. This appendix gives an evaluation of the amount of energy transferred through the spacer in two different glazings in order to establish the maximum error that will result if no insulation is applied on the edge of glazing during measurements.

2. Equations

The heat flow through the spacer can be calculated by treating each glass pane as a fin with base at the spacer and by using a number of assumptions. In figure 1 is shown the heat flow through the edge construction in a glazing where the outer glazing is warmer than the inner.

Figure 1.
Heat flow through edge of glazing.

q_1 , q_2 and q_s denotes the heat flow in glass pane 1 and 2 and through the spacer respectively.



The assumptions are:

There is no “horizontal” heat flow through the spacer in figure 1

The space between the glass panes is replaced by a solid with an equivalent thermal conductivity

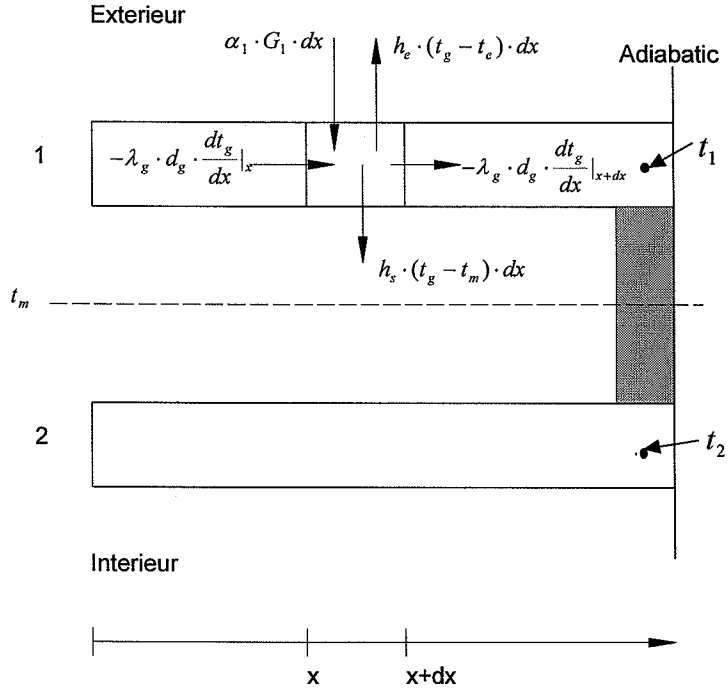
The external and internal heat transfer coefficients h_e and h_i are both constant
There exist a plane halfway between the glass panes where the temperature is constant t_m

$$q_1 = q_2 = q_s.$$

In figure 2 is shown the heat balance for a segment of the outer glass pane.

Figure 2.

Heat balance of a segment in a glass fin.
 t_1 and t_2 represents the temperatures at the base of the fins



The energy balance for the segment in figure 2 can be written as:

$$\alpha_1 \cdot G_1 \cdot dx - h_e (t_g - t_e) \cdot dx - h_s \cdot (t_g - t_m) \cdot dx + (-\lambda_g \cdot d_g \cdot \frac{dt_g}{dx} |_x) - (-\lambda_g \cdot d_g \cdot \frac{dt_g}{dx} |_{x+dx}) = 0 \quad (1)$$

where α_1 is the solar absorptance of layer 1
 G_1 is the solar irradiation on layer 1
 h_e is the outside surface heat transfer coefficient
 h_s is the heat transfer coefficient from the outer glass pane to the plane halfway between the glass panes
 t_g , t_e and t_m are respectively the temperatures of the glazing segment, the outside environment and the plane between the glass panes
 λ_g is the thermal conductivity of the glass
 d_g is the thickness of the glass.

(1) can be transformed to:

$$\frac{d^2 t_g}{dx^2} = \frac{h_e \cdot (t_g - t_e) + h_s \cdot (t_g - t_m) - S_1}{\lambda_g \cdot d_g} \quad (2)$$

where S_1 is $\alpha_1 \cdot G_1$

Two boundary conditions are known :

$$\left. \frac{dt_g}{dx} \right|_{x=0} = 0 \quad (b1)$$

corresponding to no temperature gradient on the middle of the glass pane,
and

$$t_g|_{x=W/2} = t_1 \quad (b2)$$

corresponding to the temperature of the glass pane at the spacer (base of the fin), W denotes the width of the investigated sample. The temperature t_1 is not known by now, but can be found later by iteration. (2) can be rewritten as:

$$\frac{d^2 t_g}{dx^2} = \frac{h_e + h_s}{\lambda_g \cdot d_g} \cdot \left(t_g - \frac{h_e \cdot t_e + h_s \cdot t_m}{h_e + h_s} - \frac{S_1}{h_e + h_s} \right) \quad (3)$$

Using

$$m_1 = \sqrt{\frac{h_e + h_s}{\lambda_g \cdot d_g}} \quad (4)$$

and

$$Y = t_g - \frac{h_e \cdot t_e + h_s \cdot t_m}{h_e + h_s} - \frac{S_1}{h_e + h_s} \quad (5)$$

equation (3) can be rewritten as:

$$\frac{d^2 Y}{dx^2} = m_1^2 \cdot Y \quad (6)$$

which has the general solution:

$$Y = C_1 \cdot \sinh(m_1 \cdot x) + C_2 \cdot \cosh(m_1 \cdot x) \quad (7)$$

Using (b1) and (b2) gives boundary conditions for equation (6):

$$\left. \frac{dY}{dx} \right|_{x=0} = 0 \quad (b3)$$

and

$$Y|_{x=W/2} = t_1 - \frac{h_e \cdot t_e + h_s \cdot t_m}{h_e + h_s} - \frac{S_1}{h_e + h_s} \quad (b4)$$

C_1 and C_2 are found by means of the boundary conditions and t_g can now be found from:

$$t_g = \left(t_1 - \frac{h_e \cdot t_e + h_s \cdot t_m + S_1}{h_e + h_s} \right) \frac{\cosh(m_1 \cdot x)}{\cosh(m_1 W / 2)} + \frac{h_e \cdot t_e + h_s \cdot t_m + S_1}{h_e + h_s} \quad (8)$$

$$\frac{dt_g}{dx} = \left(t_1 - \frac{h_e \cdot t_e + h_s \cdot t_m + S_1}{h_e + h_s} \right) \cdot \frac{m_1 \cdot \sinh(m_1 \cdot x)}{\cosh(m_1 W / 2)} \quad (9)$$

$x = W/2$ yields:

$$\frac{dt_g}{dx} \Big|_{x=W/2} = \left(t_1 - \frac{h_e \cdot t_e + h_s \cdot t_m + S_1}{h_e + h_s} \right) \cdot m_1 \cdot \tanh(m_1 W / 2) \quad (10)$$

q_1 can now be found from:

$$q_1 = -\lambda_g \cdot d_g \cdot \frac{dt_g}{dx} \Big|_{x=W/2} \quad (11)$$

Using (10) in (11) yields:

$$q_1 = \frac{W}{2} \cdot F_1 \cdot (S_1 + h_e \cdot t_e + h_s \cdot t_m - t_1 \cdot (h_e + h_s)) \quad (12)$$

where F_1 is the fin factor:

$$F_1 = \frac{\tanh(m_1 W / 2)}{m_1 W / 2} \quad (13)$$

In similar way q_3 can be found as:

$$q_2 = -\frac{W}{2} \cdot F_2 \cdot (S_2 + h_i \cdot t_i + h_s \cdot t_m - t_2 \cdot (h_i + h_s)) \quad (14)$$

The heat flow through the spacer can be found as:

$$q_s = \Lambda_s \cdot (t_1 - t_2) \quad (15)$$

The spacer conductance Λ_s is calculated from:

$$\Lambda_s = \frac{\lambda_{spacer}}{d_{spacer}} \cdot h_{spacer}$$

where λ_{spacer} is the equivalent thermal conductivity of the spacer, d_{spacer} is the extension of the spacer in the heat flow direction and h_{spacer} is the height of the spacer (see also figure 1). For most cases Λ_s is between 0.5 and 5 W/mK.

By using (12), (14), (15) and the assumption that $q_1 = q_2 = q_s$ the heat flow through the spacer can now be found.

APPENDIX F

MONOLITHIC SILICA AEROGEL IN SUPERINSULATING GLAZINGS

K. DUER and S. SVENDSEN

DEPARTMENT OF BUILDINGS AND ENERGY, TECHNICAL UNIVERSITY
OF DENMARK, BUILDING 118, DK-2800 LYNGBY, DENMARK

PHONE + 45 45 93 44 77, FAX +45 45 93 44 30

Abstract

Silica aerogel is an open-pored porous transparent material with optical and thermal properties that makes the material very interesting as an insulation material in windows. A number of different aerogels have been investigated for their optical and thermal performance. High thermal resistance of aerogel was found for all the investigated samples and the samples showed very high solar as well as light transmittance. However all the investigated aerogel samples showed a tendency to scatter the transmitted light resulting in a reduced optical quality when the aerogels are integrated in glazings. This phenomenon is considered being the main obstacle to incorporate the material in clear glazings but a significant improvement of the optical quality of aerogel has been observed during the last five years. A number of prototypical evacuated 500x500x28 mm aerogel double glazed units employing a new edge seal technique were manufactured and characterised for their optical and thermal properties. As expected the same scattering of light was found in the aerogel glazings as in the aerogel samples, but excellent thermal performance was found, indicating a glazing type that from a thermal point of view is without competition in heating dominated climates.

1. INTRODUCTION

This paper summarises the work that has been carried out within the aerogel project of the International Energy Agency, Solar Heating and Cooling Programme, Task 18, "Advanced Glazings and Associated Materials For Solar And Building Applications" (IEA SHCP Task 18). The scope of the aerogel project was to perform an evaluation of the aerogel material in order to identify some of the strengths and weaknesses that can be expected of aerogel as a material for window applications. The aerogel project has been carried out with partition of the following nations: Denmark, Finland, France, Germany, Japan, Norway, Sweden and the United Kingdom.

Super insulating windows with U-values below $1 \text{ Wm}^{-2}\text{K}^{-1}$ can be constructed in several ways. Most common is triple glazed systems using coatings with low

emissivity and noble gas filling of the gap between the transparent layers. By increasing the number of glass-panes in the window, the U-value can be even further reduced. However the price for the very low U-value will be a low transmission of solar energy and to a lesser extend daylight, both of which will have a negative impact on the total energy balance of the window in especially heating dominated climates. Studies within IEA SHCP Task 18 (Hutchins et al., 1997) have shown that the center U-value of an evacuated glazing with two hard low-e coatings (in position 2 and 3) is about $1.3 \text{ Wm}^{-2}\text{K}^{-1}$. The edge seal in the vacuum glazings is critical and in (Hutchins et al., 1997) it is found that the edge seal increases the over all U-value for a $1.0 \times 1.0 \text{ m}$ glazing with about $0.3 \text{ Wm}^{-2}\text{K}^{-1}$. By applying more advanced coatings it may be possible to obtain over all U-values of about $1.0 \text{ Wm}^{-2}\text{K}^{-1}$, but again the cost for this is a relatively low solar gain. It has so far not been possible to construct a glazing that at the same time has very high thermal resistance and high transmittance of solar energy and daylight.

By providing at the same time high thermal resistance and high transmittance of solar radiation and daylight, the silica aerogel is a very attractive material for the purpose of improving the thermal performance of windows. The main goals of the aerogel project were to carry out an optical and thermal characterisation of the aerogel and to show that it will be possible to construct a glazing with a U-value below $0.5 \text{ Wm}^{-2}\text{K}^{-1}$ and at the same time achieve a total solar energy transmittance (g-value) above 0.75.

2. SILICA AEROGEL

Silica aerogel is an open-pored porous transparent material with optical and thermal properties that makes the material very interesting as an insulation material in windows. Silica aerogel is not a new invention - it is described by S.S. Kistler already in 1931 and has since then been the subject of more or less interest.

Silica aerogel is usually manufactured from two types of precursor (Hutchins et al., 1997): Tetramethoxysilane (TMOS) or Tetraethoxylane (TEOS). The precursor is mixed with water, alcohol and different cathalysts into a mixture called an alcosol. After a while the silica particles form a structure. At this stage the mixture is called an alcogel and consists of a material with very small pores filled with solvent. Now the solvent must be removed without causing a collapse in the silica structure. The silica structure is rather fragile and an attempt to dry out the gel in an oven at atmospheric pressure will result in a break down of the silica structure. However by a supercritical drying it is possible to carry out the drying process and keeping the silica structure intact. This happens in an autoclave at a high pressure and at a temperature above the critical temperature of the solvent. For alcohol-solvents typical values are 90 bar and 280°C . The pressure is slowly reduced and the solvent can now be extracted from the gel leaving the silica structure undamaged. This process is

rather time- and energy consuming and implies of course a risk of explosion in the high temperature alcohol. Therefore effort has been shown to develop methods to avoid the supercritical alcohol extraction and two ways have been shown: At Lawrence Berkely Laboratory, California, USA a method has been developed where CO₂ is substituted for alcohol at a temperature far below the critical temperature of the alcohol-solvent (Hunt and Martin, 1991). After the substitution the CO₂ is extracted by rising the temperature above the critical for CO₂ (31°C). This method is fast and energy efficient compared to the supercritical drying of the alcohol-solvent and reduces the explosion danger considerably. Such a production method has been developed at the laboratory level in the LACE Laboratory at University Claude Bernard in Lyon to produce the "carbogel" samples described later in this paper.

Another method to avoid the high pressure and temperature drying is used at the University of Trondheim, Norway, where new monomers are added to the alcogel in order to strengthen the alcogel network and in this way making it possible to perform the drying process of the alcogel at atmospheric pressure and at temperatures below 100°C. The product of this process is the so called xerogel. As the silica skeleton has been reinforced the xerogel is somewhat more dense than aerogel (typically a factor of 2-5 in density). Also the thermal conductivity of the Xerogel in non-evacuated condition is higher than that of aerogel (typically a factor of 2 in thermal conductivity). However, German investigations shows only small differences in the thermal conductivity of aerogel and xerogel in evacuated condition (Hutchins et al., 1997).

Aerogel is very vulnerable to tensile stress and also to moisture and if liquid water comes in contact with the aerogel, the aerogel will rapidly be destroyed. That means that the material has to be effectively protected from the environment if used for ordinary building applications like in windows. Luckily aerogel is very strong in compression, making it possible to use the material in a sandwich construction, e.g. between two sheets of glass.

The material has under atmospheric pressure a relatively low thermal conductivity, around 15-20 mWm⁻¹K⁻¹, and the open-pored structure of the aerogel in combination with the small pore size makes it possible to achieve vacuum-like properties of the aerogel at a very moderate vacuum ($p < 5000$ Pa). By exposing the aerogel to a pressure below 5000 Pa the heat transport through the material happens mainly by heat conduction through the structure (silica skeleton) and by radiation. As up to 97% of the aerogel consists of air voids it is evident that the heat conduction through the skeleton is very limited and thermal conductivity below 10 mWm⁻¹K⁻¹ can be expected. The thermal resistance of a 20 mm evacuated aerogel tile will be about the same as the thermal resistance of 100 mm conventional mineral wool.

The pore size is about 10-20 nm ($\sim 1/40$ of the wavelength of visible light) and besides the high thermal resistance at a moderate vacuum this small pore size makes aerogel transparent and translucent. This is the property that makes aerogel applicable as an insulation material in windows and in solar applications in general.

In theory the small pore size makes it possible to produce a silica aerogel that is perfectly transparent with no significant distortion of the transmitted light, but in practice difficulties arise during the production processes of the aerogel. Many local disorders in the material result in scattering of the transmitted light, mainly in the blue part of the visible spectrum. This scattering gives objects a hazy look when observed through the aerogel and changes also the colors in such a way that the aerogel appears slightly bluish when the background is black or dark and appears slightly yellow when the background is white or bright.

3. MEASUREMENTS

Two fields of properties for the aerogel have been investigated: The optical and the thermal characteristics and the investigation described here deals with several aerogel-like materials considered as candidates to be used between two plane glass panes for a super insulating double glazed unit.

Main focus has been on transparency as this property is considered to be the main difficulty for monolithic aerogel in clear windows. Secondly the thermal resistance is investigated, expected to be high and permitting anyway a significant increase in the thermal resistance compared to the actual highly insulated glazing units. The purpose is merely to check that the thermal conductivity remains in the range of the expected value for aerogels.

A number of aerogel samples have been investigated. IEA SHCP Task 18 has had a duration of five years and a development of aerogel materials has been seen during the time of the project. Five samples have been selected to give a good picture of the range of especially optical properties that are characteristic for different aerogel materials. Key parameters for the five samples are described in table 1.

JAPAN submitted two samples: a low density monolithic silica aerogel manufactured by supercritical drying of alcohol, referred as JAP1 and a monolithic silica aerogel produced by supercritical treatment in 2-propanol, referred as JAP2.

SWEDEN submitted the same type of material with a higher density, referred as SWE1. FRANCE submitted a monolithic silica aerogel (carbogel) obtained by supercritical drying of CO₂, previously substituted to alcohol, it is referred as FRA1. NORWAY submitted a monolithic xerogel sample produced by atmospherical pressure drying, referred as NOR1.

The JAP2 sample was produced and investigated in 1996, the other four samples were investigated in the period from 1992 to 1994.

Table 1. Key parameters of test specimen

JAP1	NOR1	SWE1	FRA1	JAP2
------	------	------	------	------

Type	Aerogel	Xerogel	Aerogel	Carbogel	Aerogel
Density	90 kg/m ³	500 kg/m ³	150 kg/m ³	173 kg/m ³	116 kg/m ³
Thickness	12 mm	9 mm	7 mm	11 mm	9 mm

3.1 Measured solar and visible properties

The spectral measurements have been performed in spectrophotometers by several laboratories and for each sample all laboratories produced rather uniform measurement results, allowing the presentation of only a selected number of results here. The spectral normal-normal transmittance (τ_{λ}^{nn}) and the spectral normal-hemispherical transmittance (τ_{λ}^{nh}) have been obtained in the spectral range from 300 to 2500 nm, using when necessary an integrating sphere.

The results are shown in fig. 1 to fig. 5.

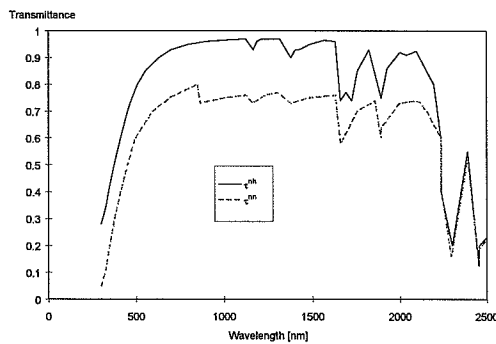


Figure 1. Spectral normal-hemispherical and normal-normal transmittance. Sample JAP1.

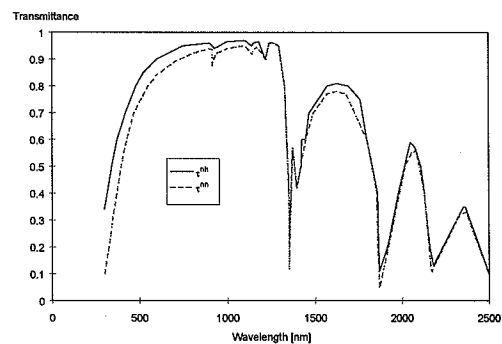


Figure 2. Spectral normal-hemispherical and normal-normal transmittance. Sample NOR1.

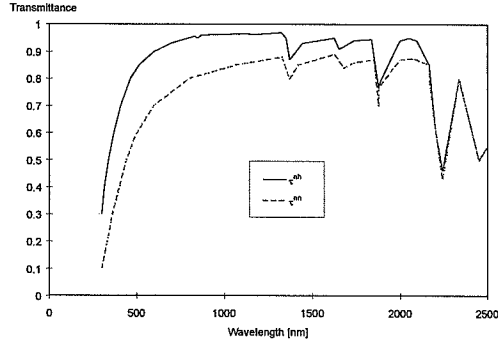


Figure 3. Spectral normal-hemispherical and normal-normal transmittance. Sample SWE1.

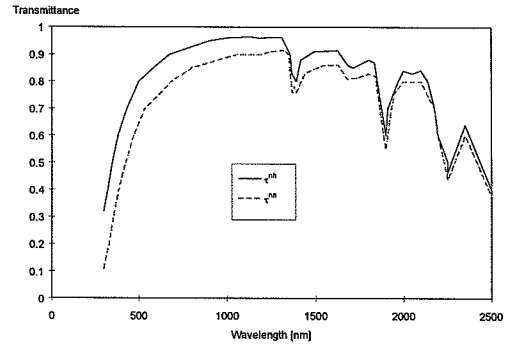


Figure 4. Spectral normal-hemispherical and normal-normal transmittance. Sample FRA1.

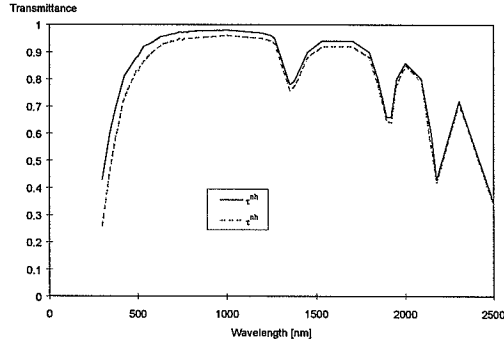


Figure 5. Spectral normal-hemispherical and normal-normal transmittance. Sample JAP2.

From the measured spectra the integrated values have been calculated using standard documents (ASTM - E891; CEN: Pr EN 410). Table 2 shows the solar properties indicated with subscript e and table 3 shows the visible light properties indicated with subscript v.

TR is the Transparency Ratio (Elaloui et al., 1992), expressed as the ratio:

$$TR = \frac{\tau_v^{nn}}{\tau_v^{nh}} \quad (1)$$

where subscript v indicates visible light parameters. TR is expected to be as high as possible to guarantee a good transparency and vision quality.

Table 2. Solar properties

	JAP1	NOR1	SWE1	FRA1	JAP2
Type	Aerogel	Xerogel	Aerogel	Carbogel	Aerogel
τ_e^{nh} [%]	87.3	86.0	89.7	86.7	92.1
τ_e^{nn} [%]	68.4	80.5	73.6	76.1	89.0
τ_e^{ndiff} [%]	20.9	5.5	16.3	-	3.1
ρ_e^{nh} [%]	2.9	3.3	3.8	-	1.9

Table 3. Light properties

	JAP1	SWE1	NOR1	FRA1	JAP2
Type	Aerogel	Aerogel	Xerogel	Carbogel	Aerogel
τ_v^{nh} [%]	84.1	87.2	86.7	89.9	92.1
τ_v^{nn} [%]	65.3	65.4	79.6	77.4	88.0
τ_v^{ndiff} [%]	18.8	21.8	7.1	-	4.0
ρ_v^{nh} [%]	4.0	4.8	4.6	-	2.8
TR	0.78	0.75	0.92	0.86	0.96

As shown in table 2 and 3 the aerogel, carbogel and xerogel samples are found to have high transmittance (84-92%) for radiation in the solar spectrum as well as in the visible part of the solar spectrum. These values are about the same as for conventional clear glass. However, part of the solar radiation is being diffused when transmitted through the material. Measurements have shown that the scattering is taking place mainly at shorter wavelength i.e. in the visible part of the solar spectrum. This means that the aerogel is the reason for more or less hazy pictures when objects are viewed through the material.

If the structures in a transparent material are similar to or smaller than the wavelength of the transmitted light, the scattering is considered to be dependant on the wavelength. The structures in the bulk of the aerogels are small in comparison to the wavelength of the light and the scattering in the aerogel is indeed wavelength

dependant and can approximately be described as Rayleigh scattering where the scattering will be proportional to the wavelength in the power of -4.

When the structures in the transparent material are much larger than the wavelength of the incoming light the scattering is considered to be wavelength independent. The surface irregularities of the aerogel are in general relatively large (scratches and cracks etc.) and the surface scattering is therefore considered independent of the wavelength.

The scattering $S(\lambda)$ can be expressed by the following model:

$$S(\lambda) = S_{\text{bulk}}(\lambda) + S_{\text{surface}} \quad (2)$$

where $S_{\text{bulk}}(\lambda)$ is the wavelength dependant bulk scattering and S_{surface} is the wavelength independent surface scattering.

By reducing the typical dimension of pores, cavities and silicon oxide particles in the aerogel it may be possible to push the scattering towards shorter wavelength into the ultraviolet and thereby out of the visible, resulting in less visible scattering (Hutchins et al., 1997).

The surface scattering can only be reduced by careful production and handling of the aerogel.

The value of the Transparency Ratio TR is a simple way of quantifying the scattering phenomenon. For the sake of comparison ordinary float glass has a TR value of about 0.99, where the TR value for the investigated samples were in the range of 0.75 to 0.96.

It is worth noticing that the JAP2 sample has a lower visible scattering (~4%) and at the same time a higher solar and visible transmittance than all other investigated samples in this way showing a significant improvement in especially the visible properties of the aerogel. However one should bear in mind that the investigated samples are of different thickness. The thickness is an important parameter for the optical properties, partly because of absorption in the aerogel and partly because a large part of the scattering of light is taking place as bulk scattering. In this way the scattering and absorption of light will be dependent on the sample thickness. By using the simple scattering model in (2) it is possible to perform a comparison between different thickness of aerogel (Jensen et al., 1996).

Anyway, large transmittances has been measured also on thicker samples (20 mm Swedish aerogel from Airglass), where the visible transmittance was found to 86.3% and the solar transmittance was found to 87.7% (Hutchins et al., 1997).

3.2 Measured thermal properties

The heat transport in aerogel happens by conduction through the silica skeleton, conduction through the pore gas and by radiation. Because of the very small pore size the convection in aerogel is considered negligible for building application from a thermal point of view. By evacuating the aerogel the conduction through the pore gas is reduced dramatically and the heat transport through the aerogel is now reduced to conduction in the silica skeleton and radiation. Measurements of the thermal conductivity as a function of the pore pressure shows that already after reducing the pore pressure to 5000 Pa the conduction in the pore gas has almost come to a stop. Previous investigations have showed the high thermal resistance of evacuated aerogel and values for the thermal conductivity around 11-12 $\text{mWm}^{-1}\text{K}^{-1}$ have been reported (Kistler, 1935, 1942; Heinemann et al., 1986).

Depending on the density of the aerogel the non-evacuated and evacuated thermal conductivity for the samples investigated in this paper have been measured to 15-17 $\text{mWm}^{-1}\text{K}^{-1}$ and 9-11 $\text{mWm}^{-1}\text{K}^{-1}$ respectively. The xerogels showed higher thermal conductivity in non-evacuated condition (25 $\text{mWm}^{-1}\text{K}^{-1}$) but the same thermal conductivity as aerogels in evacuated state (Hutchins et al., 1997).

4. AEROGEL DOUBLE GLAZED UNIT

4.1. Production of an aerogel glazing

An aerogel glazing can be constructed as a sandwich by inserting a 20 mm thick aerogel disk between two glass panes, sealing the unit and evacuating the interior of the aerogel glazing to a level below 5000 Pa. Of course this is much easier said than done.

The center U-value (U_{center}) of such evacuated glazings has previously been investigated and values around 0.5 $\text{Wm}^{-2}\text{K}^{-1}$ (depending on the aerogel) have been found (Rubin and Lampert, 1983; Jensen, 1992). To maintain this low U_{center} of the evacuated glazing it is essential that the edge sealing is sufficiently vapour and air tight during the expected lifetime of the glazing. The ideal edge seal for an evacuated aerogel glazing should be airtight, vapour tight and resulting in no or only little cold bridge effect.

The first and second of these requirements are essential and in order to meet them, edge seals with rather poor thermal properties have so far been proposed, resulting in a significantly higher U_{glazing} in comparison to the U_{center} . Typical values are $U_{\text{glazing}} = 1.7 \times U_{\text{center}}$ for a 1x1 m glazing, i.e. an increase of 70%. Clearly this is not very satisfying and efforts have been shown to find an edge seal design that results in a U_{glazing} close to the U_{center} .

In a recent work a promising edge seal for an evacuated aerogel glazing has been described (Jensen et al., 1996). The principle of the edge seal is very simple: Instead of the stainless steel that so far has been used, a special plastic laminate with glass

dust is used in the sealing. The plastic laminate is wrapped around the aerogel disk along the periphery, a layer of butyl is applied on the plastic laminate on both sides of the aerogel/plastic and the aerogel/plastic is assembled to the two glass panes, see figure 6 (Jensen et al., 1996). Finally the unit is evacuated through a suction pipe in the edge seal.

Investigations have been carried out to characterise the properties of the plastic laminate with respect to water vapour tightness and UV-resistance and it was found that the plastic foil requires a protection against water vapour diffusion and mechanical overload. This protection can be achieved by a two-step cover of the edge of the glazing: innermost a 0.5mm layer of butyl, forming an effective barrier to water vapour and outermost a 1 mm layer of polysulfide, see figure 6. The polysulfide will also serve as a bond between the two glass panes if the vacuum in the aerogel glazing should disappear.

As the sealing is about 1.6 mm thick (including plastic foil, butyl and polysulfide) it results only in small cold bridge effect in the final edge seal. In table 4 is shown calculated U-values for aerogel glazings (20 mm aerogel sheet) of different sizes, all using the described edge seal. Values are including the effect of the butyl and polysulfide layers.

Four evacuated aerogel double glazed units in small scale have been constructed in Denmark, all using the basic principle of the edge seal described above. Four glazings were manufactured in order to allow investigations in four different laboratories in Europe. Each glazing was made of a 20 mm thick Swedish Airglass disk and two 4 mm low iron hardened glass panes. The overall size of each unit is 500x500x28 mm with an aperture of about 450x450 mm.

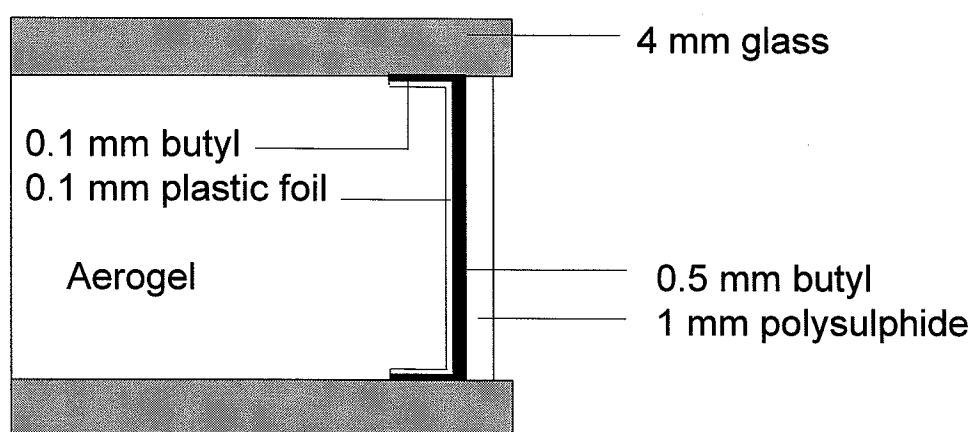


Figure 6. *Edge seal based on a 0.1 mm glass-coated plastic laminate.*
(Jensen et al., 1996)

As the edge seal is rather fragile even when the butyl and polysulfide is applied it was at his stage necessary to apply a thick layer of silicone to the edge seal in order to protect it against mechanical damages during transportation of the glazings. In figure 7 is shown the design of the edge seal in the tested aerogel glazings. The two-step protection with butyl and polysulfide was replaced with of a thick layer of silicone in order to obtain a very robust edge seal. Of course this silicone more or less ruins the good thermal performance of the edge seal, thus the focus for the thermal measurements was on the center value.

Table 4. Calculated total U-values (U_{2D}) for different sizes of aerogel glazings with rim seal of 0.1 mm laminated plastic foil and 0.5 mm of butyl protected with a 1 mm polysulfide sealant. (Jensen et al., 1996)

Spacer material	Glazing size	Peri meter	Area	Equivalent thermal conductivity	U_{centre}	U_{2D}
	m × m	m	m ²	Wm ⁻¹ K ⁻¹	Wm ⁻² K ⁻¹	Wm ⁻² K ⁻¹
	0.5×0.5	2.0	0.25			0.44
Plastic foil	1.0×1.0	4.0	1.00	0.20	0.40	0.42
	1.5×1.5	6.0	2.25			0.41

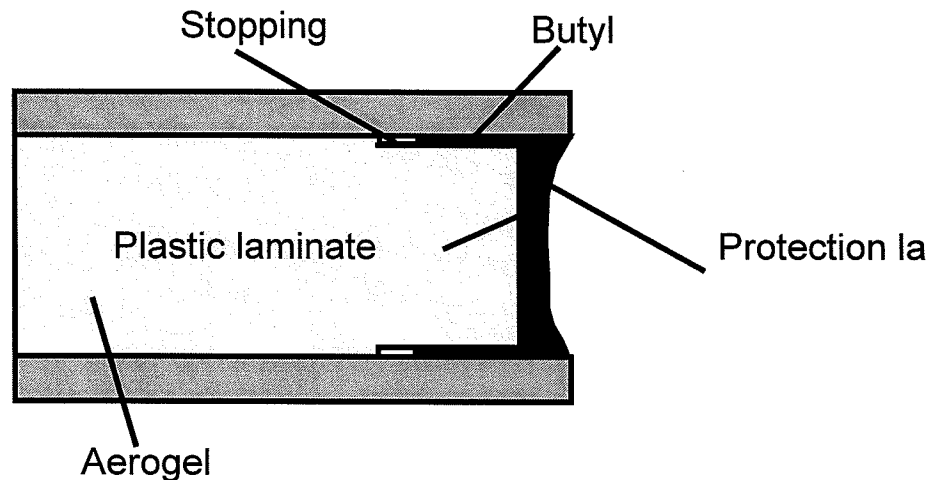


Figure 7. Plastic laminate edge seal of the tested units. (Jensen et al., 1996)

4.2. Measurement of key performance parameters

The key performance parameters (U-value, g-value, solar transmittance $\tau_{\text{e}}^{\text{nh}}$ and light transmittance $\tau_{\text{v}}^{\text{nh}}$), have been measured at different laboratories.

The results of the measurements are shown in table 5. The optical results shown are integrated values of normal-hemispherical transmittance in the solar and visible

spectrum respectively, i.e. τ_e^{nh} and τ_v^{nh} . U-value measurements were carried out using hot-plate devices and the results are shown for a mean temperature of the glazing of 10°C and including total surface resistance of 0.17 m²K/W. The g-value was measured by means of an illuminated calorimetric apparatus using an artificial sun (CSI-lamps)

As it shows in table 5 the measurements indicates that the aerogel glazings that have been tested exhibit very high thermal resistance as well as very high solar and visible transmittance. The goal initially set ($U < 0.5 \text{ Wm}^{-2}\text{K}^{-1}$ and $g > 0.75$) seem to be reached.

Table 5. Key performance parameters for aerogel glazing

Laboratory	FIN	FRA	FRG	DK	
U_{center}	0.42	-	0.41	0.47	[Wm ⁻² K ⁻¹]
τ_e^{nh}	78.0	74.1	75.0	-	[%]
τ_v^{nh}	73.7	71.7	72.0	-	[%]
g	-	-	-	0.79 ¹	-

¹ Incidence angle = 22.5°

5. CONCLUSION

Several candidate materials of the aerogel type have been investigated from an optical and thermal point of view. The expected high thermal resistance of aerogel was found for all the investigated samples and the samples showed very high values for the transmittance of radiation in the solar spectrum as well as in the visible part of the solar spectrum. As expected the measurements showed that the investigated materials all have a tendency to scatter the transmitted light resulting in a hazy picture when objects are viewed through the material. This phenomenon is considered to be one of the major problems for the use of aerogel-type materials in clear windows. However the sample labelled JAP2 represents a significant improvement of the visible properties of aerogel and must clearly be seen as a step towards an aerogel suitable for window applications from an optical as well as thermal point of view.

Until a clear aerogel is available the aerogel materials are at the present state of optical and thermal development very well suited for day-lighting applications provided that the production can be scaled up and that the production can be carried out at a moderate cost.

The measurements of the thermal key parameters of the aerogel glazings showed that very high values for thermal resistance and total solar energy transmittance were reached, resulting in a glazing type that from a thermal point of view is without competition for especially heating dominated climates.

For the further development of aerogel-type materials it is important to characterise the material especially concerning the optical and thermal properties. Some of the characterisations needed have taken place within IEA SHCP, Task 18 but will of course have to continue as long as new and hopefully improved materials appear. These characterisations can together with results from work carried out in other fields of advanced glazings serve as input to a common solution to the problems that arises on the way to a clear window with aerogel-like super insulation.

ACKNOWLEDGEMENT

This work was to a large extend carried out as a contribution to the International Energy Agency Solar Heating & Cooling Programme, Task 18 Advanced Glazing Materials. This paper is written by the Danish IEA Task 18 participants in their capacity of project leaders of the aerogel project in Task 18. The content of the paper is mainly based on work carried out by all the participants in the aerogel project in Task 18. The authors wish to thank the Danish Energy Ministry's Research Programme for supporting the Danish participation in IEA Task 18.

REFERENCES

- Elaloui, E.; Achard, P.; Chevalier, B.; Chevalier, J.L.; Durant, M.; Pajonk, G.M.: Improved monolithic aerogel for transparent glass spacer in innovative windows. Proceedings of SPIE v 1727 p. 402-417, 1992.
- Heinemann, U.; Hümmer, E.; Büttner, D.; Caps, R.; Fricke, J.: Silica aerogel - a light-transmitting thermal super insulator. High Temperatures High Pressures v 18 n5 1986 p. 517-526
- Hunt, Arlon J.; Martin, Marlo
Scaling up production of silica aerogel using the CO₂ substitution method
Proceedings of International Symposium on Aerogels. Sept. 30 - Oct. 2, 1991
- Hutchins, M.G.; Aschehoug, O.; Ballinger, J. (eds): International Energy Agency Solar Heating & Cooling Programme Task 18, Advanced Glazing Materials, Technical Reports of Subtask A and Subtask B. To be published. (1997).
- Jensen, K.I.; Schultz, J.M.; Svendsen, S. (eds): Development and investigation of evacuated windows based on monolithic silica aerogel spacers.

- EU-contract JOU2-CT92-0192. (1992-1995).
- Jensen, K.I.: Passive solar component based on evacuated monolithic silica aerogel.
J. of Non-Crystalline Solids v 145 n 1-3 Aug 1 1992, p237-239
- Kistler, S.S.: Nature 127, 1931
- Kistler, S.S.; J. Phys. Chem 39 1935
- Kistler, S.S.; J. Phys. Chem 46 1942
- Rubin, M.; Lampert, C.M.: Transparent Silica Aerogels for Window
Insulation Solar Energy Materials 7 (1983) 393-400.

